

UNIVERZITA OBRANY
FAKULTA VOJENSKÉHO ZDRAVOTNICTVÍ

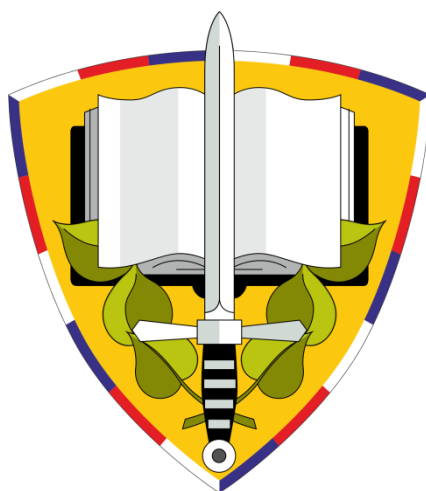
DISERTAČNÍ PRÁCE

HRADEC KRÁLOVÉ 2019

Mgr. Lukáš Górecki

UNIVERZITA OBRANY
FAKULTA VOJENSKÉHO ZDRAVOTNICTVÍ

Doktorský studijní program Toxikologie



DISERTAČNÍ PRÁCE

Development of novel cholinesterase modulators

Zpracoval: Mgr. Lukáš Górecki

Školitel: PharmDr. Jan Korábečný, Ph.D.

HRADEC KRÁLOVÉ 2019

Acknowledgements

I would like to thank all the people who supported me during my postgraduate studies. First and the most important thanks belong to my current supervisor Dr. Jan Korábečný and my former supervisor Dr. Kamil Musílek. I would like to thank them for their advices, experiences and guidance through my studies. Especially, I am grateful to Dr. Jan Korábečný, who has the greatest influence on me as well as he is responsible for all I have become during PhD. Next thanks belong to all my colleagues at the Department of Toxicology and Military pharmacy and at Biomedical Research Center for creating a pleasant working environment in our laboratories and also for their help with biochemical studies and analytical characterization of the final products. I would also like to thank all my relatives and especially Monika Elisová for the support during these years.

My special thanks belong to prof. Maria Laura Bolognesi for accepting me for the internship at her lab (Universita di Bologna). She gave me invaluable lessons for my career in the science.

Other special thanks belong to Dr. Zoran Radić, Dr. Carlo Ballatore and prof. Palmer Taylor. I am grateful to Zoran and Carlo for accepting me for the internship at their labs (UCSD). Thanks to Zoran, this period of my life was priceless experience in personal as well as in career life.

Finally, I acknowledge the financial support by University of Defense (Faculty of Military Health Sciences, Long-term Development Plan – 1011 and SV/FVZ201601) and University Hospital Hradec Kralove (No. 00179906).

Declaration

I declare that this thesis is my original work. All used literature sources are listed in the list of references and properly cited within the text.

In Hradec Králové

Mgr. Lukáš Górecki

Abstract

The enzyme acetylcholinesterase (AChE) is a key component in cholinergic synapses and at the neuromuscular junctions. Its physiological function is essential in humans, as well as in animal species, including insects. In pathological conditions, AChE is also involved in various disorders such as Alzheimer's disease (AD) or myasthenia gravis. The significance of the enzyme has also been demonstrated by its successful use as a target in insecticides. In addition, it is the key mediator in the manifestation of symptoms of intoxication after exposure to Chemical warfare agents (CWA) (Nerve agents; NA). Herein, I report my study of three different aspects of this enzyme: as an anti-AD target; as an insecticidal target; and as an enzyme to be reactivated after intoxication by organophosphorus compounds (OPCs).

Since the introduction of tacrine in 1993 as an anti-AD drug, much attention has been paid to the development of novel AChE inhibitors; some, such as donepezil, have been successfully marketed. At present, there is still a need for efficient drugs against AD. As AD is a multifactorial disorder, it is believed that it cannot be treated by simply targeting one pathological condition. Therefore, the so-called multi-target directed ligands (MTDLs) have been developed to overcome this limitation. Within this thesis, the development of two families of MTDLs is described.

Specifically targeting harmful insect species (e.g., those responsible for vector-borne diseases) and not beneficial ones, such as honey bees or other animals, appears to be an almost impossible task. However, AChE is considered as one of the most promising targets, even though currently used insecticides have very poor selectivity. Two series of insecticides have been discovered and are reported herein. The ones with the highest efficacy also proved to have very promising selectivity towards insect AChE.

AChE reactivators represent the only available causal protection against OPC intoxication. At present, there is no reliable enzyme reactivator that would ensure sufficient protection. Within this work, three series of AChE reactivators were prepared. Based on a survey of the literature, some of them exert the most promising reactivation profiles yet to be presented.

Keywords: nerve agent, acetylcholinesterase, reactivator, oxime, synthesis, *in vitro*

Abstrakt

Enzym acetylcholinesterasa (AChE) je klíčovým komponentem cholinergních synapsí a nervosvalových spojích. Její biologická funkce je nezbytná pro všechny zástupce živočišné říše. Z patofyziologického hlediska je zapojena do řady onemocnění jako Alzheimerova choroba (AD, z anglického Alzheimer's disease) nebo *Myasthenia gravis*. Význam tohoto enzymu může taktéž být prokázán tím, že se AChE stala spolehlivým terčem pro řadu insekticidů. Mimo jiné nejtoxičtější skupina chemických bojových látek (nervově paralytické látky; NPL) rovněž cílí na tento enzym. V této disertační práci jsme se zaměřili na AChE ze tří různých aspektů, jako cíl proti AD, jako insekticidy a jako enzym, který musí být reaktivován po intoxikaci organofosforovými sloučeninami.

Už od dob nástupu takrinu jako prvního léčivého přípravku proti AD v roce 1993, AChE inhibitory jsou velkou skupinou látek cílící proti tomuto onemocnění. Některé z nich byly i úspěšně uvedeny do klinické praxe (např. donepezil). V dnešní době však stále neexistuje úspěšná léčba tohoto multifaktoriálního onemocnění. Moderní postupy vývoje léčiv se snaží zaměřit na více cílů najednou přípravou takzvané multi-cílové látky (MTDL, z anglického multi-targeted directed ligand). V této práci je popsán vývoj dvou sérií těchto MTDL sloučenin.

Skoro nemyslitelným úkolem se zdálo cílení AChE od určitých druhů hmyzu (přenášče tropických nemocí) a zároveň zanechat nedotknutelný enzym u prospěšného hmyzu (např. včely), enzym savčí anebo např. ptačí. Napovídá tomu i fakt, že všechny klinicky dostupné insekticidy útočící na AChE mají jen velmi nepatrnou selektivitu. My jsme v této práci využili nových vědeckých poznatků a připravili dvě série látek. Ty nejlepší se ukázaly být významnými selektivními insekticidy.

Reaktivátory AChE představují jedinou kauzální ochranu před organofosforovou intoxikací. V dnešní době stále není účinná protekce, která by zaručovala dobrou prognózu otráveného. V této práci popisujeme vývoj třech nových sérií reaktivátorů AChE, přičemž některé z těchto látek disponují nejúčinnějším profilem, který kdy byl prezentován.

Klíčová slova: nervově paralytické látky, acetylcholinesterasa, reaktivátor, oxim, syntéza, *in vitro*

Content

Abbreviations	11
List of figures	14
List of tables	17
1. Introduction	18
1.1 Acetylcholinesterase	18
1.2 Alzheimer's disease	22
1.2.1 Treatment.....	25
1.3 Insecticides.....	27
1.3.1 Common issues with current insecticides.....	28
1.3.2 AChE-targeted insecticides	29
1.4 Organophosphorus intoxication.....	30
1.4.1 Treatment options	33
1.4.2 Novel approaches to the treatment of OP intoxication.....	34
2. Objectives.....	37
3. Results.....	38
3.1 Design	38
3.1.1 Tacrine-phenothiazine derivatives.....	38
3.1.2 Tacrine derivatives with dual-targeting of AChE and the NMDA receptors	40
3.1.3 AChE-targeting insecticides	41
3.1.4 Second subset of insecticides	42
3.1.5 Mono-quaternary permanently charged AChE reactivators.....	43
3.1.6 Tacroximes	43
3.1.7 Uncharged bis-oxime reactivators	45
3.2 Synthesis	48

3.2.1	Tacrine-phenothiazine derivatives.....	48
3.2.2	Tacrine derivatives with dual-targeting of AChE and the NMDA receptor	54
3.2.3	AChE-targeting insecticides.....	56
3.2.4	Second subset of insecticides	58
3.2.5	Mono-quaternary permanently charged AChE reactivators.....	60
3.2.6	Tacroximes	64
3.2.7	Uncharged bis-oxime reactivators.....	65
3.3	Biological evaluation	68
3.3.1	Tacrine-phenothiazine derivatives.....	68
3.3.2	Tacrine derivatives with dual-targeting of AChE and the NMDA receptor	71
3.3.3	AChE-targeting insecticides.....	73
3.3.4	Second subset of insecticides	75
3.3.5	Mono-quaternary permanently charged AChE reactivators.....	76
3.3.6	Tacroximes	81
3.3.7	Uncharged bis-oxime reactivators.....	83
4.	Discussion	88
4.1	Synthesis	88
4.1.1	Tacrine-phenothiazine derivatives.....	88
4.1.2	Tacrine derivatives with dual-targeting of AChE and the NMDA receptor	89
4.1.3	AChE-targeting insecticides.....	89
4.1.4	Second subset of insecticides	91
4.1.5	Mono-quaternary permanently charged AChE reactivators.....	92
4.1.6	Tacroximes	93
4.1.7	Uncharged bis-oxime reactivators.....	94

4.2	Biological evaluation and structure-activity relationship	95
4.2.1	Tacrine-phenothiazine derivatives.....	95
4.2.2	Tacrine derivatives with dual-targeting of AChE and the NMDA receptors	96
4.2.3	AChE-targeting insecticides	96
4.2.4	Second subset of insecticides	97
4.2.5	Mono-quaternary permanently charged AChE reactivators.....	98
4.2.6	Tacroximes	98
4.2.7	Uncharged bis-oxime reactivators.....	99
4.3	Overview of contribution to the development of cholinesterase modulators 100	
4.3.1	Anti-AD drugs	102
4.3.2	AChE-targeted insecticides	103
4.3.3	AChE reactivators	103
5.	Conclusion.....	105
6.	Experimental part	106
6.1	General synthetic methods.....	106
6.1.1	Tacrine-phenothiazine derivatives.....	106
6.1.2	Tacrine derivatives with dual-targeting of AChE and the NMDA receptor	132
6.1.3	AChE-targeting insecticides	141
6.1.4	Second subset of insecticides	157
6.1.5	Mono-quaternary permanently charged AChE reactivators.....	166
6.1.6	Tacroximes	182
6.1.7	Uncharged bis-oxime reactivators.....	190
6.2	Biological evaluation	201
6.2.1	Inhibitory assays.....	201

6.2.2	Reactivation assays.....	202
6.2.3	BBB penetration estimation assays	204
6.2.4	Additional measurements	205
7.	References	207
8.	Outputs	225
9.	Attachments.....	228

Abbreviations

ACh – acetylcholine

AChE – acetylcholinesterase

AD – Alzheimer's disease

APP – A β precursor protein

A β – amyloid β

BBB – blood-brain barrier

BCh – butyrylcholine

BChE – butyrylcholinesterase

CAS – catalytic active site

Cdk5 – cyclin dependent kinase 5

CNS – central nervous system

CNS MPO – central nervous system multi-parameter optimization

CWA – Chemical warfare agent

CWC – Chemical Weapon Convention

DCM – dichloromethane

DIBAL-H – diisobutylaluminium hydride

DMF – *N,N*-dimethylformamide

DMSO – dimethylsulfoxide

EtOH – ethanol

FDA – Food and Drug Administration

GSK-3 β – glycogen synthase kinase β

*h*AChE – human acetylcholinesterase

*h*BChE – human butyrylcholinesterase

IC₅₀ – median inhibitory concentration

IRS – indoor residual spraying
ITN – insecticide-treated nets
MeCN – acetonitrile
MeOH – methanol
MTDL – multi-targeted directed ligands
MW – microwave
NA – Nerve Agent
NBS – *N*-bromosuccinimide
NMDA - *N*-methyl-*D*-aspartate
NMR – nuclear magnetic resonance (spectroscopy)
OP – organophosphorous
OPC – organophosphorous compounds
PAS – peripheral anionic site
PERNOD – *p*-anisaldehyde TLC detection stain
PHT – phenothiazine
PMA - phosphomolybdic acid TLC detection stain
PPh₃ – triphenylphospine
PSL – peripheral anionic site ligand
SAR – structure-activity relationship
TBAF – tetrabutylamonium fluoride
TBDMSOTf – *tert*-butyldimethylsilyl triflate
TBS – *tert*-butyldimethylsilyl protecting group
*Tc*AChE – Torpedo californica acetylcholinesterase
TEA – triethylamine
TFA – trifluoroacetic acid
TFAA – trifluoroacetic acid anhydride

THA – 1,2,3,4-tetrahydroacridine

TLC – thin layer chromatography

TsOH - *p*-toluenesulfonic acid

WHO – World Health Organization

WMD – Weapons of mass destruction

List of figures

Figure 1 Schematic drawing of the function of the neurotransmitter ACh for the function in various parts of nervous system. (page 18)

Figure 2 Schematic representation of the active and peripheral site of *TcAChE*, including the amino acids residues of the catalytic triad, anionic site, narrow aromatic gorge, and peripheral site. (page 20)

Figure 3 The global impact of dementia. Taken from World Alzheimer Report 2015 by WHO. (page 22)

Figure 4 Currently available drugs for the treatment of AD. (page 25)

Figure 5 Tacrine and its analog, 7-MEOTA and 6-chlorotacrine. (page 26)

Figure 6 Plausible strategies for the development of novel MTDLs. (page 26)

Figure 7 A: Pyrethroid family compounds targeting the voltage-gated sodium ion channels, permethrin and deltamethrin; and the organochlorine insecticide DDT. B: Organophosphorus-based insecticides targeting AChE: paraoxon, dichlorvos, malathion, and the methylcarbamates, bendiocarb and propoxur. (page 28)

Figure 8 Representative NAs from the G-family (tabun, sarin, soman, and cyclosarin) and the V family (VX, Russian VX, and Chinese VX). (page 31)

Figure 9 A: Clinically approved causal antidotes against organophosphorus intoxication: pralidoxime, obidoxime, asoxime, methoxime, and trimedoxime (X⁻ represents chloride, bromide, iodide, or methansulfonate anion); B: Examples of symptomatic antidotes: the anticonvulsive diazepam and the anticholinergic atropine. (page 34)

Figure 10 Designed compounds based on tacrine and phenothiazine scaffolds. (page 40)

Figure 11 Substituted tacrine derivatives and their analogs with five- to seven-membered saturated rings. (page 40)

Figure 12 The first series of Cys-targeted insecticides developed from already published models described by Pang et al. in 2012 and Dou et al. in 2013. (page 41)

Figure 13 *In silico* representation of **134** in the *AgAChE1* active site (PDB ID: 5YDH). The close-up view of the ligand is presented as a three-dimensional (A, left) and two-

dimensional (B, right) representations. Generally, A, **134**, is presented in green, important amino acid residues are presented in blue, and the catalytic triad is presented in yellow. (page 42)

Figure 14 Our second series of Cys-targeted insecticides, which were derived from the first series. (page 42)

Figure 15 Design of mono-quaternary compounds based on 2-[(1E)-(hydroxyimino)methyl]pyridin-3-ol scaffold and charged PAS ligands. (page 43)

Figure 16. Top-scoring docking poses of compounds **tacroxime 2** in the non-aged VX-inhibited-AChE active site (PDB ID: 2Y2U translated to 4EY7). The close-up is presented in three-dimensional (A) and two-dimensional (B) diagrams, respectively. Generally, for A: **tacroxime 2** is shown with carbon sticks in dark blue, important amino acid residues in green, catalytic triad residues in yellow, and the VX agent in purple. Dashed lines (in all figure parts) represent the crucial intermolecular interactions of different origin (hydrogen bonds, π - π / π -cation stacking, van der Waal interactions, and other hydrophobic forces). Figure A was created with PyMOL Molecular Graphics System, Version 2.0 Schrödinger, LLC. Figure B was rendered by using Dassault Systèmes BIOVIA, Discovery Studio Visualizer, v 17.2.0.16349, San Diego: Dassault Systèmes, 2016. (page 45)

Figure 17 The crystal structure of RS194B and VX-inhibited acetylcholinesterase. The unfavorable conformation of the molecule is clearly displayed. (page 46)

Figure 18 Design of RS194B analogs with a second oxime group. (page 46)

Figure 19 Molecular docking results of the best two candidates, **229** and **230**. Different conformations are evident in the enzyme. However, one of the oxime groups is always pointing towards the phosphorus atom and both central rings are stacked above Trp286. (page 47)

Figure 20 General structure of tacrine-phenothiazine derivatives. (page 68)

Figure 21 General structure of tacrine derivatives. (page 71)

Figure 22 General structure of mono-quaternary AChE reactivators. (page 76)

Figure 23 *In vitro* reactivation of sarin-inhibited AChE by 10 μ M of the test compound. (page 77)

Figure 24 *In vitro* reactivation of VX-inhibited AChE by 10 μ M of the test compound. (page 78)

Figure 25 *In vitro* reactivation of tabun-inhibited AChE by 10 μ M of the test compound. (page 78)

Figure 26 *In vitro* reactivation of dichlorvos-inhibited AChE by 10 μ M of the test compounds. (page 79)

Figure 27 *In vitro* reactivation of paraoxon-inhibited AChE by 10 μ M of the test compounds. (page 79)

Figure 28 *In vitro* reactivation of OP-inhibited BChE by 10 μ M of the test compounds. (page 80)

Figure 29 The reactivating potency of 10 μ M and 100 μ M tacroximes compared with the standards pralidoxime and obidoxime against OP-inhibited *h*AChE and *h*BChE. (page 82)

Figure 30 Reactivation kinetics of AChE inhibited by sarin measured at three concentrations (0.1 mM, 0.5 mM, and 1.0 mM). (page 85)

Figure 31 Reactivation kinetics of AChE inhibited by VX measured at three concentrations (0.1 mM, 0.5 mM, and 1.0 mM). (page 85)

List of tables

Table 1 The best designed candidates based on molecular docking calculations. (page 46-47)

Table 2 Tacrine-phenothiazine derivatives. (page 52)

Table 3 Prepared tacrine derivatives with dual targeting to AChE and the NMDA receptor. (page 54-55)

Table 4 Prepared mono-quaternary permanently charged AChE reactivators. (page 63)

Table 5 Inhibitory activity against *hAChE* and *hBChE* with the calculated selectivity index for *hAChE*. (page 68-70)

Table 6 Antioxidant activity, cytotoxicity of tested compounds in HepG2 cells after 24 h and the MDCK determination of potential BBB penetration ability. (page 70)

Table 7 *In vitro* anticholinesterase activity and CNS MPO calculation. (page 71-73)

Table 8 The inhibitory effects of novel compounds and standards on *hAChE*, *hBChE*, and *AgAChE1*. (page 73)

Table 9 The comparison between modified Ellman's methods and potentiometric methods. (page 74)

Table 10: Inhibition mechanisms and maximum inhibition time of novel compounds. (page 74)

Table 11 The inhibitory effect of novel compounds and standards on *hAChE*, *hBChE*, and *AgAChE1*. (page 75)

Table 12 Prepared mono-quaternary reactivators with predicted solubility, *ClogP*, *in vitro* determined AChE IC_{50} , and SH-SY5Y cytotoxicity IC_{50} values. (page 76-77)

Table 13. Pampa and MDCK determination of potential BBB penetration ability. (page 80)

Table 14. The inhibitory activities on *hAChE* and *hBChE*, the cytotoxicity in HepG2 cells, and the prediction of BBB penetration. (page 81)

Table 15 *In vitro* experimental determination of the kinetic parameter k_r . (page 83)

Table 16 *In vitro* experimental determination of the kinetic parameter k_2 . (page 83-84)

Table 17 *In vitro* experimental determination of the kinetic parameter K_{ox} . (page 84)

Table 18 Experimental determination of pK_a , $\log D_{7.4}$, and $\log P_{neutral}$. (page 86-87)

1. Introduction

1.1 Acetylcholinesterase

From an evolutionary perspective, acetylcholinesterase (AChE; E.C. 3.1.1.7.), belonging to the α/β hydrolase family, can be considered as a perfect functional tool. This family contains other cholinesterases (i.e. butyrylcholinesterase), carboxylesterases, and lipases. The biological function of AChE is to rapidly hydrolyze the neurotransmitter acetylcholine (ACh), which leads to the termination of nerve impulses. Therefore, it is an inextricable component of the cholinergic system and the neuromuscular junctions (Figure 1) [1, 2]. The physiological role of its companion, butyrylcholinesterase (BChE; E.C. 3.1.1.8.), is unclear; however, it is most probably responsible for the detoxification of xenobiotics, such as aspirin, cocaine, and other esters [3].

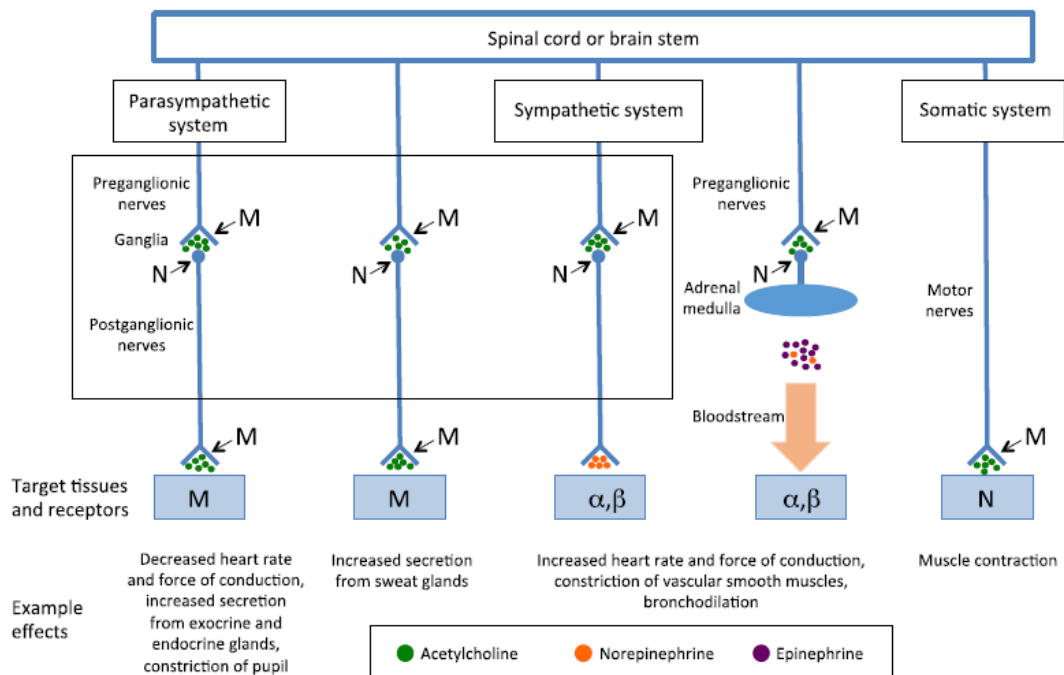


Figure 1 Schematic drawing of the function of the neurotransmitter ACh for the function in various parts of nervous system. Taken from Costanzi et al. 2018 [4].

The first insight into the structure of AChE was detailed in 1991 by J. Sussman when refining the crystal structure of *Torpedo californica* AChE (*TcAChE*). It contains 537 amino acids with an active gorge composed of two sub-sites connected with narrow gorge: the proximally lodged catalytic active site (CAS) and the distally accommodated

peripheral anionic site (PAS) [5]. The CAS is located at the bottom of deep and narrow gorge (wider at the base and approximately 20 Å deep, with a width 4.5 Å). The gorge is flanked by 14 aromatic residues capable of hydrophobic interactions (e.g. π - π , cation- π interactions) with aryl-based or positively charged substrates [2, 6, 7]. The active site consists of three major domains, including a catalytic triad (Ser200, His440, and Glu327), an esteratic site (which is 14.7 Å from Ser200), and a hydrophobic region that is contiguous with esteratic and anionic subsites [5, 7]. The catalytic triad is involved in substrate hydrolysis by the transfer of the acetyl group from ACh to Ser200 [1, 8]. The anionic site is composed of Trp84, Tyr 130, Phe330, and Phe331 residues. It is able to attract the substrate's quaternary ammonium group, and is also responsible for its correct orientation toward the catalytic triad [9]. Especially, Trp84 and Phe330 are able to form π - π , cation- π , or aliphatic- π interactions with active site ligands (Figure 2) [8–11].

The PAS region contains five residues (Tyr70, Asp72, Tyr121, Trp279, and Tyr 334) located at the rim of the cavity entrance. The key amino acid responsible for adhesion and enzyme functioning is Trp279, which can provide a variety of strong interactions (e.g. π - π stacking or cation- π interactions) [7, 12, 13]. The PAS contains a number of surface loops with high flexibility, which allow this site to fulfill its catalytic role and ensure the conformational changes necessary for enzyme activity can occur [13, 14].

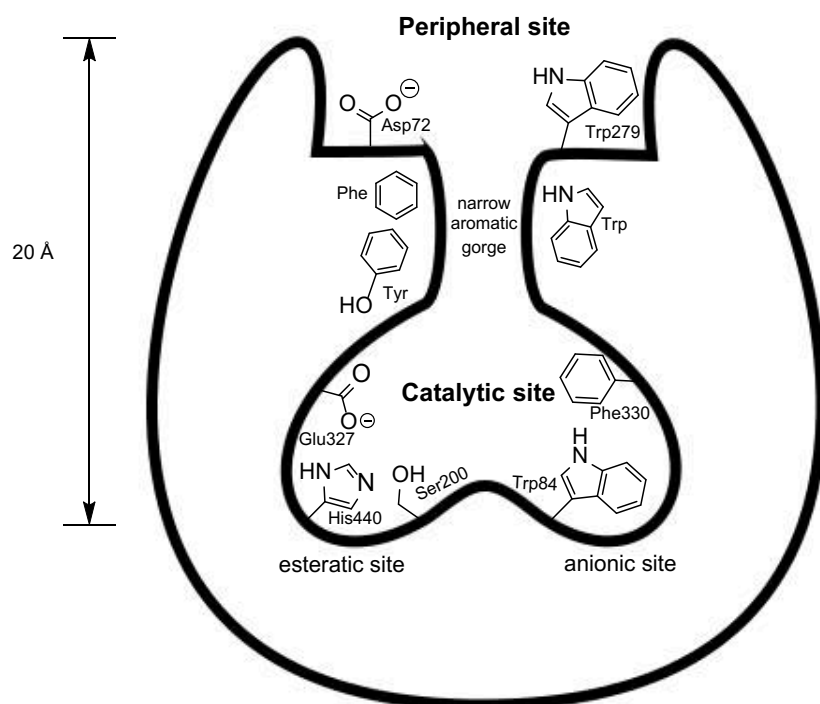
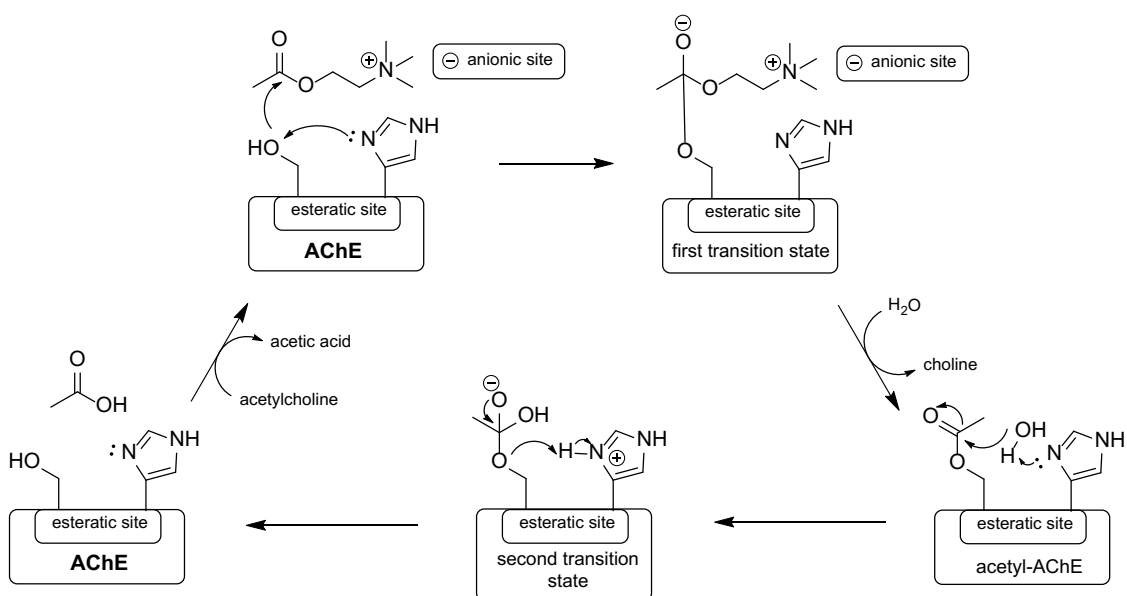


Figure 2 Schematic representation of the active and peripheral site of *TcAChE*, including the amino acids residues of the catalytic triad, anionic site, narrow aromatic gorge, and peripheral site [15].

The physiological role of AChE lies in the hydrolysis of the neurotransmitter ACh. Initially, the substrate (ACh) is bound to the PAS, which subsequently transports the substrate to the catalytic active center [14]. Hydrolysis of ACh is executed by the catalytic triad and this mechanism proceeds in two steps. First, the serine nucleophilic attack of ACh leads to a tetrahedral transition state that collapses to the acetyl-enzyme (acetyl-Ser200) and releases choline. Second, the hydrolysis through an activated water molecule occurs at the nearby histidine; this residue attacks the acetyl-serine complex and leads to the formation of the second tetrahedral transition state, which ultimately yields the free enzyme and acetic acid (Scheme 1) [1, 2, 16].



Scheme 1 Mechanism of ACh hydrolysis by AChE [15].

Modulation of the AChE activity may have some beneficial effects. Indeed, some inhibitors can be applied in the management of Alzheimer's disease (AD), myasthenia gravis, or as insecticides. Mechanistically, there are several distinct methods of AChE inhibition. Organophosphates and carbamates bind competitively and directly to the catalytic active site, whereas some other inhibitors, such as edrophonium [17], bind to the anionic site. Moreover, there are also compounds able to non-competitively bind to the PAS (e.g. gallamine [18]). Some bis-quaternary compounds, such as decamethonium (a depolarizing muscle relaxant) [19] or some potential anti-AD drugs (tacrine-related dual anionic binders) [20–24] are able to contact both anionic sites of AChE simultaneously [13, 25]. Irreversible inhibitors are highly toxic compounds; often, they are misused as warfare nerve agents or used as agricultural pesticides. In contrast, reversible inhibitors are used for the treatment of Alzheimer's disease (e.g. tacrine, donepezil); or myasthenia gravis (e.g. pyridostigmine bromide) as muscle relaxing drugs; or are present as secondary metabolites in plants or fungi (e.g. aflatoxins) [7, 19, 26–29].

The following sections are subdivided into the three different fields of interest investigated in this thesis. Initially, some aspects that contribute to the development and progression of Alzheimer's disease are outlined. Next, AChE-targeted insecticides are detailed and discussed. Finally, organophosphorus intoxication, the principal part of this work, is addressed.

1.2 Alzheimer's disease

According to the World Health Organization (WHO), 47.5 million people suffer from dementia worldwide and 7.7 million new cases are diagnosed each year. Alzheimer's disease (AD) and dementia are considered the most common causes of mortality, are predicted to comprise approximately 60%–70% of total mortality, and have huge physical, physiological, social, and economic impacts on caregivers, families, and society as a whole (Figure 3) [30]. AD is a chronic progressive illness characterized by defects in cognitive capacities that occur more severely than the normal consequences of aging. The main symptoms of AD include memory loss, difficulty in solving problems, failure to comprehend, spatial disorientation, and impaired learning ability [31]. The pathophysiology of AD comprises a plethora of intertwined mechanistic pathways, which are still not fully understood [32].

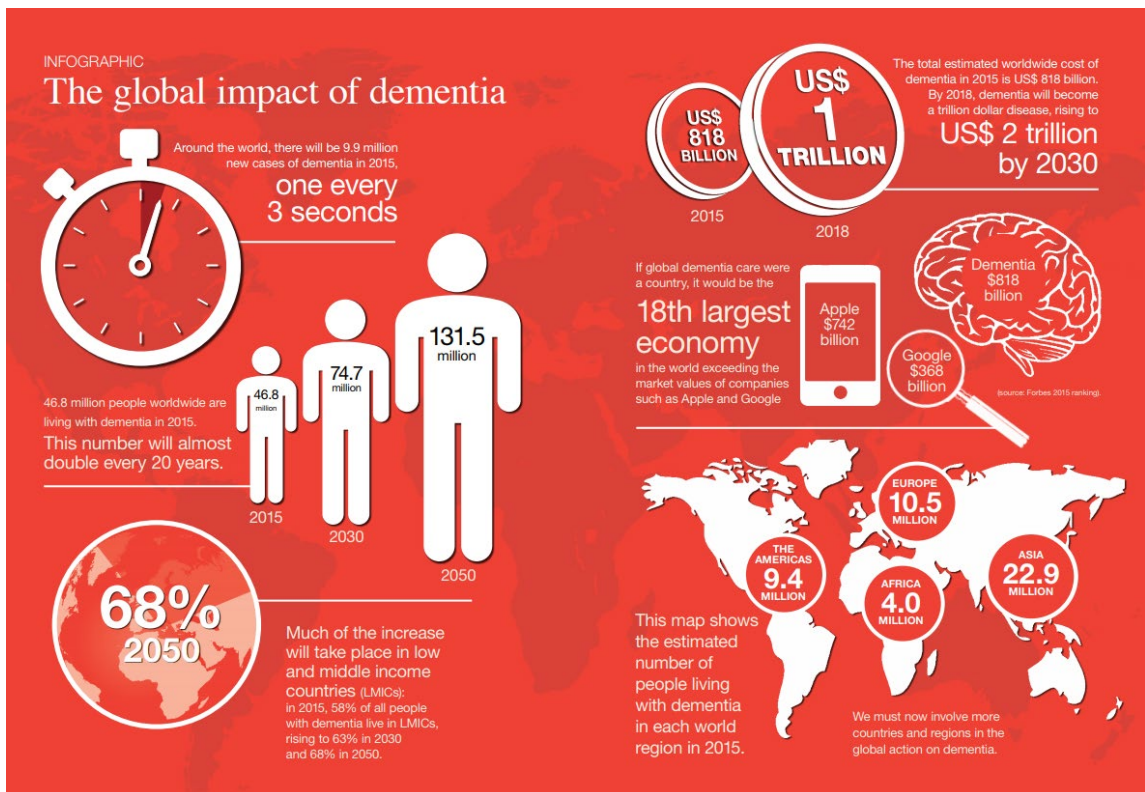


Figure 3 The global impact of dementia. Taken from World Alzheimer Report 2015 by WHO [33].

Cholinergic hypothesis

The pioneering hypothesis of AD combines the observed cognitive decline, decreased ACh levels, and the memory-enhancing role of AChE [34]. Currently, there are three FDA-approved and marketed therapeutics (donepezil, galantamine, and rivastigmine) [35]. It is important to note that another AChE inhibitor, tacrine, was the first to be approved to combat the symptoms of AD [36]. However, owing to its serious side effects, it was withdrawn from the market. In healthy people, AChE activity plays a major role in cholinergic functions, whereas BChE is considered to be of minor importance [3]. This scenario is somewhat different during AD: AChE levels remain unaltered or may even be decreased by 15%–20%, whereas BChE activity is significantly increased [37]. This provides a rational basis for the development of BChE-selective inhibitors to combat the advanced stages of AD [37].

Glutamate excitotoxicity

The *N*-methyl-D-aspartate (NMDA) receptor plays a pivotal role in the synaptic mechanisms of learning and memory, and previous work has suggested that glutamate-induced excitotoxic injury can disrupt optimal glutamate neurotransmission and glutamate receptor activation in patients with Alzheimer's disease (AD) [38]. The overactivation of NMDA receptors promotes cell death and extensively contributes to the etiology of AD. Therefore, it is obvious that drugs able to selectively block these receptors may have therapeutic benefit in AD [39].

Oxidative stress

The occurrence of reactive oxygen species (ROS) mediates cell injury in the brain of patients with AD [40]. Free radicals and ROS are highly reactive and unstable intermediates. Increased levels of ROS ultimately lead to oxidative stress. Specific regions of the brain affected by AD are more susceptible to ROS generation. It is believed that ROS production and inflammation are the very first pathological events responsible for neuronal injury during AD. Therapeutic intervention by antioxidants may therefore represent a beneficial tool to combat AD; however, none have been clinically approved yet [41].

β -Amyloid cascade hypothesis

This hypothesis is considered as one of the key pathological events of AD, and was first postulated at the beginning of the 1990s [42, 43]. Convincing evidence has demonstrated the progressive formation of amyloid-beta ($A\beta$) peptides, caused either by their increased production or decreased clearance. $A\beta$ is low molecular-weight polypeptide that is the major component of amyloid plaques [44]. Physiologically, it is produced from the $A\beta$ precursor protein (APP), which is expressed as transmembrane glycoprotein, with a large ectodomain containing the *N*-terminus and a small cytoplasmic domain containing the *C*-terminus [45, 46]. Initially, APP is processed by β -secretase (known as β -site APP-cleaving enzyme 1; memapsin 2; BACE-1). Subsequently, cleavage by γ -secretase within the transmembrane region of APP yields two C-terminal variants, $A\beta_{1-40}$ and $A\beta_{1-42}$ [47]. Of the secreted $A\beta$ peptides, $A\beta_{1-40}$ is 10 times more common than $A\beta_{1-42}$ [48]. The main difference is that $A\beta_{1-42}$ is more fibrillogenic and prone to nucleate more rapidly than $A\beta_{1-40}$ [49]. Moreover, $A\beta_{1-42}$ has been found as the dominant component of $A\beta$ plaques and plaques generated from APP mutants. In addition, depositions of this isoform are mainly observed in the brains of patients with AD [50]. Recently, a flurry of potential drug candidates have emerged based upon this hypothesis; however, remarkable promise was found only for BACE-1 inhibitors, which have reached phase III clinical trials [51].

Tau protein hypothesis

Tau protein is physiologically pervasive in neurons and plays an important role in the assembly and stabilization of the neuronal microtubule network. Increased levels of intracellularly hyperphosphorylated tau can be found in the brain of patients with AD. These levels lead to the production of aggregates, referred to as intracellular neurofibrillary tangles, which are toxic to neurons [52, 53]. Therapeutic interventions have been proposed though the modulation of the activity of glycogen synthase kinase β (GSK-3 β) or cyclin dependent kinase 5 (Cdk5), which are regulators of tau phosphorylation [54].

Biometal hypothesis

The homeostasis of biometals (e.g. Cu, Fe, Zn) is essential for normal brain function. Significantly altered concentrations of these metals have been reported during neurodegeneration [55]. Their accumulation in the neuropils of the brains of patients with AD is 3–5-fold higher than that in healthy adults. Cu and Fe are implicated in

redox reactions that, under pathological conditions, yield free radical species [56]. It is also well-described that these biometals interact with A β or APP. The interaction modulates the physicochemical properties of A β and ultimately induce the self-aggregation and oligomerization of this peptide [57]. In addition, Cu(II) or Fe(III) are reduced in the presence of A β , leading to the production of ROS, hydrogen peroxide, and hydroxyl radicals, which may contribute to neuronal damage [56]. Therefore, metal-chelating agents were developed in order to reduce the increases in biometal levels [58].

1.2.1 Treatment

At present, there is no treatment available to affect a complete cure for AD. Only palliative therapies exist; however, some symptomatic drugs have been clinically approved and improve both the quality and lifespan of patients with AD. But their therapeutic potential is insufficient, as they providing benefit only for a limited period of time (Figure 4) [35].

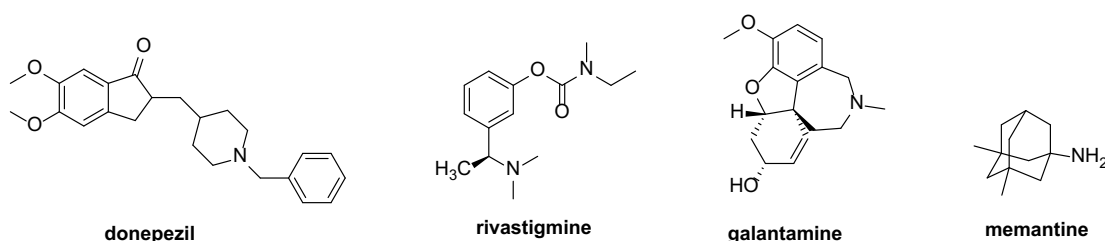


Figure 4 Currently available drugs for the treatment of AD.

Donepezil, rivastigmine, and galantamine

These drugs primarily improve cholinergic neurotransmission through the inhibition of either AChE or BChE. These leads to symptomatic relief for patients with AD [59].

Memantine

Memantine is a NMDA receptor antagonist. The involvement of these receptors in the pathology of AD is connected to excitotoxicity and the death of neurons caused by chronic neuronal activation [60, 61].

Tacrine

Tacrine was the first available therapeutic agent for AD. It was approved based on its inhibition of AChE/BChE enzymes [36]. Owing to concerns over its safety, tacrine was soon removed from clinical practice; hepatotoxicity is considered as one of its critical side effects [62]. Further research to find more potent tacrine derivatives with fewer side effects yielded 7-methoxytacrine (7-MEOTA) and 6-chlorotacrine (Figure 5) [63, 64]. These derivatives surpassed the parent drug in terms of side effects (7-MEOTA) and efficacy (6-chlorotacrine); however, none were approved for clinical use against AD. Tacrine remains extensively used as a template for the development of multifunctional molecules, possibly owing to its easy chemical synthesis [65].

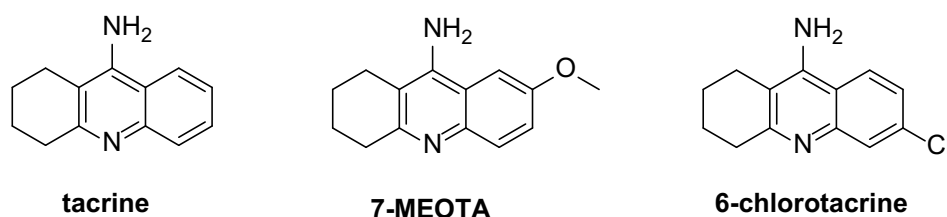


Figure 5 Tacrine and its analog, 7-MEOTA and 6-chlorotacrine

Multi-targeted directed ligand (MTDL) approach

Given the multifactorial etiology of AD, it is unlikely a single therapeutic approach will yield a cure. Therefore, researchers began to develop multifunctional compounds able to simultaneously combat multiple pathological pathways [59, 65]. There are several ways to design MTDLs, linking, fusing, or merging (Figure 6) [66].

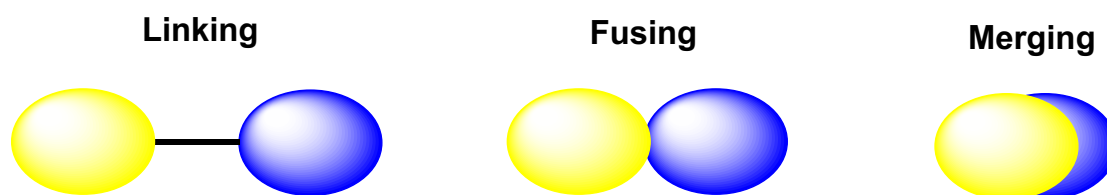


Figure 6 Plausible strategies for the development of novel MTDLs.

There are several concerns related to the development of MTDLs. The main issue when applying linking and fusing approaches arises from poor physicochemical properties that are intricately linked with their low drug-likeness [59, 65, 67]. Another critical point, especially relevant for merged or fused compounds, is to preserve the affinity or activity profiles of each ligand to different targets. The issues with balancing the physicochemical properties with high affinity/activity characteristics have resulted in none of the promising MTDL drugs reaching clinical practice. Currently, the most

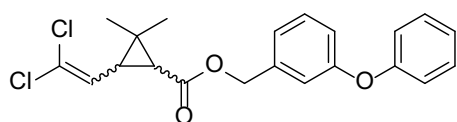
developed MTDL drug is the merged molecule ladostigil, which is in phase II clinical trials as an inhibitor of AChE/BChE and monoamine oxidase B [68].

1.3 Insecticides

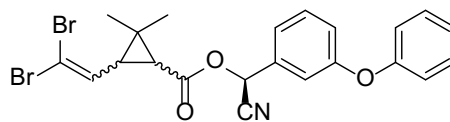
Vector-borne diseases are an enormous burden to modern society and account for more than 17% of all infectious diseases. According to the WHO, they are implicated in over 700,000 deaths annually, the most prevalent of which is malaria, estimated to be responsible for over 400,000 of those deaths. In 2017, there were approximately 219 million cases worldwide, which led to approximately 435,000 deaths. Children under 5 years of age are the most vulnerable to malaria, with a mortality rate of 61% (approximately 266,000 deaths) [69, 70]. The disease is transmitted by parasites of the genus *Plasmodium*, which are transmitted into the human body via blood feeding by adult female *Anopheline* mosquitoes (the major vector in sub-Saharan Africa is *Anopheles gambiae*). At present, the best protection lies in preventive countermeasures: insecticidal control is considered as the best tool against malaria and other vector-borne diseases [71, 72].

Chemical insecticides are the best option, given their simple practical use and cost-effectiveness [73]. They can be managed by using indoor residual spraying (IRS) or as bed nets (insecticide-treated nets; ITN). Currently, only two targets for chemical insecticides have been approved by the WHO (the voltage-gated sodium channels and acetylcholinesterase) [72, 74]. In the first family of compounds targeting the voltage-gated sodium ion channel, DDT and pyrethroids are the most cited representatives. Pyrethroids are approved for use in both ITN and IRS. The compounds targeting the AChE of mosquitos are organophosphates and methylcarbamates. These are approved only for IRS [72, 75]. Some approved insecticides are presented in Figure 7.

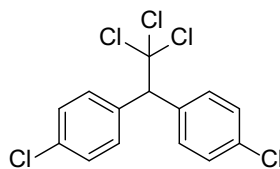
A:



permethrin

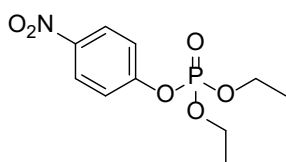


deltamethrin

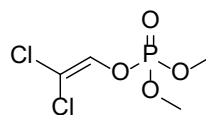


DDT

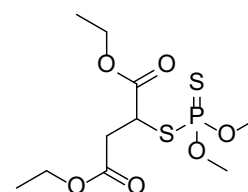
B:



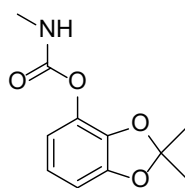
paraoxon



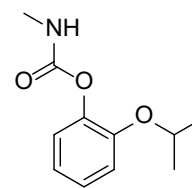
dichlorvos



malathion



bendiocarb



propoxur

Figure 7 A: Pyrethroid family compounds targeting the voltage-gated sodium ion channels, permethrin and deltamethrin; and the organochlorine insecticide DDT. B: Organophosphorus-based insecticides targeting AChE: paraoxon, dichlorvos, malathion, and the methylcarbamates, bendiocarb and propoxur.

1.3.1 Common issues with current insecticides

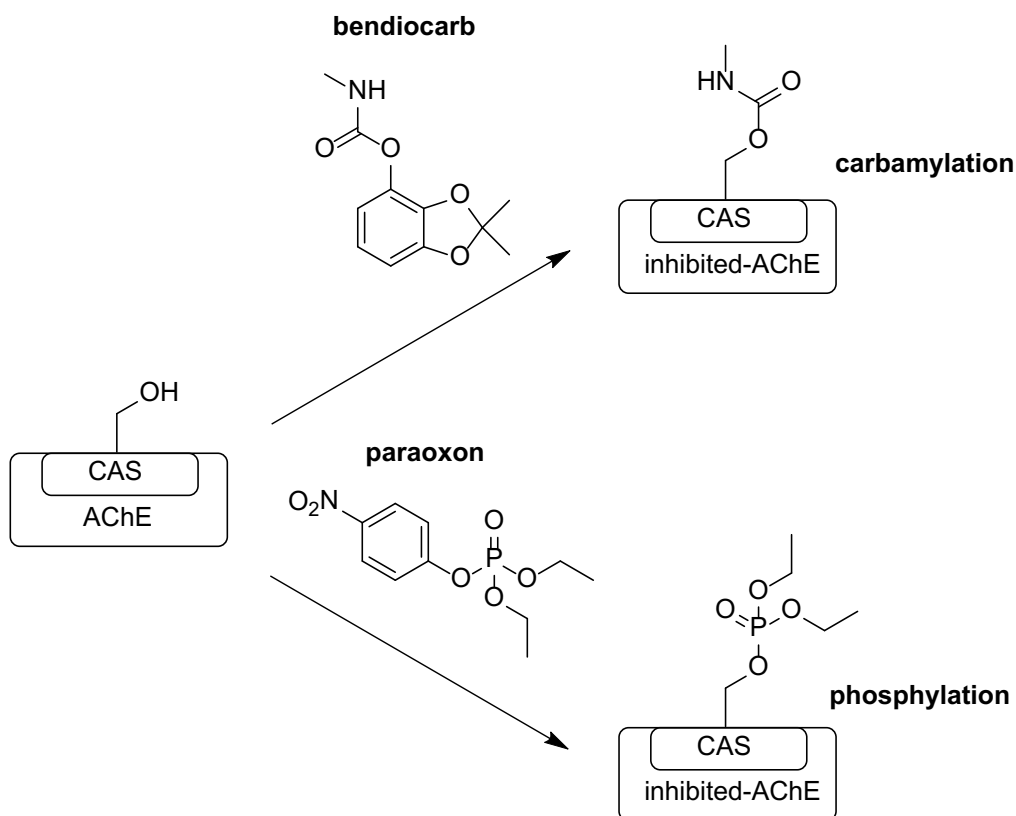
Although the beneficial effects of insecticides are clear in terms of disease control and crop protection, there is also the negative side of their excessive use over the time. Accumulation in the ecosystem results in a serious burden for the environment, with harmful effects on “non-target” species, including humans. Moreover, it fosters the development of resistance against insecticides [76, 77]. Four types of resistance have been described: i) metabolic resistance; ii) target site resistance; iii) penetration

resistance; and iv) behavioral resistance [78]. Target site and metabolic resistance have been extensively investigated [78]. Target site resistance refers to point mutations that induce the specific target of insecticides to be less sensitive to the drug [79]. Metabolic resistance refers to sequestration or detoxification of the insecticide, generally by the overproduction of specific enzymes. There are three main groups of enzymes involved: carboxylesterases; glutathione-*S*-transferases; and cytochrome P450-dependent monooxygenases. The excessive formation of these enzymes occurs mainly through two mechanisms: gene amplification and gene expression, through modifications in the promoter region or mutations in *trans*-acting regulatory genes [77, 80].

1.3.2 AChE-targeted insecticides

The enzyme AChE is the main target for organophosphorus-based and carbamate-containing insecticides. The organophosphorus insecticides are a group of organic compounds, including phosphoric, phosphonic, and phosphinic acids. Their mechanism is based on penetration through the narrow aromatic gorge of the enzyme into the CAS, where the phosphorus atom is attacked by a nucleophilic serine residue from the catalytic triad that leads to the phosphorylated adduct (a generic term that describes both phosphorylation and phosphonylation; further detail is presented in section 1.4). The first sign of intoxication by organophosphorus-based insecticides appears after 5–120 min, depending on the dose and overall toxicity, and may lead to the death of an individual after 24–48 h, dependent on the dose [73]. The major advantages are the low stability in the environment, with rapid hydrolysis occurring shortly after exposure to sunlight, air, or soil.

Carbamates are considered to have an analogical mechanism of action. Instead of phosphorylation, the enzyme is inhibited by carbamylation. From the perspective of enzyme kinetic, carbamates are classified as pseudo-reversible inhibitors, compared with the irreversible inhibition delivered by organophosphates (due to another intramolecular reaction that produces the “aged” form of the enzyme; further details are presented in section 1.4). Decarbamylation occurs within minutes; however, in some cases the time may be prolonged to a few hours. The major limitation of the use of carbamates is their high persistence in the environment. As decarbamylation occurs much more rapidly, carbamates are considered to be less toxic and dangerous to humans than organophosphates [73, 81, 82].



Scheme 2 Representative differences in the inhibition mechanism of AChE (shown with the hydroxyl group from the serine residue) by bendiocarb (carbamylation) or paraoxon (phosphylation).

The major drawback of currently used insecticides is their poor selectivity. The catalytic AChE serine residue is the key amino acid for the hydrolytic function of the enzyme and is ubiquitous in insect and non-insect species. From a structural perspective, there is only a negligible structural difference in the residues within the CAS region [83]. The general toxicity in human species is also very well characterized [73, 81]. Accordingly, there is an urgent need for a novel group of AChE-targeted insecticides that would target insects solely or at least with high specificity. Most importantly, these novel selective insecticides would form a major contribution to the reduction of the number of cases of malaria or other vector-borne diseases.

1.4 Organophosphorus intoxication

There are two main groups in the organophosphorus compounds (OPC) family. The first, organophosphorus (OP) insecticides, was introduced in the previous section (Figure 6B; section 1.3); these compounds still pose serious health and environmental

dangers [84]. OP insecticides are implicated in approximately 3,000,000 annual cases of acute intoxication; more than 200,000 of these cases are fatal. It is also estimated that pesticides are implicated in more than one third of all suicide cases worldwide [84, 85]. The second group, nerve agents (NAs), also poses a serious threat to modern society. NAs are classified as the most toxic of the chemical warfare agents (CWA) and are also weapons of mass destruction (WMD) that are easily accessible by routine chemical synthesis methods [86, 87]. NAs can be further subdivided into two families of so-called G-agents and V-agents (Figure 8). The first comprises more volatile substances, mostly liquids and gases, with low persistency in open terrain. The second comprises relatively non-volatile agents, with higher persistence and greater toxicity [88].

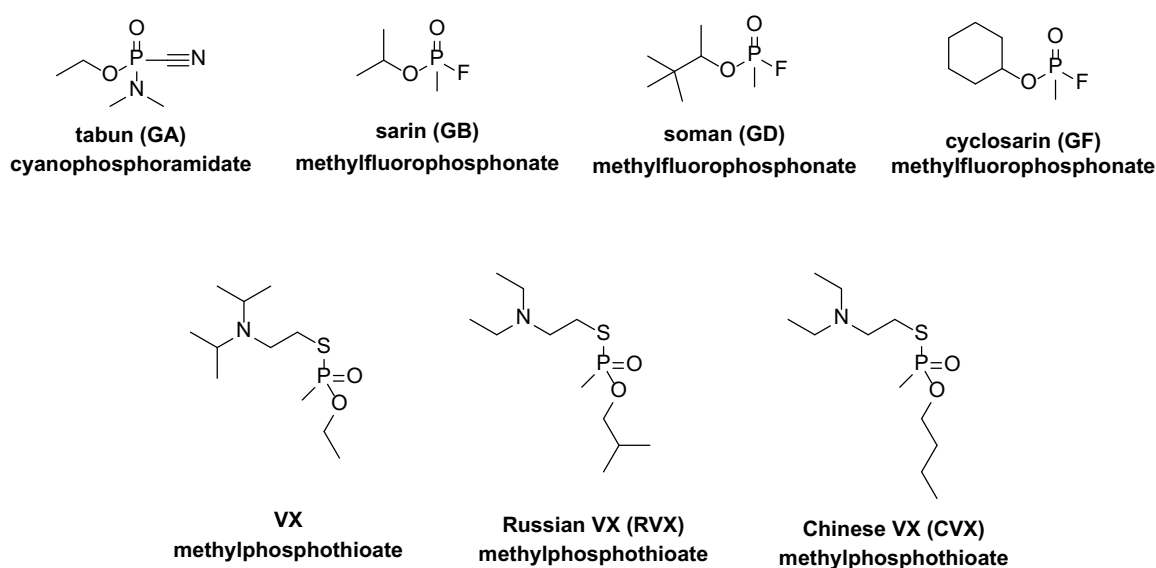
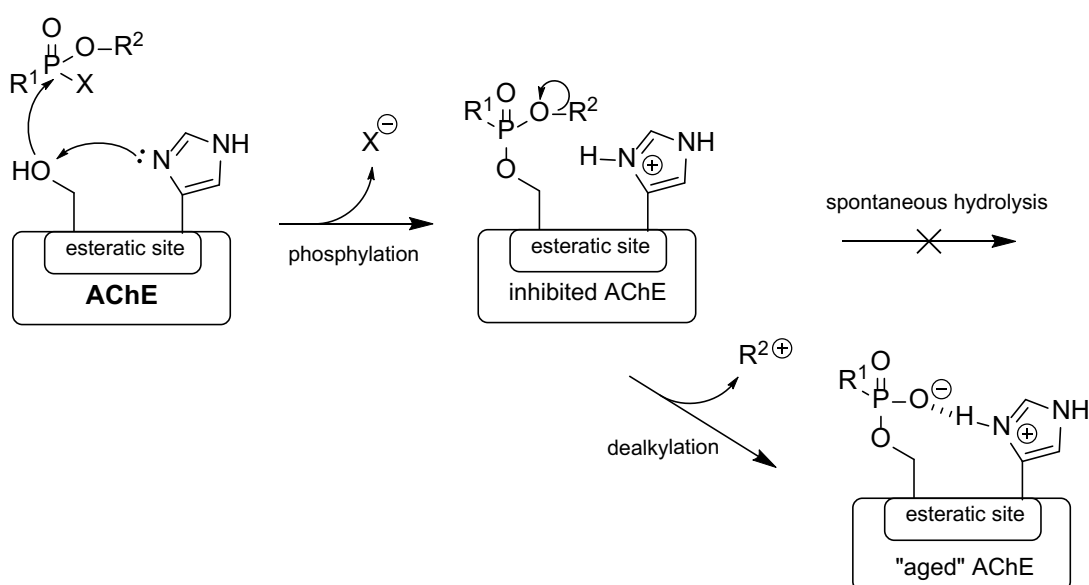


Figure 8 Representative NAs from the G-family (tabun, sarin, soman, and cyclosarin) and the V family (VX, Russian VX, and Chinese VX).

At present, the Chemical Weapons Convention (CWC) has been signed by 192 nations. The declaration should ensure protection against all the listed NAs and their intermediates used for their preparation. However, the rise in terrorist attacks, where NAs have been misused, is still alarming (e.g., in Japan 1995 and 1996, and in Syria in 2013 and 2017) [89, 90]. More recently, the assassination of some political figures (e.g., in Kuala Lumpur or in Salisbury) [91, 92] has illustrated that the power of these weapons should be considered. Each case of the misuse of NAs is accompanied by the delivery of low-levels of protection to individuals over a long period of time [4, 93]. As previously mentioned the toxic effect of OPC is based on the irreversible inhibition of AChE and requires urgent medical attention. AChE inhibition yields the excessive

accumulation of ACh in synapses and the subsequent overstimulation of cholinergic receptors [94]. This leads to severe toxic consequences mainly associated with a cholinergic crisis. The symptoms vary, depending on whether the muscarinic or nicotinic cholinergic pathomechanism prevails (see Figure 1). Vomiting, miosis, wheezing, increased nasal and submucosal secretion, and decreased blood pressure are connected to nicotinic signaling in the parasympathetic ganglia and muscarinic signaling at the synapse of the postganglionic parasympathetic nerves. Fasciculation and paralysis are associated with the alteration of the nicotinic receptors at the neuromuscular junction [4]. Overall, overstimulation leads to desensitization, and the death generally results from respiratory arrest or seizures [95].

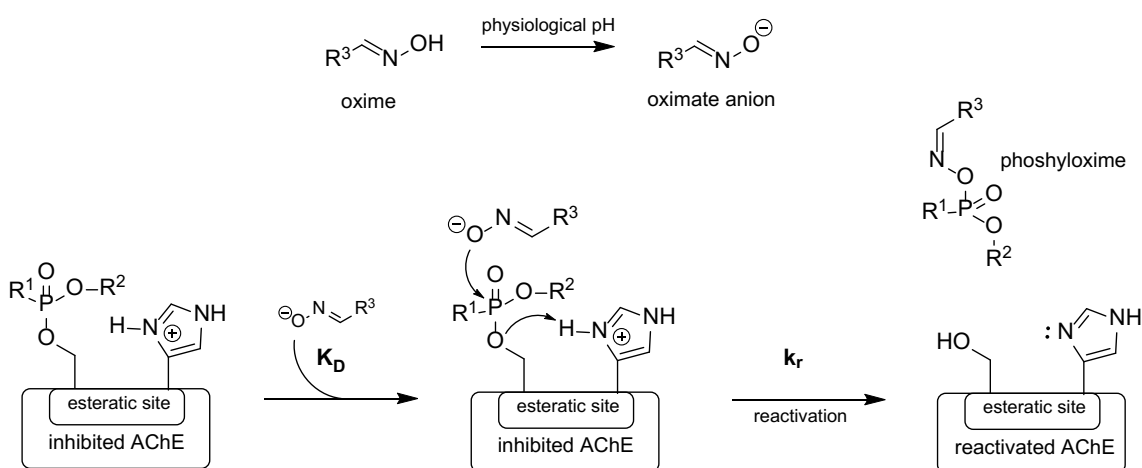
From a mechanistic perspective, the initial attack of the phosphorus atom by nucleophilic serine yields a bipyramidal transition state, followed by the release of a leaving group (dependent on the substrate, i.e. OPC). In the next step, water activation orchestrated by a histidine residue cannot be accomplished, and spontaneous hydrolysis is extremely slow, taking hours or days [15, 16]. The situation is even more serious when it comes to the intramolecular reaction that yields the dealkylated adduct called “aged-AChE”. This is considered as the ultimate stage, because the enzyme action cannot be recovered owing to the strong stabilization between the dealkylated conjugate and catalytic histidine (Scheme 3) [96]. However, some approaches to restore the activity of aged-AChE activity have recently been described [97].



Scheme 3 Inhibition of AChE by OPC and the “ageing” process. Taken from ref. [98].

1.4.1 Treatment options

The only way to revert the aging process is the introduction of a strong nucleophile that is able to attack the phosphorus atom [99, 100]. Such an attack is termed reactivation, meaning that AChE action is replenished. Upon administration in humans, only oxime-based reactivators have proved effective for the restoration of AChE. For oxime action, their activation to oximate is necessary. Their formation is indicated by the dissociation constant (pK_a), which is considered one of the most crucial factors that strongly correlates with the reactivation capability. The reactivation process yields the free enzyme and phosphoxime. Subsequently, phosphoxime is a very potent inhibitor that can mediate rebound phenomena through the alkylation of AChE *per se* (Scheme 4) [101].



Scheme 4 Reactivation of OP-inhibited AChE by oximate anion, yielding reactivated free enzyme and phosphoxime (K_D , dissociation constant of the reactivator/phosphyl-AChE complex; k_r , reactivation rate constant). Taken from ref. [15].

All the approved oxime reactivators are structurally based on permanently charged pyridinium salts (Figure 8). The first-in-class, pralidoxime, was introduced in 1955 in the USA and laid the foundations for the development of other compounds. Pralidoxime (pyridinium-2-aldoxime methyl chloride) contains only one charged pyridinium moiety [99]. Other compounds such as obidoxime, methoxime, asoxime, and trimedoxime, are bis-quaternary or bis-pyridinium aldoximes (Figure 8A) [102–105]. Although they are the only causal antidotes available, their efficiency is somewhat poor [106, 107]. Their potency is limited by several critical drawbacks. First, no compound is a broad-spectrum reactivator, as a result of the diverse chemical topology of OP-AChE

conjugates created by various OPCs. That is, none of the oximes are able to sufficiently reactivate all OP-AChE complexes [108]. Second, no marketed reactivators can restore the “aged” form of the enzyme [16]. Finally, the largest concern is their very poor ability to cross blood-brain barrier (BBB) and, therefore, to reactivate AChE in the central nervous system (CNS). This inability is mainly attributed to their permanent charge [108–110].

In addition to causal antidotes, symptomatic treatments are also important. The symptomatic antidotes are diazepam, an anticonvulsive drug, and atropine, an anticholinergic drug (Figure 9) [107].

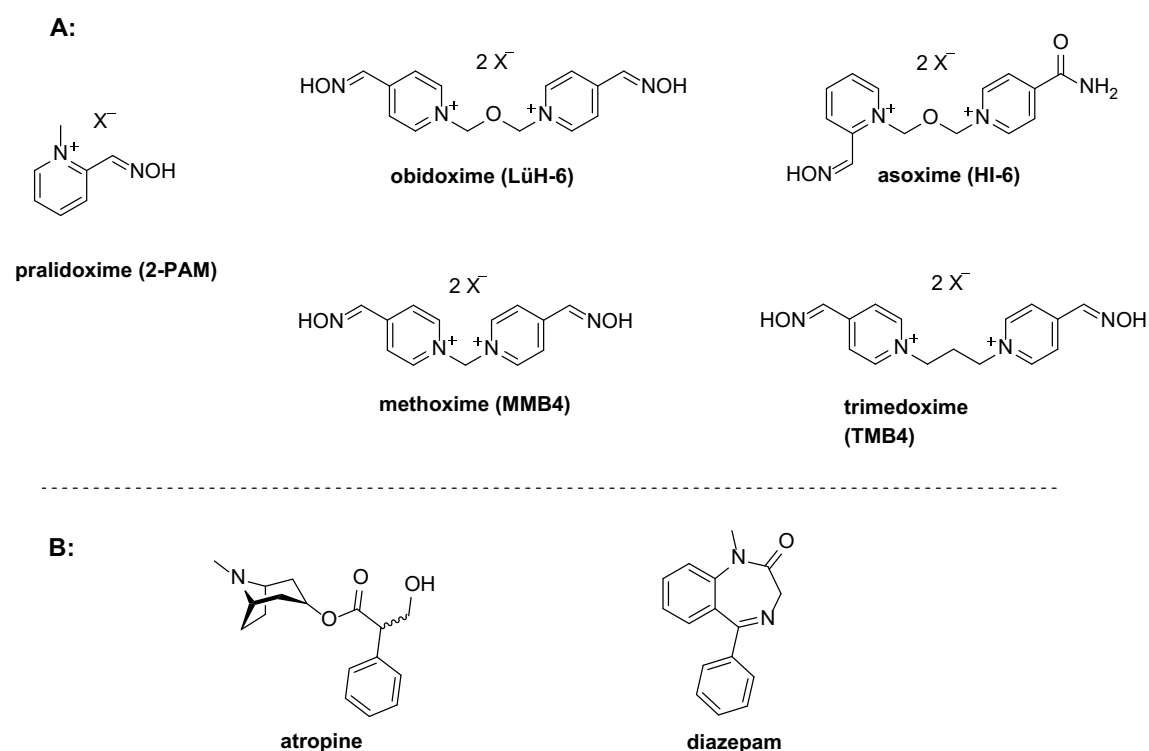


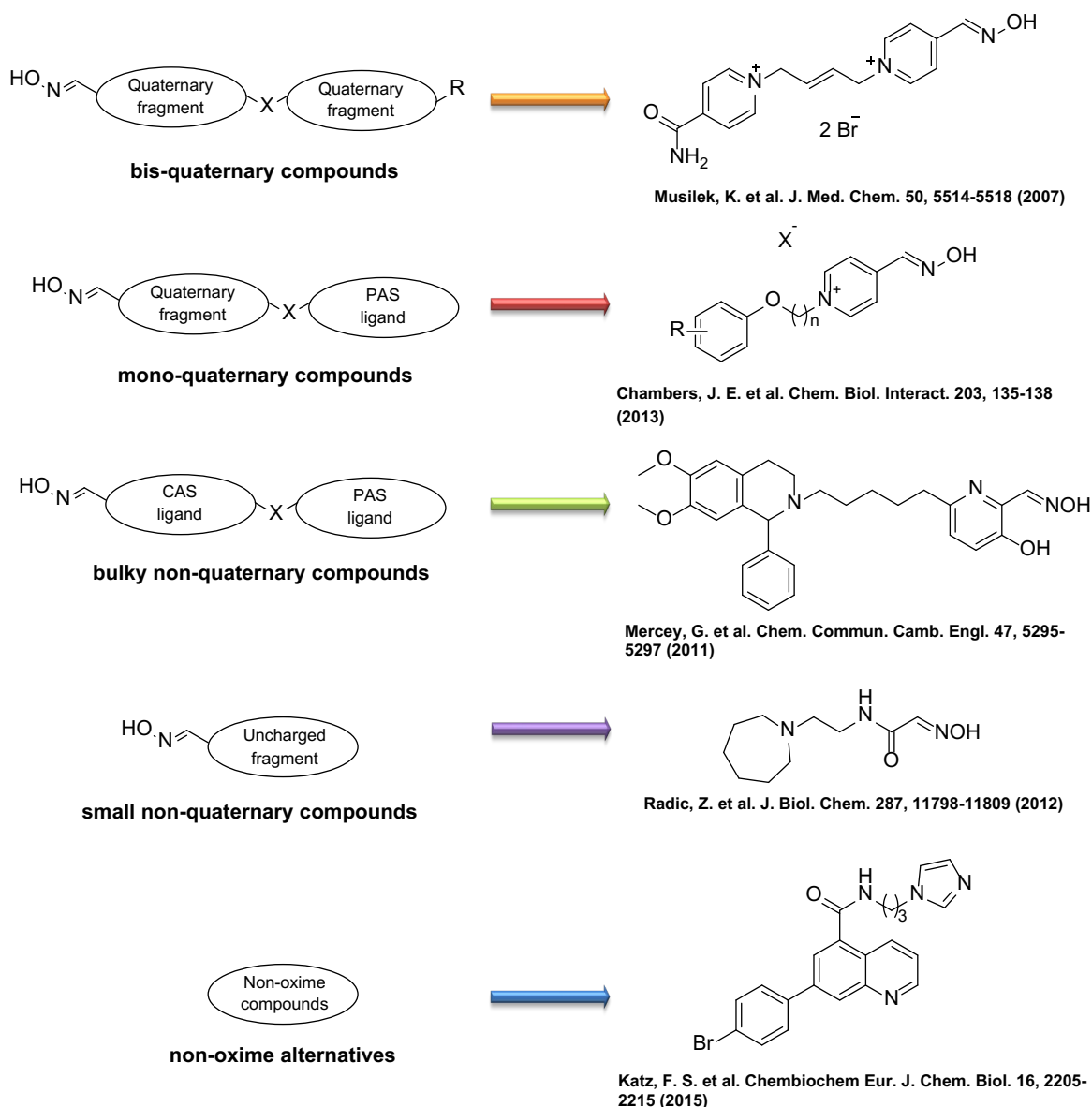
Figure 9 A: Clinically approved causal antidotes against organophosphorus intoxication: pralidoxime, obidoxime, asoxime, methoxime, and trimedoxime (X^- represents chloride, bromide, iodide, or methansulfonate anion); B: Examples of symptomatic antidotes: the anticonvulsive diazepam and the anticholinergic atropine.

1.4.2 Novel approaches to the treatment of OP intoxication

Since the introduction of asoxime in 1969, there have been thousands of new oxime reactivators developed, but none has entered clinical practice. In addition, thousands of

non-, mono- or bis-quaternary compounds have been introduced, but none has significantly surpassed the efficiency of the parent compounds. Examples of some recently discovered oxime reactivators are presented in Scheme 5. A detailed summary of recently published compounds is comprehensively described in the 2016 review article by Gorecki et al. [15] (see Attachment I). In another review in 2017, Gorecki et al. [111] summarized all patent applications connected with AChE reactivators during the years 2006–2016 (see Attachment II). In addition, in 2018, Gorecki et al. reviewed the development of K203 and outlined all the studies that have examined the properties of this potent reactivator [98] (see Attachment III).

Modern trends in the development of novel AChE reactivators are mostly based on the so-called dual site binding strategy. This approach also stimulated the development of AD drugs [112]. The concept builds upon the amalgamation of two ligands/scaffolds/pharmacophores into one lead molecule that is able to target both CAS and PAS simultaneously. Although this approach displayed minor success *in vitro*, the novel drug candidates mostly suffer from poor drug-likeness, causing failures in *in vivo* conditions [15, 108, 113].



Scheme 5 Examples illustrating progress in the design of AChE oxime reactivators over the last two decades. From top to bottom: bis-quaternary compound K203 [114]; mono-quaternary compounds from the group of Prof. J. E. Chambers [115]; bulky non-quaternary compounds from the group of Prof. Pierre-Yves Renard [116]; small uncharged compound from the UCSD group of Prof. Radić [117]; and potent non-oxime alternatives [118].

2. Objectives

The goal of this thesis was the synthesis of novel modulators of AChE that have different functions.

Initially, a family containing dozens of AChE inhibitors as multi-target directed ligands (MTDLs) is outlined. Another tacrine-related series was proposed to inspect their combined AChE and NMDA activities.

Two subsets of compounds with anti-insecticidal activity were introduced. Both series are based on a recently postulated AChE Cys-targeting approach.

Finally, three series of AChE reactivators were developed as causal antidotes of OP intoxication. The first series described contains mono-quaternary compounds with outstanding reactivation potency. Two other series, presenting completely novel approaches towards uncharged reactivators, are also depicted.

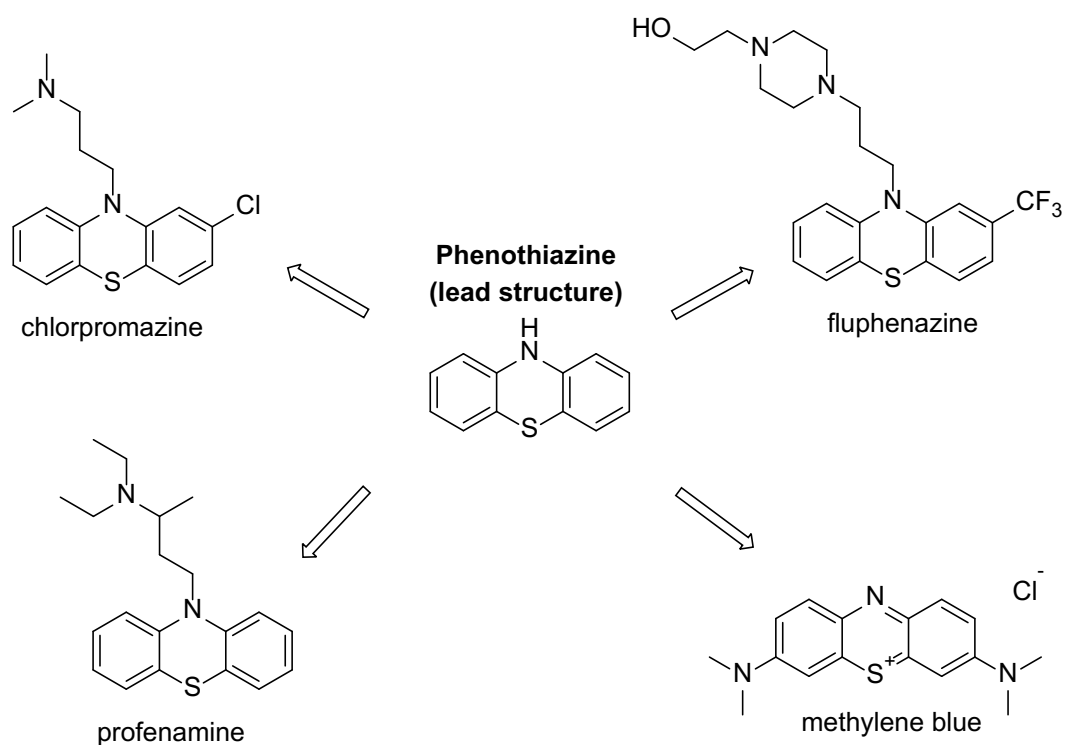
My main focus of this thesis was the design, synthesis, and determination of the physicochemical properties of the compounds in these series. I declare that all synthetic procedures were performed by me. In order to provide full insight into different research fields, I have also incorporated and briefly discussed biological data. In addition, the series of bis-oxime reactivators (sections 3.1.7, 3.2.7, and 3.3.7) discovered at UCSD were biologically evaluated by me. With regard to these compounds, I declare that I am responsible for the compound design, selections made by using virtual reality, synthesis, experimental determination of the physicochemical properties, and *in vitro* assays, including the calculation of kinetic parameters.

3. Results

3.1 Design

3.1.1 Tacrine-phenothiazine derivatives

This work is derived from a collaboration with Prof. Maria Laura Bolognesi, from the Department of Pharmacy and Biotechnology, Alma Mater Studiorum Università di Bologna. The design and synthesis were performed during three month internship at her laboratory. We designed novel multi-target directing ligands (MTDL) combining tacrine scaffolds linked to phenothiazine, a lead structure for neurological disorders [36, 119]. Tacrine is introduced in section 1.2.1. Phenothiazine is much older compound and has been applied effectively in various fields (Scheme 6): for example, as an anthelmintic (mid-20th century); as an antihistaminic agent; for anesthesia (promethazine); or as anti-schizophrenic drug (chlorpromazine) [120, 121]. It should be noted that chlorpromazine, fluphenazine, and haloperidol are mentioned in the List of Essential Medicines 2017 (WHO) for the treatment of psychotic disorders [119, 122]. Phenothiazines are also well-known for their antioxidative activity, which may offer beneficial activity with regard to the oxidative stress hypothesis of AD (see section 1.2) [123]. Finally, methylene blue, another well-known derivative of phenothiazine, was found to be effective against tau aggregation (tau-related neurotoxicity; see section 1.2) and is in phase II clinical trials for the treatment of AD [124, 125].



Scheme 6 The lead structure phenothiazine and its clinically used derivatives of chlorpromazine, fluphenazine, and profenamine; together with methylene blue, a promising anti-AD drug candidate.

We decided to connect these two efficient scaffolds with a simple methylene chain linker to obtain MTDL compounds. We believed this would provide efficient inhibitors of AChE based on a dual site binding strategy (one ligand binding in PAS and one in CAS). This would confer antioxidative activity to the compound, with anti-tau properties arising from the phenothiazine structure. 6-Chlorotacrine and 7-MEOTA were selected as tacrine derivatives, in addition the parent molecule, tacrine. 2-chlorophenothiazine and 2-trifluoromethylphenothiazine were chosen as phenothiazine derivatives, together with phenothiazine alone. Finally, the linker length was set between two and five methylene, as this seems to be the best for AChE dual site binding (Figure 10) [15, 21, 22, 126]. The compounds were inspected mainly for their inhibitory activity on the enzymes AChE/BChE, for the neuroprotective potency, and for their anti-tau aggregation properties.

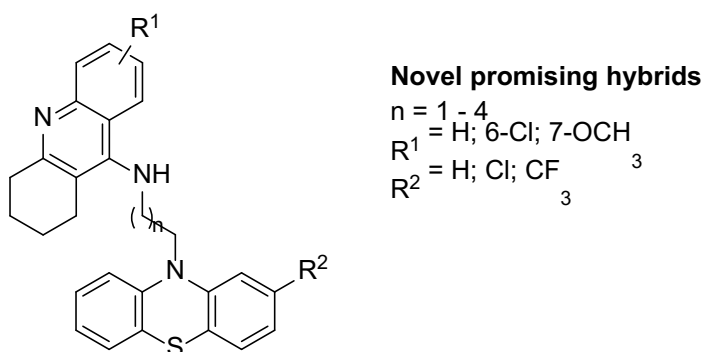


Figure 10 Designed compounds based on tacrine and phenothiazine scaffolds.

3.1.2 Tacrine derivatives with dual-targeting of AChE and the NMDA receptors

NMDA receptor antagonists are one of the therapeutic approaches towards the treatment of AD. Memantine, a clinically approved drug, was shown to have a clear proof of concept (see section 1.2). Moreover, it is believed that the efficiency of tacrine on the symptoms of AD is not only based on AChE inhibition, but may be more connected with the modulatory activity on glutamatergic neurons (direct and indirect). Indirect modulation is mediated by influencing receptors *via* the M1 receptor (mAChR subtype) activation through the inhibition of SK channels [127, 128]. This leads to the inhibition of Ca^{2+} -activated potassium channels, which re/hyperpolarize postsynaptic spines and inhibit NMDA receptor opening [127, 129]. Direct inhibition is achieved only by high (physiologically unattainable) concentrations. In contrast, it is possible that some tacrine metabolites may have increased NMDA antagonist efficiency [129].

Therefore, we decided to prepare small library of tacrine derivatives (Figure 11) and investigate them for their potential NMDA receptor antagonism.

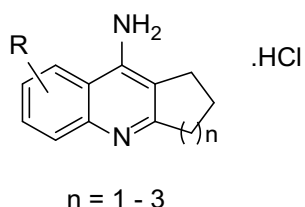


Figure 11 Substituted tacrine derivatives and their analogs with five- to seven-membered saturated rings.

3.1.3 AChE-targeting insecticides

The standard organophosphate and carbamate insecticides covalently bind Ser360 (*Anopheles gambiae* acetylcholinesterase, AgAChE) and thus prevent hydrolysis of ACh. A novel approach for the selective inhibition of AgAChE is to target the Cys447 residue in the PAS of some insect species. This Cys-targeted strategy have been proposed to overcome insecticide resistance [130]. The benefit of this approach arises from the absence of the Cys residue is in the mammalian enzymes. Moreover, the inaccessibility of the Cys residue in beneficial insects may protect them against such insecticides. Therefore, it is believed that Cys-targeted insecticides may confer significant selectivity for insect AChE over mammalian AChE [73, 131].

We decided to inspect this hypothesis though the preparation of some of the previously reported compounds. These molecules were first introduced by computational studies in 2012; but some have been prepared more recently [130, 132]. Five of the reported compounds have been enriched, and three novel compounds were enriched for a full inspection of potency. In addition, we have described a different and more straightforward synthetic strategy for compound preparation. All were then subjected to *in vitro* testing to determine their efficiency in the inhibition of the action of recombinant AgAChE1, human AChE (*hAChE*), and human butyrylcholinesterase (*hBChE*). The molecules are composed of maleimide or succinimide moieties and a pyridinium or piperidine scaffold. Both ligands were connected with long 18- or 20-methylene linkers to facilitate the binding affinity (Figure 12). It is believed that maleimide is able to covalently bind to cysteine, whereas succinimide cannot. Piperidine and pyridinium structures are both able to bind to the catalytic active site; therefore, they represent very simple CAS ligands. Molecular docking simulations were performed to improve the binding potential (Figure 13).

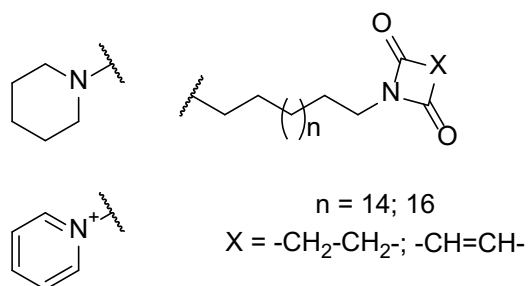


Figure 12 The first series of Cys-targeted insecticides developed from already published models described by Pang et al. [130] in 2012 and Dou et al. [132] in 2013.

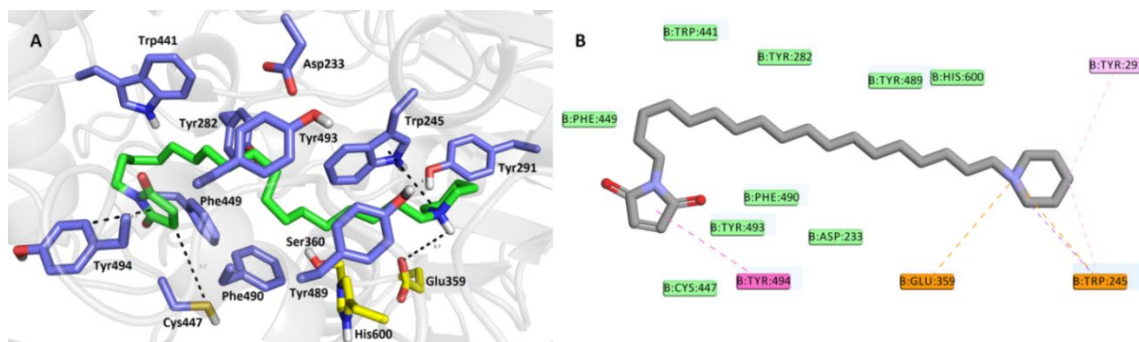


Figure 13 *In silico* representation of **134** in the *AgAChE1* active site (PDB ID: 5YDH). The close-up view of the ligand is presented as a three-dimensional (A, left) and two-dimensional (B, right) representations. Generally, A, **134**, is presented in green, important amino acid residues are presented in blue, and the catalytic triad is presented in yellow.

3.1.4 Second subset of insecticides

Based on the results from the first series, we wanted to continue with the development of Cys-targeted insecticides. The maleimide moiety was confirmed by the *in vitro* results. We decided to change the CAS ligands for the well-known ligand tacrine, 4-aminoquinoline, and 4-aminopyridine, and examined the impact on the inhibitory activity and the selectivity ratio (Figure 14).

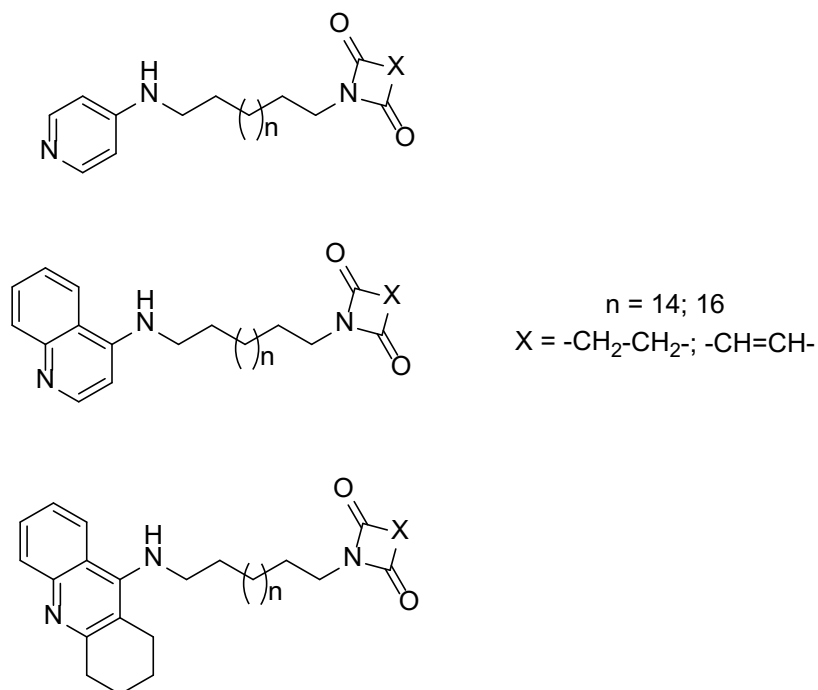


Figure 14 Our second series of Cys-targeted insecticides, which were derived from the first series.

3.1.5 Mono-quaternary permanently charged AChE reactivators

After a comprehensive literature survey of the structure-activity relationships (SARs) of the modern approaches and novel AChE reactivators, we developed a new series of mono-quaternary compounds. We selected the best approaches and molecules reported in recent literature and combined the strategies. We decided to prepare molecules based on a dual-site binding strategy. Five methylenes were chosen with the most optimal length [126]. A 2-[(1*E*)-(hydroxyimino)methyl]pyridine-3-ol scaffold was selected as the CAS ligand [116, 133]. The novelty lay in the presence of the positive charge in the PAS whereas the CAS remained uncharged. Such a strategy has not been published before. For this reason, we decided to implement new peripheral site ligands not related to AChE inhibitors such as tacrine and its derivatives. Again, this approach may be beneficial in terms of decreasing the affinity towards the enzyme. Strong inhibition is presumed to result in a strong penalty during the desolvation of the ligand and may therefore hamper the entire reactivation process [134]; consequently, the reactivator-NA complex will hardly leave the enzymatic gorge. For these reasons, novel pyridinium, quinolinium and isoquinolinium salts were designed and evaluated (Figure 15). The major advantage of this CAS ligand is the improvement in the pK_a value of the oxime group, which enhances reactivation, and the ability to stabilize phosphyloxime after reactivation [116, 133].

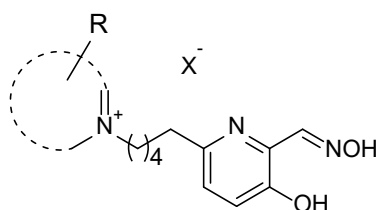
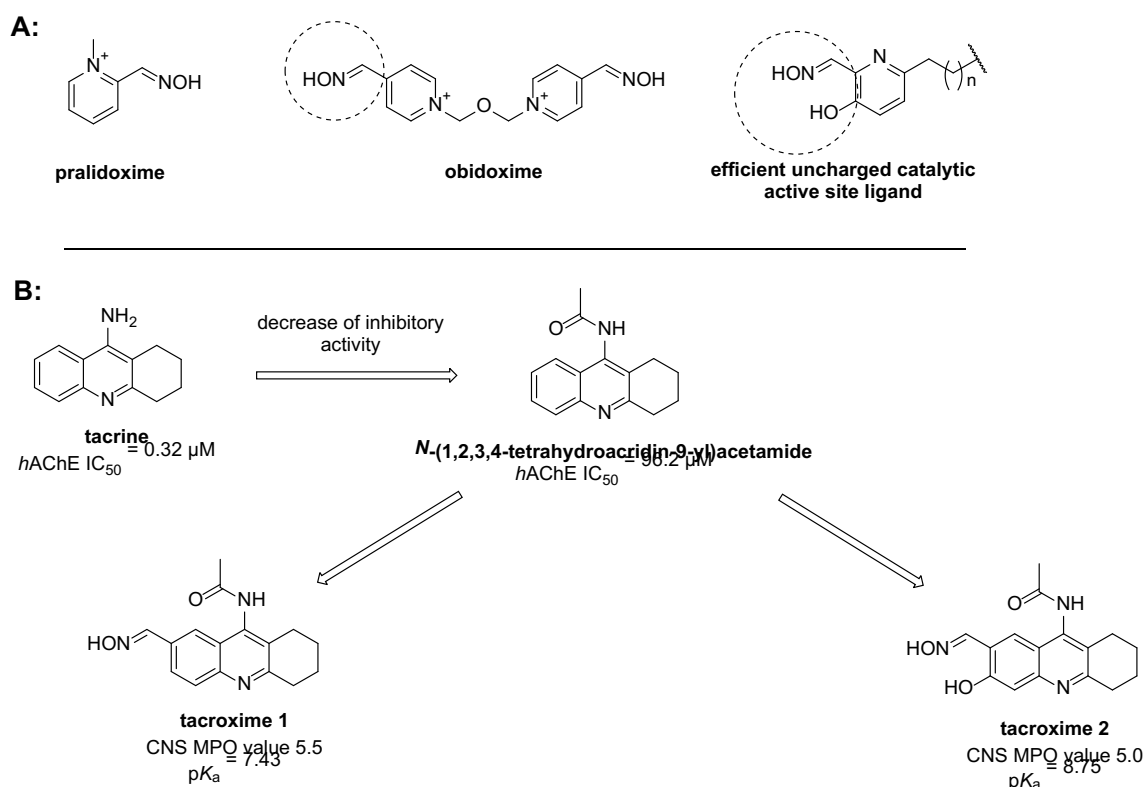


Figure 15 Design of mono-quaternary compounds based on 2-[(1*E*)-(hydroxyimino)methyl]pyridin-3-ol scaffold [133] and charged PAS ligands.

3.1.6 Tacroximes

In this small series of compounds, we proposed a completely novel approach. We repurpose small AChE inhibitors that are used in the treatment of AD. However, the compounds needed to be hampered to decrease inhibitory activity, so that affinity would be maintained but the compounds would not possess strong inhibitory activity. Again, we started from tacrine, which appears to be the best candidate. To decrease its potency, we selected an acetylated derivative. The acetylated derivative will have a lower degree

of protonation at physiological pH and the affinity for the enzyme will be slightly decreased. We amalgamated the aldoxime group to this *N*-acetyltacrine to confer reactivation ability to the compound. As well as a single aldoxime group, we also decided to put a hydroxyl group in the *ortho*-position to achieve same benefits as discussed in Scheme 7 [116, 133]. Molecular docking (MD) and physicochemical properties were calculated to predict their real potential. Indeed, MD simulation suggested a favored orientation in the enzyme (Figure 16). The calculations of the physicochemical properties were examined in the central nervous system multi-parameter optimization (CNS MPO) model [67] suggested the ability of the compounds to cross the BBB. Finally, the pK_a value of **tacroxime 1** was in the desired range (7.0–8.35) for efficient reactivation [135].



Scheme 7 A: Clinically used reactivators pralidoxime and obidoxime and the efficient CAS ligand, as previously described [15,16]. B: The optimization of the tacrine structure was conducted to obtain a potent reactivator.

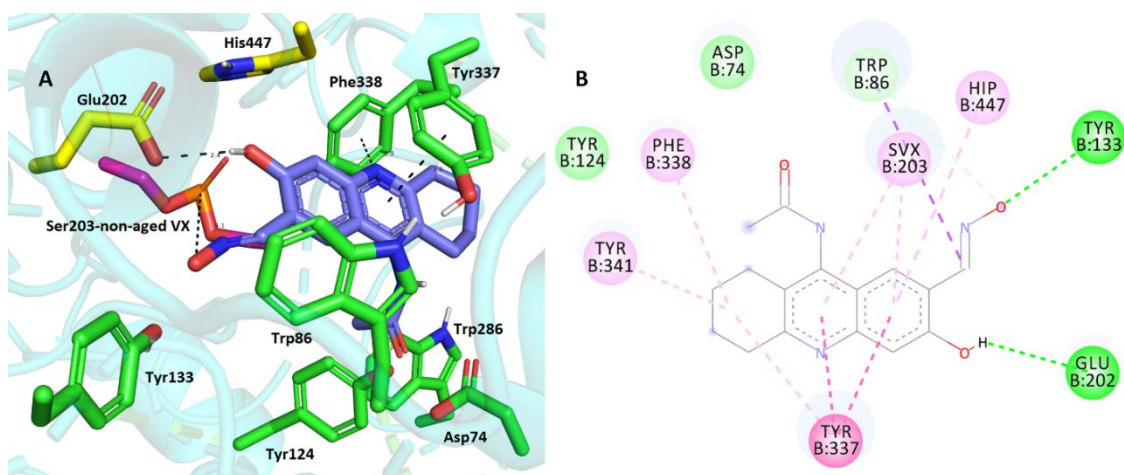


Figure 16. Top-scoring docking poses of compounds **tacroxime 2** in the non-aged VX-inhibited-AChE active site (PDB ID: 2Y2U translated to 4EY7). The close-up is presented in three-dimensional (A) and two-dimensional (B) diagrams, respectively. Generally, for A: **tacroxime 2** is shown with carbon sticks in dark blue, important amino acid residues in green, catalytic triad residues in yellow, and the VX agent in purple. Dashed lines (in all figure parts) represent the crucial intermolecular interactions of different origin (hydrogen bonds, π - π / π -cation stacking, van der Waal interactions, and other hydrophobic forces). Figure A was created with PyMOL Molecular Graphics System, Version 2.0 Schrödinger, LLC. Figure B was rendered by using Dassault Systèmes BIOVIA, Discovery Studio Visualizer, v 17.2.0.16349, San Diego: Dassault Systèmes, 2016.

3.1.7 Uncharged bis-oxime reactivators

The final series present in this thesis arose from an internship at University of California San Diego (UCSD) at the Skaggs School of Pharmacy and Pharmaceutical Sciences (SSPPS) under supervision of Assoc. Prof. Zoran Radić, Assoc. Prof. Carlo Ballatore, and Prof. Palmer Taylor. The idea for the series came from the compound RS194B, the most potent uncharged drug-like candidate for the treatment of organophosphorus intoxication [117, 136, 137]. RS194B was originally invented by UCSD in collaboration with the Scripps Research Institute. Although this compound is very efficient, the crystal structure suggests an unfavorable conformation in the gorge of AChE. In Figure 17, it can be seen that the oxime group is pointing outwards from the phosphorus atom (in orange) and is stacked in the PAS.

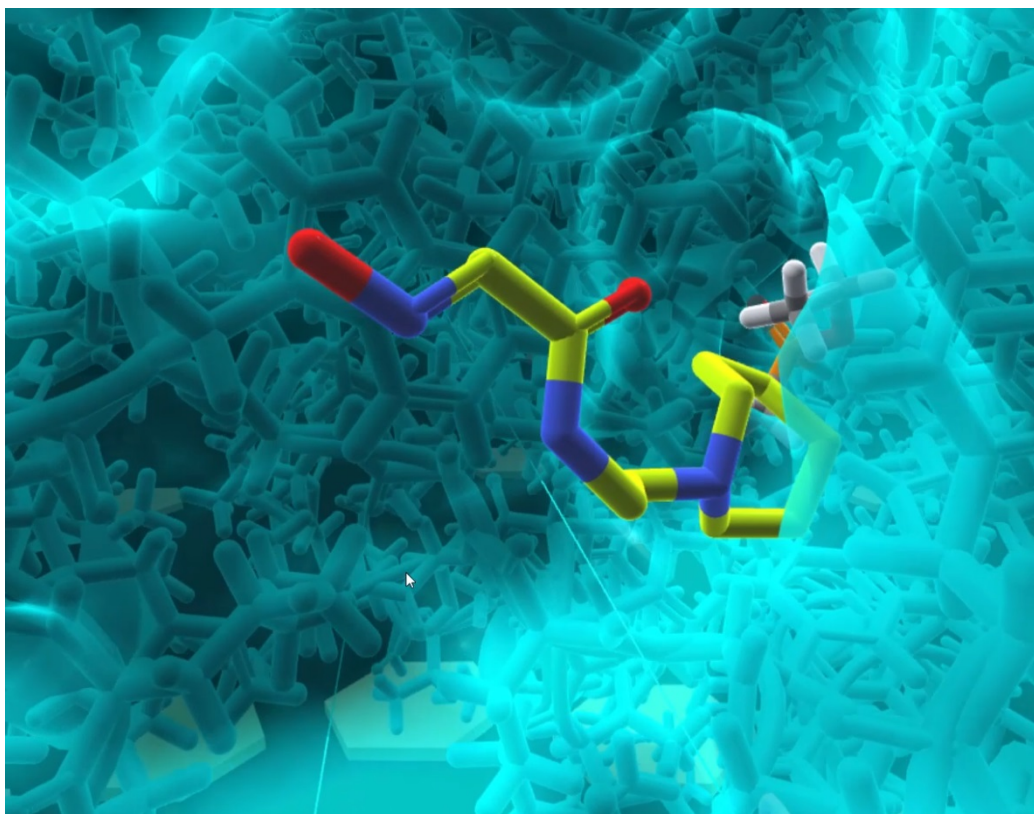


Figure 17 The crystal structure of RS194B and VX-inhibited acetylcholinesterase. The unfavorable conformation of the molecule is clearly displayed.

Our goal was to add another oxime group to the molecule, specifically on the other side of the heterocyclic ring (Figure 18). The oxime would also act as a PAS ligand (PSL). This would ensure that one of the oximes would point towards the phosphorus atom. On this basis, 17 molecules were designed. The hits were investigated by using virtual reality (VR) modeling and MD calculations (see the results and the best hits in Table 1 and Figure 19).

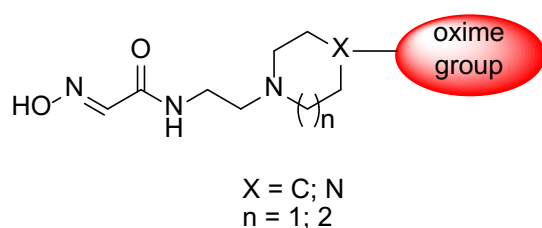


Figure 18 Design of RS194B analogs with a second oxime group.

Table 1 The best designed candidates based on molecular docking calculations.

Ranking	Structure	Score (kcal/mol)
---------	-----------	------------------

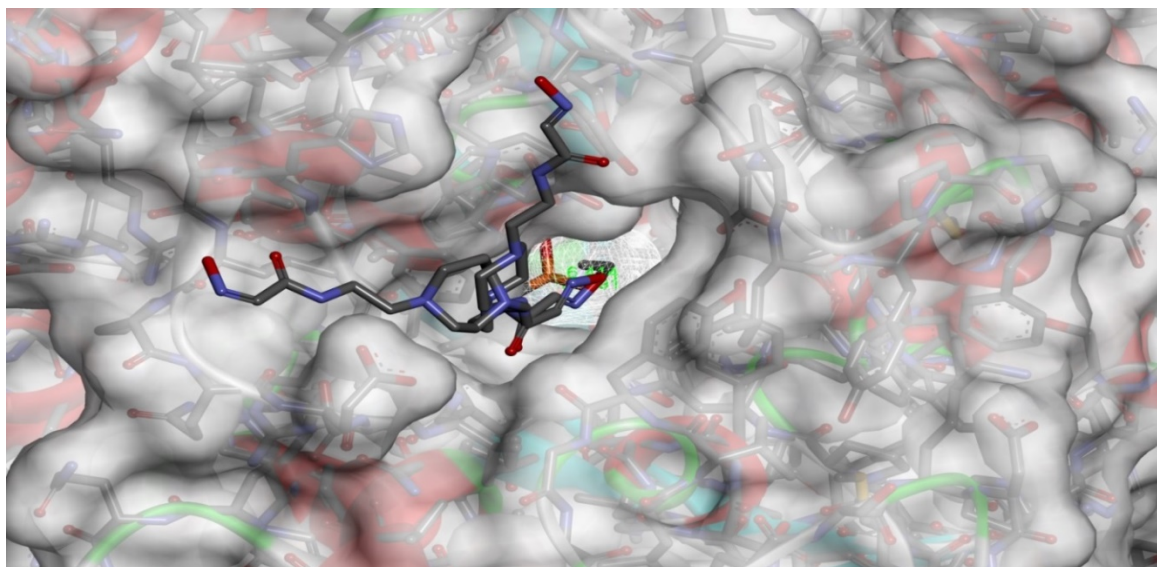
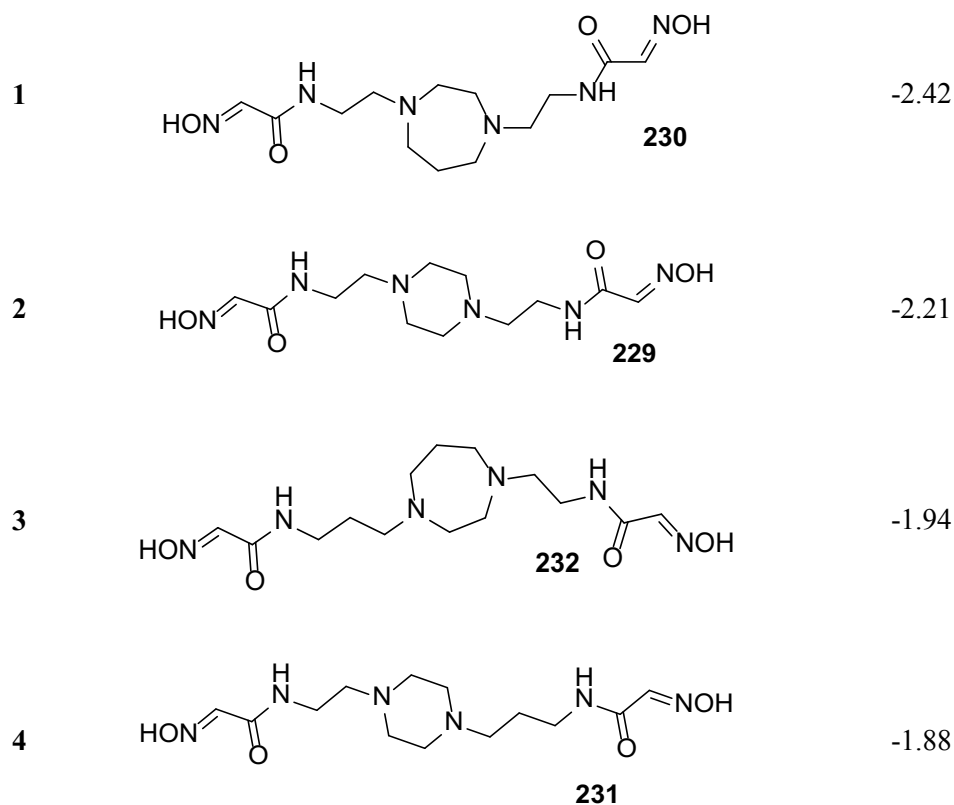


Figure 19 Molecular docking results of the best two candidates, **229** and **230**. Different conformations are evident in the enzyme. However, one of the oxime groups is always pointing towards the phosphorus atom and both central rings are stacked above Trp286.

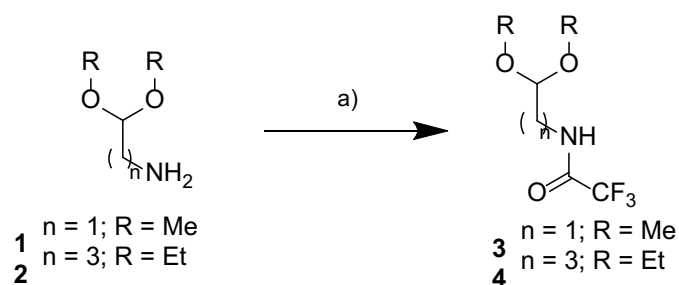
3.2 Synthesis

3.2.1 Tacrine-phenothiazine derivatives

Reductive amination was selected as the core reaction for the synthesis of tacrine-phenothiazine heterodimers. There are several different types of this reaction: we chose mild conditions using triethylsilane (TES) as the reducing agent and acetals as the reactants. The initial step was the preparation of corresponding acetals (Scheme 8). Acetals **1** and **2** were commercially available and key linker intermediates were readily prepared by the protection of amino group using trifluoroacetic acid anhydride (TFAA) (Scheme 8A). In the case of the three methylene linker, a one-pot reaction afforded the reduction of the nitrile group and immediate acetylation (Scheme 8B). Finally, the five carbon-linker had to be prepared from commercially available 5-aminopentan-1-ol (**7**). The reaction with phthalic anhydride and the subsequent Swern oxidation led to aldehyde **9**. Subsequently, reactions with triethyl orthoformate resulted in the desired acetal **10** (Scheme 8C).

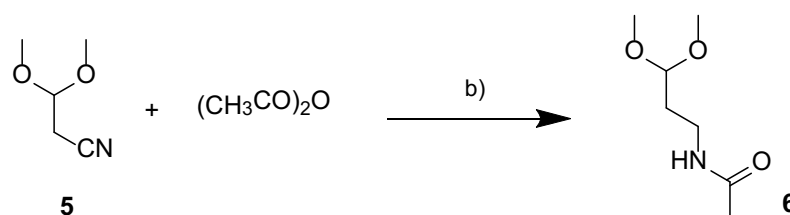
Preparation of 2C and 4C linker

A:



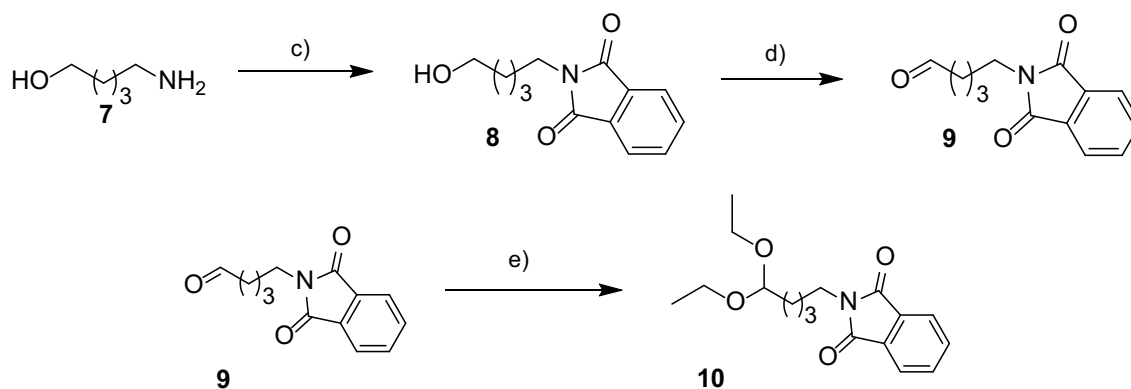
B:

Preparation of 3C linker



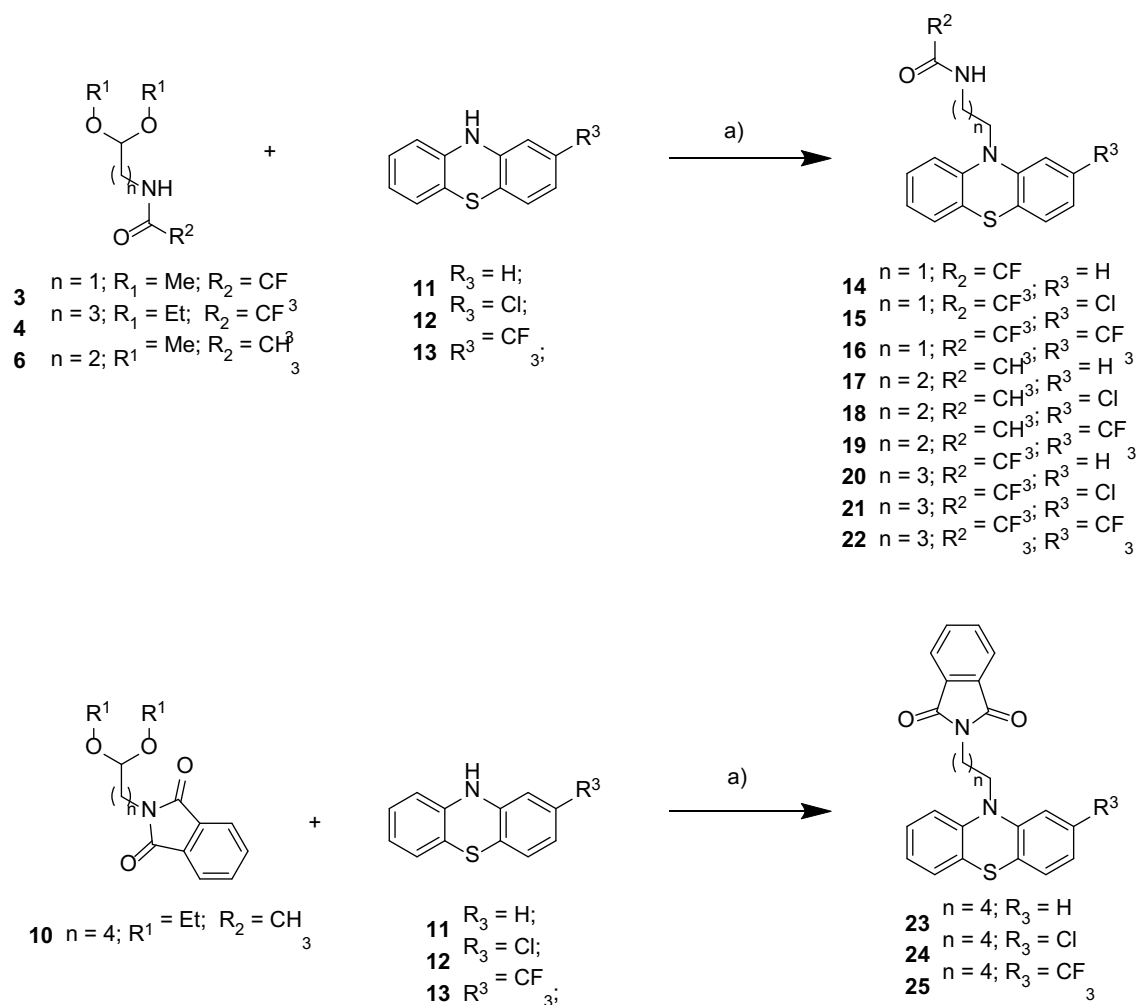
C:

Preparation of 5C linker



Scheme 8 The preparation of selected linkers. Reagents and conditions: a) TFAA, TEA, THF, 0°C to RT; b) NiSO₄, NaBH₄, MeOH, 0°C to RT; c) phthalic anhydride, 150°C; d) (COCl)₂, DMSO, DIPEA, DCM, -45°C to RT; e) TsOH, triethyl orthoformate, EtOH, RT.

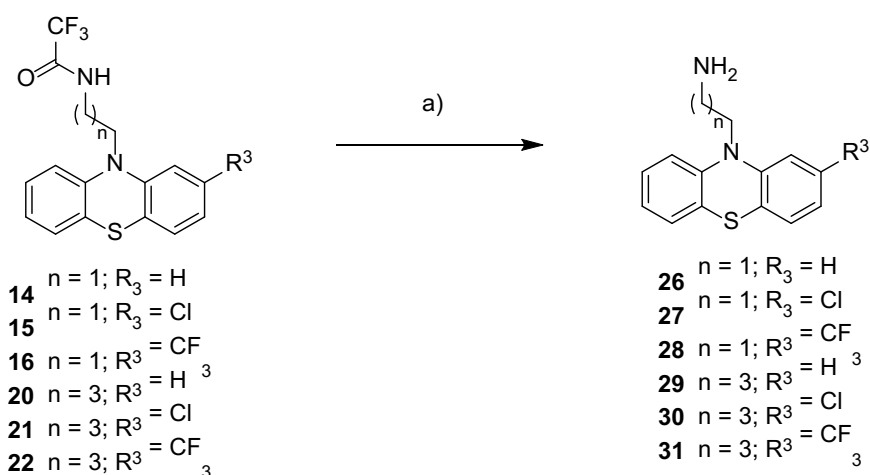
After preparation of the acetals **3**, **4**, **6** and **10**, reductive amination was performed in an acidic environment employing trifluoroacetic acid (TFA) with TES as the reductive agent (Scheme 9).



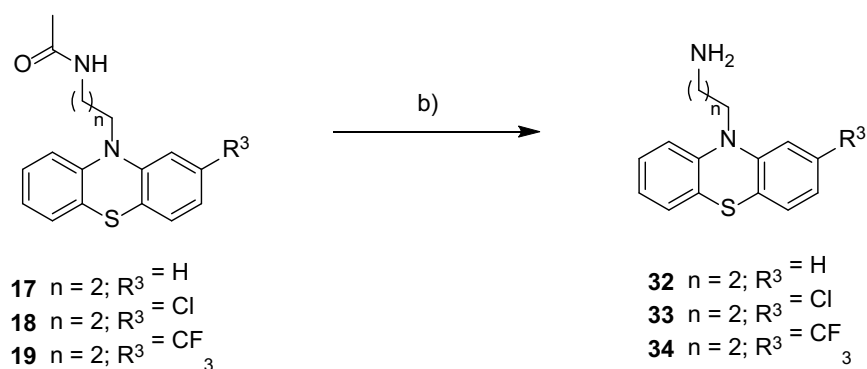
Scheme 9 Reductive amination of acetals and phenthiazines. Reagents and conditions:
a) TFA, TES, DCM, RT.

Deprotection procedures varied with the protective ligand. Trifluoroacetamides were cleaved by overnight stirring with potassium carbonate (K_2CO_3) (Scheme 10A). Harsher conditions were necessary for acetamides. Indeed, deprotection was conducted by microwave (MW) irradiation at 160°C with potassium hydroxide (KOH) (Scheme 10B). Finally, phthalimides were refluxed in EtOH with hydrazine to obtain the desired primary amines (Scheme 10C).

A: Deprotection of the trifluoroacetamide group

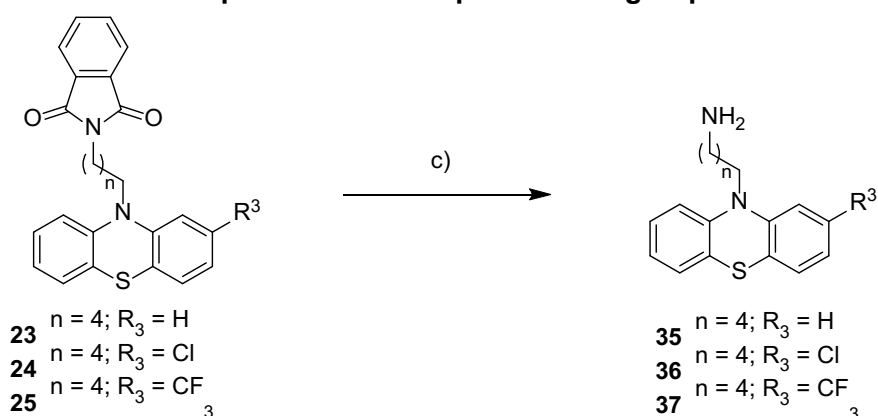


B: Deprotection of the acetamide group



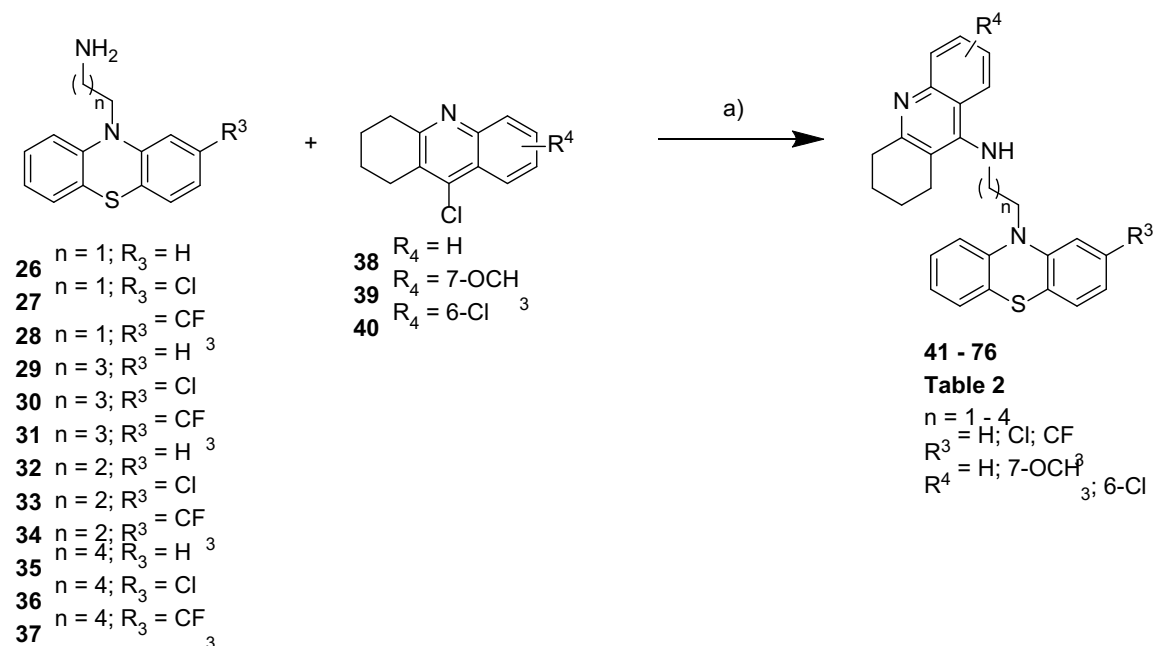
C:

Deprotection of the phthalimide group



Scheme 10 Deprotection reactions leading to primary amines (final intermediates). Reagents and conditions: a) K_2CO_3 , MeOH/H₂O (2:1), RT; b) MW, KOH, 160°C, MeOH/H₂O (2:1); c) $NH_2NH_2 \cdot H_2O$; EtOH; 90°C.

The final step, comprising *N*-(ω -aminoalkyl)phenothiazine intermediates with 9-chloro-1,2,3,4-tetrahydroacridine derivatives, led to the desired hybrids. The reaction was performed under MW irradiation at 180°C in phenol (Scheme 11).



Scheme 11 The final reaction leading to the desired hybrids. Reagents and conditions: a) MW, 180°C, phenol.

Table 2 Tacrine-phenothiazine derivatives

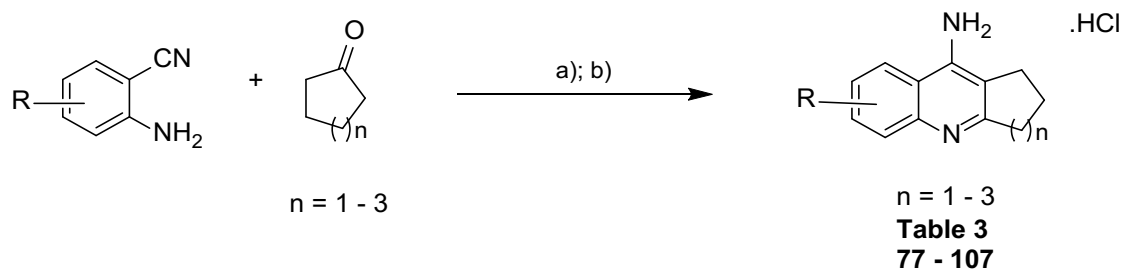
Compound	n	R ³	R ⁴
41	1	H	H
42	1	H	7-OCH ₃
43	1	H	6-Cl
44	1	Cl	H
45	1	Cl	7-OCH ₃
46	1	Cl	6-Cl
47	1	-CF ₃	H
48	1	-CF ₃	7-OCH ₃
49	1	-CF ₃	6-Cl

50	2	H	H
51	2	H	7-OCH ₃
52	2	H	6-Cl
53	2	Cl	H
54	2	Cl	7-OCH ₃
55	2	Cl	6-Cl
56	2	-CF ₃	H
57	2	-CF ₃	7-OCH ₃
58	2	-CF ₃	6-Cl
59	3	H	H
60	3	H	7-OCH ₃
61	3	H	6-Cl
62	3	Cl	H
63	3	Cl	7-OCH ₃
64	3	Cl	6-Cl
65	3	-CF ₃	H
66	3	-CF ₃	7-OCH ₃
67	3	-CF ₃	6-Cl
68	4	H	H
69	4	H	7-OCH ₃
70	4	H	6-Cl
71	4	Cl	H
72	4	Cl	7-OCH ₃
73	4	Cl	6-Cl

74	4	-CF ₃	H
75	4	-CF ₃	7-OCH ₃
76	4	-CF ₃	6-Cl

3.2.2 Tacrine derivatives with dual-targeting of AChE and the NMDA receptor

The synthesis of tacrine derivatives was optimized by using microwave irradiation. We achieved full conversion in only 10 min with yields of 37%–99% (Scheme 12). The corresponding 2-aminobenzonitriles were commercially available. Therefore, we developed a simple one-step synthesis to afford title products (see Table 3).



Scheme 12 The reaction leading to the final tacrine derivatives. ZnCl₂ or AlCl₃ were used as Lewis acids (LA). Reagents and conditions: a) LA; MW; 10 min; 150°C; b) MeOH; HCl (25% in H₂O), RT.

Table 3 Prepared tacrine derivatives with dual targeting to AChE and the NMDA receptor

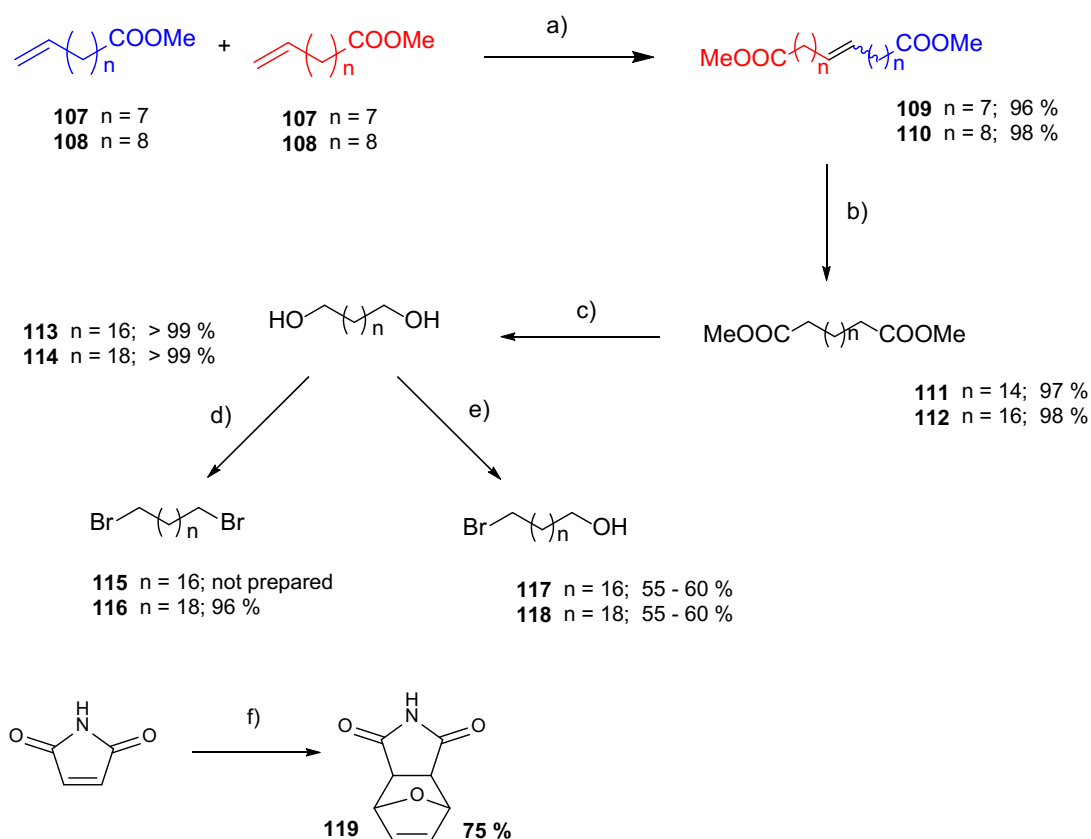
Compound	n	R	Yield
77	1	7-CH ₃	83%
78	2	7-CH ₃	98%
79	3	2-CH ₃	81%
80	1	7-Br	67%
81	2	7-Br	52%
82	3	2-Br	88%
83	1	7-Cl	82%

84	2	7-Cl	56%
85	3	2-Cl	94%
86	1	5,7-diCl	72%
87	2	5,7-diCl	86%
88	3	2,4-diCl	96%
89	1	5,7-diBr	82%
90	2	5,7-diBr	35%
91	3	2,4-diBr	65%
92	1	7-F	83%
93	2	7-F	77%
94	3	2-F	98%
95	1	8-Cl	63%
96	2	8-Cl	48%
97	3	1-Cl	89%
98	1	6-CH ₃	83%
99	2	6-CH ₃	77%
100	3	3-CH ₃	99%
101	1	8-CH ₃	58%
102	2	8-CH ₃	77%
103	3	1-CH ₃	59%
104	1	7-OCH ₃	60%
105	2	7-OCH ₃	37%
106	3	2-OCH ₃	82%

3.2.3 AChE-targeting insecticides

To obtain the long methylene chain for use as the basic core of these compounds, we suggested that the employment of methyl esters with a terminal double bond (**107** and **108**) might serve as a good starting point. Therefore, we applied olefin metathesis as the most efficient reaction prior to the use of Grignard reactions. Indeed, the Grubbs reaction yielded the dimeric intermediates, **109** and **110**, with an almost quantitative yield (Scheme 13). Owing to follow-up hydrogenation of double bond in the next step, stereoselectivity of the reaction was not solved. Therefore, the much cheaper first-generation Grubbs catalyst was preferred to the use of a second-generation Grubbs catalyst [138]. The subsequent hydrogenation of double bond and the reduction of the ester to an alcohol provided **113** and **114**, both in quantitative yields. The ester reduction can proceed via two synthetic routes. Besides lithium aluminium hydride (LiAlH₄), diisobutylaluminium hydride (DIBAL-H) can be also efficiently applied to obtain α,ω -bis-hydroxyl compound **113** and **114**, respectively (Scheme 1).

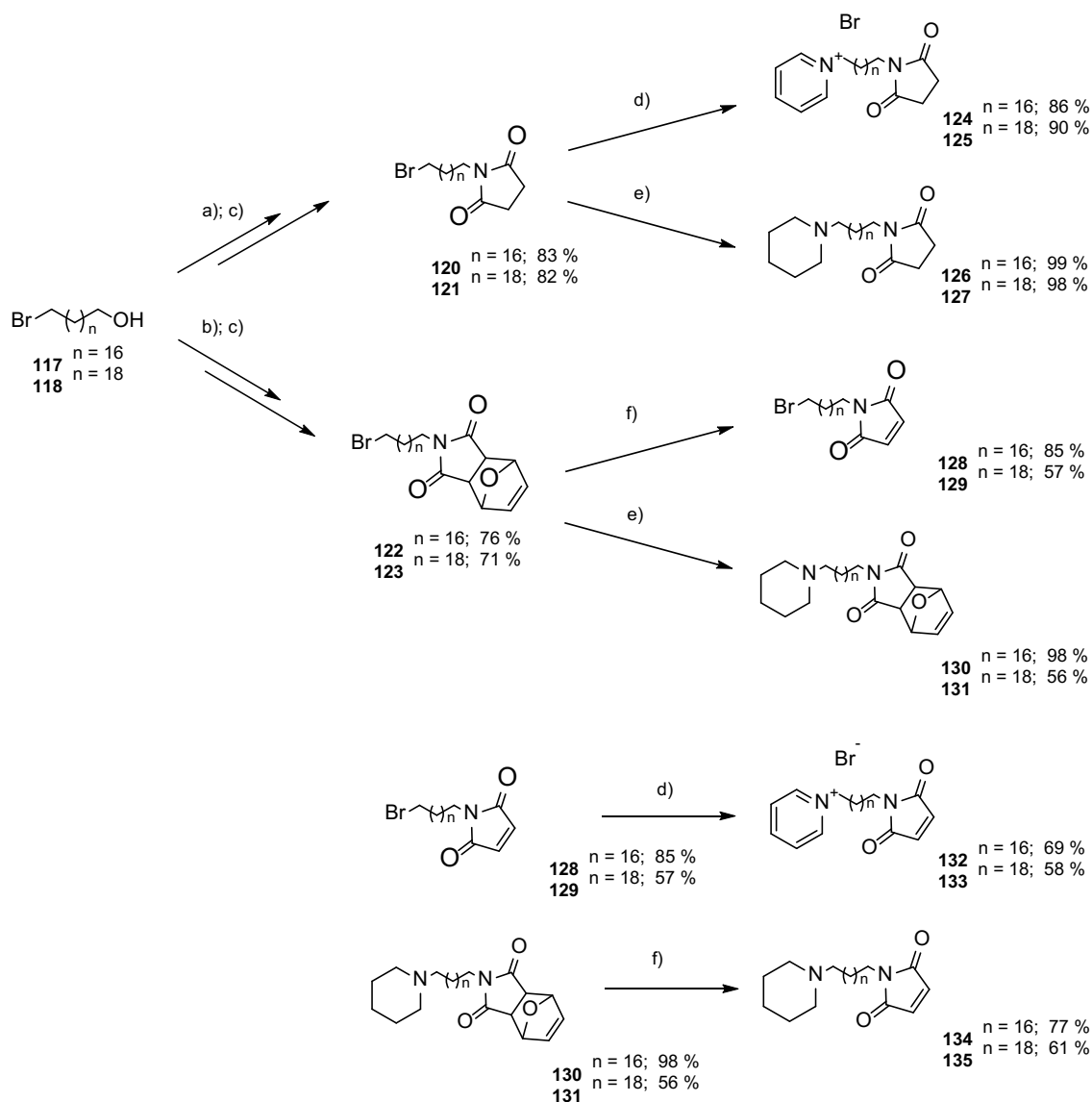
In the next step was important for the preparation of alkylating intermediates. Therefore, we applied *N*-bromosuccinimide (NBS) bromination of eicosan-1,20-diol **114**, which afforded α,ω -dibromoalkane **116** in nearly quantitative yields. Therefore, a more useful approach to obtain the mono-alkylating agents **117** and **118**, and thereby avoid the selective protection of one of the hydroxyl groups, lies in the use of hydrogen bromide (HBr) to yield ω -bromoalkan-1-ol **117** and **118** [139]. Formation of the α,ω -dibromoalkanes (**115** or **116**) was observed.



Scheme 13. The application of olefin metathesis to obtain a variety of substituted long alkanes. Reagents and conditions: a) First-generation Grubbs, reduced pressure up to 2 mbar, RT–50°C; b) Pd(OH)₂ on C (20%), H₂, MeOH/EA (2:1), RT; c) LiAlH₄ 2 M solution in THF, THF, reflux; d) NBS, PPh₃, THF, RT; e) HBr 48% solution in H₂O, toluene, reflux; f) furan, dioxane, 90°C;

To activate maleimide, a Diels-Alder reaction with furan was performed, resulting in **119** (Scheme 13) [140]. Improvement of the conditions led to the intermediates **120**–**123** in high yields (over 70%) after two steps, including the coupling reaction and subsequent NBS-bromination.

The final compounds bearing succinimide (**124**–**127**) were finally obtained by employing microwave irradiation. *N*-Alkylation enabled almost quantitative yields in the case of piperidine (**126** and **127**) and approximately 90% in the case of pyridine (**124** and **125**) (Scheme 14). The final steps for insecticides containing maleimide **132**–**135** were not straightforward. In the case of pyridinium compounds **132** and **133**, a retro-Diels-Alder reaction took place prior to *N*-alkylation. For the piperidine analogs (**134** and **135**), the *N*-alkylation had to precede the retro-Diels-Alder reaction in order to achieve the desired product. The *N*-alkylation and retro-Diels-Alder reactions resulted in good yields (over 58%; Scheme 14).

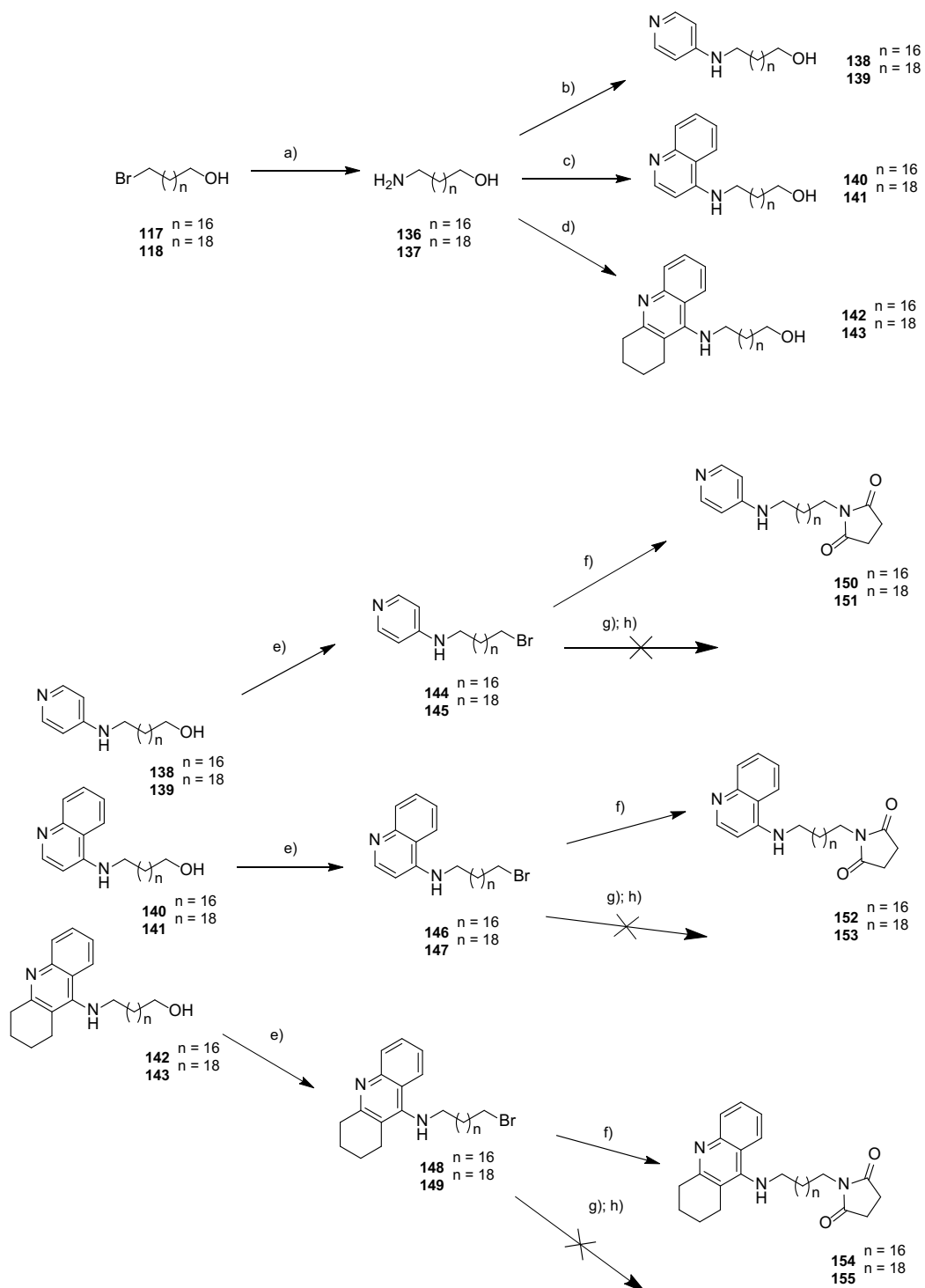


Scheme 14 Synthetic approach for Cys-targeted insecticides. Reagents and conditions: a) succinimide, K_2CO_3 , DMF, $60^\circ C$; b) imide **119**, K_2CO_3 , DMF, $60^\circ C$; c) NBS, PPh_3 , THF, RT; d) MW, pyridine, MeCN, $90^\circ C$; e) MW, piperidine, K_2CO_3 , MeCN, $90^\circ C$; f) vacuum, approximately 1 mBar, $130^\circ C$.

3.2.4 Second subset of insecticides

Alternative synthetic routes had to be used to obtain a second series of insecticides. Initially, 20-bromoeicosan-1-ol (**118**) or 18-bromooctadecan-1-ol (**117**) were prepared in accordance with previous synthetic procedures (Scheme 15). Next, 20-aminoeicosan-1-ol **137** or 18-aminooctadecan-1-ol **136** were obtained by a one-pot reaction with potassium phthalimide and hydrazine hydrate. The reactions with 4-bromopyridine

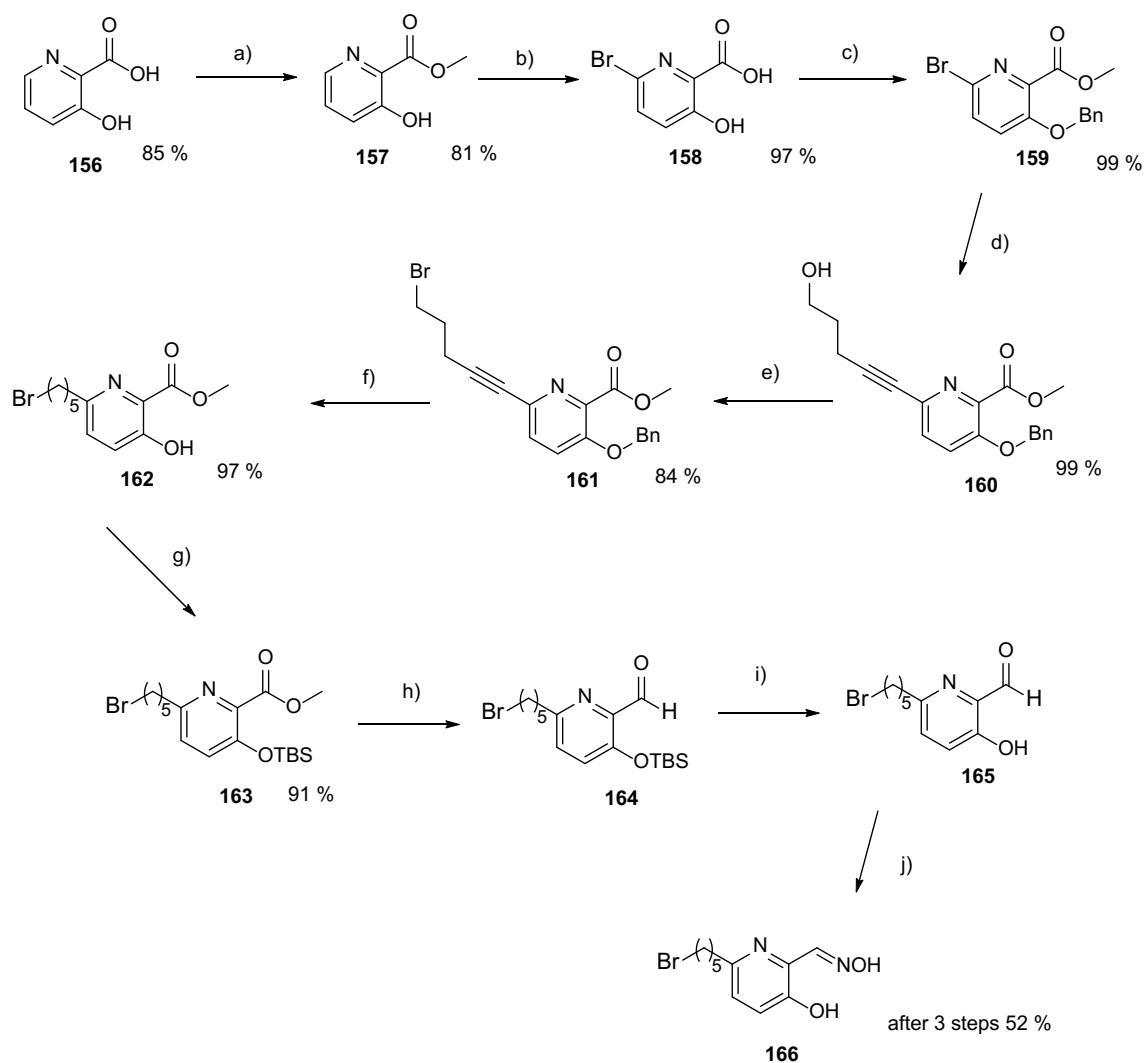
hydrochloride, 4-chloroquinoline, or 9-chloro-1,2,3,4-tetrahydroacridine produced compounds **138–143**. Then, bromination with CBr_4 took place. The final reaction with succinimide resulted in the desired final products **150–155**. Maleimide analogs were not prepared, despite several optimization attempts.



Scheme 15 The alternative synthetic route to the desired products. Reagents and conditions: a) one-pot reaction, potassium phthalimide for 8 h at 110°C with MW irradiation; NH₂NH₂·H₂O for 1 h at 90°C with MW irradiation; b) 4-bromopyridine hydrochloride, KOH, 1-pentanol, 4 h at 180°C with MW irradiation; c) 4-chloroquinoline, pentanol, 2 h at 180°C with MW irradiation; 9-chloro-1,2,3,4-tetrahydroacridine, pentanol, 2 h at 180°C with MW irradiation; e) CBr₄, PPh₃, DCM, Ar, RT; f) succinimide, K₂CO₃, DMF, Ar, 60°C; g) imide **119**, K₂CO₃, DMF, Ar, 60°C.

3.2.5 Mono-quaternary permanently charged AChE reactivators

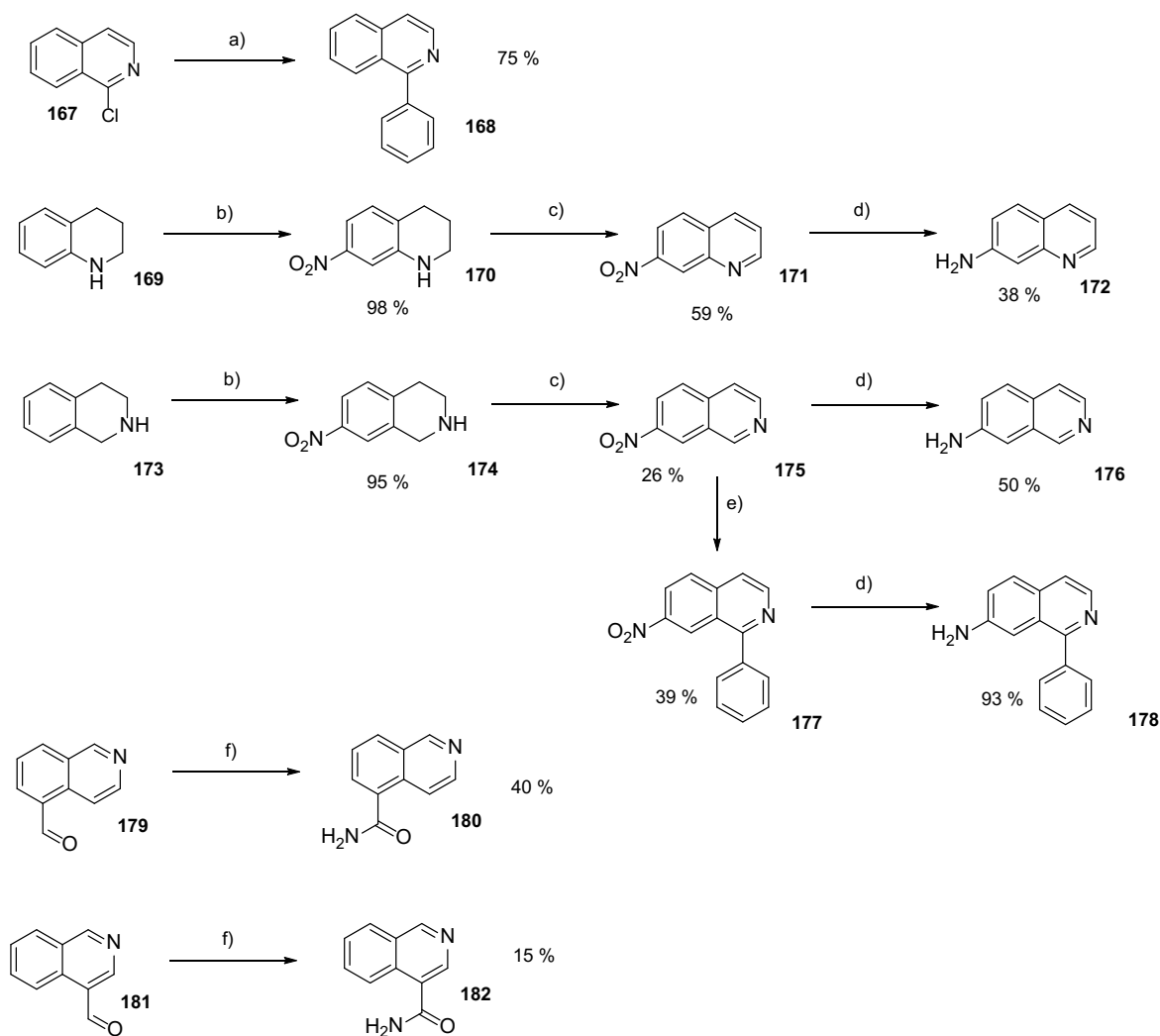
The synthesis of these compounds consists of three parts. Initially, the preparation of the oxime key intermediate **166** was conducted. Its synthesis was derived from commercially accessible 3-hydroxypicolinic acid **156** [116]. In the first step, esterification took place. Ester **157** was then brominated and the hydroxyl group was protected by benzyl bromide. All three steps resulted in excellent yields (85%, 81%, and 97%, respectively). Subsequently, the Sonogashira coupling reaction with pent-4-yn-1-ol was performed to obtain compound **160** in quantitative yields. The Appel reaction in the next step was performed to obtain bromide **161** at a good yields (84%). The hydrolysis of the triple bond with Pd(OH)₂/C also resulted in the deprotection of the phenolic group, which was protected by *tert*-butyldimethylsilyl triflate (TBDMSOTf) in the next step. The final sequence of the three step reaction was conducted in order to obtain the key intermediate **166**. The sequence started with the reduction of the ester group with DIBAL-H to the appropriate aldehyde **164**. Subsequently, deprotection of TBS was accomplished by using TBAF, and the third step, the reaction of aldehyde **165** with hydroxylamine, led to the desired product **166**. An excellent yield of 52% was obtained after these steps and the overall yield after 10 steps, from the starting compound **156** to the key intermediate **166**, was 25% (Scheme 16).



Scheme 16 The synthesis of the key intermediate **166** from commercially accessible 3-hydroxypicolinic acid **156**. Reagents and conditions: a) MeOH/H₂SO₄ (10:1), RT, 20 h; b) Br₂, H₂O, RT, 20 h; c) BnBr, K₂CO₃, acetone, RT, 20 h; d) pent-4-yn-1-ol, Pd(PPh₃)₄, CuI, DCM/Et₃N (2:1), RT, 20 h; e) CBr₄, PPh₃, DCM, RT, 1 h; f) Pd(OH)₂/C (20%), MeOH/EA (2:1), H₂, RT, 1 h; g) 2,6-lutidine, TBDMSOTf, DCM, 0°C, 1 h; h) DIBAL-H (1 M solution in DCM), DCM, -78°C, 15 min; i) TBAF (1 M solution in THF), THF, -30°C, 10 min; j) NH₂OH, absolute EtOH, RT, 30 min.

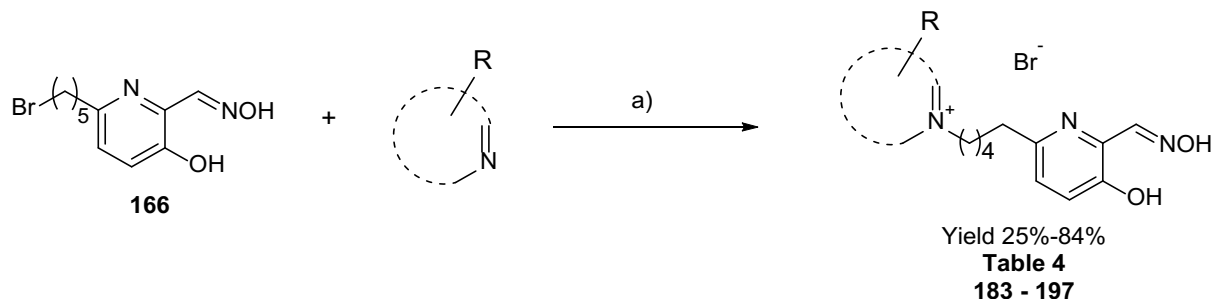
Another part of the synthesis consists of the preparation of PAS ligands (Scheme 17). The ligand **168** was obtained by Suzuki coupling with phenylboronic acid from the compound **167** (75% yield). Other quinoline- or isoquinoline-based ligands were prepared from the tetrahydroquinoline **169** or tetrahydroisoquinoline **173**. In the first step, nitration occurred in the 7-position with almost quantitative yields. The oxidative aromatization was achieved in the second step with the Pd/C catalyst in an oxygen

atmosphere. Finally, the reduction of the nitro group was performed with tin(II) chloride to obtain the final PAS ligands, **172** and **176**. Intermediate **175** was also used for the reaction with phenylboronic acid, which produced compound **177**. The reduction of the nitro group resulted in ligand **178**. The last PAS ligands were prepared from the corresponding aldehydes by the formation of the oxime and its immediate hydrolysis to amides **180** or **182**.



Scheme 17 The preparation of quinoline or isoquinoline-based PAS ligand intermediates. Reagents and conditions: a) phenylboronic acid, Pd(PPh₃)₄, K₂CO₃, dioxane, 95°C, 40 h; b) NaNO₃, H₂SO₄, 20 h, RT; c) Pd/C (10%), toluene, O₂, 200°C, 20 h; d) SnCl₂·2H₂O, absolute EtOH, 90°C, 15 h; e) phenylboronic acid, TFA, AgNO₃, K₂S₂O₈, DCM, H₂O, RT, 20 h; f) NH₂OH·HCl, Cs₂CO₃, FeCl₃, H₂O, RT, 48 h.

Commercially available pyridines and the prepared isoquinolines/quinoline, as suitable PAS ligands, were coupled with our key intermediate to obtain mono-quaternary reactivators in the final synthesis step (Scheme 18). The prepared compounds are presented in Table 4.



Scheme 18 The final *N*-alkylation reaction, which yields the desired mono-quaternary reactivators. Reagents and conditions: a) MW, MeCN, >24 h, 90°C.

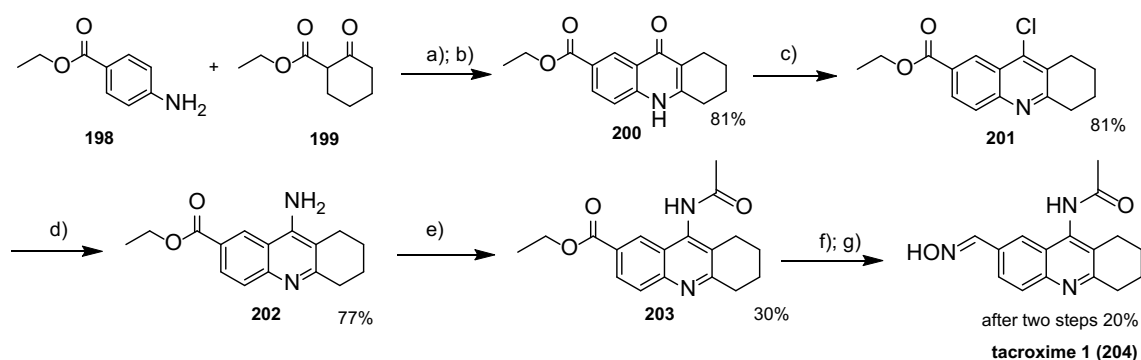
Table 4 Prepared mono-quaternary permanently charged AChE reactivators

Compound	Type of PAS ring	R
183	isoquinolinium	-
184	isoquinolinium	1-Ph
185	quinolinium	7-NH ₂
186	isoquinolinium	7-NH ₂
187	isoquinolinium	7-NH ₂ -1-Ph
188	isoquinolinium	5-CONH ₂
189	isoquinolinium	4-CONH ₂
190	pyridinium	4-CONH ₂
191	pyridinium	3-CONH ₂
192	pyridinium	4-CH ₃
193	pyridinium	4-C(CH ₃) ₃
194	pyridinium	-
195	pyridinium	4-OH
196	pyridinium	4-COOCH ₃

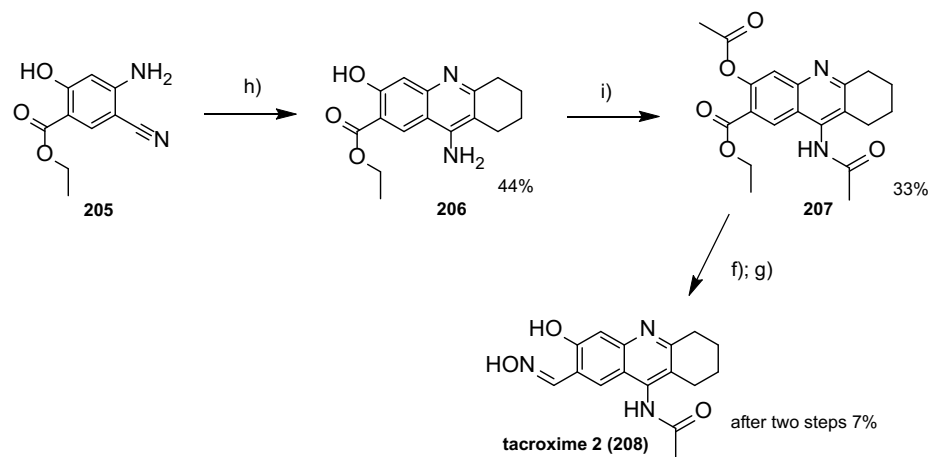
3.2.6 Tacroximes

The preparation of **tacroxime 1 (204)** apparently corresponds to the well characterized synthesis of 7-methoxytacrine [141]. Therefore, benzocaine (**198**) was used instead of 4-methoxyaniline and the synthetic route was similar up to intermediate **202**. Subsequently, acetylation with acetic anhydride was performed to afford **203**. The final two-step procedure involved the initial reduction of an ester to an aldehyde, followed by the hydroxylamine reaction to yield **204** (Scheme 19A). The synthesis of **tacroxime 2 (208)** followed a different pathway. The key intermediate **205** was obtained, as described in the literature [142]. Subsequently, compound **206** was prepared by the optimized conditions using microwave irradiation (as described in section 3.2.2). The last three steps used were as for **204** (Scheme 19B).

A:



B:

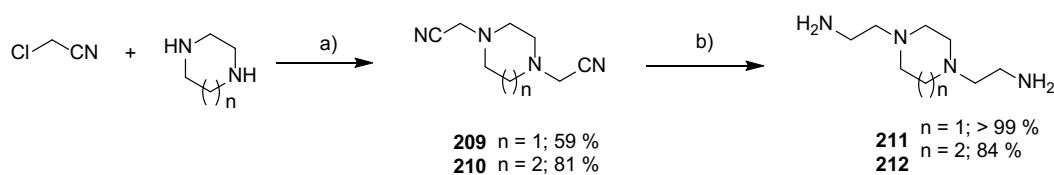


Scheme 19 A: Preparation of **tacroxime 1** from the commercially available starting points **198** and **199**. B: Preparation of **tacroxime 2** from **205**. Reagents and conditions: a) toluene, Dean-Stark trap, 150°C; b) diphenylether, Dean-Stark trap, 230°C; c) POCl₃, 140°C; d) NH₃ (g), phenol, 180°C; e) Ac₂O, pyridine, 150°C; f) DIBAL-H 1 M in DCM, DCM, -80°C; g) NH₂OH, EtOH, RT; h) ZnCl₂, cyclohexanone, MW irradiation, 150°C; i) Ac₂O, pyridine, 150°C.

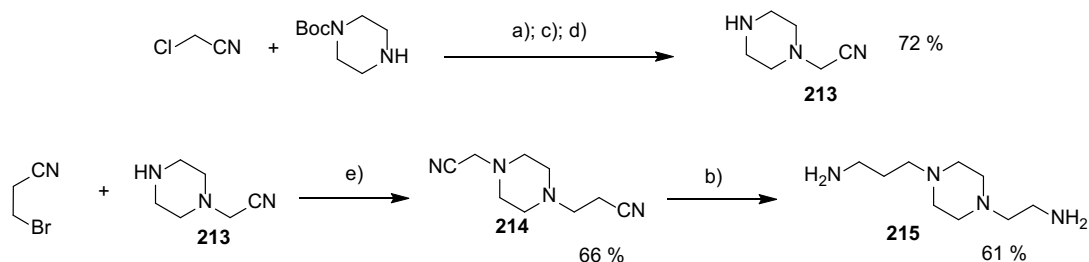
3.2.7 Uncharged bis-oxime reactivators

The core of the synthesis was the preparation of RS194B [117]. The oxime fragment was prepared in the same way (Scheme 3). Therefore, it was necessary to prepare the corresponding bis-primary amine intermediates. These preparations were not analogous and had to be optimized for almost every product (Scheme 20 and 21). The initial *N*-alkylation by either 2-chloroacetonitrile or 3-bromopropionitrile was performed by a MW reaction; at room temperature (RT) in DCM or at RT in EtOH with two different bases (TEA for DCM or Na₂CO₃ for EtOH). In the case of asymmetrical molecules, *N*-Boc-piperazine or *N*-Boc-homopiperazine was alkylated into mono-nitrilated product, followed by deprotection and another *N*-alkylation. Compounds **209**, **210**, **214**, and **225** were reduced to **211**, **212**, **215**, and **226**, respectively, by LiAlH₄. Contrary, **216**, **219**, and **223** were reduced to **217**, **220**, and **224** by Raney-nickel under H₂. Finally, the reaction with ethyl (*2E*)-2-(hydroxyimino)acetate (**227**) afforded the desired bis-oxime reactivators (Scheme 22).

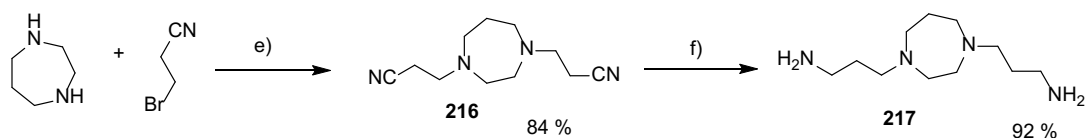
Synthesis of homopiperazine and piperazine 2C derivatives



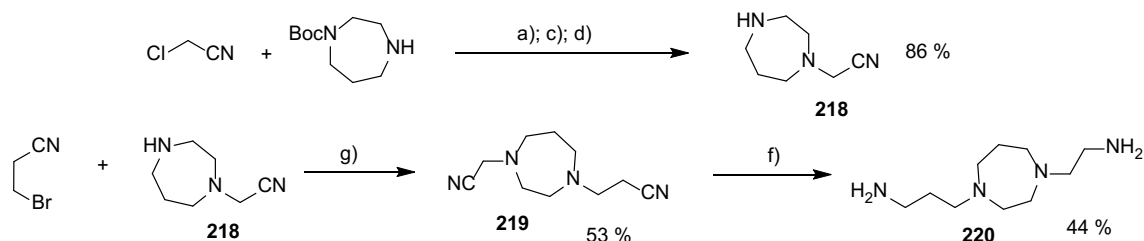
Synthesis of piperazine 2C/3C derivative



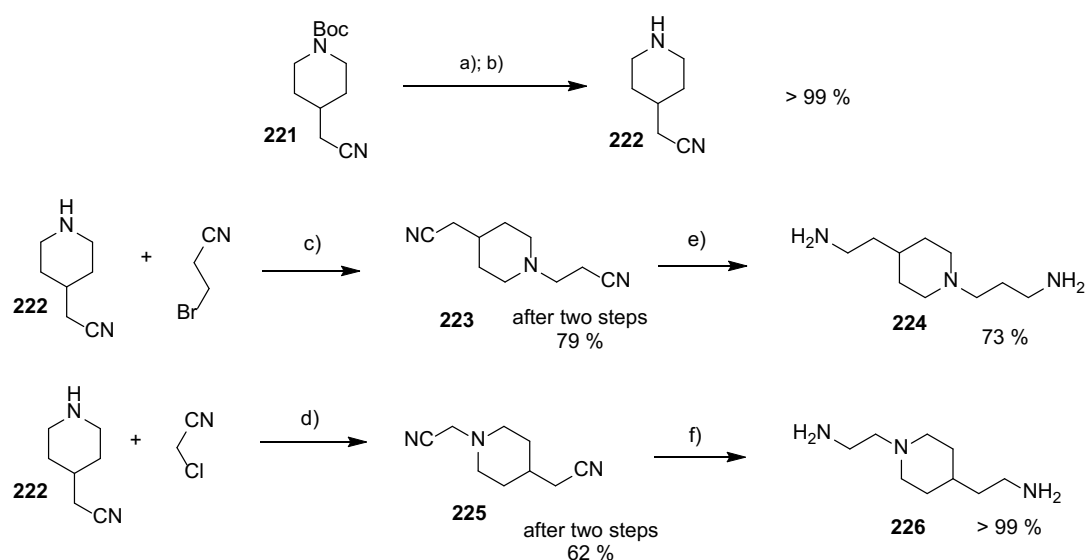
Synthesis of homopiperazine 3C derivative



Synthesis of homopiperazine 2C/3C derivative

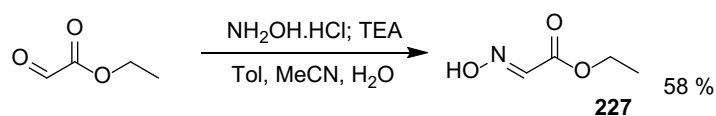


Scheme 20 The preparation of compounds **211**, **212**, **215**, **217**, and **220** with piperazine or homopiperazine central rings. Reagents and conditions: a) Na_2CO_3 , MW, 100°C , EtOH; b) LiAlH_4 , 85°C , THF; c) MeOH, 4 M HCl in dioxane, RT; d) MeOH, NH_4OH (25% in H_2O), RT; e) TEA, DCM, RT; f) Raney-nickel, H_2 , MeOH, H_2O , RT; g) Na_2CO_3 , RT, EtOH.

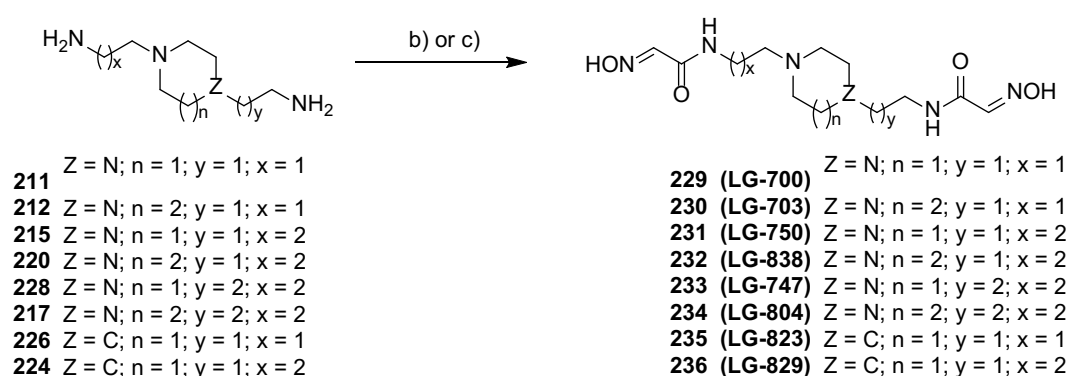


Scheme 21 Preparation of corresponding bis-primary amines with a piperidine central ring. Reagents and conditions: a) MeOH, 4 M HCl in dioxane, RT; b) MeOH, NH₄OH (25% in H₂O), RT; c) TEA, DCM, RT; d) Na₂CO₃, MW, 100°C, EtOH; e) Raney-nickel, H₂, MeOH, H₂O, RT; f) LiAlH₄, 85°C, THF.

Preparation of oxime fragment



Final step towards desired reactivators



Scheme 22 The final step in the preparation of the corresponding bis-oxime reactivators. Conditions c) were applied only for the preparation of compound **234**. Reagents and conditions: a) NH₂OH.HCl, TEA, toluene, MeCN, H₂O, RT; b) oxime **227**, EtOH, 90°C; c) oxime **227**, MeCN, 50°C.

3.3 Biological evaluation

3.3.1 Tacrine-phenothiazine derivatives

Initially, the series of tacrine-phenothiazines (Figure 20) was evaluated for the inhibitory activity against AChE and BChE (Table 5). The most potent derivatives were further evaluated for their potential antioxidant activity and cytotoxicity in HepG2 cells and for their ability to cross the BBB (Table 6).

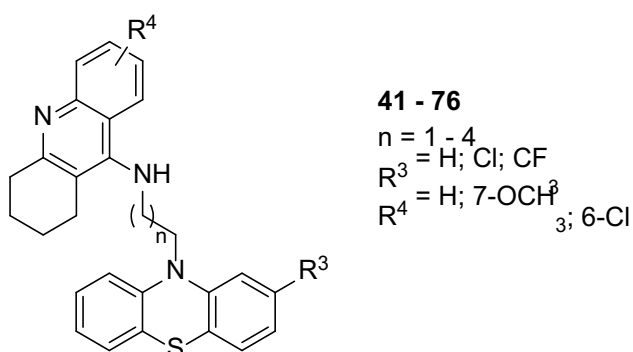


Figure 20 General structure of tacrine-phenothiazine derivatives.

Table 5 Inhibitory activity against *hAChE* and *hBChE* with the calculated selectivity index for *hAChE*.

Compound	n	R ³	R ⁴	IC ₅₀ <i>hAChE</i> (μM) ± SEM ^a	IC ₅₀ <i>hBChE</i> (μM) ± SEM ^a	Selectivity index <i>hAChE</i>
41	1	H	H	2.0 ± 0.1	0.02 ± 0.001	0.01
42	1	H	7-OCH ₃	4.0 ± 0.3	0.12 ± 0.002	0.03
43	1	H	6-Cl	0.3 ± 0.01	0.03 ± 0.001	0.09
44	1	Cl	H	1.2 ± 0.03	0.05 ± 0.001	0.04
45	1	Cl	7-OCH ₃	9.0 ± 0.8	0.10 ± 0.003	0.01
46	1	Cl	6-Cl	0.4 ± 0.02	0.09 ± 0.003	0.24
47	1	-CF ₃	H	1.7 ± 0.1	0.07 ± 0.004	0.04
48	1	-CF ₃	7-OCH ₃	18.6 ± 2.7	0.55 ± 0.01	0.03

49	1	-CF ₃	6-Cl	0.4 ± 0.02	0.30 ± 0.007	0.83
50	2	H	H	4.5 ± 0.4	0.1 ± 0.004	0.03
51	2	H	7-OCH ₃	3.5 ± 0.2	0.40 ± 0.010	0.11
52	2	H	6-Cl	0.3 ± 0.01	0.26 ± 0.010	0.81
53	2	Cl	H	0.8 ± 0.1	0.21 ± 0.005	0.25
54	2	Cl	7-OCH ₃	0.6 ± 0.02	0.81 ± 0.020	1.37
55	2	Cl	6-Cl	0.3 ± 0.02	0.95 ± 0.03	3.7
56	2	-CF ₃	H	1.7 ± 0.1	0.23 ± 0.01	0.14
57	2	-CF ₃	7-OCH ₃	5.8 ± 0.3	1.9 ± 0.05	0.32
58	2	-CF ₃	6-Cl	0.5 ± 0.02	1.04 ± 0.03	2.3
59	3	H	H	4.7 ± 0.54	0.09 ± 0.004	0.02
60	3	H	7-OCH ₃	6.3 ± 0.50	0.05 ± 0.003	0.01
61	3	H	6-Cl	0.4 ± 0.03	0.07 ± 0.002	0.15
62	3	Cl	H	1.8 ± 0.11	0.15 ± 0.002	0.08
63	3	Cl	7-OCH ₃	2.8 ± 0.25	0.13 ± 0.003	0.05
64	3	Cl	6-Cl	0.5 ± 0.04	0.23 ± 0.008	0.48
65	3	-CF ₃	H	13.1 ± 0.8	0.43 ± 0.013	0.03
66	3	-CF ₃	7-OCH ₃	24.1 ± 3.4	0.58 ± 0.02	0.02
67	3	-CF ₃	6-Cl	1.5 ± 0.15	3.8 ± 0.80	2.6
68	4	H	H	0.08 ± 0.002	0.02 ± 0.001	0.23
69	4	H	7-OCH ₃	> 100	0.83 ± 0.03	-
70	4	H	6-Cl	0.008 ± 0.0004	0.19 ± 0.01	23.5
71	4	Cl	H	0.3 ± 0.02	0.03 ± 0.001	0.10

72	4	Cl	7-OCH ₃	> 100	0.81 ± 0.03	-
73	4	Cl	6-Cl	0.03 ± 0.002	0.42 ± 0.02	14.5
74	4	-CF ₃	H	0.7 ± 0.05	0.08 ± 0.002	0.11
75	4	-CF ₃	7-OCH ₃	> 100	2.4 ± 0.09	-
76	4	-CF ₃	6-Cl	0.1 ± 0.01	4.4 ± 0.13	36.3

^a The results are expressed as the mean of at least three experiments. ^b Selectivity for *hAChE* is determined as the ratio of *hBChE* IC₅₀/*hAChE* IC₅₀

Table 6 Antioxidant activity, cytotoxicity of tested compounds in HepG2 cells after 24 h and the MDCK determination of potential BBB penetration ability.

Compounds	Antioxidant activity	HepG2 cells	BBB penetration estimation	
	% at 10 mM	IC ₅₀ (μM) ± SEM ^b	Papp ± SEM ^b (× 10 ⁻⁶ cm s ⁻¹)	CNS (+/-) ^c
41	46	8.2 ± 0.7	n.t. ^a	n.t.
44	87	6.4 ± 0.3	n.t.	n.t.
49	54	6.9 ± 0.3	n.t.	n.t.
52	91	11.8 ± 0.7	18.9 ± 5.1	+
55	63	13.5 ± 1.7	n.t.	n.t.
60	82	5.0 ± 0.2	n.t.	n.t.
68	73	7.8 ± 0.1	n.t.	n.t.
69	79	5.6 ± 0.5	n.t.	n.t.
70	93	13.1 ± 0.4	8.4 ± 3.7	+
71	71	5.6 ± 0.5	14.4 ± 7.2	+
73	63	6.0 ± 0.4	5.1 ± 1.7	+
76	71	8.2 ± 0.6	n.t.	n.t.
tacrine	n.t.	168.5 ± 3.6	25.4 ± 3.4	+
phenothiazine	EC ₅₀ = 61.53 μM	> 126	n.t.	n.t.

^a n.t. – not tested; ^b The results are expressed as the mean of a minimum of three experiments; ^c CNS + (high BBB permeation predicted): $P_{app} (\times 10^{-6} \text{ cm s}^{-1}) > 4.0$; CNS – (low BBB permeation predicted): $P_{app} (\times 10^{-6} \text{ cm s}^{-1}) < 2.0$; CNS +/- (BBB permeation uncertain): $P_{app} (\times 10^{-6} \text{ cm s}^{-1})$ from 4.0 to 2.0.

3.3.2 Tacrine derivatives with dual-targeting of AChE and the NMDA receptor

The prepared series (Figure 21) were evaluated for their inhibitory efficiency on AChE and BChE, and their ability to penetrate the BBB was calculated by using the CNS MPO model (Table 7).

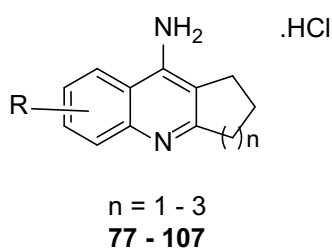


Figure 21 General structure of tacrine derivatives.

Table 7 *In vitro* anticholinesterase activity and CNS MPO calculation [67].

Compound	n	R	IC ₅₀ AChE	IC ₅₀ BChE	Selectivity	CNS MPO calculation ^d
			(μM) \pm SEM ^b	(μM) \pm SEM ^b	index hAChE ^c	
77	1	7-CH ₃	10.0 \pm 1.0	23.7 \pm 1.8	2.4	5.3
78	2	7-CH ₃	15.5 \pm 1.4	13.7 \pm 0.4	0.9	5.2
79	3	2-CH ₃	22.5 \pm 1.6	10.6 \pm 0.4	0.5	5.0
80	1	7-Br	5.7 \pm 0.3	16.9 \pm 1.5	3.0	5.7
81	2	7-Br	4.8 \pm 0.02	20.8 \pm 1.2	4.4	5.3
82	3	2-Br	13.8 \pm 0.6	15.1 \pm 1.1	1.1	4.8
83	1	7-Cl	1.6 \pm 0.1	6.9 \pm 0.7	4.3	5.7
84	2	7-Cl	1.9 \pm 0.1	6.7 \pm 0.5	3.5	5.5

85	3	2-Cl	8.6 ± 0.5	10.3 ± 0.7	1.2	5.1
86	1	5,7-diCl	13.1 ± 1.0	17.9 ± 0.1	1.4	5.0
87	2	5,7-diCl	4.3 ± 0.3	14.8 ± 0.4	3.4	4.6
88	3	2,4-diCl	9.0 ± 0.5	23.8 ± 1.0	2.6	4.2
89	1	5,7-diBr	15.1 ± 1.0	34% at 100 μM	-	4.5
90	2	5,7-diBr	5.2 ± 0.3	32.0 ± 1.1	6.2	4.0
91	3	2,4-diBr	15.1 ± 1.4	89.9 ± 7.2	6.0	3.6
92	1	7-F	0.66 ± 0.02	1.91 ± 0.1	2.9	5.7
93	2	7-F	0.98 ± 0.05	0.75 ± 0.03	0.8	5.7
94	3	2-F	0.62 ± 0.03	0.57 ± 0.02	0.9	5.5
95	1	8-Cl	6% at 100 μM	6% at 100 μM	-	5.6
96	2	8-Cl	0.033 ± 0.001	0.062 ± 0.003	1.9	5.4
97	3	1-Cl	0.22 ± 0.01	0.31 ± 0.02	1.4	5.0
98	1	6-CH ₃	0.35 ± 0.01	8.4 ± 0.5	24.3	5.3
99	2	6-CH ₃	0.07 ± 0.003	2.9 ± 0.1	41.4	5.2
100	3	3-CH ₃	0.10 ± 0.004	1.0 ± 0.03	10.0	5.0
101	1	8-CH ₃	0.42 ± 0.03	0.47 ± 0.01	1.1	5.2
102	2	8-CH ₃	0.13 ± 0.01	0.50 ± 0.02	3.8	5.2
103	3	1-CH ₃	0.26 ± 0.01	0.11 ± 0.01	0.4	5.0
104	1	7-OCH ₃	8.2 ± 0.4	10.6 ± 0.3	1.3	5.3

105	2	7-OCH ₃	10.0 ± 1.0	17.6 ± 0.8	1.8	5.3
106	3	2-OCH ₃	17.6 ± 0.7	4.4 ± 0.3	0.3	5.3

^a Percentage inhibition at 100 μM; ^b The results are expressed as the mean of at least three experiments; ^c Selectivity for *hAChE* is determined as a ratio of *hBChE* IC₅₀/*hAChE* IC₅₀; ^d Calculated according to ref. [67].

3.3.3 AChE-targeting insecticides

Initially, all eight insecticides were evaluated for their inhibitory activity on *hAChE*, *hBChE*, and *AgAChE* (Table 8). To validate Ellman's assay, we also determined IC₅₀ values by a potentiometric titration method (Table 9) [143]. Finally, the mechanism of inhibition was examined (Table 10).

Table 8 The inhibitory effects of novel compounds and standards on *hAChE*, *hBChE*, and *AgAChE*.

Compound	IC ₅₀ ± SEM (μM) ^a			Selectivity index ^b
	<i>hAChE</i>	<i>AgAChE1</i>	<i>hBChE</i>	
124	4.6 ± 0.2	4.9 ± 0.2	> 100	0.9
125	16.6 ± 1.9	2.1 ± 0.06	> 100	7.7
126	73.1 ± 4.1	3.6 ± 0.13	> 100	20.1
127	119.7 ± 15	> 100	> 100	< 1.2
132	8.8 ± 0.6	0.09 ± 0.004	> 100	100.0
133	6.1 ± 0.4	0.23 ± 0.01	> 100	26.9
134	> 100	3.6 ± 0.3	> 100	> 27.6
135	> 100	4.2 ± 0.3	> 100	> 23.6
paraoxon	0.07 ± 0.01	0.07 ± 0.003	0.07 ± 0.002	1.1
bendiocarb	0.03 ± 0.001	0.01 ± 0.0004	1.8 ± 0.07	2.8
carbofuran	0.02 ± 0.001	0.003 ± 0.0001	2.2 ± 0.12	6.7

^a IC₅₀ values measured by modified Ellman's assay [143]; ^b Selectivity for *AgAChE1* is determined as the IC₅₀ (*hAChE*)/IC₅₀ (*AgAChE1*) ratio; ^c Not determined; ^d Reversibility test was determined after 10

min by using ten times dilution; The results are expressed as the mean of at least three experiments

Table 9 The comparison between modified Ellman's methods and potentiometric methods.

Compound	IC ₅₀ ± SEM (µM)	
	<i>hAChE</i> ^a	<i>hAChE</i> ^b
124	4.6 ± 0.2	4.1 ± 0.8
125	16.6 ± 1.9	2.8 ± 0.3
126	73.1 ± 4.1	17.0 ± 4.8
127	119.7 ± 15	195.7 ± 60.0
132	8.8 ± 0.6	1.5 ± 0.1
133	6.1 ± 0.4	1.7 ± 0.1
134	> 100	> 100
135	> 100	> 100
paraoxon	0.07 ± 0.01	0.04 ± 0.002
bendiocarb	0.03 ± 0.001	n.d ^d
carbofuran	0.02 ± 0.001	n.d ^d

^a IC₅₀ values measured by modified Elman's method [143]; The results are expressed as the mean of a minimum of three experiments; ^b IC₅₀ values measured by potentiometric titration method; ^c Maximum exposure time for each compound; ^d Not determined

Table 10: Inhibition mechanisms and maximum inhibition time of novel compounds

Compound	Mechanism of inhibition ^a		Maximum inhibition time ^b	
	<i>hAChE</i>	<i>AgAChE1</i>	<i>hAChE</i>	<i>AgAChE1</i>
124	reversible	reversible	5	5
125	reversible	reversible	5	5
126	irreversible	irreversible	15	40
127	reversible	irreversible	5	15

132	reversible	reversible	5	5
133	reversible	n.d. ^c	5	5
134	reversible	irreversible	5	15
135	irreversible	reversible	5	44
paraoxon	irreversible	irreversible	60	60
bendiocarb	irreversible	irreversible	15	40
carbofuran	irreversible	irreversible	35	75

^a Mechanism of inhibition was determined by using a rapid jump dilution assay; ^b Maximum exposure time for each compound; ^c Not determined

3.3.4 Second subset of insecticides

The prepared insecticides were evaluated only for their inhibitory activity on *hAChE*, *hBChE*, and *AgAChE1* (Table 11).

Table 11 The inhibitory effect of novel compounds and standards on *hAChE*, *hBChE*, and *AgAChE1*.

Compound	IC ₅₀ ± SEM (μM) ^a		
	<i>hAChE</i>	<i>AgAChE1</i>	<i>hBChE</i>
150	4.9 ± 0.5	> 100	> 100
151	> 100	> 100	> 100
152	> 100	> 100	> 100
153	0.6 ± 0.01	> 100	> 100
154	> 100	> 100	> 100
155	> 100	> 100	> 100

^a IC₅₀ values measured by modified Ellman's assay [143]. The results are expressed as the mean of at least three experiments

3.3.5 Mono-quaternary permanently charged AChE reactivators

We have established reactivation potency of novel reactivators (Figure 22) towards OP-inhibited AChE. Sarin, VX, and tabun were selected as common NAs. Dichlorvos and paraoxon were taken as OP-based insecticides. The reactivation potencies were compared with pralidoxime, trimedoxime, obidoxime, and asoxime (Figures 23–27). Selected reactivators were also evaluated on OP-inhibited butyrylcholinesterase (BChE) and compared with obidoxime (Figure 28). The inhibitory ability of novel compounds on AChE is presented in Table 12 in section 3.2.5. We have predicted their ability to penetrate the blood-brain barrier (BBB) to select the best compounds in the series. The non-cellular model PAMPA and the cell-based model using MDCK cells were used for this evaluation (Table 13). Further, the potential cytotoxicity of all our reactivators was also determined by using an *in vitro* MTT test (colorimetric assay for the assessment of cell metabolic activity) (Table 12).

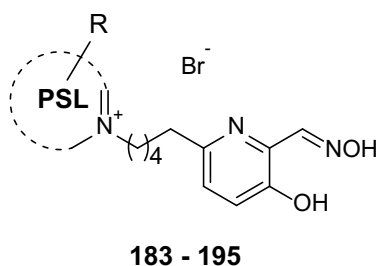


Figure 22 General structure of mono-quaternary AChE reactivators.

Table 12 Prepared mono-quaternary reactivators with predicted solubility, *ClogP*, *in vitro* determined AChE IC₅₀, and SH-SY5Y cytotoxicity IC₅₀ values.

Structure	PAS ligand	R	Predicted solubility (logS _{7.4}) ^a	<i>ClogP</i> ^a	AChE IC ₅₀ (μM) ± SEM ^{b,c}	SH-SY5Y IC ₅₀ (mM) ± SEM ^c
183	isoquinolinium	-	-2.5	-0.1	10.3 ± 0.3	0.72 ± 0.05
184	isoquinolinium	1-Ph	-4.7	1.5	165.8 ± 0.8	0.36 ± 0.05
185	quinolinium	7-NH ₂	-2.2	-0.9	2.1 ± 0.1	0.64 ± 0.03
186	isoquinolinium	7-NH ₂	-2.3	-0.9	12.9 ± 0.8	1.17 ± 0.16
187	isoquinolinium	7-NH ₂ -1-Ph	-4.5	0.6	10.3 ± 0.8	0.22 ± 0.01

188	isoquinolinium	5-CONH ₂	-3.0	-1.3	51.1 ± 9.9	> 1.3
189	isoquinolinium	4-CONH ₂	-3.0	-1.3	2.8 ± 0.2	1.07 ± 0.25
190	pyridinium	4-CONH ₂	-0.8	-2.2	75.0 ± 4.6	1.11 ± 0.05
191	pyridinium	3-CONH ₂	-0.8	-2.2	58.0 ± 3.3	1.17 ± 0.01
192	pyridinium	4-CH ₃	-1.2	-0.6	56.8 ± 4.2	> 1.0
193	pyridinium	4-C(CH ₃) ₃	-2.3	0.5	0.45 ± 0.01	0.87 ± 0.05
194	pyridinium	-	-0.7	-1.1	40.6 ± 1.2	> 1.5
195	pyridinium	4-OH	0.3	-1.4	32.5 ± 1.6	> 0.7
196	pyridinium	4-COOCH ₃	-0.9	-1.1	10.0 ± 0.4	> 1.0
197	pyridinium	4-Ph	-3.0	0.6	8.5 ± 0.5	> 1.3

^a Values calculated by using MarvinSketch software; ^b IC₅₀ values measured by modified Ellman's assay [143]; ^c The results are the mean of a minimum of three experiments

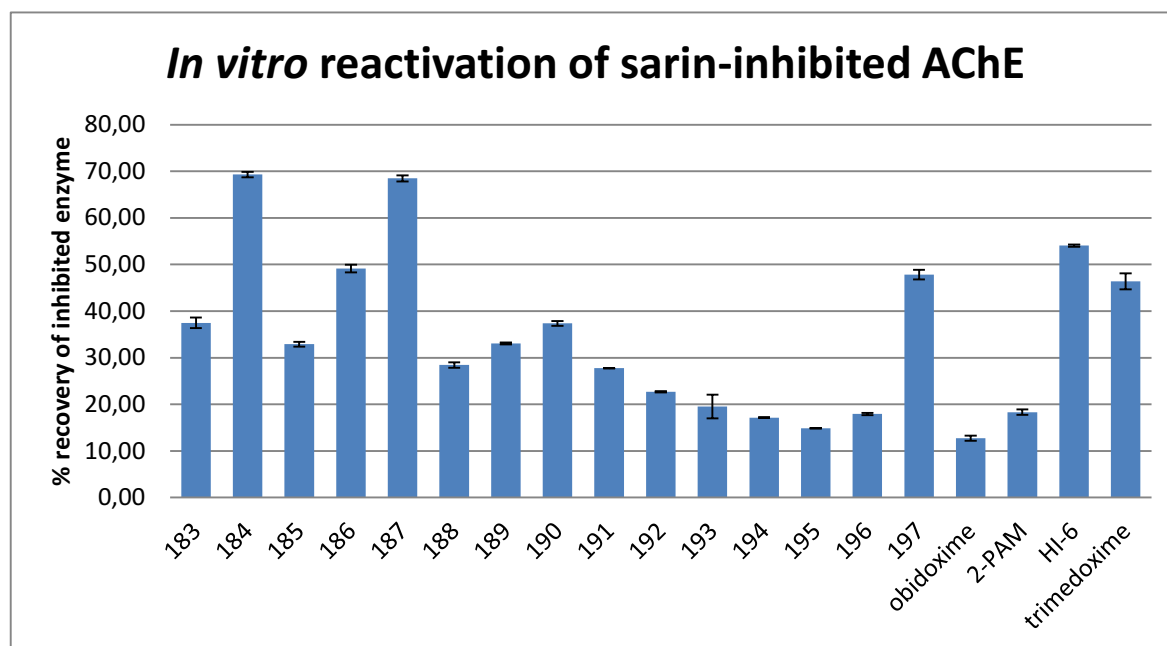


Figure 23 *In vitro* reactivation of sarin-inhibited AChE by 10 μM of the test compound.

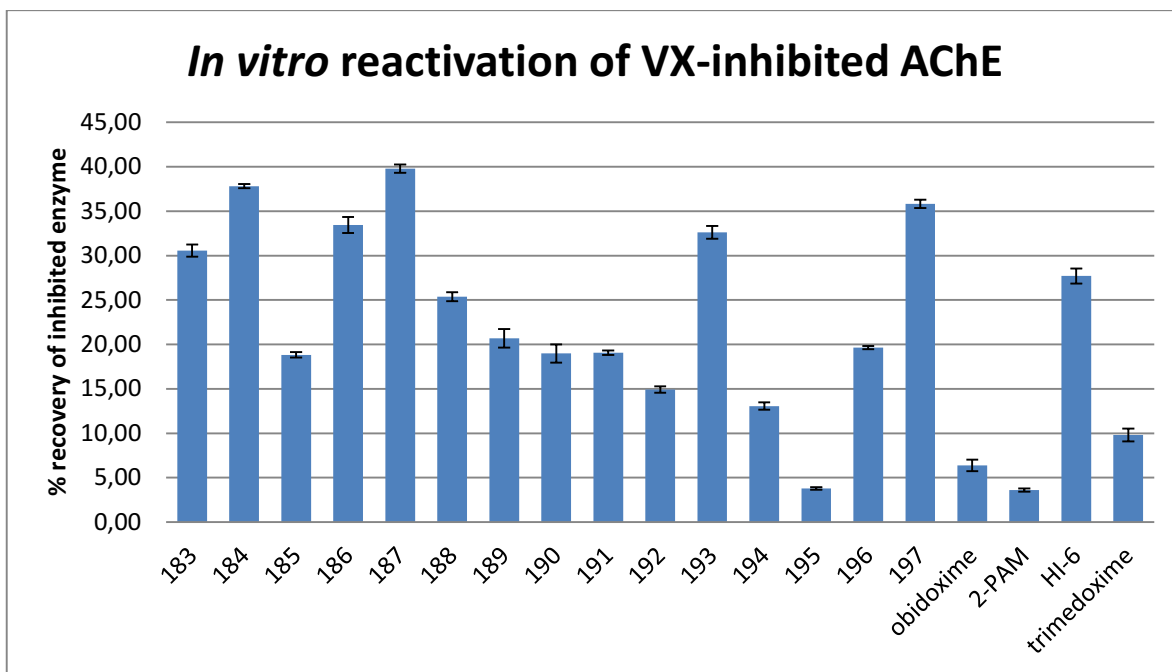


Figure 24 *In vitro* reactivation of VX-inhibited AChE by 10 μ M of the test compound.

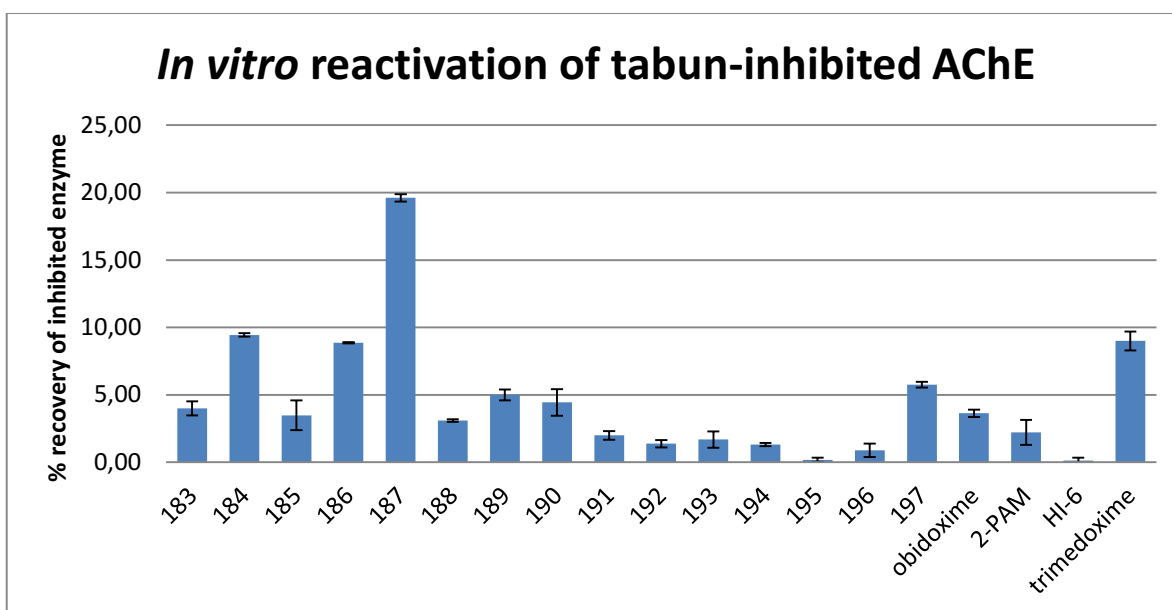


Figure 25 *In vitro* reactivation of tabun-inhibited AChE by 10 μ M of the test compound.

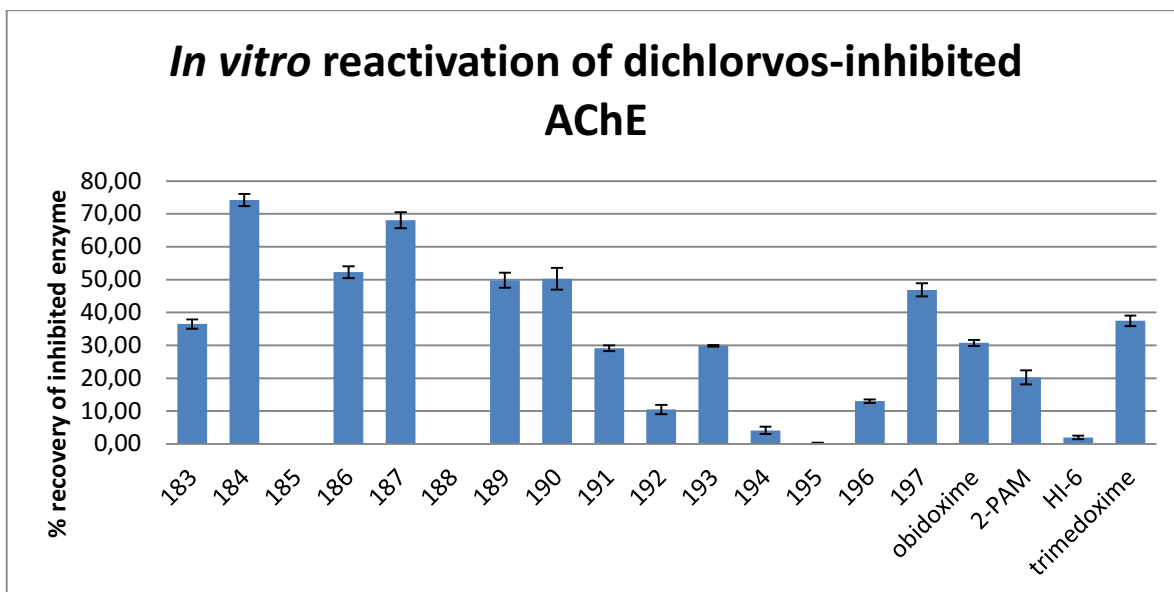


Figure 26 *In vitro* reactivation of dichlorvos-inhibited AChE by 10 μ M of the test compounds.

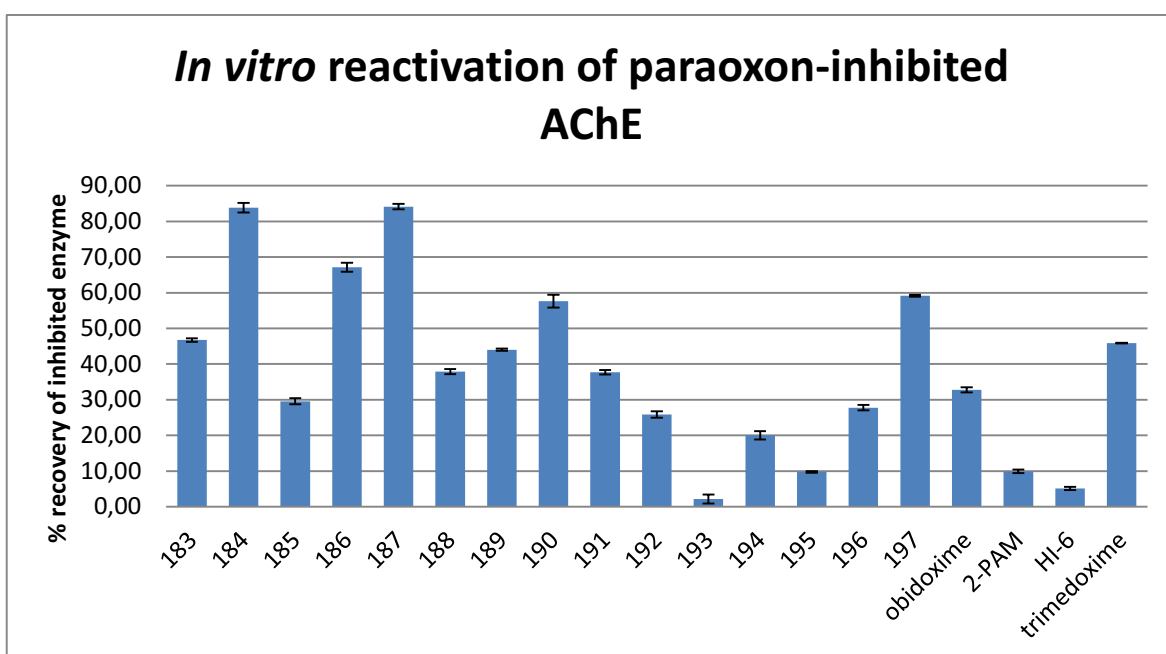


Figure 27 *In vitro* reactivation of paraoxon-inhibited AChE by 10 μ M of the test compounds.

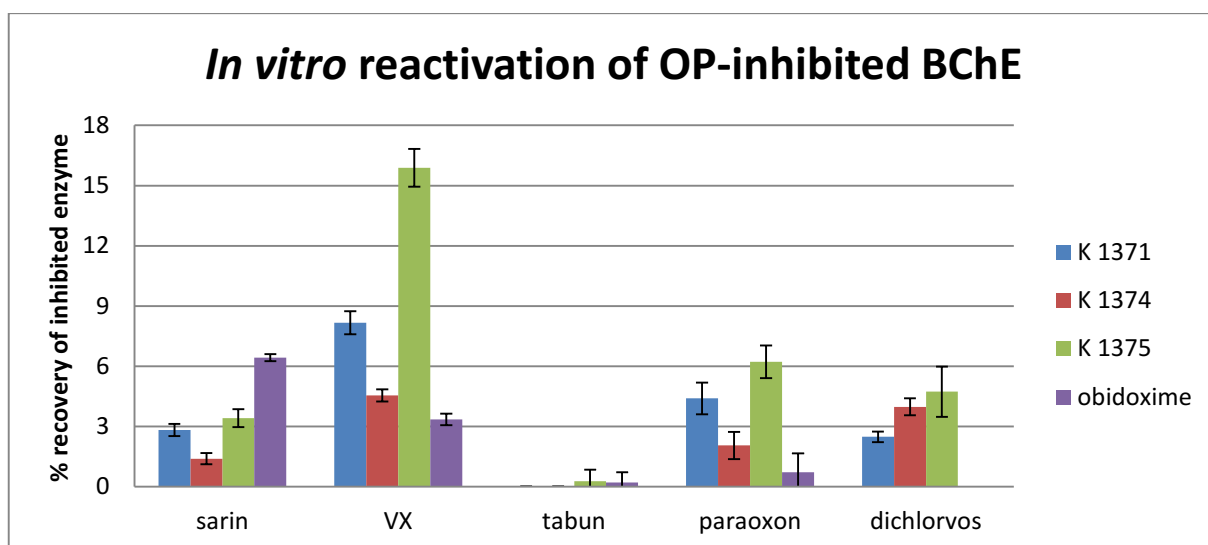


Figure 28 *In vitro* reactivation of OP-inhibited BChE by 10 μ M of the test compounds.

Table 13. Pampa and MDCK determination of potential BBB penetration ability.

Compound	BBB Penetration Estimation		CNS (+/-) ^c
	Pampa assay Pe \pm SEM ($\times 10^{-6}$ cm s ⁻¹) ^b	MDCK Papp \pm SEM ($\times 10^{-6}$ cm s ⁻¹) ^b	
184	0.00	0.00	-
186	0.57	0.28	-
187	0.37	n.d. ^a	-
190	0.48	n.d.	-
197	0.00	n.d.	-
obidoxime	0.68	1.00	-
trimedoxime	0.07	0.40	-
pralidoxime	0.36	0.00	-
asoxime	0.84	0.00	-

^a n.d. - not determined; ^b The results are expressed as the mean of a minimum of three experiments; ^c CNS + (high BBB permeation predicted): Papp or Pe ($\times 10^{-6}$ cm s⁻¹) > 4.0; CNS - (low BBB permeation predicted): Papp or Pe ($\times 10^{-6}$ cm s⁻¹) < 2.0; CNS +/- (BBB permeation uncertain): Papp or Pe ($\times 10^{-6}$ cm s⁻¹) from 4.0 to 2.0.

3.3.6 Tacroximes

Both tacroximes (**tacroxime 1** and **tacroxime 2**, corresponding to **204** and **208**, respectively) were evaluated *in vitro* for ability to reactivate *hAChE* or *hBChE* inhibited by sarin, VX, tabun, paraoxon, and dichlorvos. The potencies were compared with the clinically used standards, pralidoxime and obidoxime (Figure 29). Further, the tacroximes were inspected for their affinity towards *hAChE* and their potential cytotoxicity to HepG2 cells. Finally, an estimation of BBB penetration was evaluated in MDCK cells (Table 14).

Table 14. The inhibitory activities on *hAChE* and *hBChE*, the cytotoxicity in HepG2 cells, and the prediction of BBB penetration.

Compound	Inhibitory activity		Cytotoxicity	BBB penetration estimation	
	% <i>hAChE</i> inhibition or <i>hAChE</i> IC ₅₀ ± SEM [μM] ^b	<i>hBChE</i> IC ₅₀ ± SEM [μM] ^b	HepG2 ± SEM [μM] ^b	Papp ± SEM (× 10 ⁻⁶ cm s ⁻¹) ^b	CNS (+/-) ^c
tacroxime 1	30% at 100 μM	no inhibition at 100 μM	162 ± 9.4	9.10 ± 2.46	+
tacroxime 2	112.1 ± 12.0	no inhibition at 100 μM	335 ± 21	4.04 ± 0.66	+
pralidoxime	217.0 ± 17.0	138.0 ± 12.0	25,680	0	-
obidoxime	197.0 ± 8.0	5440.0 ± 552.0	4,280	1.0 ± 0.3	-
tacrine	0.32 ± 0.013	0.0881 ± 0.0013	168 ± 3.6	25.40 ± 3.4	+
<i>N</i>-acetyltacrine	96.2 ± 9.8	13% at 100 μM	n.t. ^a	n.t.	n.t.
7-methoxytacrine	10.0 ± 1.0	17.6 ± 0.8	44.4 ± 3.4	17.19 ± 3.56	+

^a n.t. – not tested; ^b IC₅₀ values were measured by modified Ellman's assay [143] and the results are expressed as the mean of a minimum of three experiments; ^c CNS + (high BBB permeation predicted): Papp (× 10⁻⁶ cm s⁻¹) > 4.0; CNS – (low BBB permeation predicted): Papp (× 10⁻⁶ cm s⁻¹) < 2.0; CNS +/- (BBB permeation uncertain): Papp (× 10⁻⁶ cm s⁻¹) from 4.0 to 2.0.

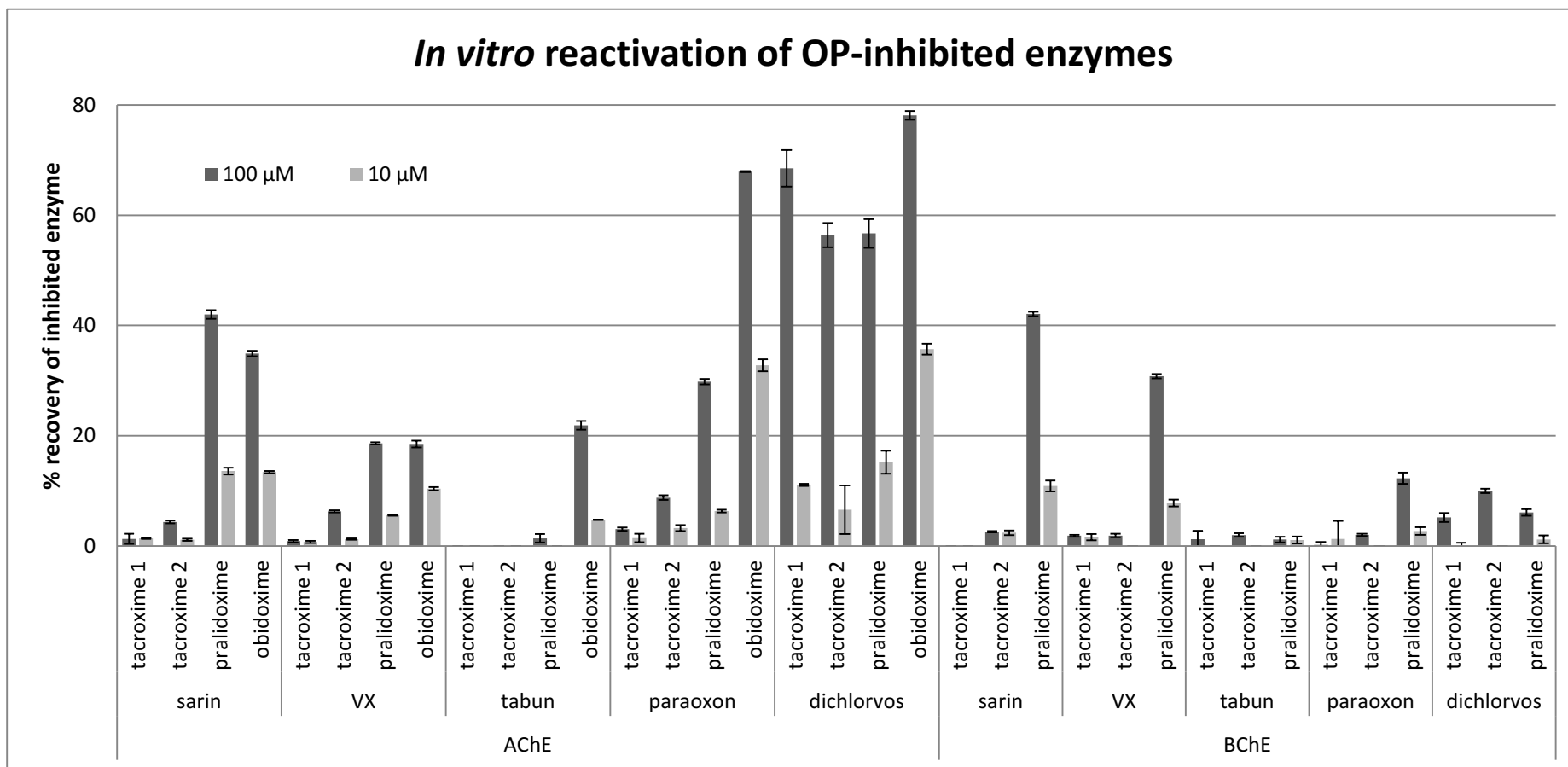


Figure 29 The reactivating potency of 10 μM and 100 μM tacroximes compared with the standards pralidoxime and obidoxime against OP-inhibited *hAChE* and *hBChE*.

3.3.7 Uncharged bis-oxime reactivators

The kinetic parameters of novel reactivators were determined in *in vitro* experiments on VX-, sarin-, paraoxon-, and cyclosarin-inhibited *hAChE* (Tables 15, 16, and 17). The following parameters were evaluated: K_{ox} (mM), describing the affinity of the reactivator towards the OP-AChE conjugate (Table 17); k_2 (min^{-1}), characterizing the ability of the oxime to cleave the covalent bond between the enzyme and OP (Table 16); and k_r , describing the velocity of whole reactivation process (Table 15). In Figures 30 and 31, the kinetics of the reactivation process are shown at three different concentrations (0.1 mM, 0.5 mM, and 1.0 mM). Finally, Table 18 shows the experimental determination of the physicochemical properties: pK_a value, $\log D_{7.4}$, and $\log P_{neutral}$. Note that many of the results are missing and will be completed for the planned publication. Missing values are indicated by a dash.

Table 15 *In vitro* experimental determination of the kinetic parameter k_r .

oxime	k_r ($\text{M}^{-1}\text{min}^{-1}$)			
	OP			
	VX	POX	sarin	cyclosarin
229 (LG-700)	1,100	9	530	120
230 (LG-703)	1,200	33	780	190
233 (LG-747)	4,600	13	1,070	84
231 (LG-750)	1,100	30	1,000	190
234 (LG-804)	2,600	- ^a	1,300	160
235 (LG-823)	810	-	1,300	183
236 (LG-829)	1,700	-	1,500	-
RS194B	840	45	550	180

^a not yet tested

Table 16 *In vitro* experimental determination of the kinetic parameter k_2 .

oxime	k_2 (min^{-1})
-------	-----------------------------

	OP			
	VX	POX	sarin	cyclosarin
229 (LG-700)	190	- ^a	0.27	-
230 (LG-703)	1,400	-	1.30	-
233 (LG-747)	390	-	0.46	-
231 (LG-750)	1,400	-	0.83	-
234 (LG-804)	1,100	-	1.50	-
235 (LG-823)	18,000	-	1.00	-
236 (LG-829)	3,200	-	2.90	-
RS194B	1,000	-	2.10	-

^a not yet tested

Table 17 *In vitro* experimental determination of the kinetic parameter K_{ox} .

oxime	K_{ox} (mM)			
	OP			
	VX	POX	sarin	cyclosarin
229 (LG-700)	0.17	- ^a	0.51	-
230 (LG-703)	1.10	-	1.70	-
233 (LG-747)	0.085	-	0.43	-
231 (LG-750)	1.30	-	0.82	-
234 (LG-804)	0.41	-	1.10	-
235 (LG-823)	22.0	-	0.78	-
236 (LG-829)	1.90	-	1.90	-
RS194B	1.20	-	3.90	-

^a not yet tested

(hAChE-Sarin) + LG oximes

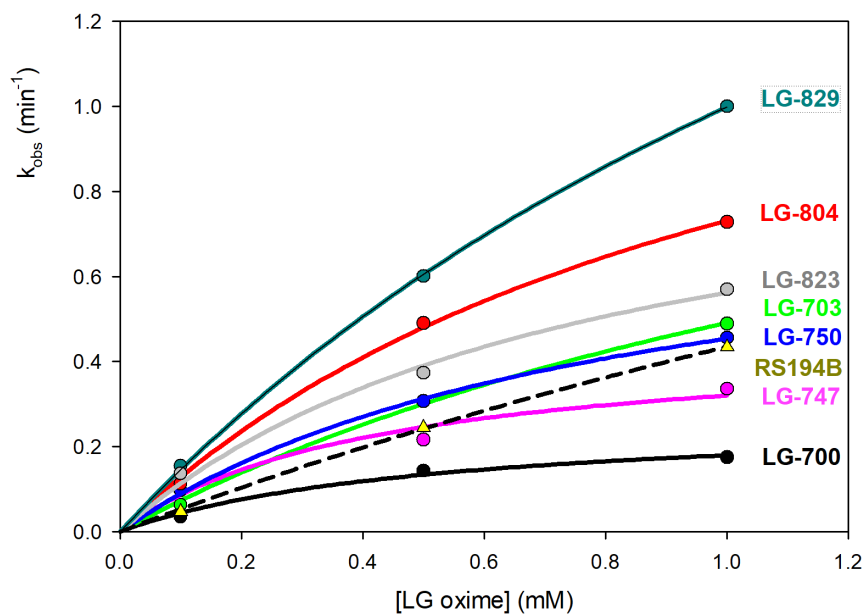


Figure 30 Reactivation kinetics of AChE inhibited by sarin measured at three concentrations (0.1 mM, 0.5 mM, and 1.0 mM).

(hAChE-VX) + LG oximes

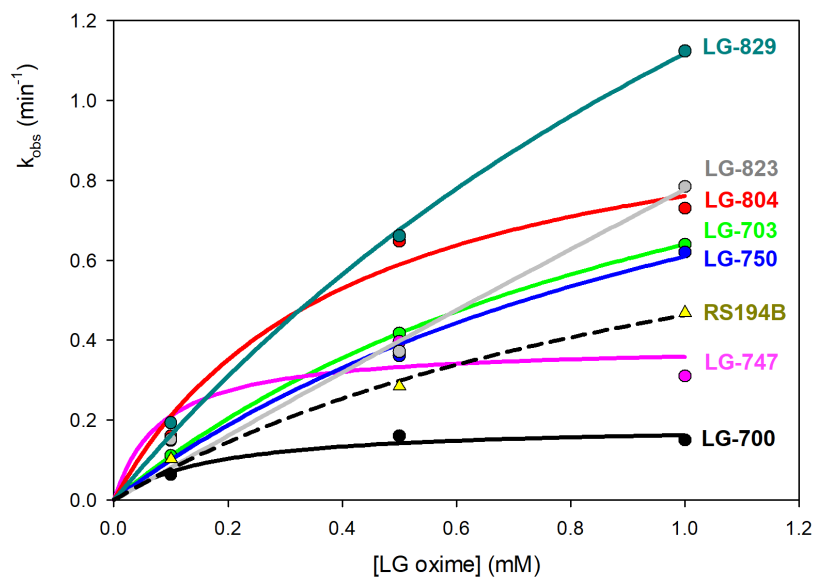
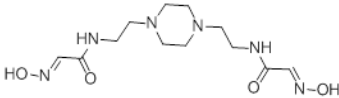
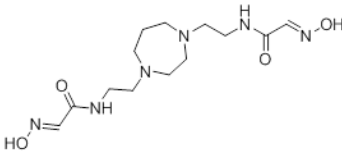
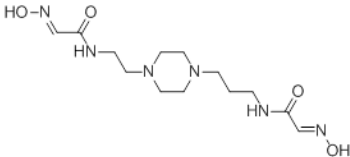
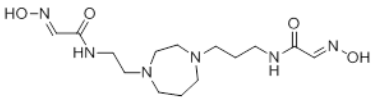
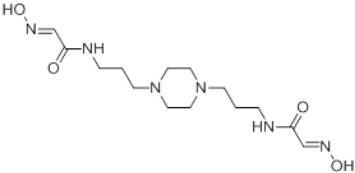
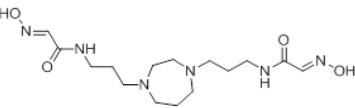
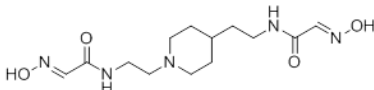
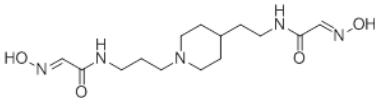
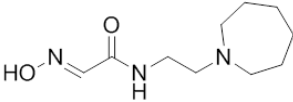


Figure 31 Reactivation kinetics of AChE inhibited by VX measured at three concentrations (0.1 mM, 0.5 mM, and 1.0 mM).

Table 18 Experimental determination of pK_a , $\log D_{7.4}$, and $\log P_{\text{neutral}}$.

Name	Structure	Sirius pK_a	Sirius $\log D_{7.4}$	Sirius $\log P_{\text{neutral}}$
229 (LG-700)		Acid 1: 8.72 Acid 2: 9.23 Base 1: 2.87 Base 2: 7.16	-0.55	-0.34
230 (LG-703)		Acid 1: 8.80 Acid 2: 9.43 Base 1: 4.51 Base 2: 7.96	-1.44	-0.77
231 (LG-750)		Acid 1: 8.72 Acid 2: 9.39 Base 1: 3.17 Base 2: 7.42	-1.42	-1.10
236 (LG-838)		- ^a	-	-
233 (LG-747)		Acid 1: 8.77 Acid 2: 9.42 Base 1: 3.69 Base 2: 7.67	-1.16	-0.70
234 (LG-804)		Acid 1: 8.99 Acid 2: 9.59 Base 1: 5.25 Base 2: 8.35	-1.45	-0.61
235 (LG-823)		Acid 1: 8.90 Acid 2: 9.45 Base 1: 8.17	-0.52	-0.62

236 (LG-829)		-	-	-
RS194B		Acid 1: 9.66	-	-
		Base 1: 8.56		

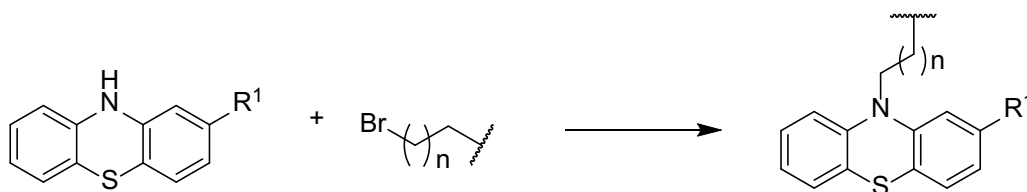
^a not yet tested

4. Discussion

4.1 Synthesis

4.1.1 Tacrine-phenothiazine derivatives

Reductive amination was used to provide a more sophisticated synthetic approach. Indeed, the derivatives could be prepared by simple consecutive *N*-alkylation reactions (see Scheme 23 for alternative approaches). However, *N*-alkylation often leads to several side products. In this case, we used acetals and TES as the core reactants. Reductive amination is commonly described as the reaction of an aldehyde with a primary or secondary amine. Sodium borohydride or sodium cyanoborohydride are often depicted as reductive agents. In contrast, such reactions processes are many times described with aliphatic amines. The conditions for the reaction were taken from the study [144] and the desired products **14–25** were obtained with good yields (over 80%). Another benefit in this case lies in the use of the more stable acetal instead of reactive and unstable aldehydes.



Scheme 23 The alternative reaction to the originally used reductive amination.

The challenging step was the preparation of the corresponding acetal intermediates of the derivatives bearing five methylene linkers. Initially, we started from 5-aminovaleric acid; however, none of the amino protective groups was suitable for the reduction of carboxylic acid or the corresponding methyl ester to aldehyde. Therefore, we switched to 5-aminopentan-1-ol and selective oxidation to the aldehyde. Unfortunately, the *tert*-butoxy carbonyl (Boc) or carboxybenzyl (Cbz) protective groups again did not afford the aldehyde in Swern or IBX oxidation conditions. Finally, the phthalimide protective group was determined as the most suitable option. Swern oxidation of the aldehyde led to the desired product without any decomposition of the protective group. The subsequent reaction to acetal proceeded without any difficulties.

The preparation of alkylated tacrine derivatives is always a difficult task. In the literature, it was often described to occur under reflux conditions in phenol for several

hours, resulting in rather poor yields [21]. In this study, we performed an optimization using MW irradiation. Indeed, the full conversion was completed in 90 min, with yields of approximately 50%.

4.1.2 Tacrine derivatives with dual-targeting of AChE and the NMDA receptor

Herein, we presented an optimized, highly efficient synthesis of several tacrine derivatives by a single one-step reaction. We also suggested that this approach could be used on any tacrine derivatives if the corresponding 2-aminobenzonitrile is available. The Friedländer type condensation (using LA) for tacrine formation is already well established in the literature. The overnight reflux reaction in 1,2-dichloroethane with excellent yields (72%–95%) was recently described [145]. Another approach, a solvent-free reaction under standard conditions at 130°C, leads to the desired product with poor to good yields (20% to 60%) [64].

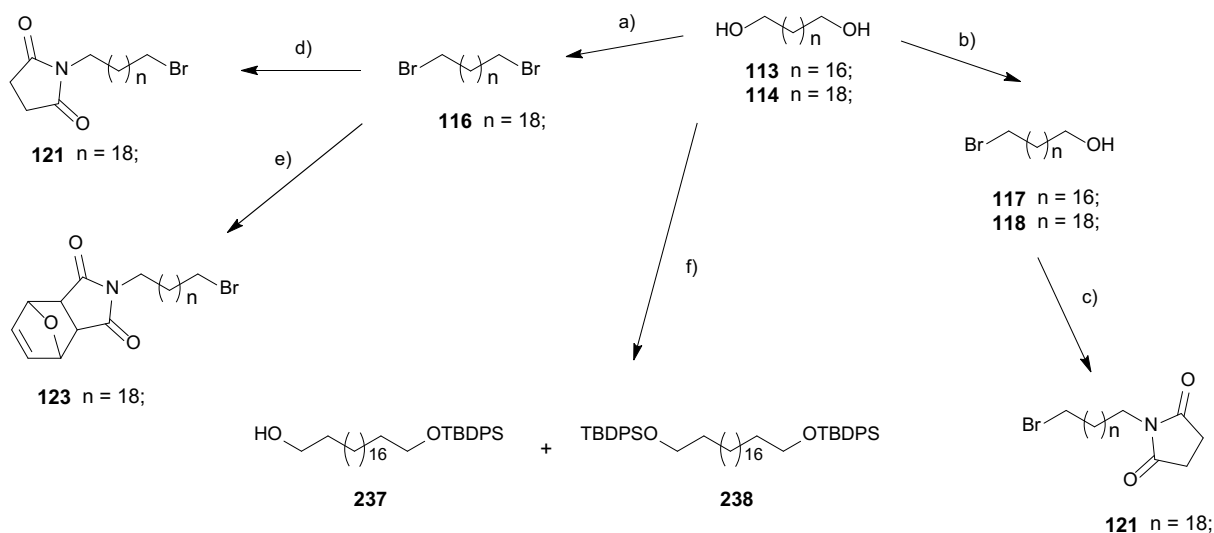
In our case, we decided to use MW irradiation to speed up the reaction. Indeed, the full conversion was completed in less than 10 minutes. Moreover, the solvent-free reaction exhibited mostly excellent yields of over 80%. We also found that not all LAs were as efficient. In some cases, ZnCl₂ led to no reaction at all. Mainly, in the case of the reaction with cyclopentanone, stronger LAs had to be used. Conversely, AlCl₃ always yielded a complete reaction.

4.1.3 AChE-targeting insecticides

The authors of the original work Dou et al. [132] did not fully describe the preparation of bromoalkyl-1-alcohol. We decided to propose a different and more straightforward approach. We applied findings from a previous study and obtained the corresponding alkanyldiols in excellent yields after three steps [138].

Subsequently, the challenging step was the selective protection of one of the hydroxyl group to successively and selectively precede towards the next step i.e. the formation of alkylating agent. Initially, this task was attempted by reaction with *tert*-butyl(chloro)diphenylsilane (TBDPSCI) [146]. Indeed, under basic conditions, mono-silylated and bis-silylated intermediates were isolated with the unsatisfied ratio 2:1, respectively, and 25% of the starting material turnover. The conditions of the reaction were extensively modified to increase selectivity for the mono-protected

adduct. However, these endeavors were fruitless. In contrast, the deprotection of the bis-silylated product with tetrabutylammonium fluoride (TBAF) yielded only the mono-silylated product. Therefore, we considered that protection might represent a “blind” step in this approach and decided to proceed directly to the alkylating agents (Scheme 24).

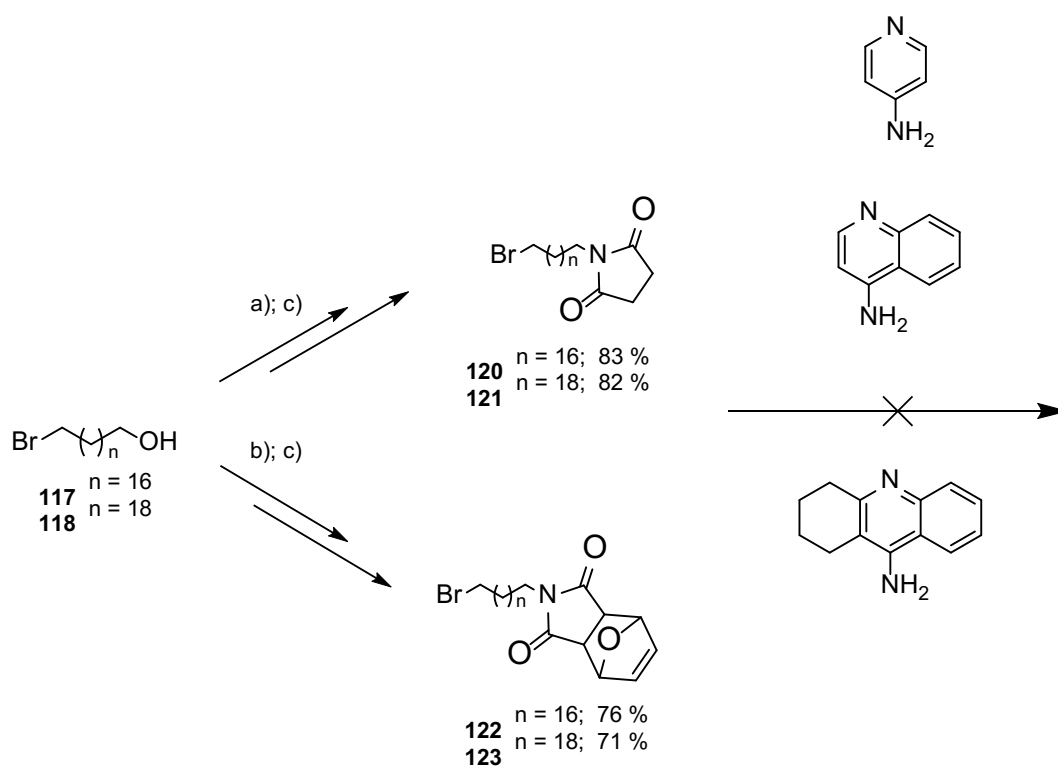


Scheme 24 Alternative pathways towards asymmetrical intermediates. Reagents and conditions: a) NBS, PPh₃, THF, RT; b) HBr 48% solution in H₂O, toluene, reflux; c) DIAD, PPh₃, THF, 0 °C – RT; d) succinimide, K₂CO₃, DMF, 60°C; e) imide **119**, K₂CO₃, DMF, 60°C; f) TBDPSCI, DIPEA, DMF, RT.

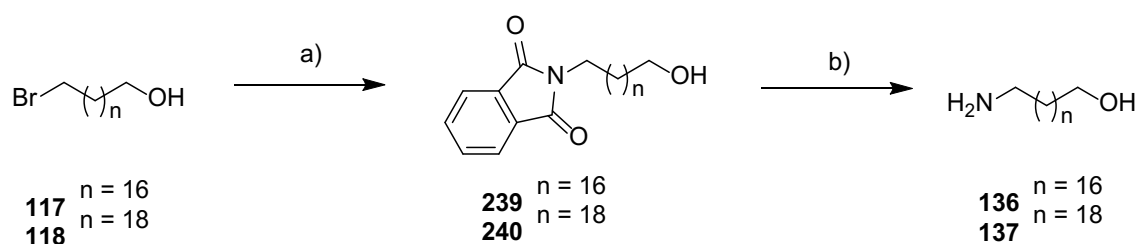
After several unsuccessful attempts we decided to use HBr for monobromination (HBr has also been employed in a previous work) (Scheme 24). The reactions were similar to those published [132]. In contrast, we simplified the original procedure by skipping the isolation of the alcohol intermediate and proceeding directly to bromination. We also used succinimide for analogical *N*-alkylation, as for **119**. In this way, we achieved better yields and avoided further reduction of the maleimide into the succinimide scaffold. Such a reduction was described in original work. Our final steps are slightly distinct from those reported, with different conditions and the implementation of MW irradiation. Note that the compounds **132** and **133** correspond to those the codenames **PM18** and **PM20**, the compounds **125**, **134**, and **126** are analogical to **PMS20**, **PY18**, and **PYS18**, respectively (only the salt is different) [132]. This is the first report of compounds **124**, **127**, and **135**.

4.1.4 Second subset of insecticides

Initially, we tried an analogical pathway to that for the first series (Scheme 25). However, our attempts were unsuccessful. Therefore, we had to design an alternative route. To overcome this situation, we invented a novel one-pot amination reaction. Indeed, ω -bromoalkane-1-ol was transformed into the corresponding ω -aminoalkane-1-ol in one step. The reaction was performed with MW irradiation and is presented in Scheme 26. Initially, *N*-alkylation of phthalimide required 6–8 hours, hydrazine was introduced, and the reaction was stirred for 1 hour further for full completion with quantitative yields. Another issue was the bromination reaction; this time, the Appel reaction was used instead of NBS bromination.



Scheme 25 Straightforward attempts for the synthesis of the second subset of insecticides. Reagents and conditions: a) succinimide K_2CO_3 , DMF, 60°C ; b) imide **119**, K_2CO_3 , DMF, 60°C ; c) NBS; PPh_3 , THF, RT.



Scheme 26 The one-pot amination. Reagents and conditions: a) one pot reaction, potassium phthalimide for 8 h at 110°C with MW irradiation; b) $\text{NH}_2\text{NH}_2 \cdot \text{H}_2\text{O}$ for 1 h at 90°C with MW irradiation.

The major issue arose in the last steps for the maleimide derivatives. These final products are unstable (based on the HPLC-MS analysis; data not shown) and could not be isolated in a pure form. Similarly, tacrine derivatives are more stable than 4-aminoquinolines and 4-aminopyridines, respectively. This presumably results from the steric hindrance around the secondary amine. Indeed, it has already been reported that maleimide could form a covalent bond with amines [147]. Therefore, we concluded that the maleimide analogs could not be prepared.

4.1.5 Mono-quaternary permanently charged AChE reactivators

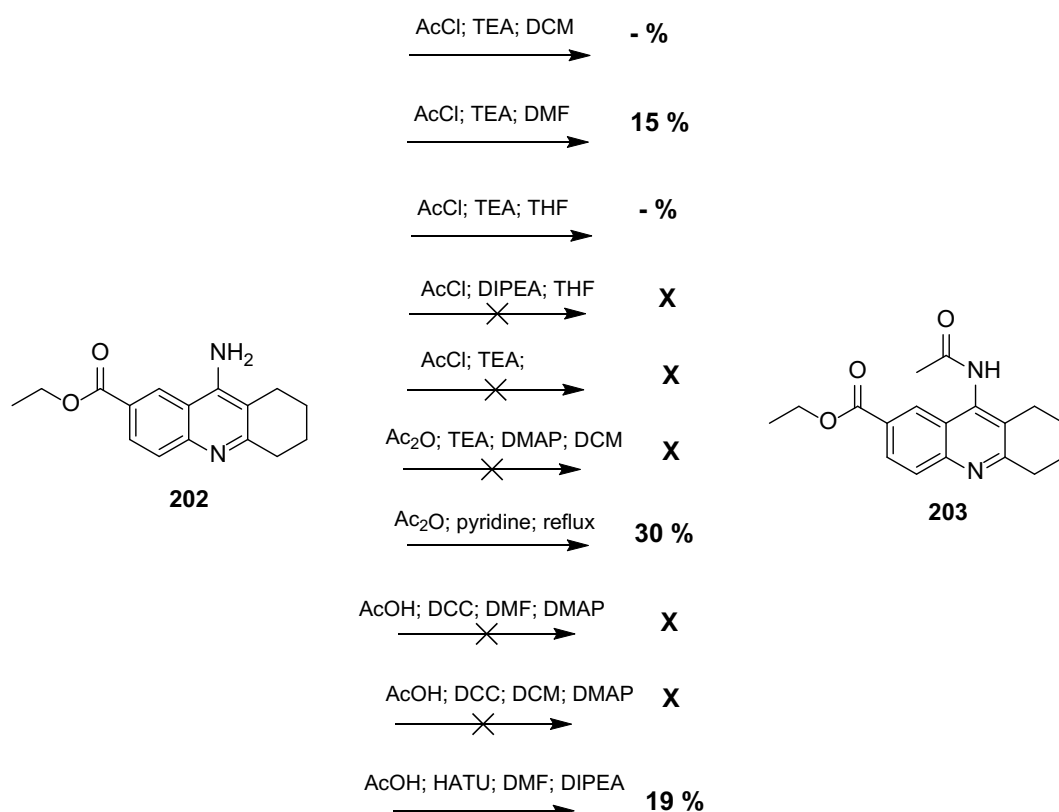
The synthesis of key oxime intermediate was the same as that of a published procedure up to Appel reaction. The authors of the previous work then coupled their compound with some of the various PAS ligands, leading to uncharged compounds [116]. Instead, our subsequent steps were innovative. In particular, the three-step reaction had excellent yields, at over 50%. The overall yield in those 10 steps was an astonishing 25%. Even a large-scale preparation (25 g of starting material) returned excellent yields.

The preparation of PAS ligands was based on common procedures, except for the aromatization step. According to the literature survey, this is the very first report of such a reaction. Indeed, very harsh conditions were needed and several side products were formed. In contrast, the reaction leads to desired intermediate and the subsequent reaction to PAS ligands.

The final step was, in some cases, very problematic and many side-products were formed. After several optimization attempts, MeCN appeared to be the most suitable solvent for the reaction. The most efficient reaction conditions were estimated to be 24 hours, with MW irradiation, at 90°C. A higher temperature led to decomposition of **166** and the product. In the case of quinoline PAS ligands, only the 7-amino derivative **186** was successfully prepared. The reaction was time prolonged, and required more than 96 hours. None of the other investigated quinoline derivatives yielded the desired product, even when other reaction conditions were attempted.

4.1.6 Tacroximes

The preparation of **tacroxime 1** corresponds to the synthesis of 7-MEOTA [148]. The issues arose in the acetylation step. Many procedures were tested (Scheme 27). Overall, the reaction with acetic anhydride appeared to be the best option. Therefore, these conditions were also used for **tacroxime 2**. The procedure for the two-step reaction, reduction and subsequent oxime formation, was used based on our experience with mono-quaternary compounds (see section 3.2.5).

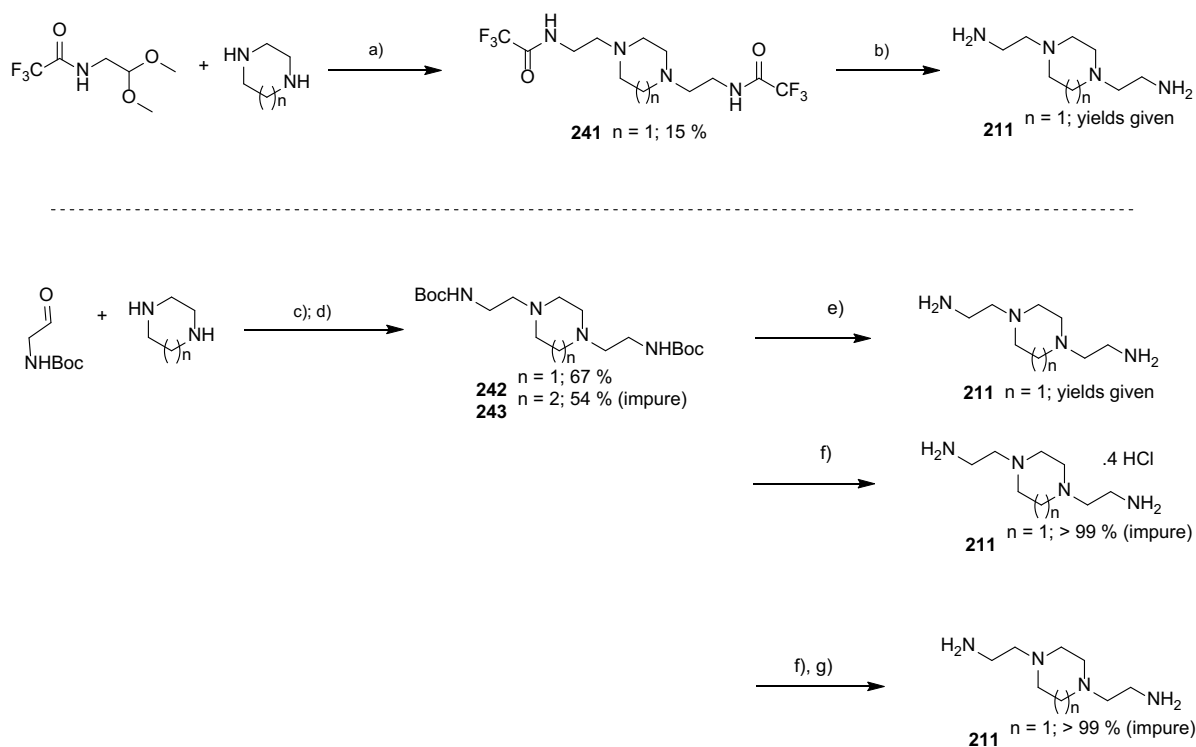


Scheme 27 The different conditions tested for acetylation of 7-substituted tacrine. A dash indicates that yields were given.

The first two reactions of tacroxime were identical to those published previously [142]. The Friedländer type condensation was based on our experiences from NMDA-targeted tacrines (see section 4.1.2). Then, we initially attempted to protect the phenolic group by reaction with *tert*-butyldimethylsilyl triflate (TBDMSOTf); however, no product was formed. Thus, we decided to acetylate both reactive groups (phenolic and aniline group). The subsequent steps were identical to **tacroxime 1**. Note that the phenolic group was acetylated prior to the aniline group.

4.1.7 Uncharged bis-oxime reactivators

The core of the synthesis came from that for RS194B. The preparation of the oxime fragment and definite bis-primary amine intermediate was required. Initially, the compounds with two methylene linkers with central homopiperazine or a piperazine ring were prepared. Our idea originated from the synthesis of THA-PHT derivatives. Indeed, several attempts were performed (Scheme 28). Although the reactions work well, deprotection step always led to an impure product that could not be purified. These impure bis-primary amines **211** did not give any product in the final step. Instead, another approach, similar to one already published [149], led to the desired pure intermediates and to those to final products.



Scheme 28 The alternative approaches for the desired products using reductive amination. Reagents and conditions: a) TES, TFA, DCM, RT; b) K_2CO_3 , MeOH, H_2O , RT; c) MeOH, AcOH, RT; d) MeOH, AcOH, $NaCNBH_3$; e) TFA, DCM, RT; f) MeOH, 4 M HCl in dioxane, RT; g) NH_4OH (25% in H_2O), MeOH, RT.

The problems arose with the longer linker intermediates. 3-Chloropropionitrile and 3-bromopropionitrile could not be used in the same procedure as 2-chloroacetonitrile. Moreover, these molecules could not be heated as they form polyacrylamide. Therefore, the same procedure was performed in the absence of heat and the reaction with TEA in DCM was used instead. Another issue arose from the reduction of nitrile groups to

amines. Again, the reaction did not work properly for the longer linkers. The reduction with LiAlH_4 always led to impure products with poor yields. In contrast, the alternative process using Raney-nickel as reductive agent under H_2 leads to the desired amines. The last step was also problematic. The reaction could not be heated to over 90°C , as side products started to form. The reaction was very slow compared with the synthesis of RS194B and returned only poor yields. One of the final products, **234**, was highly hydrophilic and could not be purified by common silica gel; instead, it was precipitated from MeOH, even though it was soluble in MeOH at RT. The piperidine derivatives **235** and **236** were purified by MeOH alone. All optimizations and alternative approaches using catalysts and/or (2*E*)-2-(hydroxyimino)acetic acid instead of ethyl ester **227** resulted in no product.

4.2 Biological evaluation and structure-activity relationship

4.2.1 Tacrine-phenothiazine derivatives

Initially, the determination of inhibitory activities on enzymes AChE and BChE were inspected. All the compounds **41–76** were potent cholinesterase inhibitors. Some of the compounds displayed nanomolar IC_{50} values, whereas others remained in the micromolar range. Based on the results, we established several SARs for cholinesterases. The superior linkers for AChE activity were those with five methylenes. In contrast, the more efficient linkers for BChE activity were those with two methylenes. Overall, derivatives with five and two methylenes were more active than those with three and four methylenes. 6-Chlorotacrines were more potent than tacrines whereas 7-methoxytacrines were always the least efficient, especially for the AChE enzyme. Based on the selection of the phenothiazine derivative, no clear conclusions could be made from the library of tested compounds for AChE. Only 2-trifluoromethyl derivatives appear to be slightly less efficient than the 2-chloro or phenothiazines alone. For BChE inhibition, a SAR was evident. Trifluoromethyl derivatives were the least efficient following chloro derivatives and the most active was phenothiazines alone. Our SAR assumptions correspond well with the most active derivatives. **70** was selected as the best inhibitor for AChE ($\text{IC}_{50} = 8 \text{ nM}$) with a BChE/AChE selectivity ratio of over 23. The structure of the compound is 6-chlorotacrine connected by five methylenes to phenothiazine. In addition, **41** was

selected as the best BChE inhibitor ($IC_{50} = 19 \text{ nM}$) with an AChE/BChE selectivity ratio of over 107.

Unfortunately, the determined antioxidative activity did not show any significant potency compared to the parent compound phenothiazine ($EC_{50} = 61 \text{ }\mu\text{M}$). Moreover, the viability of HepG2 cells was very low, indicating notable toxicity. However, the BBB penetration estimation showed the potential ability to enter the CNS.

To clearly evaluate the impact of novel compounds (mainly **41** and **70**), further assays must be performed. Indeed, planned neuroprotective determination and anti-tau properties will provide an indication for the potential of these compounds in the treatment of AD.

4.2.2 Tacrine derivatives with dual-targeting of AChE and the NMDA receptors

This series was evaluated only for the inhibitory activity of AChE/BChE. These compounds are primarily focused on modulation of the activity on NMDA receptors; however, such an assay has not yet been performed. The IC_{50} values for AChE and BChE provide some indications. There were no significantly selective BChE inhibitors, whereas 6-methyl derivatives resulted in the highest AChE selectivity. There was no evident SAR for five, six, or seven membered saturated rings. In contrast, the most efficient compound was **96**, which was an 8-chloro derivative with a six-membered saturated ring ($AChE IC_{50} = 33 \text{ nM}$; $BChE IC_{50} = 62 \text{ nM}$).

4.2.3 AChE-targeting insecticides

The concept was based on covalent bond formation with Cys447 in *AgAChE1*, resulting in its irreversible inhibition. Some *in vitro* evaluations were already presented by Dou *et al.* [132]. The inhibitory activity of our insecticides towards *hAChE*, *AgAChE1*, and *hBChE* was determined (Table 8) [143]. Maleimides **132** and **133** were found to be the most potent inhibitors of *AgAChE1*, with IC_{50} values of 87.6 nM and 227 nM. Moreover, the selectivity for *AgAChE1* over *hAChE* of compound **132** was 100. Both compounds (**132** and **133**) were found to irreversibly inhibit *AgAChE1*. The compounds containing both maleimide and piperidine scaffolds (**134** and **135**) were found to be very efficient inhibitors of *AgAChE1*, with no determined inhibition of the

human enzymes ($IC_{50} >100 \mu\text{M}$), and thus valuable selectivity for *AgAChE1*. The compounds with a succinimide scaffold (**124–127**) resulted in inconsistent and structure-related inhibition ability that was significantly lower than the presented maleimides. There was almost no activity against *hBChE*. The potentiometric titration using ACh as a substrate was conducted to elucidate whether the thiol moiety in the ATCh substrate may influence the determination of the prepared compounds. All data showed that the IC_{50} values obtained from both methods were very similar (see section 3.3.3; Table 9).

As expected, the succinimide derivatives (**124–127**) showed, in all cases, reversible inhibition of *AgAChE1* (Table 10). For the piperidine and pyridinium scaffolds, the quaternary compounds showed significantly greater affinity towards both anionic sites of the enzyme [150, 151]. The hypothesis that the compounds would act reversibly against *hAChE* and irreversibly against *AgAChE1* was not confirmed [132]. In contrast with the formerly published molecules, two of the novel compounds (**132** and **135**) presented unexpected actions and displayed the irreversible inhibition of *hAChE*. It was previously reported that the maleimide residue should be able to form a covalent bond with amino acids residues other than Cys [147]. Therefore, the interaction with His447 from the catalytic triad of *hAChE* may irreversibly inhibit the enzyme.

A docking study was performed to improve our understanding of the binding interactions between the best compound **134** and the *AgAChE1* active site (PDB ID: 5YDH) (Figure 13). Molecule **134** shows dual binding. Most importantly, it interacts hydrophobically with Cys447. These findings support the binding of the maleimide moiety of **134** to the Cys residue; that is, the formation of a covalent bond with its thiol group.

4.2.4 Second subset of insecticides

This synthesis of this series was unsuccessful. Indeed, only succinimide derivatives were prepared; therefore, no selectivity was observed. Moreover, no activity was shown against *AgAChE1* and *hBChE*. Only tacrine derivatives showed some activity against *hAChE*.

4.2.5 Mono-quaternary permanently charged AChE reactivators

All *in vitro* evaluations of the reactivating ability indicated the superior efficiency of some of our molecules compared with the standard reactivators. Moreover, our three best compounds (**184**, **187**, and **190**) showed broad-spectrum ability. For sarin- and VX-inhibited enzymes, HI-6 is considered the best reactivator available. In the case of sarin inhibition, **184** and **187** significantly surpassed HI-6. In the case of VX inhibition, six reactivators were superior. Tabun is considered as the most difficult NA to achieve reactivation from, with trimedoxime appearing to be the only efficient standard compound [152]. The oxime **187** was almost twice as efficient as trimedoxime for the reactivation of tabun-inhibited AChE.

The OP-based pesticides yielded similar results. For dichlorvos and paraoxon, six and five compounds, respectively, were significantly superior to the most potent clinically used standards (trimedoxime or obidoxime). The three best reactivators were further evaluated for the reactivation of OP-inhibited BChE and compared with obidoxime. Obidoxime was more effective than our compounds only in the case of sarin-inhibited BChE. In VX, dichlorvos, and paraoxon inhibition, our compounds were significantly superior to obidoxime. Almost no activity was shown in tabun-inhibited BChE.

Subsequently, the five best compounds were estimated for their potential ability to cross the BBB. Unfortunately, all compounds, including the standards, were able to cross MDCK cell line. However, the compounds were essentially not cytotoxic. Herein, we have presented the best reactivators ever synthesized; however, further *in vivo* assays are required to confirm the encouraging *in vitro* results.

4.2.6 Tacroximes

The expected results were obtained for the determination of inhibition potency. Both tacroximes exhibited only very poor-to-moderate activity towards both cholinesterases; these efficiencies were similar to, or even lower than the clinically used reactivators or tacrines. Tacrine is known to be hepatotoxic. Our evaluations showed that tacroximes were similarly or less toxic. Moreover, the major hepatotoxicity of tacrine is based on its metabolites after biotransformation processes [153, 154]. The CNS MPO predictions showed good prognosis for BBB penetration. This assumption was also supported by assays in MDCK cells. In contrast, under the same conditions,

pralidoxime and obidoxime were not effective. Therefore, we achieved one of our goals for centrally active drugs.

Finally, the reactivation potency of NA- and pesticide-inhibited *h*AChE and *h*BChE was inspected. Unfortunately, there were no significant efficiencies in the reactivation of NA-inhibited cholinesterase compared with the efficacies of pralidoxime and obidoxime. A reactivation potential was revealed in the case of dichlorvos-inhibited enzyme. Specifically, the reactivating ability was comparable with that 100 μ M obidoxime; note that obidoxime is still considered to be the best reactivator available against pesticides poisoning [155].

The relatively poor reactivation ability of tacroximes to various OPCs may be explained by their bulkiness. This may be surprising, because the preliminary molecular modeling simulations indicated their favorable orientation inside the cavity gorge. The constricted and narrow mid-gorge region of enzyme might represent major obstacles for tacroximes to approach the site of reactivation [156]. The efficiency in dichlorvos-inhibited AChE is probably based on the structural form of the conjugate. As the residue attached to the phosphorous atom is the methoxy group, which is undoubtedly less bulky than other OPC appendages, there is more space for the reactivator. Therefore, even bulkier compounds such as tacroximes could better fit into the CAS and easily attack the phosphorous atom.

Overall, although, the use of dichlorvos for pest control has already ceased in Europe and the USA, it is still in practice elsewhere [157]. Therefore, tacroximes (specifically **tacroxime 1**) may become centrally active candidate for the dichlorvos intoxication.

4.2.7 Uncharged bis-oxime reactivators

For this series, a more complex *in vitro* assay was selected. The evaluations of the kinetic parameters provided more clues about the reactivating abilities of the compounds and the simple percentage restoration of enzyme. Previously, only sarin and VX-agent had been fully investigated for seven of the final products. From these investigations, we made some conclusions. When the results on the central rings were compared, piperidine derivatives were superior to homopiperazines and piperazines.

Piperazine compounds were the least potent reactivators. With regard to the length of linkers, the results favored diverse linkers; three methylenes were more potent than two methylenes (mainly based on piperazine derivatives). Several novel compounds were more potent than the parent RS194B, particularly compounds **234** and **236**.

The k_r values describing the whole reactivation process indicate that the best compound for the VX-inhibited enzyme is **233**; however, these results were quite inconsistent and further evaluation is needed for confirmation. In contrast, **234** and **236** surpassed RS194B by almost three times for the sarin- and VX-inhibited enzyme. The K_{ox} values were determined to describe the affinity towards the OP-AChE conjugate. As expected, for the VX-inhibited enzyme, almost all novel compounds (except piperidine derivatives and **231**) had higher affinity than RS194B. Furthermore, they also had the weakest affinity for sarin-inhibited enzyme. Increased affinity towards the OP-AChE conjugate may result in improved reactivation ability *in vivo*. To confirm the best candidate, the results had must be completed.

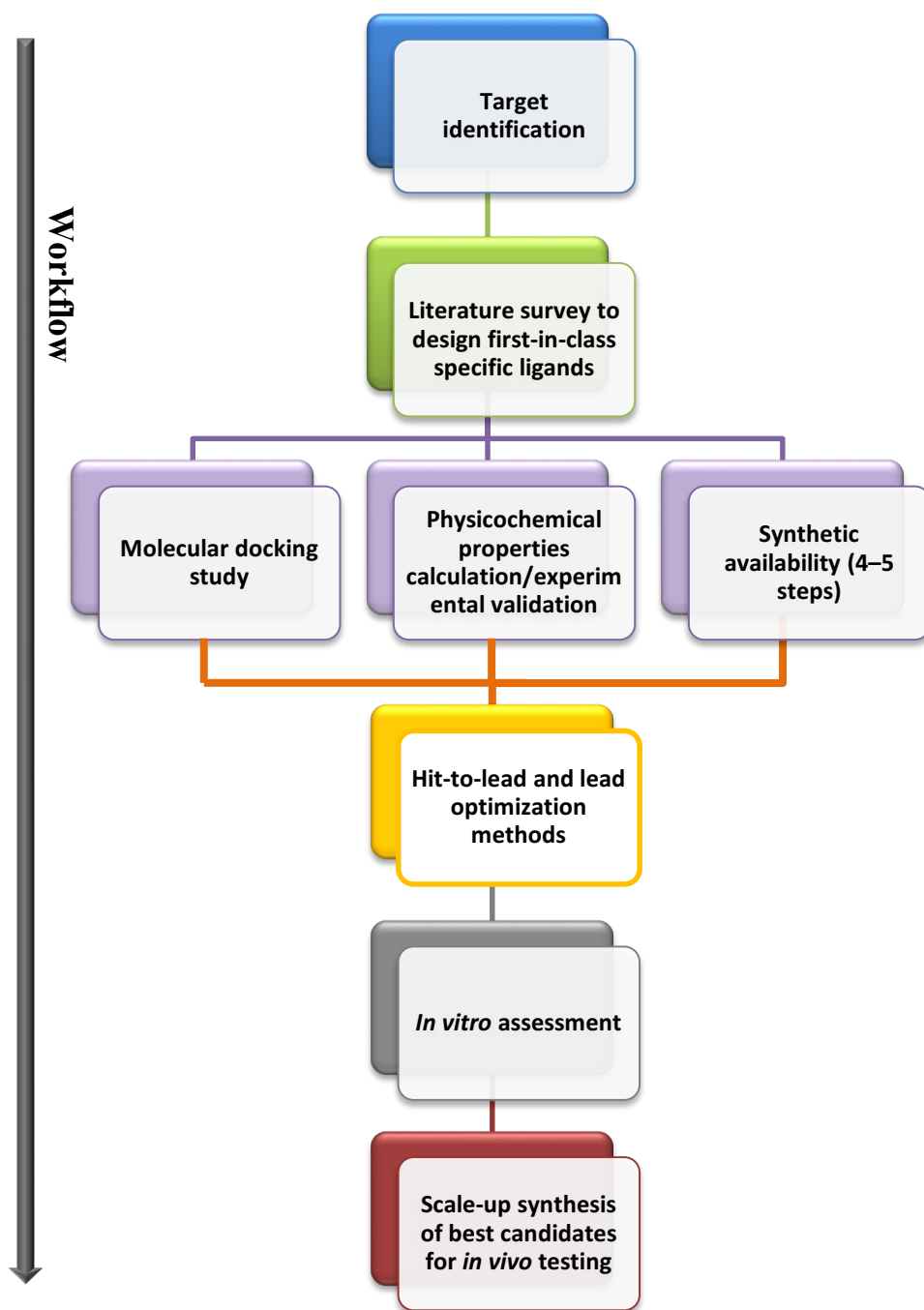
Some of the compounds have been evaluated for their physicochemical properties. The pK_a of oxime showed lower values ranging between 8.72 and 8.99, compared with RS194B ($pK_a = 9.66$). These values indicated the potential improvement of reactivation abilities. The reduction of values towards physiological pH signifies better dissociation into the active oximate anion that is responsible for the reactivation process. Another benefit of novel compounds may lay in the weaker basicity of the most basic center of the molecule. Indeed, the pK_a of our compounds ranged from 7.16 to 8.35, compared with RS194B ($pK_a = 8.56$), suggesting that there will be a less protonated portion. This could confer better ability to penetrate through the membranes. In contrast, this might be worse based on the experimentally determined $\log D_{7.4}$ and $\log P_{neutral}$.

4.3 Overview of contribution to the development of cholinesterase modulators

AChE is considered as perfect enzyme that has been investigated for several decades. Although several crystal structures are deposited in the Protein Data Bank and have been exhaustively described and analyzed, there are still several issues that remain unsolved. Some of these issues were discussed in this thesis.

Over one hundred final compounds primarily targeting AChE have been developed within this work. Some were primarily devoted to basic research, mostly to elucidate the SAR. Such tasks are also necessary to understand the fundamentals behind the pharmacology. To build on these observations, we can continue with laborious research and implement our benchmark knowledge into the medicinal chemistry pipeline (Scheme 26). The workflow could ultimately provide drug-like candidates. Good examples of generated drug candidates would be tacroximes together with uncharged bis-oxime reactivators, which are very close to being clinically useful, as successful animal studies are sufficient for their marketing.

From a synthetic perspective, several reactions and their optimization have been conducted; some were not previously documented in the literature. Specifically, reductive amination; Friedländer condensation using microwave activation with reduced reaction time; the application of olefin metathesis; one-pot efficient amination; aromatization reactions; and various *N*-alkylations are discussed in this thesis.



Scheme 29 Rational medicinal chemistry pipeline to be followed.

4.3.1 Anti-AD drugs

THA-PHT compounds do not have ideal drug-like properties. Their bulkiness and poor physicochemical properties resulted in low solubility, which may be a critical drawback for *in vivo* application. However, such compounds provide a significant contribution and insight into the development of anti-AD compounds that combine anti-tau properties and the inhibition of AChE/BChE. This unique combination is rarely

discussed in the literature. As the biological profiles of THA-PHT are still under assessment, it is hard to estimate their true therapeutic potential.

Tacrine-like compounds primarily targeting AChE/NMDA have balanced physicochemical properties and their hydrochloride analogues are readily soluble in water. Some will certainly become drug candidates. The study of their mechanism of action on NMDA receptors is a key step and can provide results of considerable interest. Owing to the developed Friedländer condensation with new specific conditions, these compounds can be obtained by a one-step synthesis in high yields over a short period of time. Preliminary data suggested that the final compounds have proven inhibition of cholinesterase and a balanced profile against NMDA receptors (data not shown).

4.3.2 AChE-targeted insecticides

The concept of maleimide moiety introduction into Cys-targeted insecticides is unique and worthy of investigation. Based on our experience with the maleimide scaffold, we conclude that it has several limitations, the major one being low stability. In contrast, this limitation may be regarded as beneficial dependent on their application. Indeed, it may result in low persistence in the environment. Another limitation to be considered is their poor solubility. The compounds are insoluble in water and barely soluble in organic solvents such as DMSO. This limitation can be overcome by the introduction of a polyethylene glycol linker instead of a methylene linker. Therefore, the optimization of molecules bearing a maleimide moiety is an essential step in the development of novel promising insecticides.

4.3.3 AChE reactivators

Initially, two review papers that were published the author provided a comprehensive overview about the current status of the development of NAs countermeasures. Strong evidence enabled the design of series of mono-quaternary charged AChE reactivators. The unique properties of this family are conferred by the presence of a positive charge in PAS ligand acting as a ligand anchor, presumably placing the molecules into both anionic subsites. Such molecules have never been reported before. Indeed, data for AChE reactivation allowed us to conclude that these unique entities were one of the most potent reactivators reported to date. Their *in vivo* efficacy is currently under investigation.

The other two series were designed to follow a short multi-step procedure. The advantage of this approach would be the potentially easier scaling up for the following *in vivo* studies. Indeed, both tacroximes were prepared in six steps. Unfortunately, the final three steps had very poor yields and more attention and, most likely, a slightly different approach is required. Similarly, optimization would be required to achieve large-scale production. We found that tacroximes are potential treatments for dichlorvos intoxication; as they are predicted to cross the BBB, they may confer sufficient protection against the OP-induced delayed neuropathy caused by dichlorvos or other pesticides. Therefore, larger quantities are needed for *in vivo* experiments and further steps will be devoted to optimization of synthesis.

Bis-oxime analogs of RS194B were remarkably interesting. Some were several times more efficient than the parent RS194B, and could be prepared in a 3–4 step synthesis. The solubility in water was also better than the parent RS194B. Important steps to enable their future application are the *in vivo* assessment and determination of their ability to cross the BBB.

5. Conclusion

My research was devoted to the design and synthesis of AChE modulators. Within my dissertation thesis, I was able to produce more than 100 final products. Of the 105 products, there were 66 compounds targeting the multifactorial nature of AD; 14 Cys-targeted insecticides, and 25 AChE reactivators.

From the biological data obtained for the anti-AD compounds and insecticides, we can draw some clear SARs that will be useful for further development. Moreover, the approaches to obtain them have yielded several novel reactions. Reductive amination, Friedländer condensation using microwave activation with reduced reaction time, the potent application of olefin metathesis, and one-pot amination were described.

Each of the three series of AChE reactivators offered a completely novel approach for the development of highly potent compounds. **187**, the most potent reactivator, is currently undergoing *in vivo* investigation to reveal its true potential. The activity of tacroximes was not interesting; however, we propose that drugs like tacrine with small structural changes can be repurposed for different indications. Finally, uncharged bis-oxime compounds have not been published before. They sufficiently surpassed the reference compound RS194B, which is awaiting FDA approval. Several optimized reaction steps with excellent yields compared with those already published, such as aromatization reactions and *N*-alkylations, were described in detail.

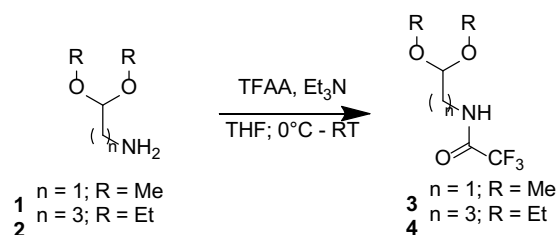
6. Experimental part

6.1 General synthetic methods

The column chromatography was performed using silica gel 100 at atmospheric pressure (70 – 230 mesh ASTM, Fluka, Prague Czech Republic) or silica gel 40 (0.0400063 mm; Merck). The analytical thin-layer chromatography was carried out using plates coated with silica gel 60 with a fluorescent indicator F254 (Merck, Prague Czech Republic). Thin-layer chromatography plates were visualized by exposure to ultraviolet light (254 nm) or by detection reagents phosphomolybdic acid (PMA) and *p*-anisaldehyde (PERNOD). NMR spectra were recorded on a Varian S500 spectrometer (500 MHz for ^1H and 126 MHz for ^{13}C); Varian MR 400 (400 MHz for ^1H and 100 MHz for ^{13}C) and Bruker Avance III (600 MHz for ^1H and 150 MHz for ^{13}C). Chemical shifts are reported in δ ppm referenced to an internal SiMe_4 standard for ^1H NMR and chloroform-*d* (CHCl_3 -*d*₁; 7.26 (D); 77.16 (C) ppm), CD_3OD (CH_3OH -*d*₄; 3.35, 4.78 (D), 49.3 (C) ppm), or hexadeuteriodimethylsulfoxide (DMSO -*d*₆; 2.50 (D), 39.7 (C) ppm). Chemicals were purchased from Sigma-Aldrich Co. LLC and were used without additional purification. CEM Explorer SP 12 S Class and Biotage[®] Initiator+ were used for microwave irradiation. The final compounds were analyzed by LC-MS consisting of UHPLC Dionex Ultimate 3000 RS coupled with Q Exactive Plus orbitrap mass spectrometer (Thermo Fisher Scientific, Bremen, Germany) and Agilent 6230 Accurate-Mass TOFMS system features Agilent Jet Stream Thermal Focusing technology for significantly improved sensitivity, as well as enhanced MassHunter Workstation software for superior data mining and analysis capabilities and Micromass Quattro Ultima, high performance benchtop triple quadrupole mass spectrometer designed for routine LC-MS and LC-MS/MS operations to obtain high resolution mass spectra. Gradient LC analysis confirmed > 95% purity.

6.1.1 Tacrine-phenothiazine derivatives

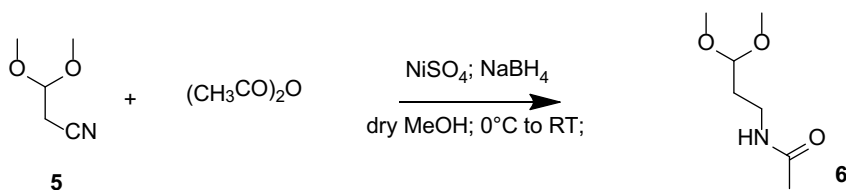
Preparation of the linker intermediates.



1 or **2** (10 mmol) was dissolved with the dried THF (15 mL) in the dried round-bottom flask, under nitrogen atmosphere. The solution was cooled to 0 °C. Trifluoroacetic acid anhydride (TFAA; 12 mmol) and triethylamine (TEA; 12 mmol) was drop wise added and the reaction mixture was stirred for 4 hours at room temperature. The reaction mixture was concentrated, diluted with dichloromethane (DCM; 20 mL), neutralized with saturated sodium bicarbonate (NaHCO₃; until pH = 7 – 8) and extracted with additional DCM 3x 20 mL. The organic layers were collected, dried with anhydrous Na₂SO₄ and filtrated. The filtrate was concentrated under reduced pressure and purified by column chromatography affording title products **3** or **4**.

N-(2,2-dimethoxyethyl)-2,2,2-trifluoroacetamide (3): The resulting residue was purified by column chromatography (PE/EA = 6:4) affording **3** as yellowish oil. Yield 99 %. ¹H NMR (401 MHz, Chloroform-*d*) δ 6.56 (bs, 1H), 4.42 (t, *J* = 5.0 Hz, 1H), 3.51 – 3.45 (m, 2H), 3.40 (s, 6H). ¹³C NMR (101 MHz, cdcl₃) δ 157.48, 157.11, 117.15, 114.30, 101.67, 54.68, 41.19.

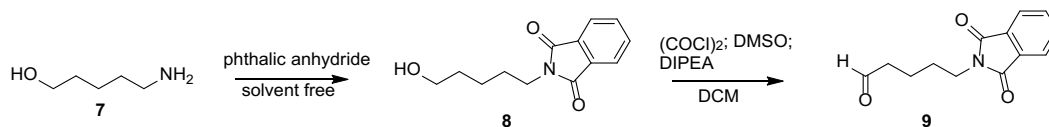
N-(4,4-diethoxybutyl)-2,2,2-trifluoroacetamide (4): The resulting residue was purified by column chromatography (PE/EA = 6:4) affording **4** as yellowish oil. Yield 99 %. ¹H NMR (401 MHz, Chloroform-*d*) δ 7.09 (s, 1H), 4.52 – 4.44 (m, 1H), 3.70 – 3.57 (m, 2H), 3.55 – 3.42 (m, 2H), 3.40 – 3.30 (m, 2H), 1.72 – 1.63 (m, 4H), 1.18 (t, *J* = 7.1 Hz, 6H). ¹³C NMR (101 MHz, cdcl₃) δ 157.29, 156.92, 117.33, 114.48, 102.40, 61.97, 39.63, 30.88, 23.21, 15.15.



N-(3,3-dimethoxypropyl)acetamide (6): In the dried round-bottom three neck flask **5** (10 mmol), acetic anhydride (20 mmol) and NiSO₄ (10 mmol) was dissolved in the dried methanol under nitrogen atmosphere. The mixture was cooled to 0 °C and stirred for 15 min. Then, NaBH₄ (70 mmol) was slowly added by portions during 30 min. The reaction mixture was stirred for 5 hours at room temperature. The reaction mixture was then neutralized by saturated NaHCO₃ (3 mL) and multiple times filtrated through the CELITE pad until obtaining clear filtrate. The filtrate was concentrated

under reduced pressure and purified by column chromatography (DCM/MeOH = 24:1) affording **6** as yellowish oil. Yield 51 %.

^1H NMR (401 MHz, Chloroform-*d*) δ 5.99 (s, 1H), 4.41 (t, J = 5.3 Hz, 1H), 3.41 – 3.25 (m, 8H), 1.94 (s, 3H), 1.86 – 1.76 (m, 2H).



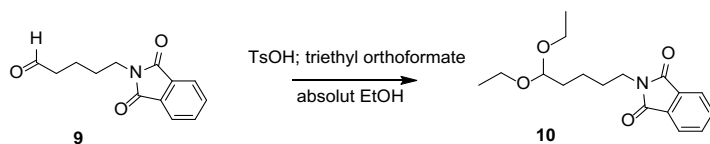
5-(1,3-dioxo-2,3-dihydro-1H-isoindol-2-yl)pentanal (**9**):

A: 5-amino-1-pentanol (**7**; 33.93 mmol) and phthalic anhydride (33.93 mmol) were added into the oven dried round-bottom flask. The mixture was stirred at 145 °C under constant stream of Ar for 30 min. The resulting residue was dried on vacuum pump affording **8** as light yellow oil with quantitative yields. ^1H NMR (500 MHz, Chloroform-*d*) δ 7.86 – 7.81 (m, 2H), 7.73 – 7.69 (m, 2H), 3.70 (t, J = 7.2 Hz, 2H), 3.64 (t, J = 6.5 Hz, 2H), 1.78 – 1.67 (m, 2H), 1.67 – 1.57 (m, 2H), 1.48 – 1.38 (m, 2H). ^{13}C NMR (126 MHz, cdCl_3) δ 168.45, 133.85, 132.08, 123.14, 62.57, 37.81, 32.14, 28.31, 22.99.

B: $(\text{COCl})_2$ (40.72 mmol) was added to anhydrous DCM (60 mL) containing DMSO (74.65 mmol) at -45 °C under Ar atmosphere. After 5 min of stirring **8** (33.93 mmol) dissolved in anhydrous DCM was slowly drop wise added. After another 15 min of stirring diisopropylethylamine (DIPEA; 101.79 mmol) was slowly drop wise added. The reaction was heated to -30 °C and stirred for additional 30 min. Finally, the solvent was removed and the residue was diluted with EA. After dilution, white precipitate was formed, mixture was filtrated. The filtrate was washed with 6 % NaHCO_3 150 mL and 3x with H_2O 150 mL. The organic layer was dried with anhydrous Na_2SO_4 and concentrated affording title product **9** as light red oil. Yield 77 % after two steps.

^1H NMR (500 MHz, Chloroform-*d*) δ 9.73 (s, 1H), 7.84 – 7.77 (m, 2H), 7.73 – 7.66 (m, 2H), 3.68 (t, J = 6.8 Hz, 2H), 2.51 – 2.45 (m, 2H), 1.76 – 1.60 (m, 4H). ^{13}C NMR (126 MHz, cdCl_3) δ 201.80, 168.32, 133.93, 132.01, 123.18, 43.15, 37.39, 27.93, 19.19.

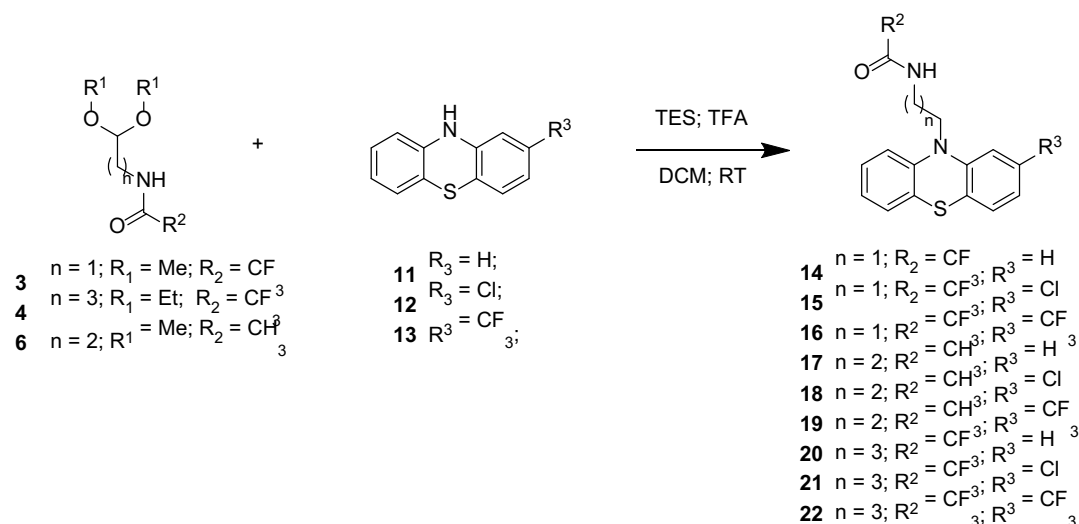
2-(5,5-diethoxypentyl)-2,3-dihydro-1H-isoindole-1,3-dione (**10**):

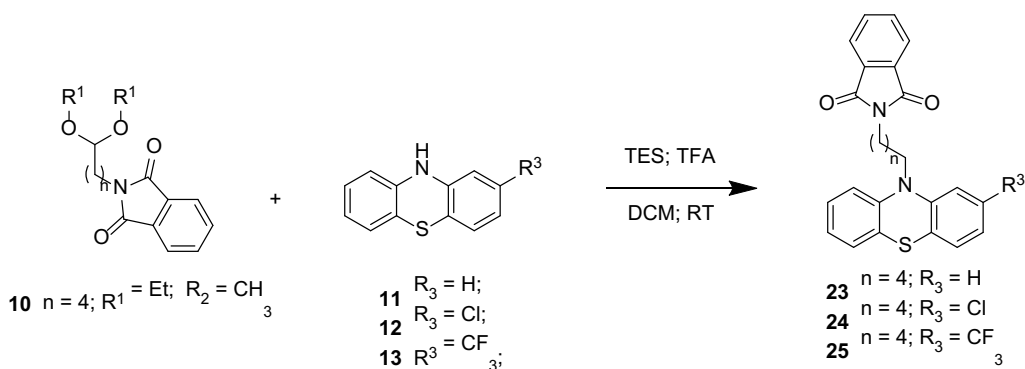


9 (5.01 mmol) and *p*-toluenesulfonic acid hydrate (0.05 mmol) were dissolved in absolute EtOH under Ar atmosphere. The solution was bubbled with additional Ar stream. Then, triethyl orthoformate was slowly added and the mixture was stirred and bubbled with Ar for 3 hours at RT. EtOH was evaporated and the residue was diluted with DCM (70 mL) and saturated NaHCO₃ (100 mL). The mixture was extracted 3 times with DCM (3x 70 mL) and the organic layers were collected, dried with anhydrous NaSO₄ and filtrated. The filtrate was concentrated under reduced pressure and purified by column chromatography (PE/EA = 5:1) affording title products **10** as colorless oil. Yield 74 %.

¹H NMR (500 MHz, Chloroform-*d*) δ 7.86 – 7.81 (m, 2H), 7.73 – 7.68 (m, 2H), 4.47 (t, *J* = 5.7 Hz, 1H), 3.69 (t, *J* = 7.3 Hz, 2H), 3.66 – 3.59 (m, 2H), 3.52 – 3.44 (m, 2H), 1.76 – 1.62 (m, 4H), 1.46 – 1.38 (m, 2H), 1.23 – 1.14 (m, 6H). ¹³C NMR (126 MHz, cdcl₃) δ 168.35, 133.80, 132.14, 123.11, 102.66, 61.03, 37.88, 33.14, 28.38, 22.06, 15.29.

Preparation of phenothiazine intermediates.





In the dried round-bottom flask **3**; **4**; **6**; or **10** (2.4 mmol) and **11**; **12** or **13** (2 mmol) was dissolved in the dry DCM (20 mL) under nitrogen atmosphere. Trifluoroacetic acid (TFA; 26 mmol) and triethylsilane (TES; 5 mmol) was then drop wise added and the reaction mixture was stirred for 2 hours at room temperature. The reaction mixture was cooled to 0 °C and slowly neutralized but addition of saturated NaHCO_3 (until pH = 7 - 8). The mixture was extracted with DCM 3x 20 mL. The organic layers were collected, dried with anhydrous Na_2SO_4 and filtrated. The filtrate was concentrated under reduced pressure and purified by column chromatography affording products **14** – **25**.

N-[2-(10H-phenothiazin-10-yl)ethyl]-2,2,2-trifluoroacetamide (14): The resulting residue was purified by column chromatography (PE/EA = 9:1) affording **14** as dark yellow viscous oil. Yield 41 %.

^1H NMR (401 MHz, Chloroform-*d*) δ 7.23 – 7.16 (m, 4H), 7.03 – 6.89 (m, 4H), 6.80 (bs, 1H), 4.14 (t, $J = 5.9$ Hz, 2H), 3.71 (q, $J = 5.9$ Hz, 2H). ^{13}C NMR (101 MHz, cdCl_3) δ 144.55, 127.90, 127.61, 126.80, 123.49, 116.16, 46.05, 36.82.

N-[2-(2-chloro-10H-phenothiazin-10-yl)ethyl]-2,2,2-trifluoroacetamide (15): The resulting residue was purified by column chromatography (PE/EA = 9:1) affording **15** as purple viscous oil. Yield 99 %.

^1H NMR (401 MHz, Chloroform-*d*) δ 7.28 – 7.15 (m, 2H), 7.15 – 7.07 (m, 1H), 7.07 – 6.85 (m, 3H), 6.83 – 6.68 (m, 1H), 4.11 (t, $J = 5.9$ Hz, 2H), 3.71 (q, $J = 5.9$ Hz, 2H). ^{13}C NMR (101 MHz, cdCl_3) δ 145.94, 143.78, 133.65, 128.38, 127.99, 127.82, 126.39, 125.14, 123.91, 123.40, 116.53, 116.37, 46.13, 36.75.

N-{2-[2-(trifluoromethyl)-10H-phenothiazin-10-yl]ethyl}-2,2,2-trifluoroacetamide (16): The resulting residue was purified by column chromatography (PE/EA = 9:1) affording **16** as dark yellow viscous oil. Yield 99 %.

^1H NMR (401 MHz, Chloroform-*d*) δ 7.36 – 7.14 (m, 4H), 7.14 – 6.91 (m, 2H), 6.73 – 6.59 (m, 1H), 4.17 (t, $J = 5.9$ Hz, 2H), 3.73 (q, $J = 5.9$ Hz, 2H).

N-[3-(10H-phenothiazin-10-yl)propyl]acetamide (17): The resulting residue was purified by column chromatography (EA/DCM = 1:1) affording **17** as white-brown solid. Yield 99 %.

^1H NMR (401 MHz, Chloroform-*d*) δ 7.24 – 7.13 (m, 4H), 7.01 – 6.86 (m, 4H), 6.16 (bs, 1H), 3.96 (t, $J = 6.0$ Hz, 2H), 3.33 (q, $J = 6.0$ Hz, 2H), 1.99 (p, $J = 6.1$ Hz, 2H), 1.75 (s, 3H). ^{13}C NMR (101 MHz, cdCl_3) δ 170.16, 145.34, 127.75, 127.55, 125.64, 122.95, 115.87, 45.92, 38.53, 26.05, 22.97.

N-[3-(2-chloro-10H-phenothiazin-10-yl)propyl]acetamide (18): The resulting residue was purified by column chromatography (PE/EA = 1:1) affording **18** as white sticky foam. Yield 94 %.

^1H NMR (401 MHz, Chloroform-*d*) δ 7.24 – 7.16 (m, 2H), 7.13 – 7.06 (m, 1H), 7.04 – 6.80 (m, 4H), 6.04 (s, 1H), 3.94 (t, $J = 6.1$ Hz, 2H), 3.35 (q, $J = 6.1$ Hz, 2H), 2.02 (q, $J = 6.2$ Hz, 2H), 1.83 – 1.78 (m, 3H).

N-{3-[2-(trifluoromethyl)-10H-phenothiazin-10-yl]propyl}acetamide (19): The resulting residue was purified by column chromatography (EA/DCM = 1:1) affording **19** as yellow viscous oil. Yield 83 %.

^1H NMR (401 MHz, Chloroform-*d*) δ 7.28 – 7.13 (m, 4H), 7.08 – 7.02 (m, 1H), 7.02 – 6.94 (m, 1H), 6.93 – 6.87 (m, 1H), 5.94 (bs, 1H), 3.97 (t, $J = 6.2$ Hz, 3H), 3.34 (q, $J = 6.3$ Hz, 2H), 2.06 – 1.95 (m, 2H), 1.80 (s, 3H). ^{13}C NMR (101 MHz, cdCl_3) δ 170.15, 145.80, 144.31, 127.92, 127.83, 127.78, 124.53, 123.54, 119.53, 119.49, 116.18, 112.17, 112.13, 45.74, 38.06, 26.20, 23.02.

N-[4-(10H-phenothiazin-10-yl)butyl]- 2,2,2-trifluoroacetamide (20): The resulting residue was purified by column chromatography (PE/EA = 7:1) affording **20** as dark yellow viscous oil. Yield 99 %.

^1H NMR (401 MHz, Chloroform-*d*) δ 7.20 – 7.12 (m, 4H), 6.98 – 6.89 (m, 2H), 6.89 – 6.81 (m, 2H), 6.31 (bs, 1H), 3.92 (t, $J = 6.3$ Hz, 2H), 3.33 (q, $J = 6.7$ Hz, 2H), 1.91 – 1.77 (m, 2H), 1.74 – 1.64 (m, 2H). ^{13}C NMR (101 MHz, cdCl_3) δ 145.09, 127.68, 127.33, 125.57, 122.76, 115.64, 46.36, 39.42, 26.37, 23.54.

N-[4-(2-chloro-10H-phenothiazin-10-yl)butyl]-2,2,2-trifluoroacetamide (21): The resulting residue was purified by column chromatography (PE/EA = 9:1) affording **21** as dark yellow viscous oil. Yield 84 %.

¹H NMR (401 MHz, Chloroform-*d*) δ 7.20 – 7.13 (m, 2H), 7.07 – 7.03 (m, 1H), 6.99 – 6.92 (m, 1H), 6.92 – 6.88 (m, 1H), 6.87 – 6.83 (m, 1H), 6.83 – 6.80 (m, 1H), 3.88 (t, *J* = 6.3 Hz, 2H), 3.34 (q, *J* = 6.7 Hz, 2H), 1.87 – 1.77 (m, 2H), 1.75 – 1.66 (m, 2H). ¹³C NMR (101 MHz, cdcl₃) δ 146.45, 144.31, 133.37, 128.13, 127.75, 127.51, 125.31, 124.06, 123.21, 122.59, 115.98, 115.94, 46.53, 39.38, 26.34, 23.56.

N-{4-[2-(trifluoromethyl)-10H-phenothiazin-10-yl]butyl}-2,2,2-trifluoroacetamide (22): The resulting residue was purified by column chromatography (PE/EA = 7:1) affording **22** as yellow viscous oil. Yield 85 %.

¹H NMR (401 MHz, Chloroform-*d*) δ 7.28 – 7.11 (m, 4H), 7.05 – 6.93 (m, 2H), 6.92 – 6.84 (m, 1H), 6.29 (bs, 1H), 3.94 (t, *J* = 6.3 Hz, 2H), 3.34 (q, *J* = 6.6 Hz, 2H), 1.87 – 1.76 (m, 2H), 1.77 – 1.65 (m, 2H). ¹³C NMR (101 MHz, cdcl₃) δ 156.66, 145.63, 144.14, 127.79, 127.74, 127.71, 124.59, 123.41, 119.38, 119.34, 116.01, 111.98, 46.61, 39.38, 26.32, 23.57.

2-[5-(10H-phenothiazin-10-yl)pentyl]-2,3-dihydro-1H-isoindole-1,3-dione (23): The resulting residue was purified by column chromatography (PE/EA = 5:1) affording **23** as dark yellow viscous oil. Quantitative yield.

¹H NMR (500 MHz, Chloroform-*d*) δ 7.87 – 7.80 (m, 2H), 7.75 – 7.68 (m, 2H), 7.17 – 7.11 (m, 2H), 7.11 – 7.07 (m, 2H), 6.95 – 6.81 (m, 3H), 3.90 – 3.79 (m, 2H), 3.71 – 3.66 (m, 2H), 1.91 – 1.81 (m, 2H), 1.76 – 1.67 (m, 2H), 1.54 – 1.44 (m, 2H). ¹³C NMR (126 MHz, cdcl₃) δ 168.36, 133.80, 132.10, 127.39, 127.15, 123.14, 123.10, 122.36, 115.40, 70.28, 47.00, 37.73, 28.13, 24.04.

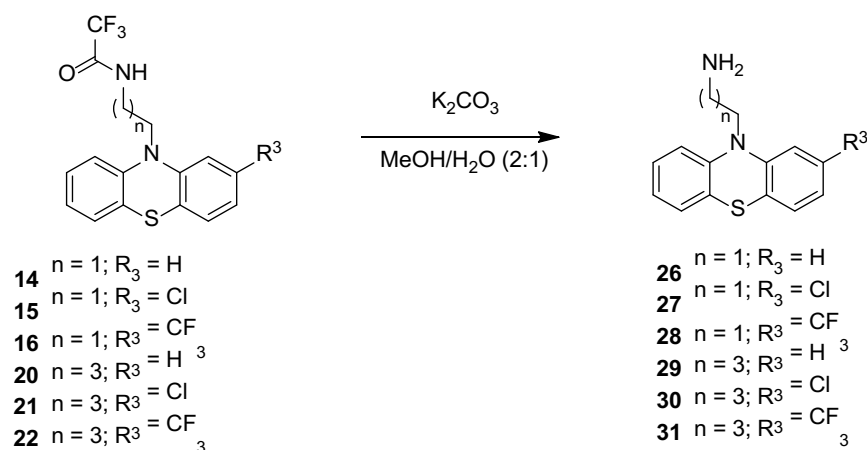
2-[5-(2-chloro-10H-phenothiazin-10-yl)pentyl]-2,3-dihydro-1H-isoindole-1,3-dione (24): The resulting residue was purified by column chromatography (PE/EA = 5:1) affording **24** as dark purple viscous oil. Yield 89 %.

¹H NMR (500 MHz, Chloroform-*d*) δ 7.87 – 7.81 (m, 2H), 7.74 – 7.68 (m, 2H), 7.18 – 7.12 (m, 1H), 7.11 – 7.06 (m, 1H), 7.00 – 6.96 (m, 1H), 6.95 – 6.89 (m, 1H), 6.89 – 6.82 (m, 2H), 6.83 – 6.78 (m, 1H), 3.82 (t, *J* = 7.0 Hz, 2H), 3.68 (t, *J* = 7.1 Hz, 2H), 1.89 – 1.80 (m, 2H), 1.76 – 1.66 (m, 2H), 1.53 – 1.44 (m, 2H). ¹³C NMR (126 MHz,

cdcl₃) δ 168.36, 146.49, 144.41, 133.82, 133.80, 132.10, 127.85, 127.47, 127.35, 123.16, 123.11, 122.83, 122.19, 115.74, 115.71, 47.09, 37.68, 28.10, 26.23, 23.95.

2-{5-[2-(trifluoromethyl)-10H-phenothiazin-10-yl]pentyl}-2,3-dihydro-1H-isoindole-1,3-dione (25): The resulting residue was purified by column chromatography (PE/EA = 5:1) affording **25** as dark yellow viscous oil. Quantitative yield.

¹H NMR (500 MHz, Chloroform-*d*) δ 7.87 – 7.80 (m, 2H), 7.76 – 7.68 (m, 2H), 7.21 – 7.10 (m, 3H), 7.10 – 7.07 (m, 1H), 7.02 – 6.99 (m, 1H), 6.97 – 6.90 (m, 1H), 6.90 – 6.84 (m, 1H), 3.88 (t, *J* = 7.0 Hz, 2H), 3.70 – 3.65 (m, 2H), 1.90 – 1.79 (m, 2H), 1.79 – 1.66 (m, 2H), 1.53 – 1.46 (m, 2H).



14 – 16; or **20 – 22** (1.5 mmol) and K₂CO₃ (12 mmol) was dissolved in MeOH/H₂O 2:1 (12:6 mL). The mixture was stirred overnight at room temperature. The solvents were evaporated and the precipitate was diluted with H₂O (20 mL) and extracted with DCM 3x 20 mL. The organic layers were collected, dried with anhydrous Na₂SO₄ and filtrated. The filtrate was concentrated under reduced pressure to afford title product **26 – 31** without any further purification.

2-(10H-phenothiazin-10-yl)ethan-1-amine (26): Dark yellow viscous oil with yield 88 %.

¹H NMR (401 MHz, Chloroform-*d*) δ 7.22 – 7.08 (m, 4H), 7.03 – 6.83 (m, 4H), 3.99 (t, *J* = 5.9 Hz, 2H), 3.06 (t, *J* = 5.9 Hz, 2H), 1.45 (bs, 2H). ¹³C NMR (101 MHz, cdcl₃) δ 145.22, 127.59, 127.23, 125.88, 122.69, 115.77, 50.52, 38.85.

2-(2-chloro-10H-phenothiazin-10-yl)ethan-1-amine (27): Dark purple viscous oil with yield 99 %.

^1H NMR (401 MHz, Chloroform-*d*) δ 7.23 – 7.10 (m, 2H), 7.10 – 7.03 (m, 1H), 7.01 – 6.80 (m, 4H), 3.96 (t, $J = 5.9$ Hz, 2H), 3.06 (t, $J = 5.9$ Hz, 2H), 1.29 (bs, 2H).

2-[2-(trifluoromethyl)-10H-phenothiazin-10-yl]ethan-1-amine (28): Dark yellow viscous oil with yield 99 %.

^1H NMR (401 MHz, Chloroform-*d*) δ 7.25 – 7.12 (m, 4H), 7.08 – 7.04 (m, 1H), 7.00 – 6.93 (m, 1H), 6.93 – 6.88 (m, 1H), 4.00 (t, $J = 5.9$ Hz, 2H), 3.06 (t, $J = 5.9$ Hz, 2H), 1.34 (bs, 2H).

4-(10H-phenothiazin-10-yl)butan-1-amine (29): Dark brown viscous oil with yield 82 %.

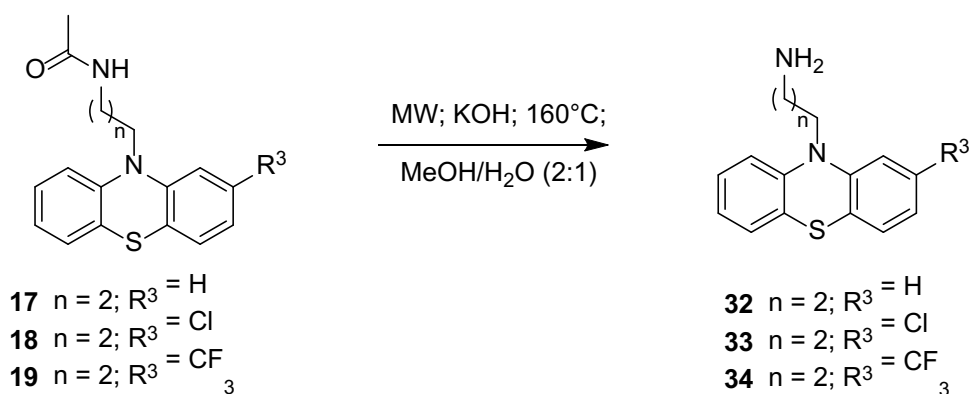
^1H NMR (401 MHz, Chloroform-*d*) δ 7.16 – 7.09 (m, 4H), 6.92 – 6.87 (m, 2H), 6.87 – 6.82 (m, 2H), 3.86 (t, $J = 7.0$ Hz, 2H), 2.68 (t, $J = 7.0$ Hz, 2H), 1.89 – 1.77 (m, 2H), 1.55 (p, $J = 7.2$ Hz, 2H), 1.29 – 1.17 (bs, 2H). ^{13}C NMR (101 MHz, cdCl_3) δ 145.23, 127.45, 127.15, 125.11, 122.38, 115.41, 47.10, 41.85, 31.12, 24.32.

4-(2-chloro-10H-phenothiazin-10-yl)butan-1-amine (30): Dark brown viscous oil with yield 93 %.

^1H NMR (401 MHz, Chloroform-*d*) δ 7.20 – 7.06 (m, 2H), 7.06 – 6.96 (m, 1H), 6.97 – 6.77 (m, 4H), 3.82 (t, $J = 7.0$ Hz, 2H), 2.69 (t, $J = 7.0$ Hz, 2H), 1.88 – 1.73 (m, 2H), 1.62 – 1.44 (m, 2H), 1.11 (bs, 2H). ^{13}C NMR (101 MHz, cdCl_3) δ 146.53, 144.50, 133.16, 127.89, 127.52, 127.35, 124.87, 123.60, 122.85, 122.20, 115.75, 115.73, 47.23, 41.79, 31.00, 24.19.

4-[2-(trifluoromethyl)-10H-phenothiazin-10-yl]butan-1-amine (31): Dark yellow viscous oil with yield 90 %.

^1H NMR (401 MHz, Chloroform-*d*) δ 7.20 – 7.15 (m, 2H), 7.15 – 7.09 (m, 2H), 7.03 – 6.99 (m, 1H), 6.97 – 6.90 (m, 1H), 6.89 – 6.84 (m, 1H), 3.88 (t, $J = 7.0$ Hz, 2H), 2.69 (t, $J = 7.0$ Hz, 2H), 1.90 – 1.74 (m, 2H), 1.62 – 1.50 (m, 2H), 1.21 – 1.14 (bs, 2H). ^{13}C NMR (101 MHz, cdCl_3) δ 145.68, 144.35, 130.02, 129.70, 127.59, 127.57, 127.46, 124.15, 123.06, 119.03, 119.00, 115.81, 111.84, 111.80, 47.27, 41.76, 30.94, 24.13.



17 – 19 (1.5 mmol) and KOH (11.25 mmol) were dissolved with MeOH/H₂O 2:1 (6:3 mL) in the microwave tube. The mixture was challenged with microwave irradiation (150 W) at 160 °C for 2 hours. The reaction mixture was concentrated under reduced pressure and purified by column chromatography affording products **32 – 34**.

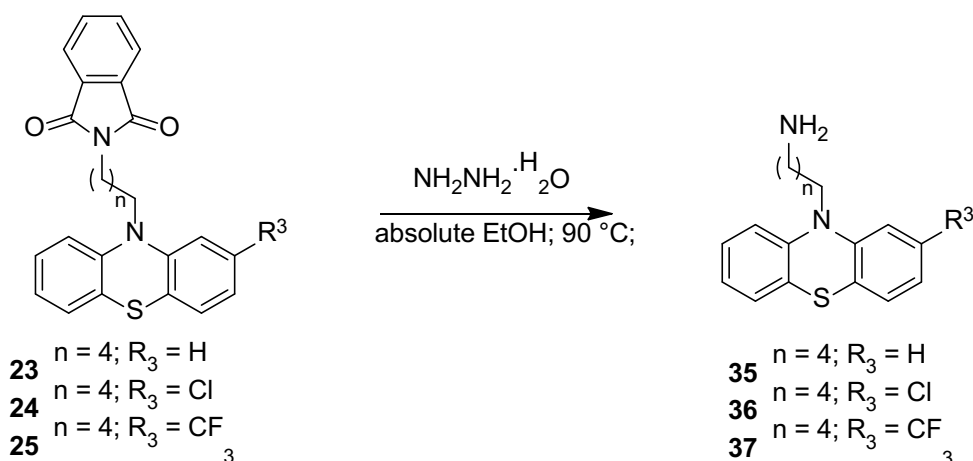
3-(10H-phenothiazin-10-yl)propan-1-amine (32): The resulting residue was purified by column chromatography (DCM/MeOH/NH₃ = 15:1:01) affording **32** as yellow viscous oil. Yield 91 %. Without characterization used into the next reactions.

3-(2-chloro-10H-phenothiazin-10-yl)propan-1-amine (33): The resulting residue was purified by column chromatography (DCM/MeOH/NH₃ = 14:1:01) affording **33** as yellow viscous oil. Yield 65 %.

¹H NMR (401 MHz, Chloroform-*d*) δ 7.18 – 7.07 (m, 2H), 7.03 – 6.96 (m, 1H), 6.96 – 6.82 (m, 4H), 3.93 (t, $J = 6.6$ Hz, 2H), 3.32 (t, $J = 6.7$ Hz, 2H), 2.11 (p, $J = 6.6$ Hz, 2H). ¹³C NMR (101 MHz, cdcl₃) δ 168.14, 146.47, 144.53, 133.20, 127.75, 127.38, 124.66, 123.38, 122.77, 122.13, 115.97, 115.89, 48.09, 44.86, 29.20, 27.71.

3-[2-(trifluoromethyl)-10H-phenothiazin-10-yl]propan-1-amine (34): The resulting residue was purified by column chromatography (DCM/MeOH/NH₃ = 14:1:01) affording **34** as yellow viscous oil. Yield 85 %.

¹H NMR (401 MHz, Chloroform-*d*) δ 7.20 – 7.01 (m, 4H), 6.99 – 6.84 (m, 3H), 3.97 (t, $J = 6.6$ Hz, 2H), 3.31 (t, $J = 6.6$ Hz, 2H), 2.10 (p, $J = 6.6$ Hz, 2H). ¹³C NMR (101 MHz, cdcl₃) δ 145.67, 144.34, 129.77, 127.61, 127.43, 127.32, 123.92, 122.99, 118.94, 115.98, 112.05, 112.01, 48.00, 44.86, 29.11, 27.63.



23 – 25 (2.0 mmol) were dried in round-bottom flask and dissolved in absolute EtOH under Ar atmosphere. Hydrazine hydrate (50 – 60 % solution in H₂O; 1.0 mL) was slowly added, the mixture was heated to reflux (90 °C) and kept stirred under Ar overnight (16 hours). The next day the white precipitate was filtrated and washed with EtOH. The filtrate was concentrated under reduced pressure and purified by column chromatography affording products **35 – 37**.

5-(10H-phenothiazin-10-yl)pentan-1-amine (35): The resulting residue was purified by column chromatography (DCM/MeOH/NH₃ = 9:1:0.1) affording **35** as light yellow viscous oil. Yield 82 %.

¹H NMR (500 MHz, Chloroform-*d*) δ 7.18 – 7.11 (m, 4H), 6.94 – 6.89 (m, 2H), 6.89 – 6.83 (m, 2H), 3.91 – 3.81 (m, 2H), 2.73 – 2.63 (m, 2H), 2.07 (bs, 2H), 1.87 – 1.76 (m, 2H), 1.51 – 1.41 (m, 4H). ¹³C NMR (126 MHz, cdcl₃) δ 145.23, 127.41, 127.13, 125.04, 122.34, 115.40, 47.08, 41.73, 32.67, 26.61, 24.08.

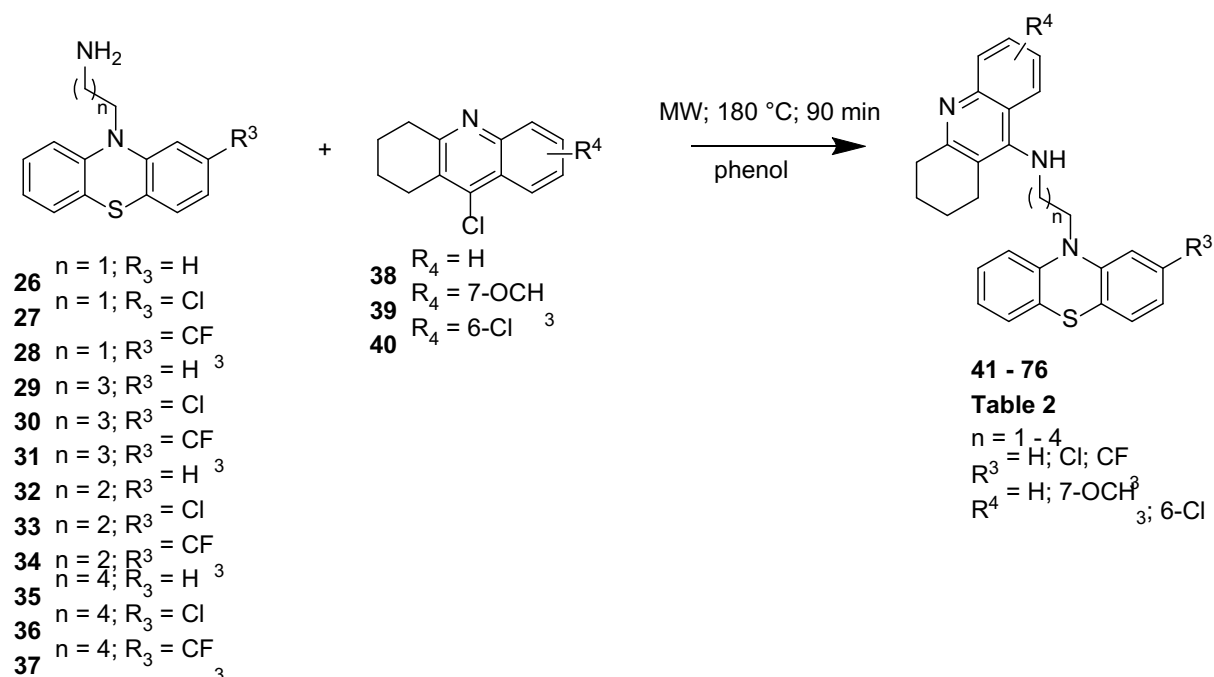
5-(2-chloro-10H-phenothiazin-10-yl)pentan-1-amine (36): The resulting residue was purified by column chromatography (DCM/MeOH/NH₃ = 9:1:0.1) affording **36** as light yellow viscous oil. Yield 74 %.

¹H NMR (500 MHz, Chloroform-*d*) δ 7.19 – 7.11 (m, 2H), 7.04 – 7.00 (m, 1H), 6.96 – 6.91 (m, 1H), 6.91 – 6.87 (m, 1H), 6.87 – 6.83 (m, 1H), 6.84 – 6.79 (m, 1H), 3.83 (t, *J* = 7.0 Hz, 2H), 2.69 (t, *J* = 6.5 Hz, 2H), 2.11 (bs, 2H), 1.85 – 1.76 (m, 2H), 1.54 – 1.41 (m, 4H). ¹³C NMR (126 MHz, cdcl₃) δ 146.54, 144.50, 133.15, 127.88, 127.50, 127.35, 124.82, 123.57, 122.84, 122.18, 115.74, 47.22, 41.69, 32.51, 26.49, 24.03.

5-[2-(trifluoromethyl)-10H-phenothiazin-10-yl]pentan-1-amine (37): The resulting residue was purified by column chromatography (DCM/MeOH/NH₃ = 9:1:0.1) affording **37** as light yellow viscous oil. Yield 75 %.

¹H NMR (500 MHz, Chloroform-*d*) δ 7.22 – 7.10 (m, 4H), 7.04 – 7.00 (m, 1H), 6.98 – 6.93 (m, 1H), 6.90 – 6.85 (m, 1H), 3.88 (t, *J* = 7.0 Hz, 2H), 2.74 – 2.64 (m, 2H), 1.87 – 1.84 (m, 2H), 1.84 – 1.76 (m, 2H), 1.54 – 1.41 (m, 4H). ¹³C NMR (126 MHz, cdcl₃) δ 145.72, 144.41, 130.02, 129.69, 129.43, 127.60, 127.58, 127.48, 125.24, 124.13, 123.07, 119.06, 119.03, 119.00, 118.97, 115.84, 111.88, 111.85, 111.82, 111.79, 47.33, 41.83, 32.84, 26.51, 24.08.

The final N-alkylation coupling of phenothiazines intermediates with tacrine derivatives.



Compounds **26 – 37** (0.20 mmol) and 1,2,3,4-tetrahydroacridine derivatives **38 – 40** (0.22 mmol) were melted and dissolved in phenol (300 μl) by heating gun at 90 °C in the microwave tube. The mixture was then challenged by the microwave irradiation (150 W) at 180 °C for 90 mins. The reaction mixture was diluted with DCM 20 mL and 20 % solution of KOH 20 mL and then extracted with additional DCM 3x 20 mL. The organic layers were collected, dried with anhydrous Na₂SO₄ and filtrated. The filtrate

was concentrated under reduced pressure and purified by column chromatography affording products **41** – **76**.

***N*-[2-(10H-phenothiazin-10-yl)ethyl]-1,2,3,4-tetrahydroacridin-9-amine (41):**

The resulting residue was purified by column chromatography (PE/DCM/Tol/EtOH/NH₃ = 15:6:3:1:0.1) affording **41** as yellow viscous oil. Yield 52 %.

¹H NMR (401 MHz, Chloroform-*d*) δ 8.08 – 7.81 (m, 2H), 7.60 – 7.44 (m, 1H), 7.32 – 7.20 (m, 3H), 7.20 – 7.10 (m, 2H), 7.05 – 6.92 (m, 2H), 6.91 – 6.81 (m, 2H), 4.76 (bs, 1H), 4.05 (t, *J* = 5.2 Hz, 2H), 3.86 (t, *J* = 4.9 Hz, 2H), 2.99 (t, *J* = 6.5 Hz, 2H), 2.50 (t, *J* = 6.4 Hz, 2H), 1.81 – 1.67 (m, 2H), 1.69 – 1.54 (m, 2H). ¹³C NMR (101 MHz, cdcl₃) δ 144.76, 128.70, 127.81, 127.46, 126.74, 123.95, 123.31, 122.89, 115.85, 47.19, 45.05, 33.23, 24.09, 22.59, 22.41. HRMS (ESI⁺): [M]⁺: calculated for C₂₇H₂₆N₃S⁺ (m/z): 424.18419; found: 424.18423. LC-MS > 95 %.

7-methoxy-*N*-[2-(10H-phenothiazin-10-yl)ethyl]-1,2,3,4-tetrahydroacridin-9-amine (42): The resulting residue was purified by column chromatography (PE/DCM/Tol/EtOH/NH₃ = 15:6:3:1:0.1) affording **42** as yellow viscous oil. Yield 50 %.

¹H NMR (401 MHz, Chloroform-*d*) δ 7.85 – 7.73 (m, 1H), 7.26 – 7.09 (m, 6H), 7.05 – 6.90 (m, 2H), 6.91 – 6.80 (m, 2H), 4.39 (bs, 1H), 4.05 – 3.95 (m, 2H), 3.79 (s, 3H), 3.78 – 3.73 (m, 2H), 2.92 (t, *J* = 6.5 Hz, 2H), 2.51 (t, *J* = 6.4 Hz, 2H), 1.79 – 1.64 (m, 2H), 1.62 – 1.48 (m, 2H). ¹³C NMR (101 MHz, cdcl₃) δ 156.37, 156.14, 148.86, 144.90, 143.28, 130.31, 129.00, 128.19, 127.77, 127.42, 126.68, 123.21, 121.74, 120.38, 119.29, 115.82, 101.25, 55.39, 47.26, 44.77, 33.71, 24.25, 22.75. HRMS (ESI⁺): [M]⁺: calculated for C₂₈H₂₈N₃OS⁺ (m/z): 454.19476; found: 454.19476. LC-MS > 96 %.

6-chloro-*N*-[2-(10H-phenothiazin-10-yl)ethyl]-1,2,3,4-tetrahydroacridin-9-amine (43): The resulting residue was purified by column chromatography (PE/DCM/Tol/EtOH/NH₃ = 15:6:3:1:0.1) affording **43** as yellow viscous oil. Yield 42 %.

¹H NMR (401 MHz, Chloroform-*d*) δ 7.88 – 7.73 (m, 2H), 7.31 – 7.20 (m, 2H), 7.21 – 7.09 (m, 3H), 7.05 – 6.94 (m, 2H), 6.90 – 6.78 (m, 2H), 4.56 (bs, 1H), 4.11 –

3.96 (m, 2H), 3.85 – 3.72 (m, 2H), 2.92 (t, $J = 6.5$ Hz, 2H), 2.59 – 2.42 (m, 2H), 1.83 – 1.70 (m, 2H), 1.66 – 1.54 (m, 2H). ^{13}C NMR (101 MHz, cdCl_3) δ 159.92, 150.02, 144.75, 133.85, 128.99, 128.18, 127.82, 127.59, 127.45, 126.74, 124.47, 124.29, 123.30, 119.17, 118.33, 115.82, 47.22, 45.17, 33.98, 24.18, 22.62, 22.56. HRMS (ESI⁺): $[\text{M}]^+$: calculated for $\text{C}_{27}\text{H}_{25}\text{N}_3\text{ClS}^+$ (m/z): 458.14522; found: 458.14557. LC-MS > 98 %.

***N*-[2-(2-chloro-10H-phenothiazin-10-yl)ethyl]-1,2,3,4-tetrahydroacridin-9-amine (44):** The resulting residue was purified by column chromatography (PE/DCM/Tol/EtOH/NH₃ = 15:6.5:3:0.5:0.05) affording **44** as yellow viscous oil. Yield 49 %.

^1H NMR (401 MHz, Chloroform-*d*) δ 7.88 – 7.81 (m, 2H), 7.56 – 7.45 (m, 1H), 7.32 – 7.19 (m, 2H), 7.20 – 7.07 (m, 2H), 7.07 – 6.93 (m, 2H), 6.84 – 6.80 (m, 2H), 4.45 (bs, 1H), 4.09 – 3.95 (m, 2H), 3.80 (t, $J = 5.3$ Hz, 2H), 2.97 (t, $J = 6.5$ Hz, 2H), 2.53 (t, $J = 6.4$ Hz, 2H), 1.86 – 1.70 (m, 2H), 1.69 – 1.56 (m, 2H). ^{13}C NMR (101 MHz, cdCl_3) δ 158.76, 149.64, 147.37, 146.15, 144.17, 133.46, 128.99, 128.82, 128.25, 127.83, 127.62, 126.34, 125.12, 123.89, 123.64, 123.09, 122.58, 120.88, 118.32, 116.25, 116.08, 47.48, 45.04, 34.02, 24.34, 22.76, 22.71. HRMS (ESI⁺): $[\text{M}]^+$: calculated for $\text{C}_{27}\text{H}_{25}\text{ClN}_3\text{S}^+$ (m/z): 458.14522; found: 458.14542. LC-MS > 99 %.

***N*-[2-(2-chloro-10H-phenothiazin-10-yl)ethyl]-7-methoxy-1,2,3,4-tetrahydroacridin-9-amine (45):** The resulting residue was purified by column chromatography (PE/DCM/Tol/EtOH/NH₃ = 15:6.5:3:0.5:0.05) affording **45** as yellow viscous oil. Yield 41 %.

^1H NMR (401 MHz, Chloroform-*d*) δ 7.82 – 7.77 (m, 1H), 7.28 – 7.07 (m, 5H), 7.03 – 6.93 (m, 2H), 6.88 – 6.80 (m, 2H), 4.30 (bs, 1H), 3.99 (t, 2H), 3.81 (s, 3H), 3.78 – 3.73 (m, 2H), 2.93 (t, $J = 6.5$ Hz, 2H), 2.51 (t, $J = 6.4$ Hz, 2H), 1.82 – 1.67 (m, 2H), 1.64 – 1.50 (m, 2H). ^{13}C NMR (101 MHz, cdCl_3) δ 156.22, 148.58, 146.18, 144.22, 133.47, 130.40, 128.99, 128.25, 128.18, 127.82, 127.63, 126.33, 125.11, 123.64, 123.08, 121.73, 120.39, 119.32, 116.24, 116.07, 101.16, 55.42, 47.51, 44.62, 33.71, 24.30, 22.75, 22.75. HRMS (ESI⁺): $[\text{M}]^+$: calculated for $\text{C}_{28}\text{H}_{27}\text{ClN}_3\text{OS}^+$ (m/z): 488.15579; found: 488.15591. LC-MS > 98 %.

6-chloro-*N*-[2-(2-chloro-10H-phenothiazin-10-yl)ethyl]-1,2,3,4-tetrahydroacridin-9-amine (46): The resulting residue was purified by column chromatography (EA/DCM = 1:1) affording **46** as yellow viscous oil. Yield 64 %.

¹H NMR (401 MHz, Chloroform-*d*) δ 7.87 – 7.83 (m, 1H), 7.83 – 7.78 (m, 1H), 7.28 – 7.11 (m, 5H), 7.07 – 6.95 (m, 2H), 6.88 – 6.81 (m, 2H), 4.57 – 4.39 (m, 1H), 4.07 – 3.95 (m, 2H), 3.89 – 3.74 (m, 2H), 2.95 (t, *J* = 6.5 Hz, 2H), 2.51 (t, *J* = 6.4 Hz, 2H), 1.85 – 1.71 (m, 2H), 1.71 – 1.57 (m, 2H). ¹³C NMR (101 MHz, cdcl₃) δ 159.97, 149.79, 147.91, 146.04, 144.07, 133.92, 133.51, 128.29, 127.87, 127.66, 126.37, 125.14, 124.58, 124.11, 123.72, 123.18, 119.16, 118.35, 116.25, 116.07, 109.99, 47.50, 45.03, 33.97, 24.26, 22.63, 22.56. HRMS (ESI⁺): [M]⁺: calculated for C₂₇H₂₄Cl₂N₃S⁺ (m/z): 492.10625; found: 492.10651. LC-MS > 97 %.

***N*-{2-[2-(trifluoromethyl)-10H-phenothiazin-10-yl]ethyl}-1,2,3,4-tetrahydroacridin-9-amine (47):** The resulting residue was purified by column chromatography (PE/DCM/Tol/EtOH/NH₃ = 15:6.5:3:0.5:0.05) affording **47** as yellow viscous oil. Yield 32 %.

¹H NMR (401 MHz, Chloroform-*d*) δ 7.89 – 7.82 (m, 2H), 7.53 – 7.46 (m, 1H), 7.33 – 7.11 (m, 5H), 7.07 – 6.97 (m, 2H), 6.90 – 6.82 (m, 1H), 4.42 (s, 1H), 4.12 – 4.00 (m, 2H), 3.90 – 3.74 (m, 2H), 2.97 (t, *J* = 6.5 Hz, 2H), 2.52 (t, *J* = 6.4 Hz, 2H), 1.89 – 1.69 (m, 2H), 1.68 – 1.52 (m, 2H). ¹³C NMR (101 MHz, cdcl₃) δ 158.76, 149.58, 147.35, 145.38, 143.96, 131.52, 128.99, 128.83, 128.23, 128.18, 127.87, 125.58, 125.26, 123.94, 123.86, 122.48, 121.84, 120.90, 119.84, 118.36, 116.17, 112.27, 47.61, 44.98, 33.99, 24.35, 22.74, 22.69. HRMS (ESI⁺): [M]⁺: calculated for C₂₈H₂₅F₃N₃S⁺ (m/z): 492.17158; found: 492.17157. LC-MS > 99 %.

7-methoxy-*N*-{2-[2-(trifluoromethyl)-10H-phenothiazin-10-yl]ethyl}-1,2,3,4-tetrahydroacridin-9-amine (48): The resulting residue was purified by column chromatography (PE/DCM/Tol/EtOH/NH₃ = 15:6.5:3:0.5:0.05) affording **48** as yellow viscous oil. Yield 29 %.

¹H NMR (401 MHz, Chloroform-*d*) δ 7.85 – 7.75 (m, 1H), 7.34 – 7.27 (m, 1H), 7.25 – 7.13 (m, 4H), 7.11 – 7.07 (m, 1H), 7.06 – 6.97 (m, 2H), 6.89 – 6.84 (m, 1H), 4.29 (bs, 1H), 4.11 – 4.01 (m, 2H), 3.80 (s, 3H), 3.76 (t, *J* = 6.4 Hz, 3H), 2.93 (t, *J* = 6.5 Hz, 2H), 2.49 (t, *J* = 6.4 Hz, 2H), 1.79 – 1.67 (m, 2H), 1.60 – 1.49 (m, 2H). ¹³C NMR (101 MHz, cdcl₃) δ 156.25, 145.40, 143.99, 131.52, 130.32, 130.01, 128.99, 128.18, 127.87,

127.85, 125.57, 125.25, 123.86, 121.70, 120.38, 119.83, 116.15, 101.17, 47.65, 44.54, 33.62, 24.28, 22.71, 22.69. HRMS (ESI⁺): [M]⁺: calculated for C₂₉H₂₇F₃N₃OS⁺ (m/z): 522.18214; found: 522.18280. LC-MS > 96 %.

6-chloro-*N*-{2-[2-(trifluoromethyl)-10H-phenothiazin-10-yl]ethyl}-1,2,3,4-tetrahydroacridin-9-amine (49): The resulting residue was purified by column chromatography (EA/DCM = 1:1) affording **49** as yellow viscous oil. Yield 34 %.

¹H NMR (401 MHz, Chloroform-*d*) δ 7.88 – 7.81 (m, 1H), 7.81 – 7.73 (m, 1H), 7.32 – 7.26 (m, 1H), 7.26 – 7.12 (m, 4H), 7.05 – 6.96 (m, 2H), 6.88 – 6.80 (m, 1H), 4.45 (bs, 1H), 4.10 – 4.01 (m, 2H), 3.87 – 3.74 (m, 2H), 2.93 (t, *J* = 6.5 Hz, 2H), 2.48 (t, *J* = 6.4 Hz, 2H), 1.84 – 1.68 (m, 2H), 1.67 – 1.54 (m, 2H). ¹³C NMR (101 MHz, cdcl₃) δ 159.86, 149.80, 145.26, 143.82, 134.00, 131.52, 130.05, 129.72, 127.90, 127.56, 125.59, 124.63, 124.03, 123.94, 119.95, 119.91, 119.10, 118.32, 116.15, 112.32, 112.28, 112.24, 47.62, 44.96, 33.86, 24.25, 22.59, 22.50. HRMS (ESI⁺): [M]⁺: calculated for C₂₈H₂₄ClF₃N₃S⁺ (m/z): 526.1326; found: 526.13263. LC-MS > 99 %.

***N*-[3-(10H-phenothiazin-10-yl)propyl]-1,2,3,4-tetrahydroacridin-9-amine (50):** The resulting residue was purified by column chromatography (PE/DCM/Tol/EtOH/NH₃ = 15:5.5:3:1.5:0.1) affording **50** as yellow viscous oil. Yield 67 %.

¹H NMR (401 MHz, Chloroform-*d*) δ 7.91 – 7.82 (m, 1H), 7.78 – 7.71 (m, 1H), 7.54 – 7.44 (m, 1H), 7.26 – 7.19 (m, 1H), 7.19 – 7.08 (m, 4H), 6.96 – 6.88 (m, 2H), 6.84 – 6.77 (m, 2H), 3.97 (t, *J* = 6.2 Hz, 2H), 3.54 (t, *J* = 6.5 Hz, 2H), 2.99 (t, *J* = 6.4 Hz, 2H), 2.48 (t, *J* = 6.3 Hz, 2H), 2.13 – 2.03 (m, 2H), 1.87 – 1.78 (m, 2H), 1.79 – 1.68 (m, 2H). ¹³C NMR (101 MHz, cdcl₃) δ 158.52, 150.15, 147.25, 145.03, 129.00, 128.71, 128.17, 127.62, 127.30, 125.95, 125.27, 123.76, 122.80, 122.27, 120.36, 116.71, 115.65, 45.80, 44.03, 33.96, 28.11, 24.72, 22.98, 22.72. HRMS (ESI⁺): [M]⁺: calculated for C₂₈H₂₈N₃S⁺ (m/z): 438.19985; found: 438.19971. LC-MS > 99 %.

7-methoxy-*N*-[3-(10H-phenothiazin-10-yl)propyl]-1,2,3,4-tetrahydroacridin-9-amine (51): The resulting residue was purified by column chromatography (PE/DCM/Tol/EtOH/NH₃ = 15:5.5:3:1.5:0.1) affording **51** as yellow viscous oil. Yield 68 %.

¹H NMR (401 MHz, Chloroform-*d*) δ 7.82 – 7.74 (m, 1H), 7.27 – 7.07 (m, 6H), 6.95 – 6.87 (m, 2H), 6.83 – 6.77 (m, 2H), 3.98 (t, *J* = 6.2 Hz, 2H), 3.81 (s, 3H), 3.50 (t,

$J = 6.5$ Hz, 2H), 3.01 – 2.92 (m, 2H), 2.49 (t, $J = 6.3$ Hz, 2H), 2.14 – 2.05 (m, 2H), 1.89 – 1.77 (m, 2H), 1.78 – 1.68 (m, 2H). ^{13}C NMR (101 MHz, cdCl_3) δ 156.16, 156.02, 149.32, 145.00, 143.19, 130.21, 129.00, 128.19, 127.61, 127.28, 125.82, 125.26, 122.79, 121.25, 120.24, 117.80, 115.58, 101.19, 55.43, 45.71, 44.25, 33.65, 28.32, 24.58, 22.99, 22.77. HRMS (ESI⁺): $[\text{M}]^+$: calculated for $\text{C}_{29}\text{H}_{30}\text{N}_3\text{OS}^+$ (m/z): 468.21041; found: 468.21042. LC-MS > 98 %.

6-chloro-*N*-[3-(10H-phenothiazin-10-yl)propyl]-1,2,3,4-tetrahydroacridin-9-amine (52): The resulting residue was purified by column chromatography (EA/DCM = 1:1) affording **52** as yellow viscous oil. Yield 60 %.

^1H NMR (401 MHz, Chloroform-*d*) δ 7.87 – 7.76 (m, 1H), 7.68 – 7.61 (m, 1H), 7.18 – 7.08 (m, 5H), 6.97 – 6.89 (m, 2H), 6.84 – 6.77 (m, 2H), 3.98 (t, $J = 6.1$ Hz, 2H), 3.54 (t, $J = 6.4$ Hz, 2H), 2.94 (t, $J = 6.4$ Hz, 2H), 2.44 (t, $J = 6.3$ Hz, 2H), 2.08 (p, $J = 6.3$ Hz, 2H), 1.86 – 1.78 (m, 2H), 1.77 – 1.69 (m, 2H). ^{13}C NMR (101 MHz, cdCl_3) δ 159.61, 150.27, 147.88, 144.96, 133.83, 127.66, 127.56, 127.30, 126.06, 124.36, 123.99, 122.87, 118.56, 116.62, 115.65, 45.93, 43.95, 33.96, 28.08, 24.50, 22.85, 22.58. HRMS (ESI⁺): $[\text{M}]^+$: calculated for $\text{C}_{28}\text{H}_{27}\text{ClN}_3\text{S}^+$ (m/z): 472.16087; found: 472.16092. LC-MS > 99 %.

***N*-[3-(2-chloro-10H-phenothiazin-10-yl)propyl]-1,2,3,4-tetrahydroacridin-9-amine (53):** The resulting residue was purified by column chromatography (PE/DCM/Tol/EtOH/NH₃ = 15:6.5:3:0.5:0.05) affording **53** as yellow viscous oil. Yield 29 %.

^1H NMR (401 MHz, Chloroform-*d*) δ 7.89 – 7.83 (m, 1H), 7.78 – 7.72 (m, 1H), 7.55 – 7.47 (m, 1H), 7.26 – 7.21 (m, 1H), 7.17 – 7.11 (m, 2H), 7.05 – 7.01 (m, 1H), 6.99 – 6.88 (m, 2H), 6.83 – 6.76 (m, 2H), 3.95 (t, $J = 6.2$ Hz, 2H), 3.56 (t, $J = 6.4$ Hz, 2H), 3.00 (t, $J = 6.4$ Hz, 2H), 2.53 (t, $J = 6.3$ Hz, 2H), 2.14 – 2.05 (m, 2H), 1.91 – 1.81 (m, 2H), 1.81 – 1.72 (m, 1H). ^{13}C NMR (101 MHz, cdCl_3) δ 150.08, 146.33, 144.26, 133.32, 128.99, 128.70, 128.25, 128.18, 128.09, 127.70, 127.48, 125.72, 125.26, 124.46, 123.85, 123.26, 122.66, 122.16, 116.69, 116.01, 115.94, 45.62, 44.11, 33.86, 28.09, 24.81, 22.96, 22.71. HRMS (ESI⁺): $[\text{M}]^+$: calculated for $\text{C}_{28}\text{H}_{27}\text{ClN}_3\text{S}^+$ (m/z): 472.16087; found: 472.16086. LC-MS > 96 %.

***N*-[3-(2-chloro-10H-phenothiazin-10-yl)propyl]-7-methoxy-1,2,3,4-tetrahydroacridin-9-amine (54):** The resulting residue was purified by column

chromatography (PE/DCM/Tol/EtOH/NH₃ = 15:6:3:1:0.1) affording **54** as yellow viscous oil. Yield 20 %.

¹H NMR (401 MHz, Chloroform-*d*) δ 7.83 – 7.73 (m, 1H), 7.27 – 7.05 (m, 4H), 7.03 – 6.97 (m, 1H), 6.97 – 6.84 (m, 2H), 6.82 – 6.72 (m, 2H), 3.95 (t, *J* = 6.2 Hz, 2H), 3.83 (s, 3H), 3.52 (t, *J* = 6.5 Hz, 2H), 2.97 (t, *J* = 6.4 Hz, 2H), 2.52 (t, *J* = 6.3 Hz, 2H), 2.19 – 2.04 (m, 2H), 1.90 – 1.79 (m, 2H), 1.79 – 1.70 (m, 2H). ¹³C NMR (101 MHz, cdcl₃) δ 156.09, 149.42, 146.27, 144.24, 133.30, 129.91, 128.99, 128.06, 127.68, 127.46, 125.58, 124.32, 123.24, 122.63, 121.08, 120.34, 115.94, 115.86, 101.22, 55.45, 45.48, 44.32, 33.36, 28.30, 24.69, 22.94, 22.68. HRMS (ESI⁺): [M]⁺: calculated for C₂₉H₂₉ClN₃OS⁺ (m/z): 502.17144; found: 502.17139. LC-MS > 97 %.

6-chloro-*N*-[3-(2-chloro-10H-phenothiazin-10-yl)propyl]-1,2,3,4-tetrahydroacridin-9-amine (55): The resulting residue was purified by column chromatography (EA/DCM = 1:1) affording **55** as yellow viscous oil. Yield 26 %.

¹H NMR (401 MHz, Chloroform-*d*) δ 7.85 – 7.81 (m, 1H), 7.70 – 7.64 (m, 1H), 7.22 – 7.08 (m, 2H), 7.04 – 6.99 (m, 1H), 6.98 – 6.92 (m, 1H), 6.92 – 6.87 (m, 1H), 6.87 – 6.83 (m, 1H), 6.81 – 6.76 (m, 1H), 6.76 – 6.73 (m, 1H), 3.93 (t, *J* = 6.1 Hz, 2H), 3.57 (t, *J* = 6.4 Hz, 2H), 2.96 (t, *J* = 6.3 Hz, 2H), 2.47 (t, *J* = 6.2 Hz, 2H), 2.14 – 2.05 (m, 2H), 1.88 – 1.70 (m, 4H). ¹³C NMR (101 MHz, cdcl₃) δ 159.32, 150.57, 146.22, 144.13, 134.21, 133.33, 129.47, 128.10, 127.73, 127.48, 126.96, 125.79, 124.53, 124.02, 123.35, 122.74, 119.58, 118.26, 115.99, 115.93, 115.59, 45.70, 43.98, 33.38, 28.07, 24.57, 22.75, 22.42. HRMS (ESI⁺): [M]⁺: calculated for C₂₈H₂₆Cl₂N₃S⁺ (m/z): 506.12190; found: 506.12201. LC-MS > 98 %.

***N*-{3-[2-(trifluoromethyl)-10H-phenothiazin-10-yl]propyl}-1,2,3,4-tetrahydroacridin-9-amine (56):** The resulting residue was purified by column chromatography (PE/DCM/Tol/EtOH/NH₃ = 15:6:3:1:0.1) affording **56** as yellow viscous oil. Yield 40 %.

¹H NMR (401 MHz, Chloroform-*d*) δ 7.90 – 7.83 (m, 1H), 7.77 – 7.71 (m, 1H), 7.55 – 7.47 (m, 1H), 7.25 – 7.20 (m, 2H), 7.18 – 7.10 (m, 3H), 7.04 – 6.93 (m, 2H), 6.85 – 6.77 (m, 1H), 4.01 (t, *J* = 6.2 Hz, 2H), 3.56 (t, *J* = 6.5 Hz, 2H), 2.99 (t, *J* = 6.4 Hz, 2H), 2.52 (t, *J* = 6.3 Hz, 2H), 2.11 (p, *J* = 6.4 Hz, 2H), 1.89 – 1.79 (m, 2H), 1.80 – 1.70 (m, 2H). ¹³C NMR (101 MHz, cdcl₃) δ 158.40, 150.14, 147.02, 145.47, 144.17, 130.91, 129.84, 129.52, 128.99, 128.57, 128.32, 128.18, 127.75, 127.73, 127.71, 125.26,

124.96, 123.89, 123.48, 122.12, 120.26, 119.48, 119.44, 116.69, 116.01, 112.11, 112.07, 45.65, 44.22, 33.72, 28.04, 24.78, 22.90, 22.64. HRMS (ESI⁺): [M]⁺: calculated for C₂₉H₂₇F₃N₃S⁺ (m/z): 506.18723; found: 506.18716. LC-MS > 96 %.

7-methoxy-*N*-{3-[2-(trifluoromethyl)-10H-phenothiazin-10-yl]propyl}-1,2,3,4-tetrahydroacridin-9-amine (57): The resulting residue was purified by column chromatography (PE/DCM/Tol/EtOH/NH₃ = 15:5.5:3:1.5:1) affording **57** as yellow viscous oil. Yield 41 %.

¹H NMR (401 MHz, Chloroform-*d*) δ 7.81 – 7.74 (m, 1H), 7.28 – 7.10 (m, 5H), 7.10 – 7.07 (m, 1H), 7.02 – 6.92 (m, 2H), 6.84 – 6.77 (m, 1H), 4.01 (t, *J* = 6.2 Hz, 2H), 3.82 (s, 3H), 3.51 (t, *J* = 6.6 Hz, 2H), 2.96 (t, *J* = 6.4 Hz, 2H), 2.52 (t, *J* = 6.3 Hz, 2H), 2.11 (p, *J* = 6.4 Hz, 2H), 1.90 – 1.80 (m, 2H), 1.78 – 1.71 (m, 2H). ¹³C NMR (101 MHz, cdcl₃) δ 156.11, 149.17, 145.40, 144.18, 130.22, 128.99, 128.18, 127.73, 127.71, 127.69, 125.25, 124.83, 123.45, 121.24, 120.25, 119.44, 117.87, 115.92, 112.06, 112.02, 109.99, 101.15, 55.40, 45.57, 44.46, 33.57, 28.25, 24.67, 22.94, 22.73. HRMS (ESI⁺): [M]⁺: calculated for C₃₀H₂₉F₃N₃OS⁺ (m/z): 536.19779; found: 536.19775. LC-MS > 98 %.

6-chloro-*N*-{3-[2-(trifluoromethyl)-10H-phenothiazin-10-yl]propyl}-1,2,3,4-tetrahydroacridin-9-amine (58): The resulting residue was purified by column chromatography (EA/DCM = 1:1) affording **58** as yellow viscous oil. Yield 63 %.

¹H NMR (401 MHz, Chloroform-*d*) δ 7.82 – 7.79 (m, 1H), 7.70 – 7.63 (m, 1H), 7.23 – 7.08 (m, 5H), 7.01 – 6.92 (m, 2H), 6.83 – 6.77 (m, 1H), 4.00 (t, *J* = 6.1 Hz, 2H), 3.91 (bs, 1H), 3.54 (t, *J* = 6.5 Hz, 2H), 2.94 (t, *J* = 6.4 Hz, 2H), 2.48 (t, *J* = 6.3 Hz, 2H), 2.09 (p, *J* = 6.4 Hz, 2H), 1.89 – 1.79 (m, 2H), 1.78 – 1.70 (m, 2H). ¹³C NMR (101 MHz, cdcl₃) δ 159.66, 150.13, 147.89, 145.39, 144.10, 133.88, 130.99, 129.83, 129.51, 127.78, 127.73, 127.63, 125.03, 124.45, 123.90, 123.54, 119.53, 119.49, 118.56, 116.72, 115.99, 112.10, 112.07, 45.79, 44.12, 33.92, 28.06, 24.57, 22.80, 22.55. HRMS (ESI⁺): [M]⁺: calculated for C₂₉H₂₆ClF₃N₃S⁺ (m/z): 540.14826; found: 540.14825. LC-MS > 98 %.

***N*-[4-(10H-phenothiazin-10-yl)butyl]-1,2,3,4-tetrahydroacridin-9-amine (59):** The resulting residue was purified by column chromatography (PE/DCM/Tol/EtOH/NH₃ = 15:5.5:3:1.5:0.15) affording **59** as dark yellow viscous oil. Yield 74 %.

^1H NMR (401 MHz, Chloroform-*d*) δ 7.92 – 7.85 (m, 1H), 7.85 – 7.80 (m, 1H), 7.56 – 7.46 (m, 1H), 7.29 – 7.20 (m, 1H), 7.18 – 7.07 (m, 4H), 6.95 – 6.86 (m, 2H), 6.84 – 6.76 (m, 2H), 3.86 (t, $J = 6.4$ Hz, 2H), 3.45 (t, $J = 6.9$ Hz, 2H), 3.02 (t, $J = 6.2$ Hz, 2H), 2.54 (t, $J = 6.1$ Hz, 2H), 1.92 – 1.79 (m, 6H), 1.79 – 1.70 (m, 2H). ^{13}C NMR (101 MHz, cdCl_3) δ 158.44, 150.36, 147.46, 145.11, 128.76, 128.17, 127.57, 127.22, 125.48, 123.56, 122.66, 122.59, 120.14, 115.92, 115.53, 48.81, 46.67, 34.05, 29.00, 24.71, 24.16, 23.04, 22.75. HRMS (ESI $^+$): $[\text{M}]^+$: calculated for $\text{C}_{29}\text{H}_{30}\text{N}_3\text{S}^+$ (m/z): 452.21550; found: 452.21527 LC-MS > 98 %.

7-methoxy-*N*-[4-(10H-phenothiazin-10-yl)butyl]-1,2,3,4-tetrahydroacridin-9-amine (60): The resulting residue was purified by column chromatography (PE/DCM/Tol/EtOH/NH $_3$ = 15:5.5:3:1.5:0.15) affording **60** as dark yellow viscous oil. Yield 57 %.

^1H NMR (401 MHz, Chloroform-*d*) δ 7.83 – 7.77 (m, 1H), 7.23 – 7.18 (m, 1H), 7.15 – 7.07 (m, 5H), 6.93 – 6.86 (m, 2H), 6.83 – 6.77 (m, 2H), 3.87 (t, $J = 6.5$ Hz, 2H), 3.80 (s, 3H), 3.38 (t, $J = 7.0$ Hz, 2H), 3.00 (t, $J = 6.1$ Hz, 2H), 2.58 (t, $J = 6.0$ Hz, 2H), 1.94 – 1.80 (m, 6H), 1.79 – 1.70 (m, 2H). ^{13}C NMR (101 MHz, cdCl_3) δ 156.15, 155.87, 149.50, 145.11, 143.38, 130.27, 127.55, 127.19, 125.47, 122.58, 121.20, 120.27, 117.40, 115.49, 101.47, 55.39, 48.58, 46.72, 33.78, 29.00, 24.64, 24.35, 23.05, 22.80. HRMS (ESI $^+$): $[\text{M}]^+$: calculated for $\text{C}_{30}\text{H}_{32}\text{N}_3\text{OS}^+$ (m/z): 482.22606; found: 482.22583. LC-MS > 99 %.

6-chloro-*N*-[4-(10H-phenothiazin-10-yl)butyl]-1,2,3,4-tetrahydroacridin-9-amine (61): The resulting residue was purified by column chromatography (EA/DCM = 1:1) affording **61** as yellow sticky foam. Yield 61 %.

^1H NMR (401 MHz, Chloroform-*d*) δ 7.86 – 7.81 (m, 1H), 7.76 – 7.70 (m, 1H), 7.17 – 7.06 (m, 5H), 6.93 – 6.86 (m, 2H), 6.82 – 6.76 (m, 2H), 3.87 (t, $J = 6.3$ Hz, 2H), 3.44 (t, $J = 6.9$ Hz, 2H), 2.98 (t, $J = 6.1$ Hz, 2H), 2.47 (t, $J = 6.0$ Hz, 2H), 1.90 – 1.78 (m, 6H), 1.78 – 1.69 (m, 2H). ^{13}C NMR (101 MHz, cdCl_3) δ 159.46, 150.42, 148.06, 145.08, 133.84, 127.60, 127.53, 127.21, 125.58, 124.39, 124.14, 122.64, 118.27, 115.74, 115.55, 48.85, 46.55, 34.00, 28.97, 24.46, 24.02, 22.90, 22.59. HRMS (ESI $^+$): $[\text{M}]^+$: calculated for $\text{C}_{29}\text{H}_{29}\text{ClN}_3\text{S}^+$ (m/z): 486.17652; found: 486.17636. LC-MS > 97 %.

***N*-[4-(2-chloro-10H-phenothiazin-10-yl)butyl]-1,2,3,4-tetrahydroacridin-9-amine (62):** The resulting residue was purified by column chromatography (EA/DCM = 1:1) affording **62** as yellow viscous oil. Yield 50 %.

¹H NMR (401 MHz, Chloroform-*d*) δ 7.90 – 7.76 (m, 2H), 7.57 – 7.47 (m, 1H), 7.30 – 7.22 (m, 1H), 7.15 – 7.06 (m, 2H), 7.03 – 6.97 (m, 1H), 6.96 – 6.83 (m, 2H), 6.82 – 6.74 (m, 2H), 3.84 (t, *J* = 6.3 Hz, 2H), 3.45 (t, *J* = 6.9 Hz, 2H), 3.02 (t, *J* = 6.1 Hz, 2H), 2.55 (t, *J* = 6.0 Hz, 2H), 1.92 – 1.80 (m, 6H), 1.79 – 1.69 (m, 2H). ¹³C NMR (101 MHz, cdcl₃) δ 158.39, 150.31, 147.38, 146.41, 144.37, 133.21, 128.72, 128.22, 128.03, 127.64, 127.40, 125.25, 123.61, 123.06, 122.60, 122.43, 120.11, 115.95, 115.87, 115.84, 109.99, 48.76, 46.82, 34.01, 28.92, 24.72, 24.04, 23.02, 22.73. HRMS (ESI⁺): [M]⁺: calculated for C₂₉H₂₉ClN₃S⁺ (m/z): 486.17652; found: 486.17633. LC-MS > 98 %.

***N*-[4-(2-chloro-10H-phenothiazin-10-yl)butyl]-7-methoxy-1,2,3,4-tetrahydroacridin-9-amine (63):** The resulting residue was purified by column chromatography (PE/DCM/Tol/EtOH/NH₃ = 15:5.5:3:1.5:0.15) affording **63** as yellow viscous oil. Yield 50 %.

¹H NMR (401 MHz, Chloroform-*d*) δ 7.83 – 7.76 (m, 1H), 7.23 – 7.17 (m, 1H), 7.15 – 7.08 (m, 3H), 7.02 – 6.96 (m, 1H), 6.95 – 6.88 (m, 1H), 6.88 – 6.84 (m, 1H), 6.81 – 6.76 (m, 2H), 3.88 – 3.76 (m, 5H), 3.38 (t, *J* = 7.0 Hz, 2H), 3.00 (t, *J* = 6.0 Hz, 2H), 2.59 (t, *J* = 5.9 Hz, 2H), 1.93 – 1.79 (m, 6H), 1.80 – 1.69 (m, 2H). ¹³C NMR (101 MHz, cdcl₃) δ 156.11, 155.90, 149.46, 146.41, 144.38, 143.28, 133.19, 130.19, 128.01, 127.62, 127.39, 125.24, 123.99, 123.05, 122.42, 121.18, 120.30, 117.39, 115.84, 115.81, 101.46, 55.40, 48.52, 46.87, 33.70, 28.92, 24.66, 24.22, 23.03, 22.78. HRMS (ESI⁺): [M]⁺: calculated for C₃₀H₃₁ClN₃OS⁺ (m/z): 516.18709; found: 516.18701. LC-MS > 97 %.

6-chloro-*N*-[4-(2-chloro-10H-phenothiazin-10-yl)butyl]-1,2,3,4-tetrahydroacridin-9-amine (64): The resulting residue was purified by column chromatography (EA/DCM = 1:1) affording **64** as yellow viscous oil. Yield 47 %.

¹H NMR (401 MHz, Chloroform-*d*) δ 7.86 – 7.81 (m, 1H), 7.76 – 7.71 (m, 1H), 7.18 – 7.08 (m, 3H), 7.02 – 6.96 (m, 1H), 6.95 – 6.89 (m, 1H), 6.89 – 6.84 (m, 1H), 6.81 – 6.74 (m, 2H), 3.84 (t, *J* = 6.2 Hz, 2H), 3.45 (t, *J* = 6.9 Hz, 2H), 2.98 (t, *J* = 6.0 Hz, 2H), 2.49 (t, *J* = 6.0 Hz, 2H), 1.92 – 1.78 (m, 6H), 1.78 – 1.68 (m, 2H). ¹³C NMR (101

MHz, cdCl_3) δ 159.40, 150.38, 147.95, 146.34, 144.34, 133.92, 133.21, 128.05, 127.66, 127.48, 127.40, 125.32, 124.32, 124.20, 124.08, 123.10, 122.47, 118.23, 115.89, 115.84, 115.76, 48.80, 46.70, 33.93, 28.88, 24.48, 23.90, 22.88, 22.56. HRMS (ESI⁺): [M]⁺: calculated for $\text{C}_{29}\text{H}_{28}\text{Cl}_2\text{N}_3\text{S}^+$ (m/z): 520.13755; found: 520.13733. LC-MS > 97 %.

***N*-{4-[2-(trifluoromethyl)-10H-phenothiazin-10-yl]butyl}-1,2,3,4-tetrahydroacridin-9-amine (65):** The resulting residue was purified by column chromatography (PE/DCM/Tol/EtOH/NH₃ = 15:5.5:3:1.5:0.1) affording **65** as yellow viscous oil. Yield 63 %.

¹H NMR (401 MHz, Chloroform-*d*) δ 7.89 – 7.80 (m, 2H), 7.55 – 7.47 (m, 1H), 7.29 – 7.22 (m, 1H), 7.22 – 7.16 (m, 1H), 7.17 – 7.10 (m, 3H), 7.01 – 6.98 (m, 1H), 6.98 – 6.91 (m, 1H), 6.84 – 6.79 (m, 1H), 3.91 (t, *J* = 6.4 Hz, 2H), 3.84 (bs, 1H), 3.52 – 3.41 (m, 2H), 3.02 (t, *J* = 6.1 Hz, 2H), 2.57 (t, *J* = 6.1 Hz, 2H), 1.95 – 1.71 (m, 8H). ¹³C NMR (101 MHz, cdCl_3) δ 158.50, 150.23, 147.49, 145.65, 144.17, 128.84, 128.18, 127.71, 127.62, 124.57, 123.61, 123.28, 122.53, 120.19, 119.25, 119.21, 116.08, 115.93, 111.95, 111.91, 48.79, 46.90, 34.07, 28.93, 24.74, 24.05, 23.01, 22.74. HRMS (ESI⁺): [M]⁺: calculated for $\text{C}_{30}\text{H}_{29}\text{F}_3\text{N}_3\text{S}^+$ (m/z): 520.20288; found: 520.20264. LC-MS > 98 %.

7-methoxy-*N*-{4-[2-(trifluoromethyl)-10H-phenothiazin-10-yl]butyl}-1,2,3,4-tetrahydroacridin-9-amine (66): The resulting residue was purified by column chromatography (PE/DCM/Tol/EtOH/NH₃ = 15:5.5:3:1.5:1) affording **66** as yellow viscous oil. Yield 53 %.

¹H NMR (401 MHz, Chloroform-*d*) δ 7.84 – 7.78 (m, 1H), 7.23 – 7.07 (m, 6H), 7.01 – 6.97 (m, 1H), 6.97 – 6.90 (m, 1H), 6.84 – 6.78 (m, 1H), 3.90 (t, *J* = 6.5 Hz, 2H), 3.80 (s, 3H), 3.38 (t, *J* = 7.0 Hz, 2H), 3.00 (t, *J* = 6.0 Hz, 2H), 2.59 (t, *J* = 6.0 Hz, 2H), 1.94 – 1.80 (m, 6H), 1.79 – 1.71 (m, 2H). ¹³C NMR (101 MHz, cdCl_3) δ 156.11, 155.93, 149.50, 145.63, 144.18, 143.19, 130.46, 130.09, 129.73, 129.41, 127.69, 127.61, 124.54, 123.28, 121.19, 120.33, 119.23, 119.20, 117.41, 115.91, 111.92, 111.88, 101.45, 55.36, 48.51, 46.94, 33.57, 28.91, 24.66, 24.19, 22.99, 22.74. HRMS (ESI⁺): [M]⁺: calculated for $\text{C}_{31}\text{H}_{31}\text{F}_3\text{N}_3\text{OS}^+$ (m/z): 550.21344; found: 550.21301. LC-MS > 95 %.

6-chloro-*N*-{4-[2-(trifluoromethyl)-10H-phenothiazin-10-yl]butyl}-1,2,3,4-tetrahydroacridin-9-amine (67): The resulting residue was purified by column chromatography (EA/DCM = 1:1) affording **67** as yellow viscous oil. Yield 52 %.

¹H NMR (401 MHz, Chloroform-*d*) δ 7.87 – 7.81 (m, 1H), 7.76 – 7.71 (m, 1H), 7.21 – 7.09 (m, 5H), 7.01 – 6.97 (m, 1H), 6.97 – 6.90 (m, 1H), 6.83 – 6.77 (m, 1H), 3.91 (t, *J* = 6.3 Hz, 2H), 3.45 (t, *J* = 6.9 Hz, 2H), 2.98 (t, *J* = 6.0 Hz, 2H), 2.50 (t, *J* = 6.0 Hz, 2H), 1.94 – 1.80 (m, 6H), 1.79 – 1.70 (m, 2H). ¹³C NMR (101 MHz, cdcl₃) δ 159.47, 150.33, 148.01, 145.60, 144.14, 133.91, 130.53, 127.73, 127.64, 127.62, 127.55, 124.63, 124.26, 124.22, 123.32, 119.27, 119.23, 118.29, 115.93, 115.87, 111.96, 111.92, 48.83, 46.78, 33.97, 28.88, 24.48, 23.91, 22.86, 22.56. HRMS (ESI⁺): [M]⁺: calculated for C₃₀H₂₈ClF₃N₃S⁺ (*m/z*): 554.16391; found: 554.16364. LC-MS > 98 %.

***N*-[5-(10H-phenothiazin-10-yl)pentyl]-1,2,3,4-tetrahydroacridin-9-amine (68):** The resulting residue was purified by column chromatography (PE/DCM/Tol/EtOH/NH₃ = 15:5.5:3:1.2:0.1) affording **68** as yellow viscous oil. Yield 78 %.

¹H NMR (500 MHz, Chloroform-*d*) δ 7.96 – 7.87 (m, 2H), 7.58 – 7.51 (m, 1H), 7.36 – 7.27 (m, 1H), 7.21 – 7.10 (m, 4H), 6.96 – 6.88 (m, 2H), 6.88 – 6.81 (m, 2H), 5.30 (bs, 1H), 3.88 (t, *J* = 6.7 Hz, 2H), 3.45 (t, *J* = 7.1 Hz, 2H), 3.06 (t, *J* = 6.1 Hz, 2H), 2.65 (t, *J* = 5.9 Hz, 2H), 1.97 – 1.78 (m, 6H), 1.72 – 1.61 (m, 2H), 1.61 – 1.48 (m, 2H). ¹³C NMR (126 MHz, cdcl₃) δ 158.34, 150.65, 147.31, 145.22, 128.60, 128.25, 127.50, 127.16, 125.30, 123.58, 122.74, 122.47, 120.15, 115.90, 115.47, 49.28, 46.91, 33.89, 31.25, 26.45, 24.75, 24.24, 23.02, 22.72. HRMS (ESI⁺): [M]⁺: calculated for C₃₀H₃₂N₃S⁺ (*m/z*): 466.23115; found: 466.23074. LC-MS > 96 %.

7-methoxy-*N*-[5-(10H-phenothiazin-10-yl)pentyl]-1,2,3,4-tetrahydroacridin-9-amine (69): The resulting residue was purified by column chromatography (PE/DCM/Tol/EtOH/NH₃ = 15:5.5:3:1.2:0.1) affording **69** as yellow viscous oil. Yield 45 %.

¹H NMR (500 MHz, Chloroform-*d*) δ 7.89 – 7.84 (m, 1H), 7.26 – 7.22 (m, 1H), 7.20 – 7.10 (m, 5H), 6.95 – 6.88 (m, 2H), 6.86 – 6.80 (m, 2H), 3.91 – 3.81 (m, 5H), 3.37 (t, *J* = 7.1 Hz, 2H), 3.04 (t, *J* = 6.0 Hz, 2H), 2.66 (t, *J* = 5.9 Hz, 2H), 1.94 – 1.77 (m, 6H), 1.70 – 1.60 (m, 2H), 1.58 – 1.48 (m, 2H). ¹³C NMR (126 MHz, cdcl₃) δ 155.87, 155.78, 149.80, 145.11, 142.95, 129.84, 127.40, 127.09, 125.16, 122.38, 121.05,

120.28, 117.08, 115.38, 101.55, 55.32, 48.85, 46.82, 33.44, 31.20, 26.42, 24.57, 24.25, 22.92, 22.65. HRMS (ESI⁺): [M]⁺: calculated for C₃₁H₃₄N₃OS⁺ (m/z): 496.24171; found: 496.24121. LC-MS > 97 %.

6-chloro-*N*-[5-(10H-phenothiazin-10-yl)pentyl]-1,2,3,4-tetrahydroacridin-9-amine (70): The resulting residue was purified by column chromatography (EA/DCM = 1:1) affording **70** as yellow viscous oil. Yield 43 %.

¹H NMR (500 MHz, Chloroform-*d*) δ 7.94 – 7.87 (m, 1H), 7.86 – 7.79 (m, 1H), 7.25 – 7.20 (m, 1H), 7.20 – 7.11 (m, 4H), 6.92 (t, *J* = 7.4 Hz, 2H), 6.89 – 6.81 (m, 3H), 3.87 (t, *J* = 6.6 Hz, 2H), 3.42 (t, *J* = 7.0 Hz, 2H), 3.01 (t, *J* = 5.9 Hz, 2H), 2.58 (t, *J* = 5.6 Hz, 2H), 1.95 – 1.77 (m, 6H), 1.68 – 1.59 (m, 2H), 1.57 – 1.46 (m, 2H). ¹³C NMR (126 MHz, cdcl₃) δ 159.36, 150.62, 147.94, 145.13, 133.83, 127.45, 127.36, 127.13, 125.24, 124.48, 124.07, 122.43, 118.23, 115.64, 115.45, 49.28, 46.76, 33.83, 31.16, 26.28, 24.46, 24.11, 22.82, 22.52. HRMS (ESI⁺): [M]⁺: calculated for C₃₀H₃₁ClN₃S⁺ (m/z): 500.19217; found: 500.19183. LC-MS > 96 %.

***N*-[5-(2-chloro-10H-phenothiazin-10-yl)pentyl]-1,2,3,4-tetrahydroacridin-9-amine (71):** The resulting residue was purified by column chromatography (PE/DCM/Tol/EtOH/NH₃ = 15:5.5:3:1.2:0.1) affording **71** as yellow viscous oil. Yield 71 %.

¹H NMR (500 MHz, Chloroform-*d*) δ 7.97 – 7.87 (m, 2H), 7.57 – 7.51 (m, 1H), 7.35 – 7.27 (m, 1H), 7.17 – 7.09 (m, 2H), 7.03 – 6.98 (m, 1H), 6.96 – 6.90 (m, 1H), 6.90 – 6.85 (m, 1H), 6.85 – 6.78 (m, 2H), 3.82 (t, *J* = 6.7 Hz, 2H), 3.44 (t, *J* = 7.1 Hz, 2H), 3.06 (t, *J* = 6.0 Hz, 2H), 2.63 (t, *J* = 5.9 Hz, 2H), 1.95 – 1.84 (m, 4H), 1.84 – 1.76 (m, 2H), 1.69 – 1.60 (m, 2H), 1.55 – 1.46 (m, 2H). ¹³C NMR (126 MHz, cdcl₃) δ 158.12, 150.65, 147.01, 146.41, 144.36, 133.08, 128.30, 128.26, 127.86, 127.47, 127.29, 124.92, 123.69, 123.53, 122.86, 122.67, 122.20, 119.96, 115.72, 115.67, 49.12, 46.92, 33.60, 31.11, 26.21, 24.65, 24.05, 22.90, 22.58. HRMS (ESI⁺): [M]⁺: calculated for C₃₀H₃₁ClN₃S⁺ (m/z): 500.19217; found: 500.19162. LC-MS > 95 %.

***N*-[5-(2-chloro-10H-phenothiazin-10-yl)pentyl]-7-methoxy-1,2,3,4-tetrahydroacridin-9-amine (72):** The resulting residue was purified by column chromatography (PE/DCM/Tol/EtOH/NH₃ = 15:5.5:3:1.2:0.1) affording **72** as yellow viscous oil. Yield 39 %.

¹H NMR (500 MHz, Chloroform-*d*) δ 7.88 – 7.82 (m, 1H), 7.26 – 7.21 (m, 1H), 7.20 – 7.09 (m, 3H), 7.03 – 6.98 (m, 1H), 6.96 – 6.90 (m, 1H), 6.89 – 6.86 (m, 1H), 6.85 – 6.79 (m, 2H), 3.86 (s, 3H), 3.83 (t, *J* = 6.7 Hz, 2H), 3.37 (t, *J* = 7.1 Hz, 2H), 3.03 (t, *J* = 6.0 Hz, 2H), 2.66 (t, *J* = 5.8 Hz, 2H), 1.93 – 1.85 (m, 4H), 1.85 – 1.78 (m, 2H), 1.70 – 1.61 (m, 2H), 1.58 – 1.49 (m, 2H). ¹³C NMR (126 MHz, cdcl₃) δ 155.86, 149.79, 146.44, 144.41, 142.96, 133.11, 129.87, 127.90, 127.51, 127.31, 124.96, 123.73, 122.89, 122.24, 121.08, 120.30, 117.13, 115.74, 115.72, 101.60, 55.37, 48.86, 47.00, 33.45, 31.20, 26.35, 24.63, 24.22, 22.96, 22.68. HRMS (ESI⁺): [M]⁺: calculated for C₃₁H₃₃ClN₃OS⁺ (m/z): 530.20274; found: 530.20233. LC-MS > 96 %.

6-chloro-*N*-[5-(2-chloro-10H-phenothiazin-10-yl)pentyl]-1,2,3,4-tetrahydroacridin-9-amine (73): The resulting residue was purified by column chromatography (EA/DCM = 1:1) affording **73** as yellow viscous oil. Yield 45 %.

¹H NMR (500 MHz, Chloroform-*d*) δ 7.90 – 7.86 (m, 1H), 7.84 – 7.79 (m, 1H), 7.25 – 7.20 (m, 1H), 7.18 – 7.09 (m, 2H), 7.03 – 6.98 (m, 1H), 6.96 – 6.90 (m, 1H), 6.90 – 6.86 (m, 1H), 6.84 – 6.78 (m, 2H), 3.83 (t, *J* = 6.6 Hz, 2H), 3.41 (t, *J* = 7.1 Hz, 2H), 3.05 – 2.96 (m, 2H), 2.64 – 2.54 (m, 2H), 1.93 – 1.85 (m, 4H), 1.85 – 1.75 (m, 2H), 1.68 – 1.59 (m, 2H), 1.55 – 1.47 (m, 2H). ¹³C NMR (126 MHz, cdcl₃) δ 159.41, 150.54, 148.00, 146.42, 144.39, 133.84, 133.13, 127.90, 127.52, 127.43, 127.33, 124.99, 124.43, 124.11, 123.76, 122.92, 122.88, 122.26, 118.29, 115.77, 115.75, 49.27, 46.91, 33.91, 31.14, 26.20, 24.49, 24.05, 22.84, 22.55. HRMS (ESI⁺): [M]⁺: calculated for C₂₉H₂₇Cl₂N₃S⁺ (m/z): 534.15320; found: 534.15295. LC-MS > 98 %.

***N*-{5-[2-(trifluoromethyl)-10H-phenothiazin-10-yl]pentyl}-1,2,3,4-tetrahydroacridin-9-amine (74):** The resulting residue was purified by column chromatography (PE/DCM/Tol/EtOH/NH₃ = 15:5.5:3:1.2:0.1) affording **74** as yellow viscous oil. Yield 64 %.

¹H NMR (500 MHz, Chloroform-*d*) δ 7.96 – 7.87 (m, 2H), 7.57 – 7.52 (m, 1H), 7.35 – 7.29 (m, 1H), 7.20 – 7.10 (m, 4H), 7.03 – 7.00 (m, 1H), 6.98 – 6.92 (m, 1H), 6.86 – 6.81 (m, 1H), 3.88 (t, *J* = 6.7 Hz, 2H), 3.44 (t, *J* = 7.1 Hz, 2H), 3.06 (t, *J* = 6.0 Hz, 2H), 2.64 (t, *J* = 6.0 Hz, 2H), 1.94 – 1.86 (m, 4H), 1.82 (p, *J* = 7.0 Hz, 2H), 1.70 – 1.60 (m, 2H), 1.58 – 1.49 (m, 2H). ¹³C NMR (126 MHz, cdcl₃) δ 158.24, 150.58, 147.17, 145.58, 144.24, 128.44, 128.24, 127.54, 127.46, 124.22, 123.54, 123.09, 122.65, 120.04, 119.04, 119.01, 115.80, 115.78, 111.81, 111.78, 49.15, 47.02, 33.73, 31.15,

26.22, 24.67, 24.08, 22.92, 22.62. HRMS (ESI⁺): [M]⁺: calculated for C₃₁H₃₁F₃N₃S⁺ (m/z): 534.21853; found: 534.21808. LC-MS > 99 %.

7-methoxy-*N*-{5-[2-(trifluoromethyl)-10H-phenothiazin-10-yl]pentyl}-1,2,3,4-tetrahydroacridin-9-amine (75): The resulting residue was purified by column chromatography (PE/DCM/Tol/EtOH/NH₃ = 15:5.5:3:1.2:0.1) affording **75** as yellow viscous oil. Yield 78 %.

¹H NMR (500 MHz, Chloroform-*d*) δ 7.88 – 7.84 (m, 1H), 7.26 – 7.21 (m, 1H), 7.21 – 7.10 (m, 5H), 7.03 – 6.99 (m, 1H), 6.99 – 6.92 (m, 1H), 6.88 – 6.81 (m, 1H), 3.89 (t, *J* = 6.7 Hz, 2H), 3.86 (s, 3H), 3.39 (t, *J* = 7.1 Hz, 2H), 3.03 (t, *J* = 6.2 Hz, 2H), 2.66 (t, *J* = 5.8 Hz, 2H), 1.92 – 1.78 (m, 6H), 1.67 (p, *J* = 7.4 Hz, 2H), 1.60 – 1.50 (m, 2H). ¹³C NMR (126 MHz, cdcl₃) δ 155.90, 155.73, 149.94, 145.60, 144.28, 142.63, 130.19, 129.64, 129.60, 127.58, 127.56, 127.50, 124.25, 123.12, 120.97, 120.41, 119.07, 119.04, 119.01, 116.90, 115.80, 111.82, 111.79, 111.76, 101.64, 55.35, 48.81, 47.07, 33.25, 31.23, 26.33, 24.63, 24.22, 22.92, 22.60. HRMS (ESI⁺): [M]⁺: calculated for C₃₂H₃₃F₃N₃OS⁺ (m/z): 564.22909; found: 564.22833. LC-MS > 97 %.

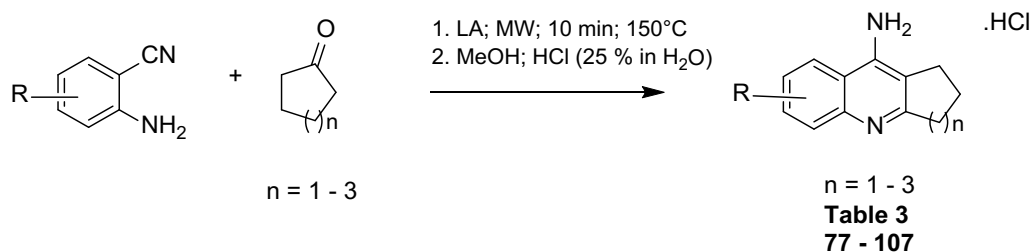
6-chloro-*N*-{5-[2-(trifluoromethyl)-10H-phenothiazin-10-yl]pentyl}-1,2,3,4-tetrahydroacridin-9-amine (76): The resulting residue was purified by column chromatography (EA/DCM = 1:1) affording **76** as yellow viscous oil. Yield 33 %.

¹H NMR (500 MHz, Chloroform-*d*) δ 7.92 – 7.89 (m, 1H), 7.84 – 7.80 (m, 1H), 7.25 – 7.11 (m, 5H), 7.04 – 7.00 (m, 1H), 6.99 – 6.93 (m, 1H), 6.88 – 6.84 (m, 1H), 3.90 (t, *J* = 6.6 Hz, 2H), 3.44 (t, *J* = 7.1 Hz, 2H), 3.05 – 2.98 (m, 2H), 2.64 – 2.55 (m, 2H), 1.94 – 1.78 (m, 6H), 1.66 (p, *J* = 7.0 Hz, 2H), 1.59 – 1.48 (m, 2H). ¹³C NMR (126 MHz, cdcl₃) δ 159.32, 150.67, 147.81, 145.59, 144.27, 133.98, 130.22, 129.62, 129.37, 128.96, 128.25, 128.15, 127.61, 127.58, 127.52, 127.28, 124.43, 124.29, 124.17, 123.16, 119.11, 119.07, 118.19, 115.84, 115.61, 111.86, 111.83, 49.27, 46.98, 33.71, 31.18, 26.17, 24.47, 24.06, 22.81, 22.49.

HRMS (ESI⁺): [M]⁺: calculated for C₃₁H₃₀ClF₃N₃S⁺ (m/z): 568.17956; found: 568.17956. LC-MS > 97 %.

6.1.2 Tacrine derivatives with dual-targeting of AChE and the NMDA receptor

General procedure for tacrine derivatives formation



A: The starting 2-amino-benzonitrile (1.0 eq); lewis acid (LA; 2.0 eq) and cyclopentanone; cyclohexanone or cyclohexanone (2 mL) were challenged by MW irradiation for 10 min at 150 °C. The resulting solid was diluted with 2 M NaOH (3 mL) and DCM 2 mL and stirred for 30 min. The solution was diluted by another 2 M NaOH (20 mL) and three times washed by DCM (3x 20 mL). The organic layers were collected, dried by anhydrous Na₂SO₄, filtered and the filtrate was concentrated. The residue was purified by column chromatography to give crude product as a base.

B: The base was dissolved by MeOH (10 mL) and HCl (25 % in H₂O; 1.5 mL) and stirred overnight. The solution was concentrated and dried to give crude product.

7-methyl-1H,2H,3H-cyclopenta[b]quinolin-9-amine hydrochloride (77): 2-amino-5-methylbenzonitrile (180 mg; 1.36 mmol); AlCl₃ (363 mg; 2.72 mmol). Purified by column chromatography using mobile phase DCM/MeOH/NH₄OH (7:1:0.1) to give crude product as a brownish solid. Yield 83 %.

¹H NMR (500 MHz, DMSO-*d*₆) δ 8.04 (s, 1H), 7.64 (d, *J* = 8.5 Hz, 1H), 7.47 – 7.39 (m, 1H), 7.06 (bs, 2H), 2.96 (t, *J* = 7.7 Hz, 2H), 2.81 (t, *J* = 7.3 Hz, 2H), 2.44 (s, 3H), 2.08 (p, *J* = 7.6 Hz, 2H). ¹³C NMR (126 MHz, dmsO) δ 163.06, 148.31, 143.37, 132.99, 131.37, 125.08, 121.73, 116.91, 113.89, 33.55, 27.82, 22.30, 21.29. HRMS (ESI⁺): [M]⁺: calculated for C₁₃H₁₅N₂⁺ (m/z): 199.12297; found: 199.12291. HPLC purity > 99 %.

7-methyl-1,2,3,4-tetrahydroacridin-9-amine hydrochloride (78): 2-amino-5-methylbenzonitrile (315 mg; 2.38 mmol); ZnCl₂ (648 mg; 4.76 mmol). Purified by column chromatography using mobile phase DCM/MeOH/NH₄OH (9:1:0.1) to give crude product as a brownish solid. Yield 98 %.

^1H NMR (500 MHz, Methanol- d_4) δ 7.81 (dd, $J = 1.9, 1.0$ Hz, 1H), 7.59 (d, $J = 8.6$ Hz, 1H), 7.40 (dd, $J = 8.6, 1.8$ Hz, 1H), 2.88 (t, $J = 6.1$ Hz, 2H), 2.58 (t, $J = 6.2$ Hz, 2H), 2.48 (s, 3H), 1.97 – 1.83 (m, 4H). ^{13}C NMR (126 MHz, cd_3od) δ 156.99, 151.01, 144.28, 134.76, 132.35, 126.31, 121.47, 117.96, 110.54, 33.31, 24.51, 23.75, 23.63, 21.60. HRMS (ESI $^+$): $[\text{M}]^+$: calculated for $\text{C}_{14}\text{H}_{17}\text{N}_2^+$ (m/z): 213.13862; found: 213.13829. HPLC purity > 99 %.

2-methyl-6H,7H,8H,9H,10H-cyclohepta[b]quinolin-11-amine hydrochloride (79): 2-amino-5-methylbenzotrile (180 mg; 1.36 mmol); AlCl_3 (363 mg; 2.72 mmol). Purified by column chromatography using mobile phase DCM/MeOH/ NH_4OH (7:1:0.1) to give crude product as a brownish solid. Yield 81 %.

^1H NMR (500 MHz, DMSO- d_6) δ 7.99 (d, $J = 1.7$ Hz, 1H), 7.61 (d, $J = 8.5$ Hz, 1H), 7.40 (dd, $J = 8.5, 1.8$ Hz, 1H), 6.71 (bs, 2H), 3.04 – 2.95 (m, 2H), 2.83 – 2.76 (m, 2H), 2.44 (s, 3H), 1.79 (p, $J = 6.3$ Hz, 2H), 1.63 (p, $J = 5.4$ Hz, 2H), 1.55 (p, $J = 5.6$ Hz, 2H). ^{13}C NMR (126 MHz, dms) δ 161.79, 148.32, 142.30, 133.12, 130.90, 126.02, 121.68, 117.36, 114.29, 37.74, 31.64, 27.57, 26.56, 25.30, 21.41. HRMS (ESI $^+$): $[\text{M}]^+$: calculated for $\text{C}_{15}\text{H}_{19}\text{N}_2^+$ (m/z): 227.15428; found: 227.15398. HPLC purity > 99 %.

7-bromo-1H,2H,3H-cyclopenta[b]quinolin-9-amine hydrochloride (80): 2-amino-5-bromobenzotrile (154 mg; 0.782 mmol); ZnCl_2 (213 mg; 1.563 mmol). Purified by column chromatography using mobile phase DCM/MeOH/ NH_4OH (15:1:0.1) to give crude product as an orange solid. Yield 67 %

^1H NMR (500 MHz, DMSO- d_6) δ 8.39 (d, $J = 1.9$ Hz, 1H), 7.65 – 7.54 (m, 2H), 6.53 (bs, 2H), 2.87 (t, $J = 7.7$ Hz, 2H), 2.80 (t, $J = 7.3$ Hz, 2H), 2.14 – 1.95 (m, 2H). ^{13}C NMR (126 MHz, dms) δ 167.45, 147.45, 145.58, 130.77, 130.67, 124.58, 119.17, 115.48, 114.34, 34.71, 27.82, 22.31. HRMS (ESI $^+$): $[\text{M}]^+$: calculated for $\text{C}_{12}\text{H}_{12}\text{BrN}_2^+$ (m/z): 263.01784; found: 263.01758. HPLC purity > 99 %.

7-bromo-1,2,3,4-tetrahydroacridin-9-amine hydrochloride (81): 2-amino-5-bromobenzotrile (156 mg; 0.792 mmol); ZnCl_2 (216 mg; 1.58 mmol). Purified by column chromatography using mobile phase DCM/MeOH/ NH_4OH (9:1:0.1) to give crude product as a light orange solid. Yield 52 %.

^1H NMR (500 MHz, DMSO- d_6) δ 8.42 (d, $J = 1.8$ Hz, 1H), 7.60 – 7.51 (m, 2H), 6.44 (bs, 2H), 2.80 (t, $J = 6.0$ Hz, 2H), 2.53 (t, $J = 6.1$ Hz, 2H), 1.86 – 1.74 (m, 4H). ^{13}C NMR (126 MHz, dms) δ 158.29, 147.61, 145.18, 130.98, 130.42, 124.43, 118.54,

115.44, 109.96, 33.71, 23.84, 22.67, 22.56. HRMS (ESI⁺): [M]⁺: calculated for C₁₃H₁₄BrN₂⁺ (m/z): 277.03349; found: 277.03329. HPLC purity > 99 %.

2-bromo-6H,7H,8H,9H,10H-cyclohepta[b]quinolin-11-amine hydrochloride (82): 2-amino-5-bromobenzonitrile (155 mg; 0.787 mmol); ZnCl₂ (214 mg; 1.57 mmol). Purified by column chromatography using mobile phase DCM/MeOH/NH₄OH (9:1:0.1) to give crude product as an orange solid. Yield 88 %.

¹H NMR (500 MHz, DMSO-*d*₆) δ 8.44 – 8.32 (m, 1H), 7.57 (d, *J* = 2.0 Hz, 2H), 6.42 (bs, 2H), 2.99 – 2.89 (m, 2H), 2.81 – 2.74 (m, 2H), 1.78 (p, *J* = 5.9 Hz, 2H), 1.61 (p, *J* = 5.5 Hz, 2H), 1.54 (p, *J* = 5.6 Hz, 2H). ¹³C NMR (126 MHz, dmsO) δ 164.92, 146.38, 145.06, 130.82, 130.71, 124.78, 119.45, 116.03, 115.11, 31.73, 27.75, 26.71, 25.48. HRMS (ESI⁺): [M]⁺: calculated for C₁₄H₁₆BrN₂⁺ (m/z): 291.04914; found: 291.04883. HPLC purity > 99 %.

7-chloro-1H,2H,3H-cyclopenta[b]quinolin-9-amine hydrochloride (83): 2-amino-5-chlorobenzonitrile (173 mg; 1.134 mmol); AlCl₃ (302 mg; 2.27 mmol). Purified by column chromatography using mobile phase DCM/MeOH/NH₄OH (9:1:0.1) to give crude product as a brownish solid. Yield 82 %.

¹H NMR (500 MHz, DMSO-*d*₆) δ 8.25 (d, *J* = 2.4 Hz, 1H), 7.67 (d, *J* = 8.9 Hz, 1H), 7.47 (dd, *J* = 8.9, 2.3 Hz, 1H), 6.52 (bs, 2H), 2.88 (t, *J* = 7.7 Hz, 2H), 2.80 (t, *J* = 7.3 Hz, 2H), 2.10 – 1.97 (m, 2H). ¹³C NMR (126 MHz, dmsO) δ 167.38, 147.27, 145.67, 130.47, 128.19, 127.18, 121.41, 118.55, 114.34, 34.68, 27.81, 22.33. HRMS (ESI⁺): [M]⁺: calculated for C₁₂H₁₂ClN₂⁺ (m/z): 219.06835; found: 219.06808. HPLC purity > 99 %.

7-chloro-1,2,3,4-tetrahydroacridin-9-amine hydrochloride (84): 2-amino-5-chlorobenzonitrile (177 mg; 1.16 mmol); AlCl₃ (309 mg; 2.32 mmol). Purified by column chromatography using mobile phase DCM/MeOH/NH₄OH (9:1:0.1) to give crude product as a brownish solid. Yield 56 %.

¹H NMR (500 MHz, DMSO-*d*₆) δ 8.28 (d, *J* = 2.3 Hz, 1H), 7.62 (d, *J* = 8.9 Hz, 1H), 7.46 (dd, *J* = 9.0, 2.3 Hz, 1H), 6.42 (bs, 2H), 2.80 (t, *J* = 6.0 Hz, 2H), 2.53 (t, *J* = 6.1 Hz, 2H), 1.91 – 1.69 (m, 4H). ¹³C NMR (126 MHz, dmsO) δ 158.22, 147.66, 145.07, 130.30, 128.40, 127.11, 121.22, 117.92, 109.94, 33.73, 23.85, 22.70, 22.58. HRMS (ESI⁺): [M]⁺: calculated for C₁₃H₁₄ClN₂⁺ (m/z): 233.08400; found: 233.08374. HPLC purity > 99 %.

2-chloro-6H,7H,8H,9H,10H-cyclohepta[b]quinolin-11-amine hydrochloride (85): 2-amino-5-chlorobenzonitrile (181 mg; 1.186 mmol); AlCl₃ (316 mg; 1.372 mmol). Purified by column chromatography using mobile phase DCM/MeOH/NH₄OH (9:1:0.1) to give crude product as a brownish solid. Yield 94 %.

¹H NMR (500 MHz, DMSO-*d*₆) δ 8.25 (d, *J* = 2.4 Hz, 1H), 7.64 (d, *J* = 8.9 Hz, 1H), 7.47 (dd, *J* = 8.9, 2.3 Hz, 1H), 6.41 (bs, 2H), 3.01 – 2.91 (m, 2H), 2.84 – 2.73 (m, 2H), 1.78 (p, *J* = 5.8 Hz, 2H), 1.61 (p, *J* = 5.5 Hz, 2H), 1.54 (p, *J* = 5.5 Hz, 2H). ¹³C NMR (126 MHz, dms) δ 164.83, 146.48, 144.89, 130.54, 128.25, 127.70, 121.62, 118.85, 115.11, 31.74, 27.76, 26.75, 25.50. HRMS (ESI⁺): [M]⁺: calculated for C₁₄H₁₆ClN₂⁺ (m/z): 247.09965; found: 247.09950. HPLC purity > 99 %.

5,7-dichloro-1H,2H,3H-cyclopenta[b]quinolin-9-amine hydrochloride (86): 2-amino-3,5-dichlorobenzonitrile (148 mg; 0.79 mmol); AlCl₃ (211 mg; 1.58 mmol). Purified by column chromatography using mobile phase PE/EA (1:1) to give crude product as a brownish solid. Yield 72 %.

¹H NMR (500 MHz, DMSO-*d*₆) δ 8.27 (d, *J* = 2.3 Hz, 1H), 7.75 (d, *J* = 2.2 Hz, 1H), 6.70 (bs, 2H), 2.93 (t, *J* = 7.7 Hz, 2H), 2.81 (t, *J* = 7.3 Hz, 2H), 2.13 – 2.02 (m, 2H). ¹³C NMR (126 MHz, dms) δ 168.07, 146.26, 143.49, 133.27, 128.02, 126.22, 120.99, 119.31, 115.38, 34.97, 27.86, 22.23. HRMS (ESI⁺): [M]⁺: calculated for C₁₂H₁₁Cl₂N₂⁺ (m/z): 253.02938; found: 253.02911. HPLC purity > 99 %.

5,7-dichloro-1,2,3,4-tetrahydroacridin-9-amine hydrochloride (87): 2-amino-3,5-dichlorobenzonitrile (148 mg; 0.79 mmol); AlCl₃ (211 mg; 1.58 mmol). Purified by column chromatography using mobile phase PE/EA (2:1) to give crude product as a brownish solid. Yield 86 %

¹H NMR (500 MHz, DMSO-*d*₆) δ 8.30 (d, *J* = 2.3 Hz, 1H), 7.74 (d, *J* = 2.2 Hz, 1H), 6.60 (bs, 2H), 2.87 – 2.82 (m, 2H), 2.53 (t, *J* = 6.0 Hz, 2H), 1.85 – 1.76 (m, 4H). ¹³C NMR (126 MHz, dms) δ 158.97, 148.31, 141.25, 133.08, 128.12, 126.06, 120.83, 118.54, 111.02, 33.97, 23.89, 22.58, 22.38. HRMS (ESI⁺): [M]⁺: calculated for C₁₃H₁₃Cl₂N₂⁺ (m/z): 267.04503; found: 267.04489. HPLC purity > 96 %.

2,4-dichloro-6H,7H,8H,9H,10H-cyclohepta[b]quinolin-11-amine hydrochloride (88): 2-amino-3,5-dichlorobenzonitrile (145 mg; 0.775 mmol); AlCl₃ (207 mg; 1.55 mmol). Purified by column chromatography using mobile phase PE/EA (2:1) to give crude product as a brownish solid. Yield 96 %.

^1H NMR (500 MHz, DMSO- d_6) δ 8.27 (d, J = 2.2 Hz, 1H), 7.75 (d, J = 2.2 Hz, 1H), 6.58 (bs, 2H), 3.05 – 2.96 (m, 2H), 2.84 – 2.75 (m, 2H), 1.85 – 1.74 (m, 2H), 1.66 – 1.58 (m, 2H), 1.58 – 1.51 (m, 2H). ^{13}C NMR (126 MHz, dms) δ 165.46, 147.13, 141.05, 133.35, 128.02, 126.71, 121.20, 119.52, 116.09, 39.48, 31.67, 27.52, 26.60, 25.49. HRMS (ESI $^+$): $[\text{M}]^+$: calculated for $\text{C}_{14}\text{H}_{15}\text{Cl}_2\text{N}_2^+$ (m/z): 281.06083; found: 281.06042. HPLC purity > 99 %.

5,7-dibromo-1H,2H,3H-cyclopenta[b]quinolin-9-amine hydrochloride (89): 2-amino-3,5-dibromobenzonitrile (167 mg; 0.605 mmol); AlCl_3 (161 mg; 1.21 mmol). Purified by column chromatography using mobile phase PE/EA (1:1) to give crude product as a light orange solid. Yield 82 %.

^1H NMR (500 MHz, DMSO- d_6) δ 8.45 (d, J = 2.1 Hz, 1H), 8.01 (d, J = 2.1 Hz, 1H), 6.71 (bs, 2H), 2.93 (t, J = 7.7 Hz, 2H), 2.82 (t, J = 7.3 Hz, 2H), 2.06 (p, J = 7.6 Hz, 2H). ^{13}C NMR (126 MHz, dms) δ 168.38, 146.15, 144.42, 133.59, 125.12, 124.77, 119.79, 115.37, 114.56, 35.03, 27.87, 22.24. HRMS (ESI $^+$): $[\text{M}]^+$: calculated for $\text{C}_{12}\text{H}_{11}\text{Br}_2\text{N}_2^+$ (m/z): 342.92630; found: 342.92593. HPLC purity > 99 %.

5,7-dibromo-1,2,3,4-tetrahydroacridin-9-amine hydrochloride (90): 2-amino-3,5-dibromobenzonitrile (170 mg; 0.616 mmol); AlCl_3 (164 mg; 1.232 mmol). Purified by column chromatography using mobile phase PE/EA (1:1) to give crude product as a light orange solid. Yield 35 %.

^1H NMR (500 MHz, DMSO- d_6) δ 8.48 (d, J = 2.1 Hz, 2H), 7.99 (d, J = 2.0 Hz, 1H), 6.61 (bs, 3H), 2.86 – 2.80 (m, 2H), 2.55 – 2.51 (m, 2H), 1.84 – 1.78 (m, 4H). ^{13}C NMR (126 MHz, dms) δ 159.27, 148.21, 142.14, 133.66, 125.05, 124.66, 118.99, 114.39, 111.00, 34.01, 23.88, 22.57, 22.38. HRMS (ESI $^+$): $[\text{M}]^+$: calculated for $\text{C}_{13}\text{H}_{13}\text{Br}_2\text{N}_2^+$ (m/z): 356.94195; found: 356.94135. HPLC purity > 97 %.

2,4-dibromo-6H,7H,8H,9H,10H-cyclohepta[b]quinolin-11-amine hydrochloride (91): 2-amino-3,5-dibromobenzonitrile (167 mg; 0.605 mmol); AlCl_3 (161 mg; 1.21 mmol). Purified by column chromatography using mobile phase PE/EA (3:1) to give crude product as a light orange solid. Yield 65 %.

^1H NMR (500 MHz, DMSO- d_6) δ 8.45 (d, J = 2.1 Hz, 1H), 8.00 (d, J = 1.9 Hz, 1H), 6.60 (bs, 2H), 3.04 – 2.96 (m, 2H), 2.82 – 2.76 (m, 2H), 1.83 – 1.76 (m, 2H), 1.66 – 1.59 (m, 2H), 1.59 – 1.51 (m, 2H). ^{13}C NMR (126 MHz, dms) δ 165.73, 147.06, 141.93, 133.58, 125.26, 125.01, 119.95, 116.06, 115.08, 31.67, 27.53, 26.58, 25.50.

HRMS (ESI⁺): [M]⁺: calculated for C₁₄H₁₅Br₂N₂⁺ (m/z): 370.95760; found: 370.95703. HPLC purity > 99 %.

7-fluoro-1H,2H,3H-cyclopenta[b]quinolin-9-amine hydrochloride (92): 2-amino-5-fluorobenzonitrile (122 mg; 0.896 mmol); AlCl₃ (239 mg; 1.79 mmol). Purified by column chromatography using mobile phase DCM/MeOH/NH₄OH (9:1:0.1) to give crude product as a white solid. Yield 83 %.

¹H NMR (500 MHz, DMSO-*d*₆) δ 7.97 – 7.88 (m, 1H), 7.76 – 7.66 (m, 1H), 7.45 – 7.31 (m, 1H), 6.40 (bs, 2H), 2.88 (t, *J* = 7.7 Hz, 2H), 2.80 (t, *J* = 7.3 Hz, 2H), 2.05 (p, *J* = 7.5 Hz, 2H). ¹³C NMR (126 MHz, dmsO) δ 166.46, 166.44, 159.10, 157.20, 145.86, 145.84, 130.84, 130.77, 118.05, 117.98, 117.35, 117.15, 113.97, 106.14, 105.96, 34.57, 27.78, 22.43. HRMS (ESI⁺): [M]⁺: calculated for C₁₂H₁₂FN₂⁺ (m/z): 203.09790; found: 203.09758. HPLC purity > 99 %.

7-fluoro-1,2,3,4-tetrahydroacridin-9-amine hydrochloride (93): 2-amino-5-fluorobenzonitrile (177 mg; 1.30 mmol); AlCl₃ (347 mg; 2.60 mmol). Purified by column chromatography using mobile phase DCM/MeOH/NH₄OH (9:1:0.1) to give crude product as a white solid. Yield 77 %.

¹H NMR (500 MHz, DMSO-*d*₆) δ 8.08 – 8.00 (m, 1H), 7.76 – 7.69 (m, 1H), 7.49 – 7.41 (m, 1H), 6.75 (bs, 2H), 2.83 (t, *J* = 5.9 Hz, 2H), 2.53 (t, *J* = 6.1 Hz, 2H), 1.85 – 1.75 (m, 4H). ¹³C NMR (126 MHz, dmsO) δ 159.24, 157.33, 155.97, 149.41, 141.72, 128.92, 118.77, 118.57, 117.06, 109.49, 106.30, 106.12, 32.42, 23.64, 22.32. HRMS (ESI⁺): [M]⁺: calculated for C₁₃H₁₄FN₂⁺ (m/z): 217.11355; found: 217.11346. HPLC purity > 97 %.

2-fluoro-6H,7H,8H,9H,10H-cyclohepta[b]quinolin-11-amine hydrochloride (94): 2-amino-5-fluorobenzonitrile (177 mg; 1.30 mmol); AlCl₃ (347 mg; 2.60 mmol). Purified by column chromatography using mobile phase DCM/MeOH/NH₄OH (9:1:0.1) to give crude product as a white solid. Yield 98 %

¹H NMR (500 MHz, DMSO-*d*₆) δ 7.96 – 7.89 (m, 1H), 7.71 – 7.64 (m, 1H), 7.41 – 7.33 (m, 1H), 6.30 (bs, 2H), 3.01 – 2.91 (m, 2H), 2.84 – 2.74 (m, 2H), 1.86 – 1.74 (m, 2H), 1.65 – 1.50 (m, 4H). ¹³C NMR (126 MHz, dmsO) δ 160.45, 158.51, 158.05, 153.95, 153.92, 133.87, 122.53, 122.46, 122.15, 121.95, 116.82, 116.74, 114.75, 108.60, 108.40, 32.79, 31.04, 26.23, 25.47, 24.59. HRMS (ESI⁺): [M]⁺: calculated for C₁₄H₁₆FN₂⁺ (m/z): 231.12920; found: 231.12872. HPLC purity > 99 %.

8-chloro-1H,2H,3H-cyclopenta[b]quinolin-9-amine hydrochloride (95): 2-amino-6-chlorobenzonitrile (140 mg; 0.92 mmol); AlCl₃ (245 mg; 1.84 mmol). Purified by column chromatography using mobile phase DCM/MeOH/NH₄OH (15:1:0.1) to give crude product as a brownish solid. Yield 63 %.

¹H NMR (500 MHz, DMSO-*d*₆) δ 7.65 (dd, *J* = 8.4, 1.4 Hz, 1H), 7.41 (dd, *J* = 8.4, 7.5 Hz, 1H), 7.33 (dd, *J* = 7.5, 1.4 Hz, 1H), 6.51 (bs, 2H), 2.90 (t, *J* = 7.8 Hz, 2H), 2.82 – 2.76 (m, 2H), 2.12 – 2.02 (m, 2H). ¹³C NMR (126 MHz, dmsO) δ 166.75, 151.22, 146.28, 128.96, 128.27, 127.73, 125.83, 116.29, 114.60, 34.59, 28.15, 22.04. HRMS (ESI⁺): [M]⁺: calculated for C₁₂H₁₂ClN₂⁺ (m/z): 219.06835; found: 219.06815. HPLC purity > 98 %.

8-chloro-1,2,3,4-tetrahydroacridin-9-amine hydrochloride (96): 2-amino-6-chlorobenzonitrile (135 mg; 0.885 mmol); AlCl₃ (236 mg; 1.77 mmol). Purified by column chromatography using mobile phase DCM/MeOH/NH₄OH (15:1:0.1) to give crude product as a brownish solid. Yield 48 %.

¹H NMR (500 MHz, DMSO-*d*₆) δ 7.61 (dd, *J* = 8.4, 1.4 Hz, 1H), 7.44 – 7.38 (m, 1H), 7.33 (dd, *J* = 7.5, 1.4 Hz, 1H), 6.53 (bs, 2H), 2.80 (t, *J* = 6.2 Hz, 2H), 2.49 – 2.46 (m, 2H), 1.87 – 1.75 (m, 4H). ¹³C NMR (126 MHz, dmsO) δ 157.87, 148.60, 148.22, 128.68, 127.82, 127.52, 125.90, 113.89, 111.29, 33.47, 23.98, 22.51, 22.41. HRMS (ESI⁺): [M]⁺: calculated for C₁₃H₁₄ClN₂⁺ (m/z): 233.08400; found: 233.08382. HPLC purity > 99 %.

1-chloro-6H,7H,8H,9H,10H-cyclohepta[b]quinolin-11-amine hydrochloride (97): 2-amino-6-chlorobenzonitrile (135 mg; 0.885 mmol); AlCl₃ (236 mg; 1.77 mmol). Purified by column chromatography using mobile phase DCM/MeOH/NH₄OH (15:1:0.1) to give crude product as a brownish solid. Yield 89 %.

¹H NMR (500 MHz, DMSO-*d*₆) δ 7.62 (s, 1H), 7.44 – 7.38 (m, 1H), 7.35 (dd, *J* = 7.5, 1.5 Hz, 1H), 6.59 (bs, 2H), 2.99 – 2.92 (m, 2H), 2.81 – 2.72 (m, 2H), 1.79 (t, *J* = 5.7 Hz, 2H), 1.65 – 1.52 (m, 4H). ¹³C NMR (126 MHz, dmsO) δ 164.40, 148.64, 147.14, 129.09, 127.78, 127.76, 126.57, 116.44, 114.79, 39.01, 31.57, 27.37, 26.61, 25.35. HRMS (ESI⁺): [M]⁺: calculated for C₁₄H₁₆ClN₂⁺ (m/z): 247.09965; found: 247.09943. HPLC purity > 98 %.

6-methyl-1H,2H,3H-cyclopenta[b]quinolin-9-amine hydrochloride (98): 2-amino-4-methylbenzonitrile (148 mg; 1.12 mmol); AlCl₃ (299 mg; 2.24 mmol). Purified by

column chromatography using mobile phase DCM/MeOH/NH₄OH (9:1:0.1) to give crude product as a brownish solid. Yield 83 %.

¹H NMR (500 MHz, DMSO-*d*₆) δ 8.02 (d, *J* = 8.5 Hz, 1H), 7.45 (t, *J* = 1.4 Hz, 1H), 7.14 (dd, *J* = 8.5, 1.8 Hz, 1H), 6.49 (bs, 2H), 2.87 (t, *J* = 7.7 Hz, 2H), 2.78 (t, *J* = 7.4 Hz, 2H), 2.41 (s, 3H), 2.10 – 1.99 (m, 2H). ¹³C NMR (126 MHz, dms) δ 166.02, 148.26, 146.68, 137.59, 126.95, 124.87, 122.10, 115.56, 112.98, 34.53, 27.73, 22.40, 21.33. HRMS (ESI⁺): [M]⁺: calculated for C₁₃H₁₅N₂⁺ (m/z): 199.12297; found: 199.12276. HPLC purity > 99 %.

6-methyl-1,2,3,4-tetrahydroacridin-9-amine hydrochloride (99): 2-amino-4-methylbenzotrile (142 mg; 1.07 mmol); AlCl₃ (287 mg; 2.15 mmol). Purified by column chromatography using mobile phase DCM/MeOH/NH₄OH (9:1:0.1) to give crude product as a brownish solid. Yield 77 %.

¹H NMR (500 MHz, DMSO-*d*₆) δ 8.04 (d, *J* = 8.6 Hz, 1H), 7.43 – 7.38 (m, 1H), 7.12 (dd, *J* = 8.5, 1.8 Hz, 1H), 6.36 (bs, 2H), 2.80 (t, *J* = 6.0 Hz, 2H), 2.52 (t, *J* = 6.1 Hz, 2H), 2.40 (s, 3H), 1.85 – 1.74 (m, 4H). ¹³C NMR (126 MHz, dms) δ 157.03, 148.53, 146.22, 137.63, 126.58, 124.89, 121.97, 115.09, 108.51, 33.41, 23.69, 22.75, 22.68, 21.37. HRMS (ESI⁺): [M]⁺: calculated for C₁₄H₁₇N₂⁺ (m/z): 213.13862; found: 213.13840. HPLC purity > 98 %.

3-methyl-6H,7H,8H,9H,10H-cyclohepta[b]quinolin-11-amine hydrochloride (100): 2-amino-4-methylbenzotrile (142 mg; 1.07 mmol); AlCl₃ (287 mg; 2.15 mmol). Purified by column chromatography using mobile phase DCM/MeOH/NH₄OH (5:1:0.1) to give crude product as a brownish solid. Yield 99 %.

¹H NMR (500 MHz, DMSO-*d*₆) δ 8.08 (d, *J* = 8.5 Hz, 1H), 7.52 – 7.44 (m, 1H), 7.20 (dd, *J* = 8.5, 1.8 Hz, 1H), 6.75 (bs, 2H), 3.02 – 2.95 (m, 2H), 2.83 – 2.74 (m, 2H), 2.42 (s, 3H), 1.79 (p, *J* = 5.9 Hz, 2H), 1.62 (p, *J* = 5.5 Hz, 2H), 1.55 (p, *J* = 5.7 Hz, 2H). ¹³C NMR (126 MHz, dms) δ 162.56, 148.75, 144.21, 138.65, 125.84, 125.29, 122.57, 115.46, 113.79, 37.84, 31.67, 27.57, 26.55, 25.22, 21.32. HRMS (ESI⁺): [M]⁺: calculated for C₁₅H₁₉N₂⁺ (m/z): 227.15428; found: 227.15396. HPLC purity > 99 %.

8-methyl-1H,2H,3H-cyclopenta[b]quinolin-9-amine hydrochloride (101): 2-amino-6-methylbenzotrile (158 mg; 1.196 mmol); AlCl₃ (319 mg; 2.39 mmol). Purified by column chromatography using mobile phase DCM/MeOH/NH₄OH (5:1:0.1) to give crude product as a yellowish solid. Yield 58 %.

^1H NMR (500 MHz, DMSO- d_6) δ 7.51 (dd, $J = 8.4, 1.4$ Hz, 1H), 7.31 (dd, $J = 8.4, 7.0$ Hz, 1H), 7.02 (d, $J = 7.0$ Hz, 1H), 5.88 (bs, 2H), 2.92 – 2.85 (m, 5H), 2.79 (t, $J = 7.3$ Hz, 2H), 2.05 (p, $J = 7.6$ Hz, 2H). ^{13}C NMR (126 MHz, dms) δ 165.19, 150.22, 148.36, 134.19, 127.49, 126.91, 126.24, 117.92, 115.72, 34.36, 28.03, 24.24, 22.20. HRMS (ESI $^+$): $[\text{M}]^+$: calculated for $\text{C}_{13}\text{H}_{15}\text{N}_2^+$ (m/z): 199.12297; found: 199.12270. HPLC purity > 99 %.

8-methyl-1,2,3,4-tetrahydroacridin-9-amine hydrochloride (102): 2-amino-6-methylbenzotrile (160 mg; 1.21 mmol); AlCl_3 (323 mg; 2.42 mmol). Purified by column chromatography using mobile phase DCM/MeOH/ NH_4OH (9:1:0.1) to give crude product as a yellowish solid. Yield 77 %.

^1H NMR (500 MHz, Methanol- d_4) δ 7.57 – 7.53 (m, 1H), 7.50 – 7.45 (m, 1H), 7.20 – 7.16 (m, 1H), 2.94 (s, 3H), 2.90 (t, $J = 6.2$ Hz, 2H), 2.55 (t, $J = 6.3$ Hz, 2H), 1.99 – 1.87 (m, 4H). ^{13}C NMR (126 MHz, cd_3od) δ 155.34, 155.06, 145.15, 135.86, 131.20, 128.97, 122.86, 117.54, 111.72, 31.63, 24.31, 24.27, 23.40, 22.91. HRMS (ESI $^+$): $[\text{M}]^+$: calculated for $\text{C}_{14}\text{H}_{17}\text{N}_2^+$ (m/z): 213.13862; found: 213.13837. HPLC purity > 93 %.

1-methyl-6H,7H,8H,9H,10H-cyclohepta[b]quinolin-11-amine hydrochloride (103): 2-amino-6-methylbenzotrile (160 mg; 1.121 mmol); AlCl_3 (323 mg; 2.42 mmol). Purified by column chromatography using mobile phase DCM/MeOH/ NH_4OH (7:1:0.1) to give crude product as a yellowish solid. Yield 59 %.

^1H NMR (500 MHz, DMSO- d_6) δ 7.50 (dd, $J = 8.3, 1.4$ Hz, 1H), 7.34 (dd, $J = 8.4, 7.0$ Hz, 1H), 7.07 (dt, $J = 7.0, 1.2$ Hz, 1H), 6.04 (bs, 2H), 3.00 – 2.93 (m, 2H), 2.89 (s, 3H), 2.81 – 2.74 (m, 2H), 1.83 – 1.76 (m, 2H), 1.63 (p, $J = 5.7, 5.3$ Hz, 2H), 1.56 (p, $J = 5.7$ Hz, 2H). ^{13}C NMR (126 MHz, dms) δ 162.27, 149.90, 146.76, 134.00, 127.93, 127.16, 125.97, 118.22, 115.87, 38.19, 31.60, 27.54, 26.62, 25.21, 24.26. HRMS (ESI $^+$): $[\text{M}]^+$: calculated for $\text{C}_{15}\text{H}_{19}\text{N}_2^+$ (m/z): 227.15428; found: 227.15387. HPLC purity > 99 %.

7-methoxy-1H,2H,3H-cyclopenta[b]quinolin-9-amine hydrochloride (104): 2-amino-5-methoxybenzotrile (177 mg; 1.19 mmol); AlCl_3 (319 mg; 2.39 mmol). Purified by column chromatography using mobile phase DCM/MeOH/ NH_4OH (9:1:0.1) to give crude product as a white solid. Yield 60 %.

^1H NMR (500 MHz, DMSO- d_6) δ 7.59 (d, $J = 9.1$ Hz, 1H), 7.49 (d, $J = 2.8$ Hz, 1H), 7.14 (dd, $J = 9.1, 2.7$ Hz, 1H), 6.30 (bs, 2H), 3.85 (s, 3H), 2.86 (t, $J = 7.7$ Hz, 2H), 2.80 (t, $J = 7.3$ Hz, 2H), 2.10 – 1.99 (m, 2H). ^{13}C NMR (126 MHz, dms) δ 164.15, 155.28,

145.52, 144.07, 129.58, 119.44, 118.05, 113.64, 101.55, 55.67, 34.35, 27.79, 22.50. HRMS (ESI⁺): [M]⁺: calculated for C₁₃H₁₅ON₂⁺ (m/z): 215.11789; found: 215.11755. HPLC purity > 99 %.

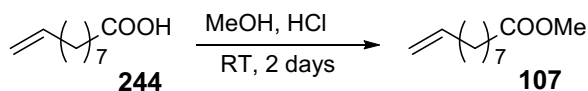
7-methoxy-1,2,3,4-tetrahydroacridin-9-amine hydrochloride (105): 2-amino-5-methoxybenzonitrile (181 mg; 1.24 mmol); AlCl₃ (330 mg; 2.48 mmol). Purified by column chromatography using mobile phase DCM/MeOH/NH₄OH (9:1:0.1) to give crude product as a yellowish solid. Yield 37 %.

¹H NMR (500 MHz, DMSO-*d*₆) δ 7.60 – 7.53 (m, 2H), 7.20 (dd, *J* = 9.1, 2.7 Hz, 1H), 6.56 (bs, 2H), 3.86 (s, 3H), 2.81 (t, *J* = 6.0 Hz, 2H), 2.54 (t, *J* = 6.2 Hz, 2H), 1.85 – 1.76 (m, 4H). ¹³C NMR (126 MHz, dmso) δ 155.54, 154.03, 148.65, 140.37, 127.96, 120.80, 117.21, 109.12, 101.28, 55.80, 32.42, 23.71, 22.50. HRMS (ESI⁺): [M]⁺: calculated for C₁₄H₁₇ON₂⁺ (m/z): 229.13354; found: 229.13313. HPLC purity > 93 %.

2-methoxy-6H,7H,8H,9H,10H-cyclohepta[b]quinolin-11-amine hydrochloride (106): 2-amino-5-methoxybenzonitrile (181 mg; 1.24 mmol); AlCl₃ (330 mg; 2.48 mmol). Purified by column chromatography using mobile phase DCM/MeOH/NH₄OH (7:1:0.1) to give crude product as a yellowish solid. Yield 82 %.

¹H NMR (500 MHz, DMSO-*d*₆) δ 7.64 (d, *J* = 9.1 Hz, 1H), 7.56 (d, *J* = 2.7 Hz, 1H), 7.23 (dd, *J* = 9.1, 2.6 Hz, 1H), 6.75 (bs, 2H), 3.87 (s, 3H), 3.02 – 2.94 (m, 2H), 2.85 – 2.77 (m, 2H), 1.80 (p, *J* = 5.9 Hz, 2H), 1.63 (p, *J* = 5.4 Hz, 2H), 1.57 (p, *J* = 5.5 Hz, 2H). ¹³C NMR (126 MHz, dmso) δ 160.14, 156.15, 156.15, 148.24, 139.03, 127.41, 120.78, 117.96, 114.38, 102.09, 55.91, 37.46, 31.62, 27.51, 26.56, 25.35. HRMS (ESI⁺): [M]⁺: calculated for C₁₄H₁₇ON₂⁺ (m/z): 243.14919; found: 243.14877. HPLC purity > 99 %.

6.1.3 AChE-targeting insecticides

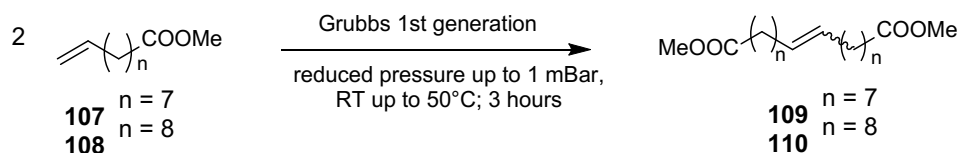


Methyl 9-decenoate (107): 9-Decenoic acid (**244**) (20 ml, 102.45 mmol) and methanol (MeOH, 150 mL) were charged into the dried round-bottom flask filled with inert atmosphere (argon; Ar). HCl (sat. aq. solution, 40 mL) was added dropwise at room temperature and final mixture was stirred for 2 days. After 2 days reaction mixture was

neutralized with 10 % NaOH (300 mL) and extracted with dichloromethane (DCM; 2 × 500 mL). The organic layers were collected, dried with anhydrous Na₂SO₄ and filtered-off. The filtrate was concentrated under reduced pressure to afford **107** (18.90 g) with quantitative yield as an orange oil. The structure of **107** was identified by NMR analysis and it was directly transferred into the next reaction.

¹H NMR (500 MHz, CDCl₃-d₁) δ 5.87 – 5.75 (m, 1H), 5.05 – 4.89 (m, 2H), 3.67 (s, 3H), 2.30 (t, *J* = 7.5 Hz, 2H), 2.10 – 1.99 (m, 2H), 1.69 – 1.57 (m, 2H), 1.42 – 1.34 (m, 2H), 1.34 – 1.27 (m, 6H). ¹³C NMR (126 MHz, CDCl₃) δ 174.24, 139.06, 114.14, 51.39, 34.06, 33.72, 29.05, 28.87, 28.80, 24.90.

General procedure for Grubbs reaction (Olefin metathesis) of methyl esters **107 and **108**:**



Methyl ester **107** or **108** (1.0 g, 5.43 mmol for **107** and 1.0 g, 5.04 mmol for **108**) and Grubbs 1st generation catalyst (2.5 % eq) were added into the dried round-bottom flask filled with inert atmosphere (Ar). The mixture was stirred for 1 hour under reduced pressure using water vacuum pump. Further, pressure was increased by using oil vacuum pump to values around 1 mBar and mixture was stirred for another 1 hour at room temperature. Finally, the mixture was heated to 50 °C for additional 1 hour at 1 mBar. The reaction mixture was purified by column chromatography (hexane/ethyl acetate 95/0.5) to afford product **109** (841 mg, 91 % yield after two steps from 9-decenoic acid (**244**)) and (petrol ether/ethyl acetate (PE/EA) = 98:2) product **110** (910 mg, 98 % yield from **108**). Both intermediates **109** and **110** were isolated as white solids.

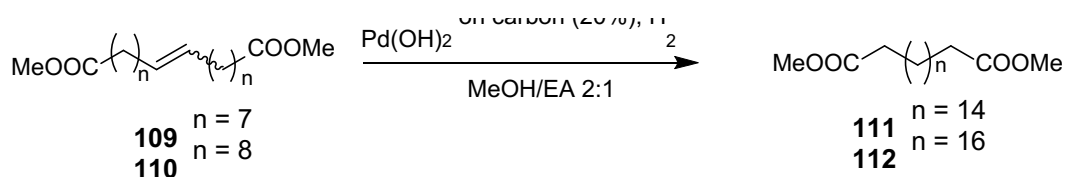
1,18-dimethyl oktadec-9-enedioate (109):

¹H NMR (500 MHz, CDCl₃-d₁) δ 5.39 – 5.36 (m, 2H), 3.67 (s, 6H), 2.30 (t, *J* = 7.5 Hz, 4H), 2.01 – 1.92 (m, 4H), 1.67 – 1.56 (m, 4H), 1.44 – 1.17 (m, 16H). ¹³C NMR (126 MHz, CDCl₃) δ 174.26, 130.28, 129.81, 51.39, 34.07, 32.51, 29.64, 29.51, 29.12, 29.08, 28.90, 27.14, 24.92.

1,20-dimethyl icos-10-enedioate (110):

^1H NMR (500 MHz, CDCl_3-d_1) δ 5.41 – 5.33 (m, 2H), 3.67 (s, 6H), 2.31 (t, $J = 7.6$ Hz, 4H), 2.07 – 1.91 (m, 4H), 1.70 – 1.54 (m, 4H), 1.45 – 1.22 (m, 20H). ^{13}C NMR (126 MHz, CDCl_3) δ 174.29, 130.30, 129.83, 51.41, 34.09, 32.55, 29.70, 29.58, 29.32, 29.27, 29.20, 29.12, 29.05, 27.17, 24.93.

General procedure for Pd-catalysed double bond reduction of **109 and **110** using hydrogen:**



The compounds **109** or **110** (913 mg, 2.68 mmol for **109** and 822 mg, 2.23 mmol for **110**) were dissolved in solution of MeOH:EA (20:40 mL) in the round flask filled with Ar. $\text{Pd}(\text{OH})_2$ on C (20 %) (0.2 eq) was added slowly in small portions at room temperature.

The atmosphere in the flask was five times removed with oil vacuum pump at values around 1 mBar. Same procedure followed with H_2 atmosphere (three times atmosphere exchange).

Finally, the mixture was stirred for 1 hour under H_2 atmosphere. The mixture was then filtered through a celite pad and the filter cake was washed three times with MeOH and EA.

The filtrate was concentrated under reduced pressure to afford title intermediates **111** (882 mg, 96 % yield) and **112** (846 mg, 98 % yield), respectively. **111** and **112** were obtained as white solids.

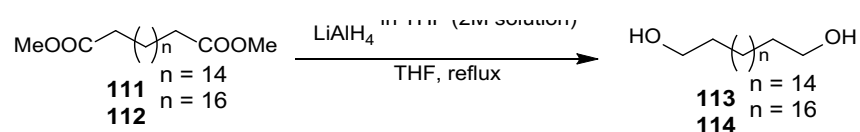
1,18-dimethyl oktadecanedioate (111):

^1H NMR (500 MHz, CDCl_3-d_1) δ 3.67 (s, 6H), 2.30 (t, $J = 7.6$ Hz, 4H), 1.66 – 1.57 (m, 4H), 1.35 – 1.21 (m, 24H). ^{13}C NMR (126 MHz, CDCl_3) δ 174.30, 51.39, 34.09, 29.63, 29.61, 29.56, 29.42, 29.23, 29.13, 24.94.

1,20-dimethyl icosanedioate (112):

^1H NMR (500 MHz, CDCl_3-d_1) δ 3.67 (s, 6H), 2.31 (t, $J = 7.6$ Hz, 5H), 1.68 – 1.57 (m, 4H), 1.26 (s, 28H). ^{13}C NMR (126 MHz, CDCl_3) δ 174.31, 51.40, 34.09, 29.64, 29.61, 29.56, 29.42, 29.23, 29.13, 24.94.

General procedure for reduction using LiAlH₄ in THF:



The compounds **111** or **112** (712 mg, 2.08 mmol for **111** and 629 mg, 1.7 mmol for **112**) were charged into an oven-dried flask following addition of anhydrous THF (34 mL) under the inert atmosphere (Ar). 2 M solution of LiAlH₄ in THF (2.5 eq) was added dropwise into vigorously stirred reaction mixture continuously within 1 hour and final reaction mixture was heated to reflux for 30 minutes. The reaction was quenched by addition of 2M solution of NaOH (8.5 mL) and mixture was extracted with DCM 3 × 100 mL. The organic layers were combined, dried with anhydrous Na₂SO₄, filtered and the filtrate was concentrated under reduced pressure to afford title product **113** (597 mg) and **114** (534 mg) with quantitative yields as white solids. No additional purification was needed.

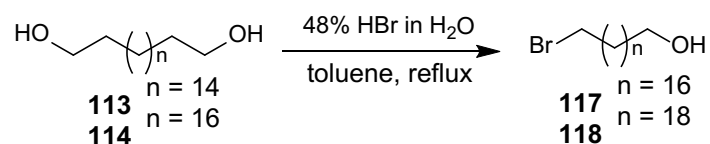
Oktadecane-1,18-diol (**113**):

¹H NMR (500 MHz, CDCl₃-*d*₁) δ 3.69 – 3.61 (m, 4H), 1.63 – 1.53 (m, 4H), 1.41 – 1.20 (m, 28H). ¹³C NMR (126 MHz, CDCl₃) δ 63.09, 32.80, 29.63, 29.59, 29.57, 29.41, 25.72.

Icosane-1,20-diol (**114**):

¹H NMR (500 MHz, CDCl₃-*d*₁) δ 3.65 (t, *J* = 6.6 Hz, 4H), 1.62 – 1.54 (m, 4H), 1.41 – 1.23 (m, 32H). ¹³C NMR (126 MHz, CDCl₃) δ 63.10, 32.81, 29.66, 29.64, 29.60, 29.58, 29.43, 25.73.

General procedure for selective mono-bromination:



The compounds **113** or **114** (705 g, 3.49 mmol for **113** and 609 mg, 1.94 mmol for **114**) were stirred in toluene (50 mL) under inert atmosphere. Solution of 48 % HBr in H₂O (4.0 eq) was added dropwise and the reaction mixture was heated at 120 °C for 48 hours. The reaction was finished by portionwise addition of saturated Na₂CO₃

(10 mL), then diluted by water (60 mL) and extracted with DCM 2 × 120 mL. The organic layers were combined, dried with anhydrous Na₂SO₄ and filtered. The filtrate was concentrated under reduced pressure and purified with column chromatography (H/EA = 9:1) to afford **117** (524 mg, 61 % yield) and **118** (440 mg, 60 % yield), respectively. **117** and **118** were obtained as light orange solids.

18-bromooktadecan-1-ol (117):

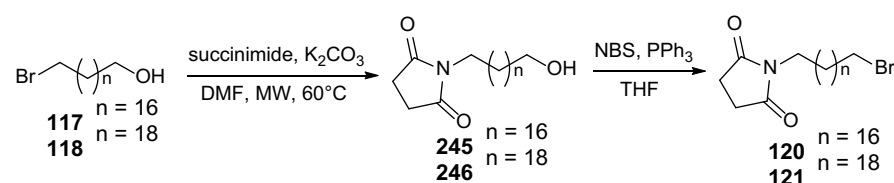
¹H NMR (500 MHz, CDCl₃-d₁) δ 3.65 (t, *J* = 6.6 Hz, 2H), 3.41 (t, *J* = 6.9 Hz, 2H), 1.92 – 1.81 (m, 2H), 1.63 – 1.53 (m, 2H), 1.46 – 1.39 (m, 2H), 1.39 – 1.22 (m, 26H). ¹³C NMR (126 MHz, CDCl₃) δ 63.08, 34.04, 32.83, 32.80, 29.65, 29.63, 29.59, 29.58, 29.52, 29.42, 28.75, 28.16, 25.72.

20-bromoicosan-1-ol (118):

¹H NMR (500 MHz, CDCl₃-d₁) δ 3.65 (t, *J* = 6.7 Hz, 2H), 3.42 (t, *J* = 6.9 Hz, 2H), 1.92 – 1.81 (m, 2H), 1.62 – 1.54 (m, 2H), 1.47 – 1.38 (m, 2H), 1.38 – 1.19 (m, 30H). ¹³C NMR (126 MHz, CDCl₃) δ 63.09, 34.04, 32.83, 32.80, 29.66, 29.64, 29.60, 29.58, 29.52, 29.42, 28.75, 28.16, 25.72.

Synthesis of compounds containing succinimide moiety 124 - 127

General procedure for synthesis of compounds 120 and 121:



The compounds **117** or **118** (671 mg, 1.92 mmol for **117** and 286 mg, 0.758 mmol for **118**), succinimide (1.2 eq) and dried K₂CO₃ (1.2 eq) were dissolved in anhydrous DMF (4 mL). The reaction mixture was stirred at 60 °C for 12 hours following extraction with brine (200 mL) and DCM 2 × 200 mL. The organic layers were combined, dried with anhydrous Na₂SO₄ and filtered. The filtrate was concentrated under reduced pressure and directly used into the next reaction. Then, **245** or **246** were initially dissolved in anhydrous THF (40 mL) under the inert atmosphere (Ar). NBS (1.5 eq) and PPh₃ (1.5 eq) were added consequently at room temperature. The final reaction mixture was stirred at room temperature for 30 min. The reaction was

diluted with water (50 mL) and extracted with DCM 2×175 mL. The organic layers were collected, dried with anhydrous Na_2SO_4 and filtrated. The filtrate was concentrated under reduced pressure and purified with column chromatography (PE/EA = 3:1) to afford **120** (702 mg, 85 % yield after two steps from **117**), **121** (286 mg, 82 % yield after two steps from **118**), respectively, as white solids.

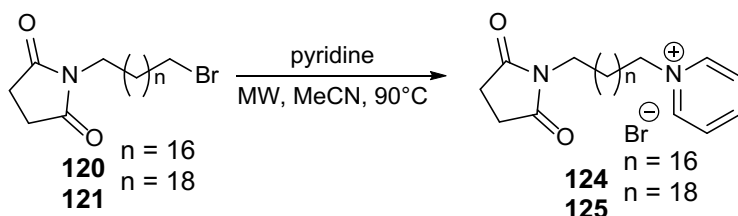
1-(18-bromooktadecyl)pyrrolidine-2,5-dione (120**):**

^1H NMR (500 MHz, CDCl_3 -*d*₁) δ 3.52 – 3.47 (m, 2H), 3.41 (t, J = 6.9 Hz, 2H), 2.70 (s, 4H), 1.91 – 1.80 (m, 2H), 1.59 – 1.53 (m, 2H), 1.46 – 1.39 (m, 2H), 1.34 – 1.22 (m, 26H). ^{13}C NMR (126 MHz, CDCl_3) δ 177.22, 38.89, 34.04, 32.82, 29.64, 29.62, 29.58, 29.52, 29.45, 29.41, 29.13, 28.74, 28.16, 28.13, 27.69, 26.84.

1-(20-bromoicosyl)pyrrolidine-2,5-dione (121**):**

^1H NMR (500 MHz, CDCl_3 -*d*₁) δ 3.50 (t, J = 7.4 Hz, 2H), 3.41 (t, J = 6.9 Hz, 2H), 2.70 (s, 4H), 1.90 – 1.82 (m, 2H), 1.59 – 1.52 (m, 2H), 1.48 – 1.39 (m, 2H), 1.36 – 1.17 (m, 30H). ^{13}C NMR (126 MHz, CDCl_3) δ 177.23, 38.90, 34.03, 32.83, 29.65, 29.60, 29.52, 29.45, 29.41, 29.14, 28.75, 28.16, 28.14, 27.70, 26.85.

General procedure for synthesis of pyridin-1-ium bromides **124 and **125**:**



Starting material, **120** or **121** (150 mg, 0.348 mmol for **120** and 136 mg, 0.297 mmol for **121**), and pyridine (2.0 eq) were added into the microwave-sealed tube and dissolved with anhydrous MeCN (2 mL). The reaction mixture was charged into microwave reactor with following settings: dynamic curve, power max cap 100 W, pressure max cap 300 PSI, 90 °C, for 24 hours. The mixture was directly purified by column chromatography (DCM/MeOH = 9:1) to afford **124** (152 mg, 86 % yield), and **125** (143 mg, 90 % yield), respectively. Both products were isolated as white solids.

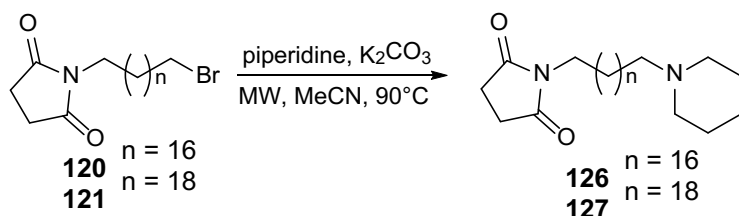
1-(18-(2,5-dioxopyrrolidin-1-yl)oktadecyl)-pyridin-1-ium bromide (124**):**

^1H NMR (500 MHz, $\text{CD}_3\text{OD}-d_4$) δ 9.08 – 9.02 (m, 2H), 8.65 – 8.59 (m, 1H), 8.18 – 8.10 (m, 2H), 4.70 – 4.65 (m, 2H), 3.51 – 3.43 (m, 2H), 2.69 (s, 4H), 2.11 – 1.96 (m, 2H), 1.62 – 1.51 (m, 2H), 1.44 – 1.23 (m, 28H). ^{13}C NMR (126 MHz, CD_3OD) δ 178.63, 145.47, 144.56, 128.13, 61.74, 38.18, 31.10, 29.33, 29.32, 29.30, 29.28, 29.25, 29.20, 29.17, 29.08, 28.84, 28.70, 27.68, 27.22, 26.47, 25.78. HRMS (ESI⁺): $[\text{M}]^+$: calculated for $\text{C}_{27}\text{H}_{45}\text{N}_2\text{O}_2^+$ (m/z): 429.3476; detected: 429.3466. LC-MS purity > 95 %.

1-(20-(2,5-dioxopyrrolidin-1-yl)icosyl)-pyridin-1-ium bromide (125):

^1H NMR (500 MHz, $\text{CD}_3\text{OD}-d_4$) δ 9.13 – 8.97 (m, 2H), 8.70 – 8.57 (m, 1H), 8.23 – 8.09 (m, 2H), 4.69 (t, $J = 7.5$ Hz, 2H), 3.46 (t, $J = 7.4$ Hz, 2H), 2.70 (s, 4H), 2.06 (qd, $J = 9.0, 8.3, 5.3$ Hz, 2H), 1.62 – 1.47 (m, 2H), 1.47 – 1.15 (m, 32H). ^{13}C NMR (126 MHz, CD_3OD) δ 179.92, 146.81, 145.93, 129.48, 63.07, 39.55, 32.50, 30.73, 30.70, 30.68, 30.64, 30.59, 30.56, 30.47, 30.23, 30.09, 29.08, 28.61, 27.87, 27.15. HRMS (ESI⁺): $[\text{M}]^+$: calculated for $\text{C}_{29}\text{H}_{49}\text{N}_2\text{O}_2^+$ (m/z): 457.3789; detected: 457.3792. LC-MS purity > 95 %.

General procedure for synthesis of compounds 126 and 127:



Compounds **120** or **121** (143 mg, 0.332 mmol for **120** and 131 mg, 0.2857 mmol for **121**), anhydrous K_2CO_3 (3.0 eq) and piperidine (2.0 eq) were charged into the microwave-sealed tube and dissolved in anhydrous MeCN (2 mL). The reaction mixture was charged into microwave reactor with following settings: dynamic curve, power max cap 100 W, pressure max cap 300 PSI, at 90 °C for 30 min. The mixture was directly purified using column chromatography (DCM/MeOH = 9:1) to afford **126** (141 mg, 98 % yield), and **127** (129 mg, 98 % yield), respectively, as white solids.

1-(18-(piperidin-1-yl)oktadecyl)pyrrolidine-2,5-dione (126):

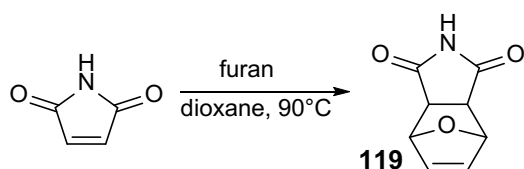
^1H NMR (500 MHz, $\text{CD}_3\text{OD}-d_4$) δ 3.49 – 3.43 (m, 2H), 3.30 – 3.07 (m, 4H), 3.07 – 3.01 (m, 2H), 2.69 (s, 4H), 1.91 – 1.81 (m, 4H), 1.78 – 1.71 (m, 2H), 1.70 – 1.63 (m, 2H), 1.55 (p, $J = 7.4$ Hz, 2H), 1.47 – 1.36 (m, 4H), 1.30 (d, $J = 4.2$ Hz, 24H). ^{13}C NMR

(126 MHz, CD₃OD) δ 180.01, 58.43, 54.31, 39.57, 30.74, 30.71, 30.65, 30.62, 30.57, 30.50, 30.24, 30.21, 29.06, 28.62, 27.87, 27.73, 25.17, 24.38, 22.83. HRMS (ESI⁺): [M+H]⁺: calculated for C₂₇H₅₁N₂O₂⁺ (m/z): 435.3945; detected: 435.3935. LC-MS purity > 95 %.

1-(20-(piperidin-1-yl)icosyl)pyrroline-2,5-dione (**127**):

¹H NMR (500 MHz, CDCl₃-d₁) δ 3.55 – 3.44 (m, 2H), 2.70 (s, 3H), 2.58 – 2.43 (m, 4H), 2.43 – 2.34 (m, 2H), 1.74 – 1.64 (m, 4H), 1.61 – 1.51 (m, 4H), 1.52 – 1.44 (m, 2H), 1.38 – 1.19 (m, 32H). ¹³C NMR (126 MHz, CDCl₃) δ 177.21, 57.80, 53.25, 38.86, 29.62, 29.60, 29.56, 29.52, 29.50, 29.43, 29.42, 29.35, 29.10, 29.04, 28.11, 27.66, 26.96, 26.82, 23.86, 22.92, 22.42. HRMS (ESI⁺): [M+H]⁺: calculated for C₂₉H₅₅N₂O₂⁺ (m/z): 463.4258; detected: 463.4260. LC-MS purity > 96 %.

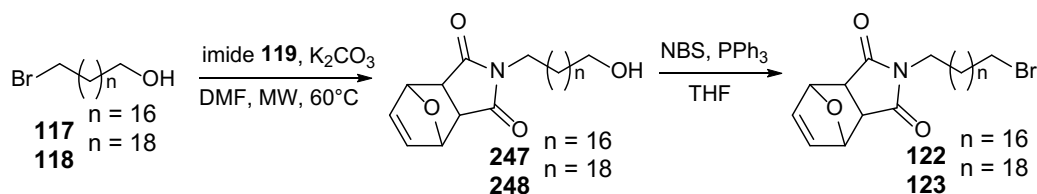
Synthesis of compounds bearing maleimide moiety **132** - **135**



10-oxa-4-azatricyclo[5.2.1.0^{2,6}]dec-8-ene-3,5-dione (119**):** Into an oven-dried flask maleimide (5.0 g, 51.51 mmol) was dissolved in anhydrous dioxane (76 mL) under the inert atmosphere (Ar). Furan (12 mL, 154.53 mmol) was added and the mixture was stirred and heated at 90 °C overnight. The reaction was diluted with water (250 mL) and extracted with EA 2 x 600 mL. The organic layers were combined, dried with anhydrous Na₂SO₄ and filtered. The filtrate was concentrated under reduced pressure to afford **119** (7.66 g, 90 % yield) as a white solid.

¹H NMR (500 MHz, DMSO-*d*₆) δ 11.13 (s, 1H), 6.52 (t, *J* = 1.0 Hz, 2H), 5.10 (t, *J* = 1.0 Hz, 2H), 3.32 (s, 2H). ¹³C NMR (126 MHz, DMSO) δ 178.29, 136.92, 80.77, 48.89.

General procedure for synthesis **122** and **123**:



The compounds **117** or **118** (296 mg, 0.847 mmol for **117** and 180 mg, 0.4769 mmol for **118**), imide **119** (1.2 eq) and anhydrous K_2CO_3 (1.2 eq) were dissolved in dry DMF (4 mL). The mixture was stirred at 60 °C for 12 hours. The resulting mixture was extracted with brine (200 mL) and DCM 2 × 200 mL. The organic layers were combined, dried with anhydrous Na_2SO_4 and filtered. The filtrate was concentrated under reduced pressure and directly used without further purification into the next reaction. **247** or **248** were then dissolved in anhydrous THF (40 mL) under the inert atmosphere (Ar). NBS (1.5 eq) and PPh_3 (1.5 eq) were added subsequently under room temperature conditions with stirring for 30 min. The reaction mixtures were diluted with water (50 mL) and extracted with DCM 2 × 175 mL. The organic layers were collected, dried with anhydrous Na_2SO_4 and filtered. The filtrate was concentrated under reduced pressure and purified with column chromatography to afford **122** (H/EA = 4:1, 320 mg, 76 % yield after two steps from **117**), and **123** (PE/EA = 5:1, 177 mg, 71 % yield after two steps from **118**) as white solids.

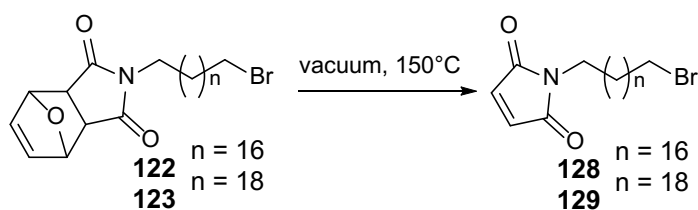
4-(18-bromooktadecyl)-10-oxa-4-azatricyclo[5.2.1.0*2,6*]-dec-8-ene-3,5-dione (122):

1H NMR (500 MHz, $CDCl_3-d_1$) δ 6.51 (s, 2H), 5.27 (s, 2H), 3.48 – 3.44 (m, 2H), 3.41 (t, $J = 6.9$ Hz, 2H), 2.83 (s, 2H), 1.91 – 1.81 (m, 2H), 1.59 – 1.50 (m, 2H), 1.46 – 1.38 (m, 2H), 1.36 – 1.19 (m, 26H). ^{13}C NMR (126 MHz, $CDCl_3$) δ 176.24, 136.51, 80.88, 47.36, 39.02, 34.04, 32.83, 29.67, 29.64, 29.63, 29.59, 29.52, 29.44, 29.42, 29.10, 28.75, 28.17, 27.58, 26.67.

4-(20-bromoicosyl)-10-oxa-4-azatricyclo[5.2.1.0*2,6*]dec-8-ene-3,5-dione (123):

1H NMR (500 MHz, $CDCl_3-d_1$) δ 6.51 (s, 2H), 5.27 (s, 2H), 3.50 – 3.44 (m, 2H), 3.41 (t, $J = 6.9$ Hz, 2H), 2.83 (s, 2H), 1.90 – 1.80 (m, 2H), 1.60 – 1.52 (m, 2H), 1.49 – 1.38 (m, 2H), 1.35 – 1.20 (m, 30H). ^{13}C NMR (126 MHz, $CDCl_3$) δ 176.26, 136.52, 80.89, 47.38, 39.04, 34.04, 32.85, 29.67, 29.65, 29.61, 29.54, 29.45, 29.43, 29.11, 28.76, 28.18, 27.59, 26.68.

General procedure for retro Diels-Alder reaction leading to 128 and 129:



122 or **123** (296 mg, 0.596 mmol for **122** and 422 mg, 0.804 mmol for **123**) were put into dried flask with reduced pressure (1 mBar). The flask was heated at 130 °C for 60 min. The product was purified by column chromatography (PE/EA = 7:1) to afford **128** (216 mg, 85 % yield), or **129** (208 mg, 57 % yield), respectively, as white solids.

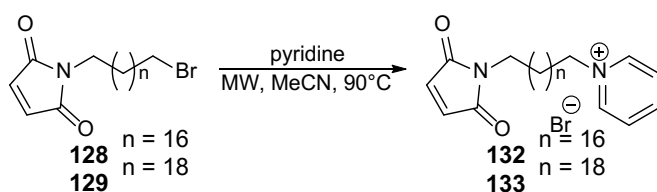
1-(18-bromooctadecyl)-2,5-dihydro-1H-pyrrole-2,5-dione (128):

¹H NMR (500 MHz, CDCl₃-d₁) δ 6.69 (s, 2H), 3.54 – 3.49 (m, 2H), 3.41 (t, *J* = 6.9 Hz, 2H), 1.92 – 1.80 (m, 2H), 1.63 – 1.52 (m, 2H), 1.50 – 1.38 (m, 2H), 1.38 – 1.16 (m, 26H). ¹³C NMR (126 MHz, CDCl₃) δ 170.86, 133.99, 37.93, 34.04, 32.83, 29.64, 29.62, 29.59, 29.52, 29.46, 29.42, 29.11, 28.75, 28.52, 28.16, 26.73.

1-(20-bromoicosyl)-2,5-dihydro-1H-pyrrole-2,5-dione (129):

¹H NMR (500 MHz, CDCl₃-d₁) δ 6.69 (s, 2H), 3.55 – 3.48 (m, 2H), 3.41 (t, *J* = 6.9 Hz, 2H), 1.94 – 1.81 (m, 2H), 1.68 – 1.53 (m, 2H), 1.48 – 1.39 (m, 2H), 1.36 – 1.20 (m, 30H). ¹³C NMR (126 MHz, CDCl₃) δ 170.88, 134.01, 37.95, 34.06, 32.85, 29.68, 29.65, 29.62, 29.54, 29.48, 29.44, 29.13, 28.77, 28.54, 28.18, 26.75.

General procedure for synthesis pyridin-1-ium bromides 132 and 133:



128 or **129** (204 mg, 0.476 mmol of **128** and 92 mg, 0.2015 mmol of **129**) and pyridine (2.0 eq) were dissolved in MeCN (2 mL) and added into the microwave-sealed tube followed by microwave-heated conditions as follows: dynamic curve, power max cap 100 W, pressure max cap 300 PSI, at 90 °C for 24 hours. The mixture was directly purified via column chromatography (DCM/MeOH = 9:1) to afford **132** (168 mg, 69 %), and **133** (63 mg, 58 % yield), respectively, as white solids.

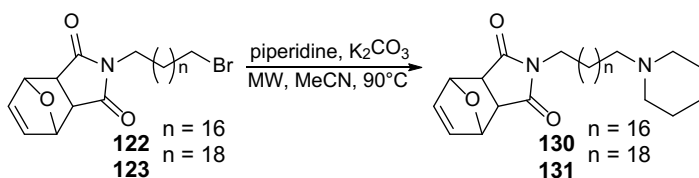
1-(18-(2,5-dioxo-2,5-dihydro-1H-pyrrol-1-yl)oktadecyl)pyridin-1-ium bromide (132):

^1H NMR (500 MHz, $\text{CD}_3\text{OD}-d_4$) δ 9.06 (d, $J = 5.8$ Hz, 2H), 8.62 (t, $J = 7.8$ Hz, 1H), 8.15 (t, $J = 7.0$ Hz, 2H), 6.81 (s, 2H), 4.71 – 4.64 (m, 2H), 3.48 (t, $J = 7.1$ Hz, 2H), 2.10 – 1.98 (m, 2H), 1.62 – 1.52 (m, 2H), 1.45 – 1.37 (m, 4H), 1.36 – 1.20 (m, 24H). ^{13}C NMR (126 MHz, CD_3OD) δ 172.57, 146.83, 145.94, 135.33, 129.50, 63.11, 38.53, 32.50, 30.71, 30.67, 30.60, 30.59, 30.55, 30.46, 30.15, 30.09, 29.46, 27.74, 27.16. HRMS (ESI $^+$): $[\text{M}]^+$: calculated for $\text{C}_{27}\text{H}_{43}\text{N}_2\text{O}_2^+$ (m/z): 427.3319; detected: 427.3310. LC-MS purity > 95 %.

1-(20-(2,5-dioxo-2,5-dihydro-1H-pyrrol-1-yl)icosyl)pyridin-1-ium bromide (133):

^1H NMR (500 MHz, $\text{CD}_3\text{OD}-d_4$) δ 9.07 – 9.01 (m, 2H), 8.70 – 8.53 (m, 1H), 8.17 – 8.10 (m, 2H), 6.81 (s, 2H), 4.72 – 4.60 (m, 2H), 3.48 (t, $J = 7.2$ Hz, 2H), 2.11 – 1.98 (m, 2H), 1.66 – 1.51 (m, 2H), 1.43 – 1.22 (m, 32H). ^{13}C NMR (126 MHz, CD_3OD) δ 172.56, 146.84, 145.93, 135.32, 129.50, 63.12, 38.53, 32.50, 30.73, 30.69, 30.62, 30.60, 30.57, 30.48, 30.17, 30.10, 29.48, 27.76, 27.18. HRMS (ESI $^+$): $[\text{M}]^+$: calculated for $\text{C}_{29}\text{H}_{47}\text{N}_2\text{O}_2^+$ (m/z): 455.3632; detected: 455.3636. LC-MS purity > 95 %.

General procedure for synthesis 130 and 131:



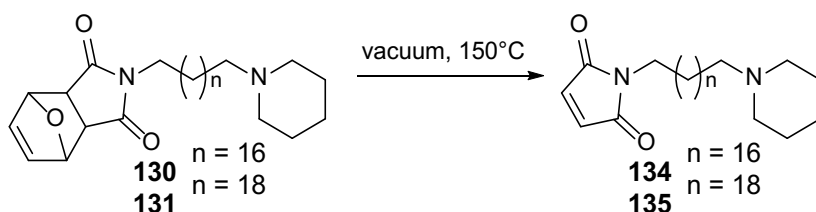
122 or **123** (207 mg, 0.417 mmol for **122** and 199 mg, 0.380 mmol for **123**), K_2CO_3 (3.0 eq) and piperidine (2.0 eq) were dissolved in MeCN (2 mL) and added into the microwave-sealed tube followed by microwave-heated conditions as follows: dynamic curve, power max cap 100 W, pressure max cap 300 PSI, at 90°C for 30 min. The mixture was directly purified by column chromatography to afford **130** (DCM/MeOH = 9:1, 209 mg, quantitative yield) and **131** (DCM/MeOH = 20:1, 111 mg, 56 % yield), respectively, as white solids.

4-(18-(piperidin-1-yl)oktadecyl)-10-oxa-4-azatricyclo[5.2.1.0*2,6*]dec-8-ene-3,5-dione (130): The compound was used into the next reaction.

4-(20-(piperidin-1-yl)icosyl)-10-oxa-4-azatricyclo[5.2.1.0*2,6*]dec-8-ene-3,5-dione (131):

^1H NMR (500 MHz, CDCl_3 - d_1) δ 6.51 (d, $J = 1.0$ Hz, 2H), 5.26 (d, $J = 1.0$ Hz, 2H), 3.52 – 3.41 (m, 2H), 2.83 (s, 2H), 2.75 – 2.60 (m, 2H), 2.59 – 2.49 (m, 2H), 1.86 – 1.72 (m, 4H), 1.70 – 1.60 (m, 2H), 1.59 – 1.49 (m, 4H), 1.36 – 1.17 (m, 34H). ^{13}C NMR (126 MHz, CDCl_3) δ 176.27, 136.53, 80.89, 58.71, 53.92, 47.38, 39.03, 29.68, 29.66, 29.62, 29.55, 29.49, 29.46, 29.34, 29.12, 27.59, 27.38, 26.68, 25.35, 24.41, 23.46.

General procedure for retro Diels-Alder reaction yielding to 134 and 135:



130 or **131** (209 mg, 0.417 mmol for **130** and 94 mg, 0.178 mmol for **131**) were charged into the dried flask. The flask was heated at 130 °C under the reduced pressure (1 mBar) for 60 min. **134** (139 mg, 77 % yield) was prepared without any further purification. **135** (50 mg, 61 % yield) had to be purified by column chromatography (PE/EA = 7:1). Both products **134** and **135** were isolated as white solids.

1-(18-(piperidin-1-yl)oktadecyl)-2,5-dihydro-1H-pyrrole-2,5-dione (134):

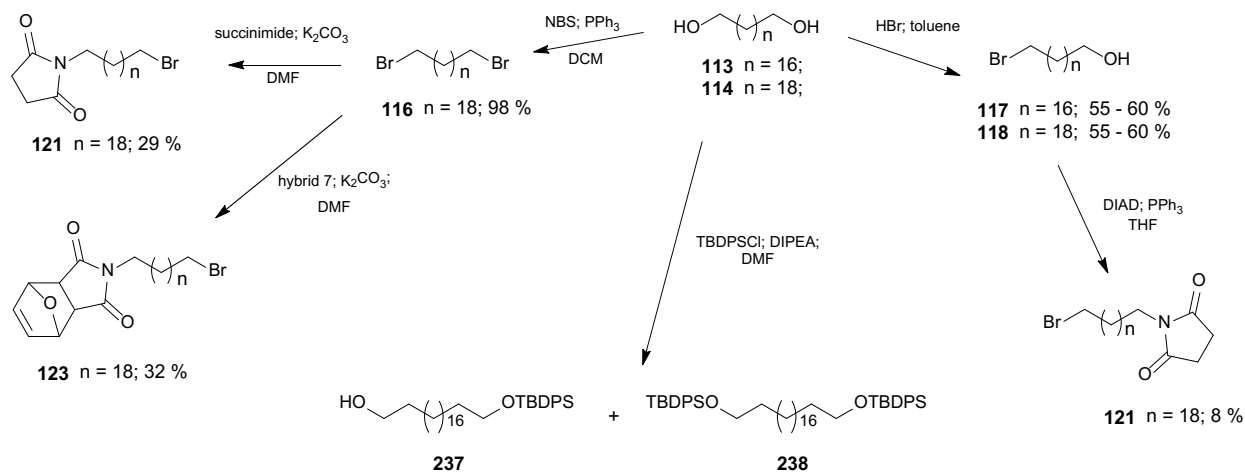
^1H NMR (500 MHz, CD_3OD - d_4) δ 6.81 (s, 2H), 3.48 (t, $J = 7.2$ Hz, 2H), 3.26 – 3.11 (m, 4H), 3.06 – 2.99 (m, 2H), 1.89 – 1.82 (m, 4H), 1.78 – 1.70 (m, 2H), 1.70 – 1.63 (m, 2H), 1.60 – 1.50 (m, 2H), 1.42 – 1.35 (m, 4H), 1.35 – 1.23 (m, 24H). ^{13}C NMR (126 MHz, CD_3OD) δ 172.55, 135.33, 58.48, 54.32, 49.51, 49.34, 49.17, 49.00, 48.83, 48.68, 48.66, 48.49, 38.53, 30.74, 30.71, 30.63, 30.58, 30.51, 30.22, 30.17, 29.48, 27.76, 25.21, 24.42, 22.90. HRMS (ESI⁺): $[\text{M}+\text{H}]^+$: calculated for $\text{C}_{27}\text{H}_{49}\text{N}_2\text{O}_2^+$ (m/z): 433.3789; detected: 433.3777. LC-MS purity > 95 %.

1-(20-(piperidin-1-yl)icosyl)-2,5-dihydro-1H-pyrrole-2,5-dione (135):

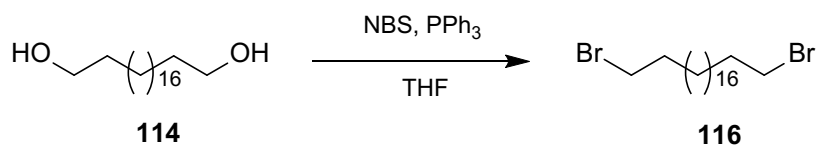
^1H NMR (500 MHz, CD_3OD - d_4) δ 6.81 (s, 2H), 3.48 (t, $J = 7.2$ Hz, 2H), 3.25 – 3.08 (m, 4H), 3.07 – 2.96 (m, 2H), 1.92 – 1.81 (m, 4H), 1.79 – 1.69 (m, 2H), 1.71 – 1.63 (m,

2H), 1.62 – 1.52 (m, 2H), 1.44 – 1.21 (m, 32H). ^{13}C NMR (126 MHz, CD_3OD) δ 172.48, 135.32, 58.49, 54.30, 38.53, 30.77, 30.74, 30.65, 30.60, 30.54, 30.24, 30.20, 29.51, 27.81, 27.78, 25.23, 24.43, 22.95. HRMS (ESI⁺): $[\text{M}+\text{H}]^+$: calculated for $\text{C}_{29}\text{H}_{53}\text{N}_2\text{O}_2^+$ (m/z): 461.4102; detected: 461.4106. LC-MS purity > 95 %.

Unsuccessful synthetic routes



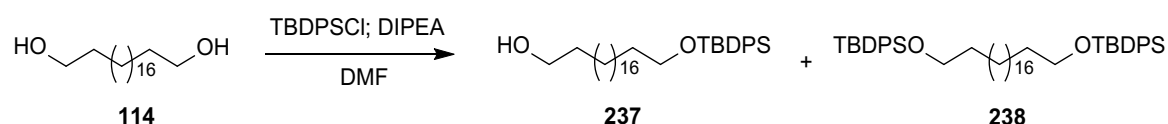
General procedure of bis-bromination:



1,20-dibromoicosane (116): The compound **114** (534 mg 1.7 mmol) was charged into the oven-dried flask and dissolved in anhydrous THF (20 ml). NBS (1.21 g, 6.8 mmol) and PPh_3 (1.784 g, 6.8 mmol) were added consequently. The reaction mixture was stirred at room temperature for 30 min. The reaction was diluted with water (50 mL) and extracted with DCM 3 × 30 mL. The organic layers were combined, dried with anhydrous Na_2SO_4 and filtered. The filtrate was concentrated under reduced pressure and purified via column chromatography (PE/EA = 299:1) to afford **116** (735 mg, 98 % yield) as a white solid.

^1H NMR (500 MHz, CDCl_3-d_1) δ 3.42 (t, J = 6.9 Hz, 4H), 1.86 (dt, J = 14.8, 6.9 Hz, 4H), 1.48 – 1.37 (m, 4H), 1.27 (s, 28H). ^{13}C NMR (126 MHz, CDCl_3) δ 34.04, 32.85, 29.67, 29.65, 29.61, 29.54, 29.44, 28.77, 28.18.

General procedure of silylation:



The icosane-1,20-diol **114** (378 mg; 1.2 mmol) was dissolved in anhydrous DMF (4 mL) under Ar atmosphere. *N,N*-Diisopropylethylamine (DIPEA; 2.1 mL; 12.0 mmol) was slowly added and the mixture was stirred for 15 min. Finally, *tert*-butyldiphenylsilyl chloride (TBDPSCI; 330 μ L; 1.26 mmol) was added dropwise and reaction mixture was stirred at RT for 2 hours. The resulting mixture was diluted with H₂O and DCM and extracted with DCM (2 \times 50 mL). The organic layers were collected and washed with 1M HCl; then with saturated NaHCO₃ and with brine. The resulting organic phase was dried with anhydrous Na₂SO₄, filtrated and concentrated under reduced pressure. The residue was purified by column chromatography using mobile phase PE/EA (8:1) to obtain **237**, **238** as white solids (**237**: 299 mg, 45 % yield; **238**: 216 mg, 23 %) and starting material turnover (**114**, 165 mg, 25 %)

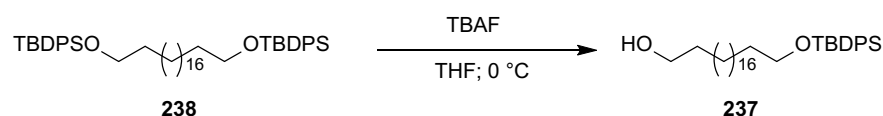
20-[(*tert*-butyldiphenylsilyl)oxy]icosan-1-ol (**237**):

¹H NMR (500 MHz, CDCl₃-*d*₁) δ 7.78 – 7.24 (m, 10H), 3.73 – 3.60 (m, 4H), 1.64 – 1.52 (m, 4H), 1.43 – 1.23 (m, 32H), 1.07 (s, 9H).

2,2,27,27-tetramethyl-3,3,26,26-tetraphenyl-4,25-dioxa-3,26-disilaoctacosane (**238**):

¹H NMR (500 MHz, CDCl₃-*d*₁) δ 7.90 – 7.19 (m, 20H), 3.67 (t, *J* = 6.5 Hz, 4H), 1.66 – 1.51 (m, 4H), 1.41 – 1.20 (m, 32H), 1.07 (s, 18H).

General procedure of monosilyl-deprotection of compound **238**:



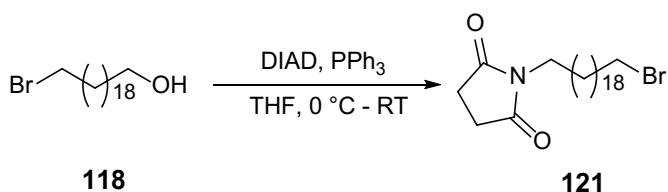
Under Ar atmosphere, **238** (168 mg; 0.2123 mmol) was dissolved in anhydrous THF (5 mL) and cooled to 0 °C. Tetrabutylammonium fluoride (TBAF; 223 μ L, 0.223 mmol) was added dropwise and the mixture was stirred for 1 hour at room temperature. The resulting reaction mixture was diluted with DCM and H₂O and extracted with DCM (3 \times 30 mL). The organic layers were combined, dried with anhydrous sodium sulfate,

filtrated and concentrated under reduced pressure. The residue was purified by column chromatography using mobile phase PE/EA (8:1) to give crude product **237** (92 mg, 78 % yield) as white solid.

20-[(tert-butylidiphenylsilyl)oxy]icosan-1-ol (**237**):

$^1\text{H NMR}$ (500 MHz, CDCl_3 -*d*₁) δ 7.78 – 7.24 (m, 10H), 3.73 – 3.60 (m, 4H), 1.64 – 1.52 (m, 4H), 1.43 – 1.23 (m, 32H), 1.07 (s, 9H).

General procedure of Mitsunobu reaction

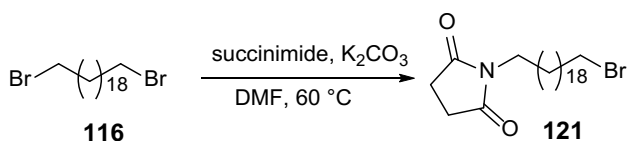


The compound **118** (170 mg, 0.3074 mmol), succinimide (40 mg, 0.40 mmol) and PPh_3 was dissolved in anhydrous THF and cooled to $0\text{ }^\circ\text{C}$ under Ar atmosphere. Diisopropyl azodicarboxylate (DIAD; 79 μL , 0.40 mmol) was drop wise added and the mixture was stirred at RT for 20 hours. The resulting mixture was diluted with H_2O and extracted with DCM (3x 30 mL). The organics were collected, dried with anhydrous Na_2SO_4 , filtrated and concentrated under reduced pressure. The residue was purified using column chromatography with mobile phase PE/EA (3:1) to give **121** (11 mg, 8 % yield).

1-(20-bromoicosyl)pyrrolidine-2,5-dione (**121**):

$^1\text{H NMR}$ (500 MHz, CDCl_3 -*d*₁) δ 3.52 (t, $J = 7.4\text{ Hz}$, 2H), 3.43 (t, $J = 6.9\text{ Hz}$, 2H), 2.72 (s, 4H), 1.92 – 1.84 (m, 2H), 1.61 – 1.54 (m, 2H), 1.50 – 1.41 (m, 2H), 1.37 – 1.19 (m, 30H).

General procedure of reactions from 1,20-dibromoicosane **116**:

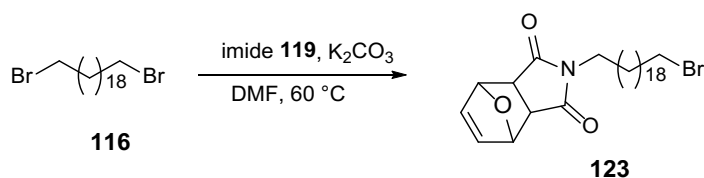


1,20-Dibromoicosane **116** (498 mg; 1.13 mmol), succinimide (124 mg; 1.244 mmol) and anhydrous K_2CO_3 (172 mg; 1.244 mmol) were dissolved in anhydrous DMF (4 mL)

under Ar atmosphere. The mixture was heated to 60 °C for 3 hours. The resulting mixture was diluted with ammonium chloride saturated solution (50 mL) and extracted with DCM (3 × 50 mL). The organic layers were combined, dried with anhydrous Na₂SO₄, filtrated and concentrated under reduced pressure. The residue was purified by column chromatography using mobile phase PE/EA (4:1) to give **121** (150 mg, 29 % yield).

1-(20-bromoicosyl)pyrrolidine-2,5-dione (121):

¹H NMR (500 MHz, CDCl₃-*d*₁) δ 3.52 – 3.47 (m, 2H), 3.41 (t, *J* = 6.9 Hz, 2H), 2.70 (t, *J* = 20.2 Hz, 4H), 1.90 – 1.80 (m, 2H), 1.60 – 1.52 (m, 2H), 1.47 – 1.38 (m, 2H), 1.35 – 1.20 (m, 30H). ¹³C NMR (126 MHz, CDCl₃) δ 177.22, 38.89, 34.03, 32.82, 29.65, 29.63, 29.59, 29.53, 29.51, 29.45, 29.41, 29.13, 28.74, 28.15, 28.13, 27.69, 26.84.

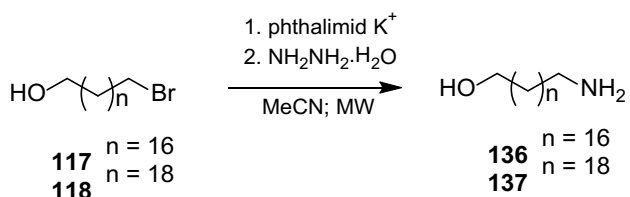


1,20-Dibromoicosane **116** (209 mg; 0.4746 mmol), imide **119** (118 mg; 0.712 mmol) and K₂CO₃ (98 mg; 0.712 mmol) were dissolved in anhydrous DMF (2 mL) under Ar atmosphere. The mixture was heated to 60 °C for 3 hours. The resulting mixture was diluted with ammonium chloride saturated solution (50 mL) and extracted with DCM (3 × 50 mL). The organic layers were combined, dried with anhydrous Na₂SO₄, filtrated and concentrated under reduced pressure. The residue was purified by column chromatography using mobile phase PE/EA (5:1) to give **123** (80 mg, 32 % yield).

4-(20-bromoicosyl)-10-oxa-4-azatricyclo[5.2.1.0*2,6*]dec-8-ene-3,5-dione (123):

¹H NMR (500 MHz, CDCl₃-*d*₁) δ 6.51 (s, 2H), 5.27 (s, 2H), 3.49 – 3.44 (m, 2H), 3.41 (t, *J* = 6.9 Hz, 2H), 2.83 (s, 2H), 1.90 – 1.82 (m, 2H), 1.60 – 1.51 (m, 2H), 1.48 – 1.38 (m, 2H), 1.36 – 1.17 (m, 30H). ¹³C NMR (126 MHz, CDCl₃) δ 176.25, 136.51, 80.87, 47.36, 39.02, 34.03, 32.83, 29.66, 29.64, 29.59, 29.52, 29.44, 29.42, 29.10, 28.75, 28.16, 27.58, 26.66.

6.1.4 Second subset of insecticides



Compound **117** or **118** (3.8 mmol) and potassium phthalimide (5.7 mmol; 1.5 eq) were dissolved in anhydrous acetonitrile (MeCN; 10 mL) in a microwave (MW) tube. The mixture was challenged with MW irradiation (dynamic curve; 100 W; 300 PSI max cap) for eight hours at 110 °C. Then, NH₂NH₂·H₂O was added and the resulting mixture was further challenged with MW irradiation (dynamic curve; 100 W; 300 PSI max cap) for 1 hour at 90 °C. The reaction mixture was filtrated and the filter cake was three times washed with 50 mL of absolute EtOH. The filtrate was concentrated and purified by column chromatography to afford title product **136** or **137**.

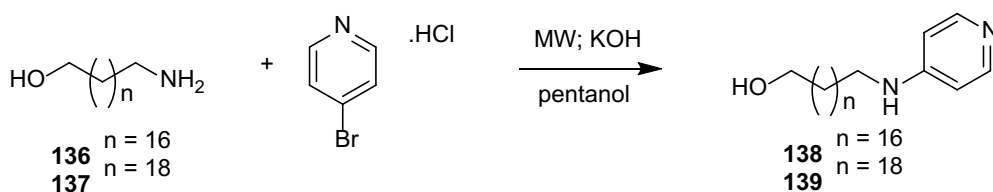
18-aminooctadecan-1-ol (136): The resulting residue was purified by column chromatography (DCM/MeOH/NH₃ = 5:1:0.1) affording **136** with quantitative yield as white powder.

¹H NMR (500 MHz, Methanol-*d*₄) δ 3.58 – 3.51 (m, 2H), 2.83 – 2.75 (m, 2H), 1.63 – 1.48 (m, 4H), 1.42 – 1.26 (m, 28H). ¹³C NMR (126 MHz, CD₃OD) δ 62.99, 41.57, 33.67, 30.90, 30.77, 30.73, 30.69, 30.61, 30.41, 27.72, 26.96.

20-aminoicosan-1-ol (137): The resulting residue was purified by column chromatography (DCM/MeOH/NH₃ = 5:1:0.1) affording **137** with quantitative yield as white powder.

¹H NMR (500 MHz, Methanol-*d*₄) δ 3.55 (t, *J* = 6.7 Hz, 2H), 2.75 – 2.67 (m, 2H), 1.53 (ttt, *J* = 10.6, 7.2, 3.4 Hz, 4H), 1.41 – 1.25 (m, 32H). ¹³C NMR (126 MHz, cd₃od) δ 61.60, 40.68, 32.29, 30.99, 29.38, 29.35, 29.33, 29.28, 29.23, 29.14, 26.50, 25.57, 8.29.

Pyridinium derivatives



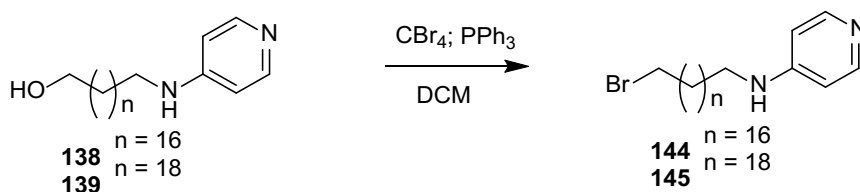
Compound **136** or **137** (0.69 mmol) and 4-bromopyridine hydrochloride (1.39 mmol; 2.0 eq) were dissolved in 3 mL pentanol in a MW tube. The mixture was challenged with MW irradiation (dynamic curve; 150 W; 300 PSI max cap) for three hours at 180 °C. The resulting mixture was concentrated and directly purified by column chromatography to afford title product **138** or **139**.

18-[(pyridine-4-yl)amino]octadecan-1-ol (138): The resulting residue was purified by column chromatography (DCM/MeOH/NH₃ = 9:1:0.1) affording **138** with 43 % yield as yellowish powder.

¹H NMR (500 MHz, Methanol-*d*₄) δ 8.12 – 8.05 (m, 2H), 6.61 – 6.57 (m, 2H), 3.63 (t, *J* = 6.6 Hz, 2H), 3.17 (t, *J* = 7.1 Hz, 2H), 1.71 – 1.62 (m, 2H), 1.60 – 1.53 (m, 2H), 1.49 – 1.25 (m, 28H). ¹³C NMR (126 MHz, cd₃od) δ 157.31, 149.85, 109.39, 63.50, 43.91, 33.84, 30.81, 30.79, 30.76, 30.68, 30.57, 30.01, 28.20, 27.03.

20-[(pyridine-4-yl)amino]icosan-1-ol (139): The resulting residue was purified by column chromatography (DCM/MeOH/NH₃ = 9:1:0.1) affording **139** with 37 % yield as yellowish powder.

¹H NMR (500 MHz, Methanol-*d*₄) δ 7.99 – 7.92 (m, 2H), 6.53 – 6.49 (m, 2H), 3.54 (t, *J* = 6.6 Hz, 2H), 3.12 (t, *J* = 7.1 Hz, 2H), 1.66 – 1.57 (m, 2H), 1.56 – 1.49 (m, 2H), 1.45 – 1.23 (m, 32H). ¹³C NMR (126 MHz, cd₃od) δ 156.31, 149.25, 108.29, 63.00, 43.27, 33.69, 30.79, 30.76, 30.72, 30.63, 30.53, 29.93, 28.14, 26.97.

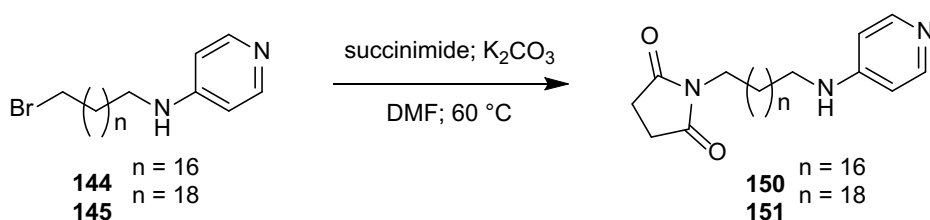


Compound **138** or **139** (0.727 mmol) was dissolved in anhydrous dichloromethane (DCM; 10 mL) under Ar atmosphere. Tetrabromomethane (CBr₄; 1.1 mmol; 1.5 eq) was added and the mixture was stirred at RT. In another oven-dried round-bottom flask triphenylphosphine (PPh₃; 1.2 mmol; 1.6 eq) was dissolved in anhydrous DCM (5 mL) under Ar atmosphere. The solution of PPh₃ was slowly drop wise added into the mixture of CBr₄ and **138** or **139** and the reaction mixture was stirred at RT for one hour. The resulting residue was concentrated and directly purified by column chromatography to afford title products **144** or **145**.

N-(18-bromooctadecyl)pyridine-4-amine (144): The resulting residue was purified by column chromatography (DCM/MeOH/NH₃ = 20:1:0.1) affording **144** with 87 % yield as brownish powder. Without characterization used into the next reaction.

N-(20-bromoicosyl)pyridine-4-amine (145): The resulting residue was purified by column chromatography (DCM/MeOH/NH₃ = 20:1:0.1) affording **145** with 79 % yield as yellowish powder.

¹H NMR (500 MHz, Methanol-*d*₄) δ 8.08 – 7.98 (m, 2H), 6.89 – 6.81 (m, 2H), 3.44 (t, *J* = 6.8 Hz, 2H), 3.32 – 3.31 (m, 3H), 1.89 – 1.80 (m, 2H), 1.72 – 1.64 (m, 3H), 1.49 – 1.21 (m, 32H).



Compound **144** or **145** (0.315 mmol), succinimide (0.4725 mmol; 1.5 eq) and K₂CO₃ (0.4725 mmol; 1.5 eq) were dissolved in anhydrous dimethylformamide (DMF; 3 mL) under Ar atmosphere. The mixture was heated to 60 °C and stirred for 15 hours. The resulting mixture was concentrated and directly purified to afford title products **150** or **151**.

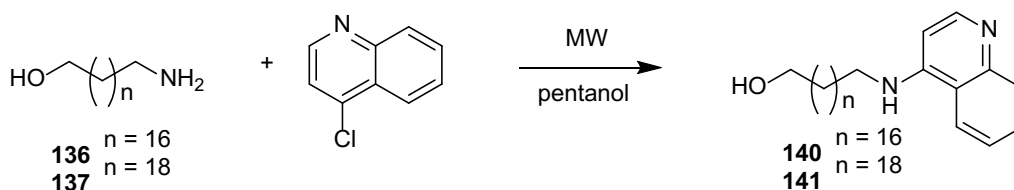
1-{18-[(pyridin-4-yl)amino]octadecyl}pyrrolidine-2,5-dione (150): The resulting residue was purified by column chromatography (DCM/MeOH = 9:1) affording **150** with 52 % yield as white powder.

¹H NMR (500 MHz, Methanol-*d*₄) δ 8.08 – 8.00 (m, 2H), 6.87 – 6.81 (m, 2H), 3.49 – 3.43 (m, 2H), 3.32 – 3.29 (m, 2H), 2.69 (s, 4H), 1.72 – 1.64 (m, 2H), 1.59 – 1.51 (m, 2H), 1.46 – 1.22 (m, 28H). ¹³C NMR (126 MHz, cd₃od) δ 178.60, 158.17, 139.92, 127.40, 42.43, 38.17, 29.33, 29.26, 29.17, 29.00, 28.84, 28.06, 27.66, 27.22, 26.56, 26.47. HRMS (ESI⁺): [M]⁺: calculated for C₂₇H₄₆N₃O₂⁺ (m/z): 444.3585; found: 444.35730. LC-MS > 96 %.

1-{20-[(pyridin-4-yl)amino]icosyl}pyrrolidine-2,5-dione (151): The resulting residue was purified by column chromatography (DCM/MeOH = 9:1) affording **151** with 67 % yield as white powder.

^1H NMR (500 MHz, Chloroform-*d*) δ 8.21 – 8.10 (m, 2H), 6.47 – 6.39 (m, 2H), 4.42 (bs, 1H), 3.49 (t, $J = 7.5$ Hz, 2H), 3.13 (q, $J = 6.6$ Hz, 2H), 2.69 (s, 4H), 1.62 (p, $J = 7.3$ Hz, 2H), 1.55 (p, $J = 7.3$ Hz, 2H), 1.43 – 1.35 (m, 2H), 1.35 – 1.19 (m, 30H). ^{13}C NMR (126 MHz, cdCl_3) δ 177.21, 153.67, 149.28, 107.39, 42.64, 38.87, 29.62, 29.60, 29.58, 29.57, 29.52, 29.50, 29.42, 29.29, 29.11, 29.06, 28.11, 27.67, 26.96, 26.82. HRMS (ESI $^+$): $[\text{M}]^+$: calculated for $\text{C}_{29}\text{H}_{50}\text{N}_3\text{O}_2^+$ (m/z): 472.3898; found: 472.38940. LC-MS > 96 %.

Quinolinium derivatives



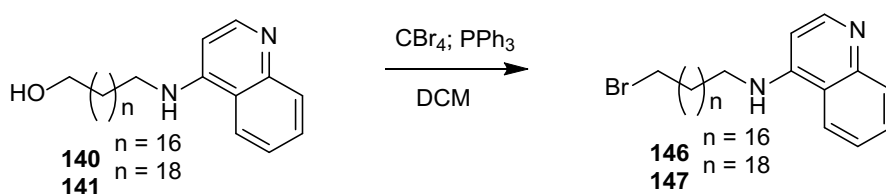
Compound **136** or **137** (1.555 mmol) and 4-chloroquinoline (1.71 mmol; 1.1 eq) were dissolved in 3 mL pentanol in a MW tube. The mixture was challenged with MW irradiation (dynamic curve; 150 W; 300 PSI max cap) for three hours at 180 °C. The resulting mixture was concentrated and directly purified by column chromatography to afford title product **140** or **141**.

18-[(quinolin-4-yl)amino]octadecan-1-ol (140): The resulting residue was purified by column chromatography (DCM/MeOH/ $\text{NH}_3 = 9:1:0.1$) affording **140** with 58 % yield as yellowish powder.

^1H NMR (500 MHz, Chloroform-*d* + Methanol-*d*₄) δ 12.30 – 12.25 (m, 1H), 11.94 – 11.88 (m, 1H), 11.78 – 11.72 (m, 1H), 11.57 – 11.50 (m, 1H), 11.39 – 11.31 (m, 1H), 10.39 – 10.32 (m, 1H), 7.47 (t, $J = 6.8$ Hz, 2H), 7.27 – 7.26 (m, 2H), 5.74 – 5.64 (m, 2H), 5.50 – 5.41 (m, 2H), 5.44 – 5.34 (m, 2H), 5.35 – 5.27 (m, 2H), 5.28 – 5.14 (m, 2H). ^{13}C NMR (126 MHz, $\text{cdCl}_3 + \text{cd}_3\text{od}$) δ 154.95, 153.86, 151.43, 133.09, 131.71, 128.27, 124.41, 122.78, 101.93, 65.97, 46.87, 36.29, 33.43, 33.41, 33.39, 33.36, 33.27, 33.19, 32.28, 30.98, 29.59.

20-[(quinolin-4-yl)amino]icosan-1-ol (141): The resulting residue was purified by column chromatography (DCM/MeOH/ $\text{NH}_3 = 9:1:0.1$) affording **141** with 64 % yield as yellowish powder.

^1H NMR (500 MHz, Chloroform-*d*) δ 8.57 – 8.52 (m, 1H), 8.01 – 7.95 (m, 1H), 7.77 – 7.71 (m, 1H), 7.67 – 7.59 (m, 1H), 7.47 – 7.39 (m, 1H), 6.47 – 6.40 (m, 1H), 5.07 (bs, $J = 5.2$ Hz, 1H), 3.65 (t, $J = 6.6$ Hz, 2H), 3.36 – 3.27 (m, 2H), 1.81 – 1.71 (m, 2H), 1.61 – 1.52 (m, 2H), 1.47 (p, $J = 7.5, 7.0$ Hz, 2H), 1.27 (d, $J = 7.6$ Hz, 30H). ^{13}C NMR (126 MHz, cdCl_3) δ 150.87, 149.74, 148.22, 129.74, 128.96, 124.52, 119.15, 118.62, 98.69, 62.91, 62.90, 43.23, 32.81, 29.64, 29.63, 29.61, 29.58, 29.56, 29.53, 29.50, 29.41, 29.33, 28.90, 27.12, 25.74.

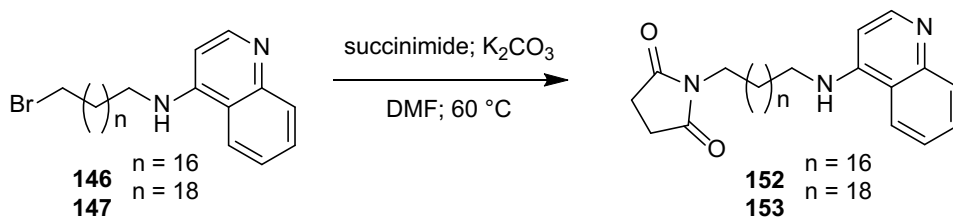


Compound **140** or **141** (0.848 mmol) was dissolved in anhydrous dichloromethane (DCM; 10 mL) under Ar atmosphere. CBr_4 (1.27 mmol; 1.5 eq) was added and the mixture was stirred at RT. In another oven-dried round-bottom flask PPh_3 (1.36 mmol; 1.6 eq) was dissolved in anhydrous DCM (5 mL) under Ar atmosphere. The solution of PPh_3 was slowly drop wise added into the mixture of CBr_4 and **140** or **141** and the reaction mixture was stirred at RT for one hour. The resulting residue was concentrated and directly purified by column chromatography to afford title products **146** or **147**.

N-(18-bromooctadecyl)quinolin-4-amine (146): The resulting residue was purified by column chromatography (DCM/MeOH/ $\text{NH}_3 = 20:1:0.1$) affording **146** with quantitative yield as yellowish powder. Without characterization used into the next reaction.

N-(20-bromoicosyl)quinolin-4-amine (147): The resulting residue was purified by column chromatography (DCM/MeOH/ $\text{NH}_3 = 20:1:0.1$) affording **147** with quantitative yield as orange powder.

^1H NMR (500 MHz, Chloroform-*d*) δ 8.59 – 8.55 (m, 1H), 8.02 – 7.96 (m, 1H), 7.79 – 7.72 (m, 1H), 7.66 – 7.60 (m, 1H), 7.44 – 7.38 (m, 1H), 6.46 – 6.41 (m, 1H), 5.06 (bs, 1H), 3.41 (t, $J = 6.9$ Hz, 2H), 3.36 – 3.29 (m, 2H), 1.90 – 1.82 (m, 2H), 1.81 – 1.73 (m, 2H), 1.52 – 1.37 (m, 4H), 1.35 – 1.23 (m, 28H). ^{13}C NMR (126 MHz, cdCl_3) δ 150.97, 149.68, 148.34, 132.95, 129.91, 124.49, 119.17, 118.66, 98.72, 43.26, 34.04, 32.81, 29.66, 29.62, 29.59, 29.57, 29.53, 29.51, 29.41, 29.36, 28.93, 28.74, 28.15, 27.15.



Compound **146** or **147** (0.282 mmol), succinimide (0.423 mmol; 1.5 eq) and K_2CO_3 (0.423 mmol; 1.5 eq) were dissolved in anhydrous DMF (3 mL) under Ar atmosphere. The mixture was heated to 60 °C and stirred for 15 hours. The resulting mixture was concentrated and directly purified to afford title products **152** or **153**.

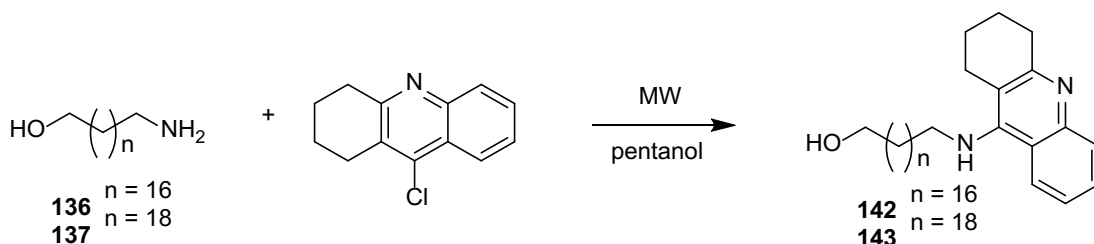
1-{18-[(quinolin-4-yl)amino]octadecyl}pyrrolidine-2,5-dione (152**):** The resulting residue was purified by column chromatography (DCM/MeOH/ NH_3 = 20:1:0.1) affording **152** with 58 % yield as white powder.

^1H NMR (500 MHz, Chloroform-*d*) δ 8.06 – 8.01 (m, 1H), 7.70 – 7.65 (m, 1H), 7.53 – 7.48 (m, 1H), 7.32 – 7.27 (m, 1H), 7.14 – 7.07 (m, 1H), 6.13 – 6.10 (m, 1H), 3.15 (t, $J = 7.4$ Hz, 2H), 3.02 (t, $J = 7.3$ Hz, 2H), 2.38 (s, 4H), 1.44 (t, $J = 7.4$ Hz, 2H), 1.22 (p, $J = 7.2$ Hz, 2H), 1.18 – 1.09 (m, 2H), 1.09 – 0.89 (m, 26H). ^{13}C NMR (126 MHz, $\text{cdCl}_3 + \text{cd}_3\text{od}$) δ 177.77, 150.59, 149.30, 146.84, 128.74, 127.17, 123.89, 120.03, 118.32, 97.51, 42.47, 38.21, 29.00, 28.99, 28.96, 28.90, 28.82, 28.79, 28.50, 27.86, 27.44, 27.00, 26.57, 26.20. HRMS (ESI $^+$): $[\text{M}]^+$: calculated for $\text{C}_{31}\text{H}_{48}\text{N}_3\text{O}_2^+$ (m/z): 494.3741; found: 494.37366. LC-MS > 96 %.

1-{20-[(quinolin-4-yl)amino]icosyl}pyrrolidine-2,5-dione (153**):** The resulting residue was purified by column chromatography (DCM/MeOH/ NH_3 = 20:1:0.1) affording **153** with 58 % yield as white powder.

^1H NMR (500 MHz, Chloroform-*d*) δ 8.59 – 8.53 (m, 1H), 8.03 – 7.94 (m, 1H), 7.77 – 7.69 (m, 1H), 7.67 – 7.59 (m, 1H), 7.46 – 7.39 (m, 1H), 6.47 – 6.40 (m, 1H), 5.02 (bs, $J = 5.3$ Hz, 1H), 3.52 – 3.45 (m, 2H), 3.36 – 3.28 (m, 2H), 2.69 (s, 4H), 1.81 – 1.73 (m, 2H), 1.60 – 1.51 (m, 2H), 1.51 – 1.43 (m, 2H), 1.42 – 1.34 (m, 2H), 1.35 – 1.21 (m, 30H). ^{13}C NMR (126 MHz, cdCl_3) δ 177.21, 151.01, 149.64, 148.38, 129.94, 128.89, 124.47, 119.12, 118.65, 98.73, 43.24, 38.88, 29.64, 29.61, 29.58, 29.55, 29.52, 29.43, 29.35, 29.12, 28.93, 28.12, 27.68, 27.14, 26.83. HRMS (ESI $^+$): $[\text{M}]^+$: calculated for $\text{C}_{33}\text{H}_{52}\text{N}_3\text{O}_2^+$ (m/z): 522.4054; found: 522.40491. LC-MS > 95 %.

Tacrine derivatives



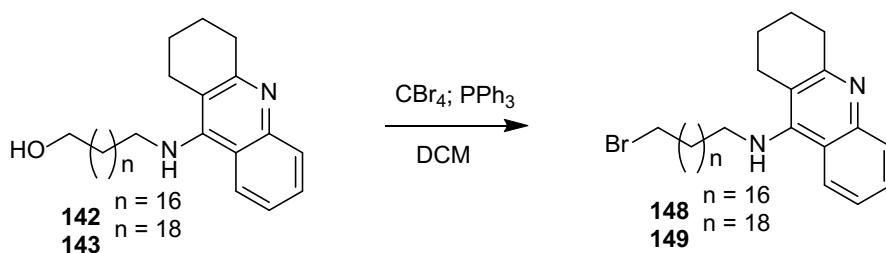
Compound **136** or **137** (1.41 mmol) and 9-chloro-1,2,3,4-tetrahydroacridine (1.55 mmol; 1.1 eq) were dissolved in 3 mL pentanol in a MW tube. The mixture was challenged with MW irradiation (dynamic curve; 150 W; 300 PSI max cap) for three hours at 180 °C. The resulting mixture was concentrated and directly purified by column chromatography to afford title product **142** or **143**.

18-[(1,2,3,4-tetrahydroacridin-9-yl)amino]octadecan-1-ol (142): The resulting residue was purified by column chromatography (DCM/MeOH = 9:1) affording **142** with 60 % yield as yellow oil.

^1H NMR (500 MHz, Methanol- d_4) δ 8.41 – 8.36 (m, 1H), 7.87 – 7.81 (m, 1H), 7.80 – 7.75 (m, 1H), 7.61 – 7.56 (m, 1H), 3.94 (t, J = 7.3 Hz, 2H), 3.54 (t, J = 6.6 Hz, 2H), 3.02 (t, J = 5.9 Hz, 2H), 2.71 (t, J = 5.8 Hz, 2H), 2.03 – 1.92 (m, 4H), 1.83 (p, J = 7.4 Hz, 2H), 1.57 – 1.48 (m, 2H), 1.47 – 1.38 (m, 2H), 1.40 – 1.23 (m, 26H). ^{13}C NMR (126 MHz, cd_3od) δ 157.83, 151.92, 140.11, 133.91, 126.42, 126.23, 120.39, 117.22, 112.98, 62.99, 33.66, 31.52, 30.75, 30.72, 30.68, 30.60, 30.54, 30.24, 29.50, 27.68, 26.95, 24.92, 23.03, 21.93.

20-[(1,2,3,4-tetrahydroacridin-9-yl)amino]icosan-1-ol (143): The resulting residue was purified by column chromatography (DCM/MeOH/ NH_3 = 9:1:0.1) affording **143** with 63 % yield as yellow oil.

^1H NMR (500 MHz, Chloroform- d) δ 8.00 – 7.93 (m, 2H), 7.59 – 7.53 (m, 1H), 7.38 – 7.32 (m, 1H), 3.68 – 3.61 (m, 2H), 3.52 (t, J = 7.2 Hz, 2H), 3.15 – 3.03 (m, 2H), 2.73 – 2.66 (m, 2H), 1.97 – 1.87 (m, 4H), 1.67 (p, J = 7.3 Hz, 2H), 1.61 – 1.52 (m, 2H), 1.43 – 1.19 (m, 32H). ^{13}C NMR (126 MHz, cdcl_3) δ 157.84, 151.19, 146.77, 128.58, 128.00, 123.64, 122.94, 119.80, 115.30, 62.94, 50.65, 49.48, 33.48, 32.79, 32.46, 31.72, 29.64, 29.62, 29.58, 29.56, 29.50, 29.48, 29.41, 29.31, 27.89, 26.88, 25.73, 24.63, 22.94, 22.59, 22.45, 14.01.



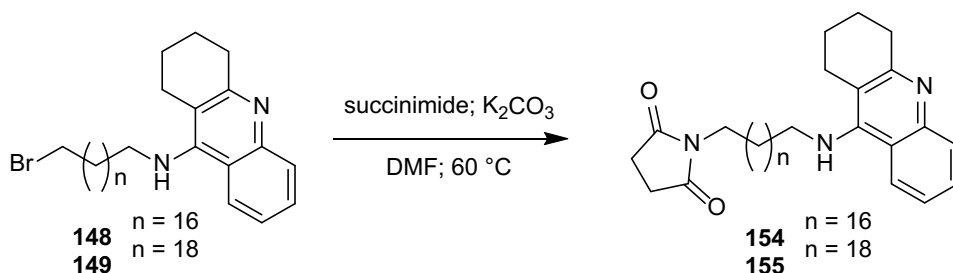
Compound **142** or **143** (0.830 mmol) was dissolved in anhydrous dichloromethane (DCM; 10 mL) under Ar atmosphere. CBr₄ (1.25 mmol; 1.5 eq) was added and the mixture was stirred at RT. In another oven-dried round-bottom flask PPh₃ (1.33 mmol; 1.6 eq) was dissolved in anhydrous DCM (5 mL) under Ar atmosphere. The solution of PPh₃ was slowly drop wise added into the mixture of CBr₄ and **142** or **143** and the reaction mixture was stirred at RT for one hour. The resulting residue was concentrated and directly purified by column chromatography to afford title products **148** or **149**.

N-(18-bromooctadecyl)-1,2,3,4-tetrahydroacridin-9-amine (148): The resulting residue was purified by column chromatography (DCM/MeOH = 9:1) affording **148** with quantitative yield as orange solid.

¹H NMR (500 MHz, Methanol-*d*₄) δ 8.41 – 8.37 (m, 1H), 7.88 – 7.82 (m, 1H), 7.80 – 7.75 (m, 1H), 7.60 – 7.58 (m, 1H), 3.99 – 3.91 (m, 2H), 3.43 (t, *J* = 6.8 Hz, 2H), 3.02 (t, *J* = 5.9 Hz, 2H), 2.71 (t, *J* = 5.8 Hz, 2H), 2.04 – 1.91 (m, 4H), 1.88 – 1.78 (m, 4H), 1.44 (p, *J* = 7.2 Hz, 4H), 1.39 – 1.23 (m, 24H). ¹³C NMR (126 MHz, cd₃od) δ 157.90, 140.00, 133.98, 132.24, 126.46, 126.25, 120.27, 117.16, 112.93, 34.44, 33.99, 31.52, 30.71, 30.68, 30.61, 30.59, 30.54, 30.24, 29.82, 29.43, 29.15, 27.68, 24.90, 23.01, 21.90.

N-(20-bromoicosyl)-1,2,3,4-tetrahydroacridin-9-amine (149): The resulting residue was purified by column chromatography (DCM/MeOH/NH₃ = 20:1:0.1) affording **149** with quantitative yield as brown solid.

¹H NMR (500 MHz, Chloroform-*d*) δ 8.00 – 7.95 (m, 1H), 7.94 – 7.89 (m, 1H), 7.68 – 7.68 (m, 1H), 7.37 – 7.31 (m, 1H), 3.53 – 3.46 (m, 2H), 3.41 (t, *J* = 6.9 Hz, 2H), 3.11 – 3.04 (m, 2H), 2.75 – 2.68 (m, 2H), 1.96 – 1.90 (m, 4H), 1.85 (p, *J* = 7.0 Hz, 2H), 1.70 – 1.62 (m, 2H), 1.46 – 1.35 (m, 4H), 1.35 – 1.22 (m, 28H).



Compound **148** or **149** (0.2719 mmol), succinimide (0.408 mmol; 1.5 eq) and K_2CO_3 (0.408 mmol; 1.5 eq) were dissolved in anhydrous DMF (3 mL) under Ar atmosphere. The mixture was heated to 60 °C and stirred for 15 hours. The resulting mixture was concentrated and directly purified to afford title products **154** or **155**.

1-{18-[(1,2,3,4-tetrahydroacridin-9-yl)amino]octadecyl}pyrrolidine-2,5-dione

(154): The resulting residue was purified by column chromatography (DCM/MeOH/ NH_3 = 20:1:0.1) affording **154** with 84 % yield as yellow sticky foam.

^1H NMR (500 MHz, Methanol- d_4) δ 8.38 – 8.33 (m, 1H), 7.84 – 7.79 (m, 1H), 7.79 – 7.75 (m, 1H), 7.58 – 7.53 (m, 1H), 3.90 (t, J = 7.3 Hz, 2H), 3.48 – 3.43 (m, 2H), 3.05 – 3.01 (m, 2H), 2.72 (t, J = 5.7 Hz, 2H), 2.68 (s, 4H), 2.02 – 1.91 (m, 4H), 1.81 (p, J = 7.4 Hz, 2H), 1.58 – 1.49 (m, 2H), 1.47 – 1.39 (m, 2H), 1.38 – 1.23 (m, 26H). ^{13}C NMR (126 MHz, cd_3od) δ 179.97, 157.34, 152.67, 140.93, 133.47, 126.21, 126.06, 121.20, 117.65, 113.38, 39.56, 31.61, 30.72, 30.67, 30.65, 30.57, 30.54, 30.25, 30.23, 30.00, 29.05, 28.62, 27.87, 27.70, 25.05, 23.15, 22.12. HRMS (ESI $^+$): $[\text{M}]^+$: calculated for $\text{C}_{35}\text{H}_{54}\text{N}_3\text{O}_2^+$ (m/z): 548.4211; found: 548.42102. LC-MS > 95 %.

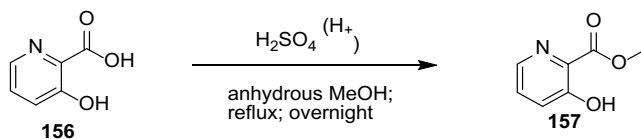
1-{20-[(1,2,3,4-tetrahydroacridin-9-yl)amino]icosyl}pyrrolidine-2,5-dione (**155**):

The resulting residue was purified by column chromatography (DCM/MeOH/ NH_3 = 20:1:0.1) affording **155** with 61 % yield as yellow sticky foam.

^1H NMR (500 MHz, Chloroform- d) δ 8.00 – 7.95 (m, 1H), 7.95 – 7.90 (m, 1H), 7.59 – 7.52 (m, 1H), 7.39 – 7.31 (m, 1H), 3.53 – 3.45 (m, 4H), 3.11 – 3.03 (m, 2H), 2.73 – 2.70 (m, 2H), 2.69 (s, 4H), 1.97 – 1.88 (m, 4H), 1.70 – 1.62 (m, 2H), 1.55 (p, J = 7.3 Hz, 2H), 1.44 – 1.35 (m, 2H), 1.35 – 1.19 (m, 30H). ^{13}C NMR (126 MHz, cdcl_3) δ 177.20, 158.12, 150.95, 147.12, 128.37, 128.37, 123.55, 122.88, 120.01, 115.55, 49.50, 38.87, 33.79, 31.74, 29.64, 29.62, 29.59, 29.52, 29.49, 29.43, 29.34, 29.12, 28.11, 27.68, 26.90, 26.83, 24.70, 23.00, 22.70. HRMS (ESI $^+$): $[\text{M}]^+$: calculated for $\text{C}_{37}\text{H}_{58}\text{N}_3\text{O}_2^+$ (m/z): 576.4524; found: 576.45166. LC-MS > 96 %.

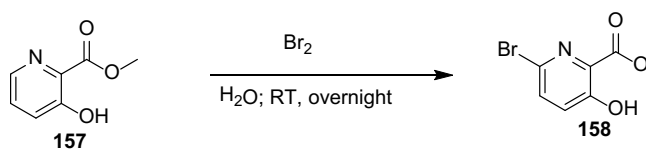
6.1.5 Mono-quaternary permanently charged AChE reactivators

Synthesis of the key intermediate 166



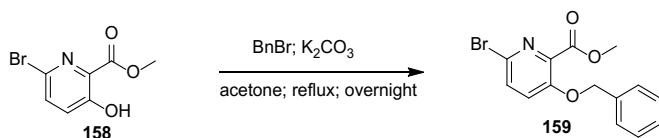
Methyl 3-hydroxypyridine-2-carboxylate (157): Into an oven-dried flask was added the starting compound **156** 3-hydroxypyridine-2-carboxylic acid (9.75 g, 70.1 mmol) and the anhydrous solvent MeOH (120 mL) under the inert atmosphere (Ar). Solution was heated to 80 °C. During the reflux and stirring, conc. H₂SO₄ (12 mL) was added drop wise within 1 hour. The reaction mixture was stirred overnight (20 hours). The solvent MeOH was evaporated and the mixture was drop wise neutralized with saturated NaCO₃ up to pH = 8. The resulting mixture was extracted with DCM 3x 200 mL and the organic layers were collected, dried with anhydrous NaSO₄ and filtered. The filtrate was concentrated under reduced pressure to afford titled product **157** (9.12 g, 85 % yield) as a white solid.

¹H NMR (500 MHz, Chloroform-*d*) δ 10.60 (s, 1H), 8.25 (dd, *J* = 4.2, 1.5 Hz, 1H), 7.40 (dd, *J* = 8.5, 4.2 Hz, 1H), 7.35 (dd, *J* = 8.5, 1.5 Hz, 1H), 4.03 (s, 3H). ¹³C NMR (126 MHz, cdCl₃) δ 169.75, 158.68, 141.37, 129.89, 129.50, 126.08, 53.04.



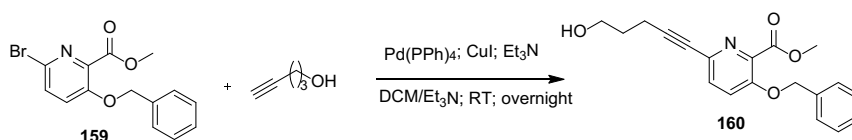
Methyl 6-bromo-3-hydroxypyridine-2-carboxylate (158): The compound **157** (9.0 g, 58.8 mmol) was dissolved in H₂O (110 mL) and cooled in ice bath at 0 °C. During the vigorous stirring, Br₂ (11.28 g, 70.56 mmol) was added drop wise within 2 hours. The mixture was stirred at room temperature overnight (20 hours). The resulting mixture was diluted with water (100 mL) and extracted with DCM 3x 200 mL. The organic layers were collected, dried with anhydrous NaSO₄ and filtered. The filtrate was concentrated under reduced pressure to afford titled product **158** (10.96 g, 81 % yield) as a yellow solid.

¹H NMR (500 MHz, Chloroform-*d*) δ 10.68 (s, 1H), 7.55 (d, *J* = 8.7 Hz, 1H), 7.27 (d, *J* = 8.7 Hz, 1H), 4.04 (s, 3H).



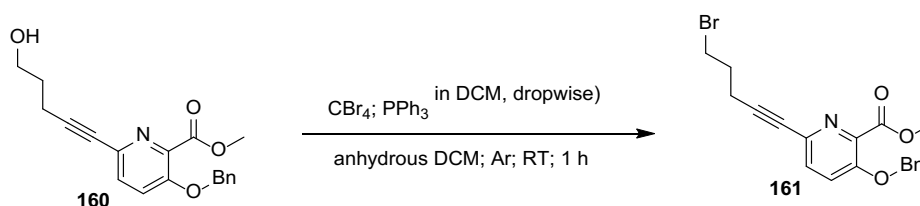
Methyl 3-(benzyloxy)-6-bromopyridine-2-carboxylate (159): The compound **158** (10.93 g, 47.32 mmol) and K_2CO_3 (29.44 g, 213.0 mmol) was dissolved in acetone (100 mL). Into the solution was added BnBr (24.3 g, 142.0 mmol) and the reaction was stirred at room temperature overnight (20 hours). The mixture was filtered and the filter cake was washed three times with 100 mL of DCM. The filtrate was concentrated under reduced pressure and purified by column chromatography (PE/EA = 9:1) to afford title product **159** (14.8 g, 97 % yield) as a yellow solid.

1H NMR (500 MHz, Chloroform-*d*) δ 7.50 (d, J = 8.8 Hz, 1H), 7.46 – 7.30 (m, 5H), 7.25 (d, J = 8.8 Hz, 1H), 5.21 (s, 2H), 3.97 (s, 3H).



Methyl 3-(benzyloxy)-6-(5-hydroxypent-1-yn-1-yl)pyridine-2-carboxylate (160): The compound **159** (10.19 g, 31.63 mmol) and 4-pentyn-1-ol (2.79 g, 33.21 mmol) was dissolved in DCM/ Et_3N (2:1 = 300:150 mL). The solution was stirred and bubbled with the Ar. After 1 hour, CuI (603 mg, 3.163 mmol) and $Pd(PPh_3)_4$ (1.826 g, 1.58 mmol) was sequentially added. The reaction was stirred and bubbled with the Ar at room temperature for 20 hours. The resulting mixture was concentrated under reduced pressure and purified by column chromatography (PE/EA = 1:1 up to PE/EA = 1:9) to afford title product **160** (10.163 g, 99 % yield) as brown viscous oil.

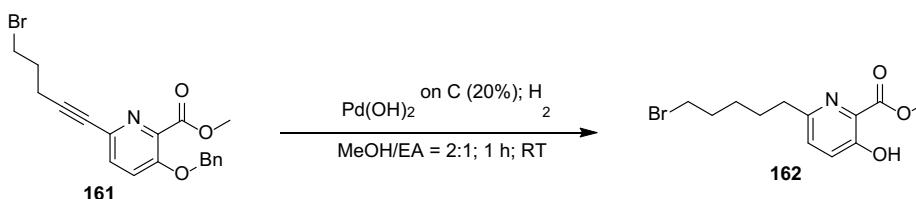
1H NMR (500 MHz, Chloroform-*d*) δ 7.44 – 7.33 (m, 5H), 7.33 – 7.28 (m, 1H), 7.28 – 7.24 (m, 1H), 5.17 (s, 2H), 3.93 (s, 3H), 3.75 (t, J = 6.2 Hz, 2H), 2.51 (t, J = 7.0 Hz, 2H), 1.87 – 1.78 (m, 2H). ^{13}C NMR (126 MHz, $cdCl_3$) δ 164.70, 152.82, 135.36, 135.20, 131.88, 129.90, 128.58, 128.09, 126.77, 121.73, 89.72, 79.44, 70.68, 61.23, 52.56, 30.82, 15.77.



Methyl 3-(benzyloxy)-6-(5-bromopent-1-yn-1-yl)pyridine-2-carboxylate (161):

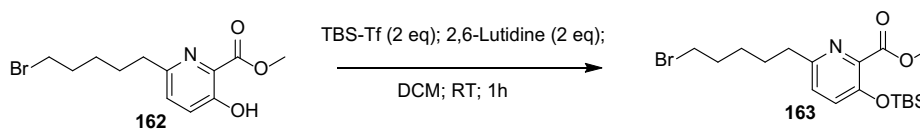
Into an oven-dried flask was added the starting compound **160** (3.67 g, 11.28 mmol), dissolved in DCM (20 mL) and the solution was cooled in ice bath to 0 °C under the inert atmosphere (Ar). Into the solution was added CBr₄ (4.86 g, 14.66 mmol). In another oven-dried flask was dissolved PPh₃ (4.14 g, 15.8 mmol) in DCM (10 mL). The solution of PPh₃ was then drop wise added into the mixture of CBr₄ and the compound **160**. The mixture was stirred at room temperature for 1 hour. The residue was concentrated under reduced pressure and purified by column chromatography (PE/EA = 3:1) to afford title product **161** (3.68 g, 84 % yield) as yellow viscous oil.

¹H NMR (500 MHz, DMSO-*d*₆) δ 7.68 (d, *J* = 8.8 Hz, 1H), 7.61 (d, *J* = 8.8 Hz, 1H), 7.46 – 7.30 (m, 5H), 5.27 (s, 2H), 3.84 (s, 3H), 3.64 (t, *J* = 6.5 Hz, 2H), 2.59 (t, *J* = 6.9 Hz, 2H), 2.07 (p, *J* = 6.7 Hz, 2H). ¹³C NMR (126 MHz, dmso) δ 165.22, 152.39, 140.65, 136.43, 134.30, 130.44, 128.97, 128.46, 127.70, 122.94, 88.36, 80.52, 70.41, 52.78, 34.13, 31.38, 17.73.



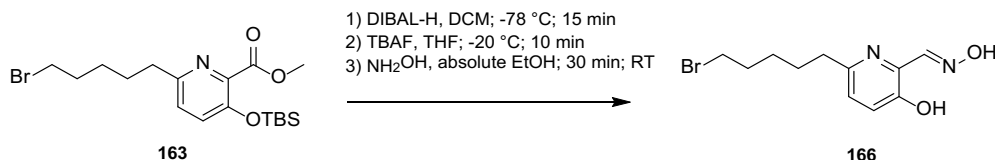
Methyl 6-(5-bromopentyl)-3-hydroxypyridine-2-carboxylate (162): The compound **161** (3.27 g, 8.42 mmol) and Pd(OH)₂ on C (20 %) (473 mg, 3.37 mmol) was dried and dissolved in EA/MeOH (1:2 = 100:200 mL) in the round flask filled with Ar. The atmosphere in the flask was multiple times removed and replaced with Ar. Same procedure were also accomplished with H₂ atmosphere. The mixture was stirred for 1 hour under H₂ atmosphere. The mixture was filtered through a celite pad and the filter cake was washed three times with 60 mL of EA. The filtrate was concentrated under reduced pressure to afford title product **162** (2.47 g, 97 % yield) as a yellow oil.

¹H NMR (500 MHz, DMSO-*d*₆) δ 7.40 (d, *J* = 8.6 Hz, 1H), 7.36 (d, *J* = 8.6 Hz, 1H), 3.88 (s, 3H), 3.51 (t, *J* = 6.7 Hz, 2H), 2.67 (t, *J* = 6.7 Hz, 2H), 1.81 (p, 2H), 1.62 (p, 2H), 1.40 (p, 2H); ¹³C NMR (126 MHz, dmso) δ 168.39, 154.52, 152.98, 131.77, 128.64, 126.72, 52.83, 36.59, 35.54, 32.51, 28.86, 27.65;



Methyl 6-(5-bromopentyl)-3-((*tert*-butyldimethylsilyloxy)pyridine-2-carboxylate (163): Into an oven-dried flask was added the starting compound **162** (2.255 g, 7.46 mmol), dissolved in DCM (20 mL) and the solution was cooled in ice bath to 0 °C under the inert atmosphere (Ar). 2,6-Lutidine (1.6 g, 14.92 mmol) and TBDMSOTf (3.94 g, 14.92 mmol) was sequentially added and the mixture was stirred up to RT for 30 min. The resulting mixture was diluted with water (100 mL) and extracted with DCM 3x 60 mL. The organic layers were collected, dried with anhydrous NaSO₄ and filtered. The filtrate was concentrated under reduced pressure and purified by column chromatography (PE/EA = 7:1) to afford title product **163** (2.812 g, 91 % yield) as a yellow oil.

¹H NMR (500 MHz, Chloroform-*d*) δ 7.18 – 7.10 (m, 2H), 3.93 (s, 3H), 3.40 (m, 2H), 2.83 – 2.72 (m, 2H), 1.94 – 1.84 (m, 2H), 1.77 – 1.68 (m, 2H), 1.56 – 1.45 (m, 2H), 1.00 (s, 9H), 0.92 (s, 6H); ¹³C NMR (126 MHz, cdcl₃) δ 166.12, 154.33, 149.18, 141.14, 128.81, 125.53, 52.40, 37.18, 33.72, 32.59, 29.07, 27.83, 25.63, 25.51, 18.14;



6-(5-bromopentyl)-2-((1*E*)-(hydroxyimino)methyl)pyridin-3-ol (166):

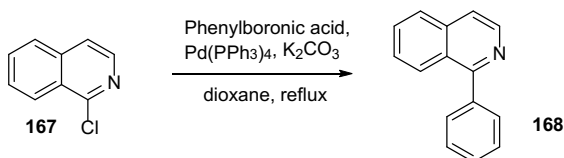
A: Into an oven-dried flask was added the starting compound **163** (2.655 g, 6.376 mmol), dissolved in DCM (20 mL) and the solution was cooled in MeOH bath to -78 °C under the inert atmosphere (Ar). The 1M solution of DIBAL-H in DCM (1.9 g, 13.39 mmol) was drop wise added and the mixture was stirred for 15 min at -78 °C. Then, MeOH 9 mL was immediately poured into the mixture and the flask was taken out of the bath, when it was out addition 30 % solution of Potassium sodium tartrate (90 mL) was added. The mixture was vigorously stirred for 1 hour. Then, the mixture was extracted with DCM 3x 100 mL. The organic layers were collected, dried with anhydrous NaSO₄, filtered and concentrated under reduced pressure. The unpurified product **164** was directly putted into the next reaction.

B: The final mixture from previous reaction was dissolved in dried THF (20 mL) and the solution was cooled in MeOH bath to -20 °C under the inert atmosphere (Ar). The 1M solution of TBAF in THF (1.834 g, 7.014 mmol) was drop wise added and the mixture was stirred for 10 min at -20 °C. The residue was diluted with water (100 mL) and extracted with DCM 3x 60 mL. The organic layers were collected, dried with anhydrous NaSO₄, filtered and concentrated under reduced pressure. The unpurified product **165** was directly putted into the next reaction.

C: The final mixture from previous reaction was dissolved in absolute EtOH (20 mL) and 50 % aqueous solution of NH₂OH (421 mg, 12.752 mmol) was drop wise added. The mixture was stirred at RT for 30 min. The resulting mixture was concentrated under reduced pressure and purified by column chromatography (PE/EA = 5:1) to afford title product **166** (944 mg, 52 % yield) as a white solid.

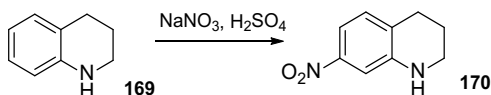
¹H NMR (500 MHz, DMSO-*d*₆) δ 11.81 (s, 1H), 10.08 (s, 1H), 8.26 (s, 1H), 7.25 (d, J = 8.4 Hz, 1H), 7.14 (d, J = 8.4 Hz, 1H), 3.51 (t, J = 6.7 Hz, 2H), 2.72 – 2.59 (m, 2H), 1.87 – 1.76 (m, 2H), 1.68 – 1.56 (m, 2H), 1.44 – 1.33 (m, 2H).; ¹³C NMR (126 MHz, dms) δ 152.82, 151.58, 151.22, 135.52, 124.21, 123.96, 36.42, 35.26, 32.25, 28.60, 27.36;

Synthesis of quinoline and isoquinoline PAS ligands



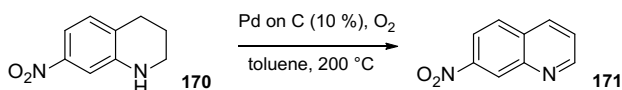
1-phenylisoquinoline (168): 1-chloroisoquinoline (285 mg, 1.742 mmol), K₂CO₃ (722 mg, 5.226 mmol) and Pd(PPh₃)₄ (61 mg, 0.052 mmol) was added into an oven-dried flask and dissolved in dried dioxane (10 mL) under the inert atmosphere (Ar). Into another oven-dried flask was phenylboronic acid (319 mg, 2.613 mmol) added and dissolved in the dried dioxane (10 mL). Such solution was drop wise added into mixture and the reaction was stirred and refluxed for 48 hours. The residue was diluted with water (30 mL) and extracted with DCM 3x 20 mL. The organic layers were collected, dried with anhydrous NaSO₄ and filtered. The filtrate was concentrated under reduced pressure and purified by column chromatography (PE/EA = 8:1) to afford title product **168** (268 mg, 75 % yield) as a yellowish solid.

^1H NMR (500 MHz, Chloroform-*d*) δ 8.65 – 8.60 (m, 1H), 8.16 – 8.09 (m, 1H), 7.93 – 7.86 (m, 1H), 7.75 – 7.64 (m, 4H), 7.58 – 7.48 (m, 4H); ^{13}C NMR (126 MHz, cdCl_3) δ 160.75, 142.09, 139.45, 136.88, 130.06, 129.91, 129.37, 128.61, 128.35, 127.62, 127.20, 126.98, 126.74, 119.99, 115.53;



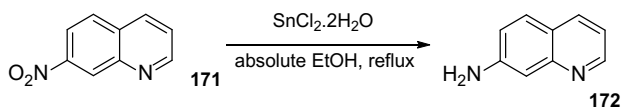
7-nitro-1,2,3,4-tetrahydroquinoline (170): H_2SO_4 (10 mL) was added into the round flask and cooled in ice bath to $0\text{ }^\circ\text{C}$. 1,2,3,4-tetrahydroquinoline (1.06 g, 7.8 mmol) was drop wise added into the acid. After 1 hour, NaNO_3 (747 mg, 8.787 mmol) was added and the reaction was stirred at RT for 20 hours. The mixture was slowly poured into the 20 % solution of NaOH (100 mL) cooled at $0\text{ }^\circ\text{C}$ and neutralized up to $\text{pH} = 10$. Then, extracted with DCM 3x 100 mL and the organic layers were collected, dried with anhydrous NaSO_4 , filtered and concentrated under reduced pressure to afford title product **170** (1.36 g, 98 %) as a brown solid.

^1H NMR (500 MHz, Chloroform-*d*) δ 7.42 – 7.37 (m, 1H), 7.30 – 7.25 (m, 1H), 7.03 – 7.00 (m, 1H), 4.20 (bs, 1H), 3.38 – 3.33 (m, 2H), 2.81 (t, $J = 6.4$ Hz, 2H), 2.00 – 1.91 (m, 2H).;



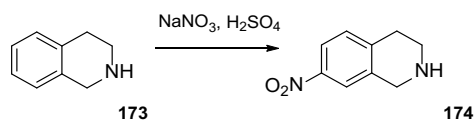
7-nitroquinoline (171): The compound **170** (1.39 g, 7.8 mmol) and Pd on C (10\%) (166 mg, 1.56 mmol) was dried and dissolved in toluene (50 mL) in the round flask filled with Ar. The atmosphere in the flask was multiple times removed and replaced with Ar. Same procedure were also accomplished with O_2 atmosphere. The mixture was stirred for 1 hour under O_2 atmosphere. The mixture was filtered through a celite pad and the filter cake was washed three times with 30 mL of EA. The filtrate was concentrated under reduced pressure to afford title product **171** (801 mg, 59 % yield) as an orange solid.

^1H NMR (500 MHz, Chloroform-*d*) δ 9.15 – 9.08 (m, 1H), 9.05 – 9.00 (m, 1H), 8.37 – 8.32 (m, 1H), 8.32 – 8.24 (m, 1H), 8.03 – 7.96 (m, 1H), 7.64 – 7.56 (m, 1H);



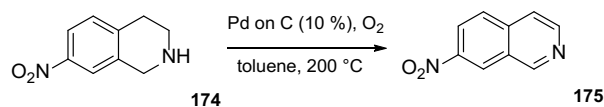
Quinolin-7-amine (172): The compound **171** (196 mg, 1.1254 mmol) was dissolved in absolute EtOH (20 mL). SnCl₂·2H₂O (1.016 g, 4.5 mmol) was added and the reaction was stirred and refluxed for 15 hours. The absolute EtOH was evaporated under the reduced pressure and the residue was diluted with 2M solution of NaOH (40 mL). The mixture was extracted with DCM 3x 30 mL. The organic layers were collected, dried with anhydrous NaSO₄ and filtered. The filtrate was concentrated under reduced pressure and purified by column chromatography (PE/EA = 1:1) to afford title product **172** (62 mg, 38 % yield) as a red solid.

¹H NMR (500 MHz, Chloroform-*d*) δ 8.92 – 8.81 (m, 1H), 8.20 – 8.11 (m, 1H), 7.62 – 7.45 (m, 2H), 7.37 – 7.22 (m, 1H), 6.88 – 6.72 (m, 1H), 4.24 (bs, 2H); ¹³C NMR (126 MHz, cdcl₃) δ 150.06, 148.95, 142.29, 129.96, 129.54, 119.86, 119.45, 118.61, 109.88;



7-nitro-1,2,3,4-tetrahydroisoquinoline (174): H₂SO₄ (10 mL) was added into the round flask and cooled in ice bath to 0 °C. 1,2,3,4-tetrahydroisoquinoline (1.06 g, 7.8 mmol) was drop wise added into the acid. After 1 hour, NaNO₃ (747 mg, 8.787 mmol) was added and the reaction was stirred at RT for 20 hours. The mixture was slowly poured into the 20 % solution of NaOH (100 mL) cooled at 0 °C and neutralized up to pH = 10. Then, extracted with DCM 3x 100 mL and the organic layers were collected, dried with anhydrous NaSO₄, filtered and concentrated under reduced pressure to afford title product **174** (1.28 g, 95 %) as a brown solid.

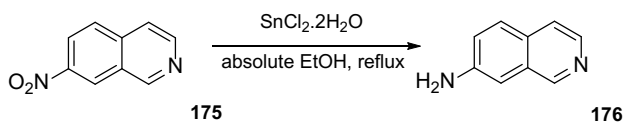
¹H NMR (500 MHz, Chloroform-*d*) δ 7.99 – 7.94 (m, 1H), 7.91 – 7.87 (m, 1H), 7.25 – 7.21 (m, 1H), 4.10 – 4.07 (m, 2H), 3.19 – 3.12 (m, 2H), 2.92 – 2.86 (m, 2H);



7-nitroquinoline (175): The compound **174** (1.26 g, 7.07 mmol) and Pd on C (10 %) (150 mg, 1.40 mmol) was dried and dissolved in toluene (50 mL) in the round flask filled with Ar. The atmosphere in the flask was multiple times removed and replaced with Ar. Same procedure were also accomplished with O₂ atmosphere. The mixture was stirred for 1 hour under O₂ atmosphere. The mixture was filtered through a

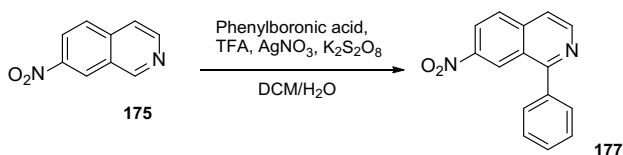
celite pad and the filter cake was washed three times with 30 mL of EA. The filtrate was concentrated under reduced pressure to afford title product **175** (326 mg, 26 % yield) as an orange solid.

^1H NMR (500 MHz, Chloroform-*d*) δ 9.48 (s, 1H), 9.00 – 8.92 (m, 1H), 8.83 – 8.71 (m, 1H), 8.53 – 8.43 (m, 1H), 8.01 (d, $J = 9.0$ Hz, 1H), 7.83 – 7.74 (m, 1H); ^{13}C NMR (126 MHz, cdCl_3) δ 154.25, 146.48, 138.17, 128.54, 127.19, 124.42, 123.74, 120.29;



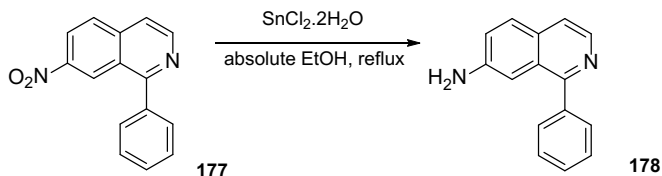
Isoquinolin-7-amine (176): The compound **175** (169 mg, 0.97 mmol) was dissolved in absolute EtOH (20 mL). $\text{SnCl}_2 \cdot 2\text{H}_2\text{O}$ (876 mg, 3.88 mmol) was added and the reaction was stirred and refluxed for 15 hours. The absolute EtOH was evaporated under the reduced pressure and the residue was diluted with 2M solution of NaOH (40 mL). The mixture was extracted with DCM 3x 30 mL. The organic layers were collected, dried with anhydrous NaSO_4 and filtered. The filtrate was concentrated under reduced pressure and purified by column chromatography (PE/EA = 1:1) to afford title product **176** (70 mg, 50 % yield) as a red solid.

^1H NMR (500 MHz, Methanol-*d*₄) δ 8.85 (s, 1H), 8.14 – 8.04 (m, 1H), 7.71 – 7.62 (m, 1H), 7.61 – 7.53 (m, 1H), 7.30 – 7.22 (m, 1H), 7.13 – 7.02 (m, 1H); ^{13}C NMR (126 MHz, cd_3od) δ 150.48, 149.20, 138.66, 132.18, 131.10, 128.51, 124.68, 122.14, 107.08;



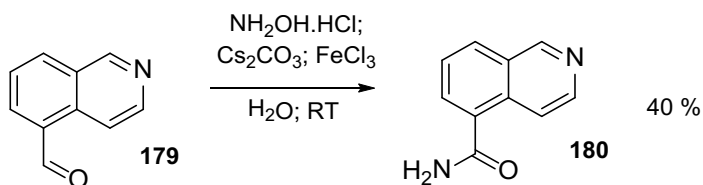
7-nitro-1-phenylisoquinoline (177): The compound **175** (420 mg, 2.4 mmol), phenylboronic acid (439 mg, 3.6 mmol), TFA (301 mg, 2.64 mmol), AgNO_3 (82 mg, 0.48 mmol) and $\text{K}_2\text{S}_2\text{O}_8$ (1.95 g, 7.2 mmol) was dissolved in DCM/ H_2O (2:1 = 20:10 mL) and the mixture was vigorously stirred for 48 hours at RT. The resulting mixture was diluted with small portion of saturated Na_2CO_3 (5 mL) and water (40 mL) and extracted with DCM 3x 30 mL. The organic layers were collected, dried with anhydrous NaSO_4 and filtered. The filtrate was concentrated under reduced pressure and purified by column chromatography (PE/EA = 5:1) to afford title product **177** (235 mg, 39 % yield) as an orange solid.

^1H NMR (500 MHz, Chloroform-*d*) δ 9.10 – 9.05 (m, 1H), 8.84 – 8.79 (m, 1H), 8.52 – 8.44 (m, 1H), 8.08 – 8.03 (m, 1H), 7.80 – 7.75 (m, 1H), 7.75 – 7.70 (m, 2H), 7.65 – 7.54 (m, 3H); ^{13}C NMR (126 MHz, cdCl_3) δ 162.99, 145.55, 139.42, 138.07, 129.96, 129.58, 128.93, 128.85, 125.41, 124.70, 123.48, 119.48;



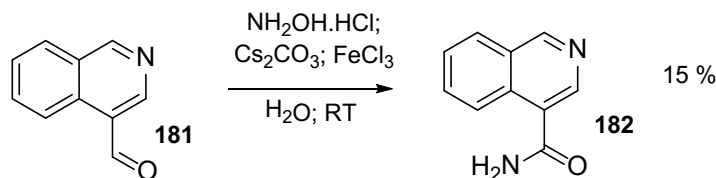
1-phenylisoquinolin-7-amine (178): The compound **177** (175 mg, 0.699 mmol) was dissolved in absolute EtOH (20 mL). $\text{SnCl}_2 \cdot 2\text{H}_2\text{O}$ (631 mg, 2.8 mmol) was added and the reaction was stirred and refluxed for 15 hours. The absolute EtOH was evaporated under the reduced pressure and the residue was diluted with 2M solution of NaOH (40 mL). The mixture was extracted with DCM 3x 30 mL. The organic layers were collected, dried with anhydrous NaSO_4 and filtered. The filtrate was concentrated under reduced pressure and purified by column chromatography (PE/EA = 3:1) to afford title product **178** (143 mg, 93 % yield) as a red solid.

^1H NMR (500 MHz, Chloroform-*d*) δ 8.41 – 8.35 (m, 1H), 7.73 – 7.64 (m, 3H), 7.57 – 7.43 (m, 4H), 7.18 – 7.15 (m, 1H), 7.14 – 7.10 (m, 1H); ^{13}C NMR (126 MHz, cdCl_3) δ 158.29, 145.39, 139.95, 139.06, 131.05, 130.73, 129.69, 128.33, 128.27, 128.25, 122.08, 119.88, 107.27;



Isoquinoline-5-carboxamide (180): Isoquinoline-5-carbaldehyde (184 mg; 1.17 mmol); FeCl_3 (10 mg; 0.06 mmol); $\text{NH}_2\text{OH} \cdot \text{HCl}$ (81 mg; 1.17 mmol) and Cs_2CO_3 (381 mg; 1.17 mmol) were dissolved in H_2O (5 mL) and heated to 110 °C for 2 days. The resulting residue was diluted with H_2O (15 mL) and three times extracted with EA (3x 15 mL). The organic layers were collected, dried with anhydrous NaSO_4 and filtered. The filtrate was concentrated under reduced pressure and purified by column chromatography using mobile phase DCM/MeOH (15:1) to afford title product **180** (81 mg, 40 % yield) as a red solid.

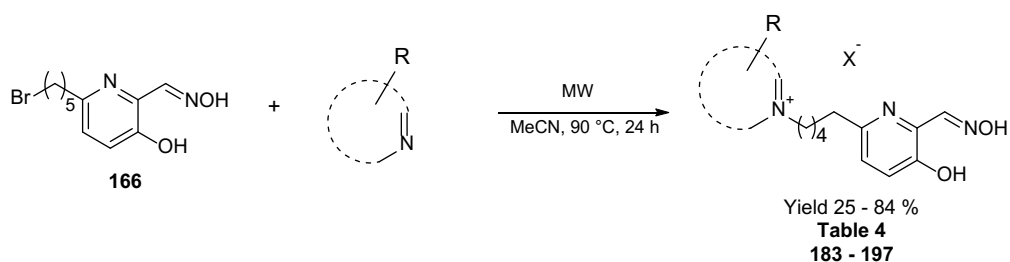
^1H NMR (500 MHz, Methanol- d_4) δ 9.32 – 9.25 (m, 1H), 8.53 – 8.46 (m, 1H), 8.32 – 8.25 (m, 1H), 8.26 – 8.18 (m, 1H), 8.06 – 8.00 (m, 1H), 7.77 – 7.66 (m, 1H). ^{13}C NMR (126 MHz, cd_3od) δ 172.98, 153.67, 143.80, 134.45, 133.85, 131.77, 131.61, 130.22, 128.01, 120.05.



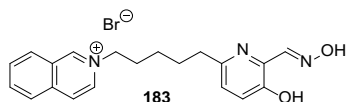
Isoquinoline-4-carboxamide (182): Isoquinoline-4-carbaldehyde (220 mg; 1.4 mmol); FeCl_3 (23 mg; 0.14 mmol); $\text{NH}_2\text{OH}\cdot\text{HCl}$ (146 mg; 2.1 mmol) and Cs_2CO_3 (684 mg; 2.1 mmol) were dissolved in H_2O (8 mL) and heated to 110 °C for 2 days. The resulting residue was diluted with H_2O (15 mL) and three times extracted with DCM (3x 15 mL). The organic layers were collected, dried with anhydrous NaSO_4 and filtered. The filtrate was concentrated under reduced pressure and purified by column chromatography using mobile phase DCM/MeOH (9:1) to afford title product **182** (36 mg, 15 % yield) as a red solid.

^1H NMR (500 MHz, Methanol- d_4) δ 9.31 (s, 1H), 8.64 (s, 1H), 8.42 – 8.33 (m, 1H), 8.20 – 8.12 (m, 1H), 7.92 – 7.83 (m, 1H), 7.78 – 7.70 (m, 1H). ^{13}C NMR (126 MHz, cd_3od) δ 162.68, 146.28, 132.51, 124.91, 123.87, 120.62, 120.13, 120.04, 119.74, 116.32.

The *N*-alkylation coupling of intermediate 166 and PAS ligands

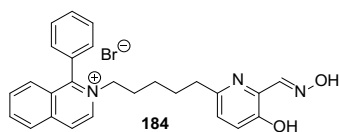


The compound **166** (1.0 eq) and the PAS ligand (2.0 eq) was dissolved in dried MeCN (2 mL) and challenged by microwave irradiation with settings: dynamic curve, power max cap 100 W, pressure max cap 300 PSI, at 90 °C for 24 hours. The solvent was evaporated under reduced pressure and the mixture was purified with column chromatography up to 3 times to afford title products.



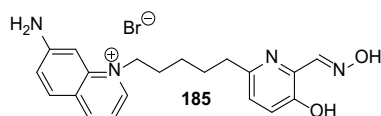
2-(5-(5-hydroxy-6-((1E)-(hydroxyimino)methyl)pyridine-2-yl)pentyl)isoquinolin-2-ium bromide (183): The resulting residue was purified by column chromatography using mobile phase DCM/MeOH (9:1) to afford title product **183** as yellowish oil. Yield 35 %.

^1H NMR (500 MHz, Methanol- d_4) δ 9.99 (s, 1H), 8.72 – 8.68 (m, 1H), 8.51 – 8.44 (m, 2H), 8.33 – 8.28 (m, 1H), 8.26 – 8.21 (m, 1H), 8.19 (s, 1H), 8.09 – 8.03 (m, 1H), 7.20 (d, $J = 8.5$ Hz, 1H), 7.14 (d, $J = 8.5$ Hz, 1H), 4.80 (t, $J = 7.5$ Hz, 2H), 2.73 (t, $J = 7.5$ Hz, 2H), 2.21 – 2.12 (m, 2H), 1.82 – 1.74 (m, 2H), 1.49 – 1.41 (m, 2H).; ^{13}C NMR (126 MHz, cd_3od) δ 152.79, 152.30, 151.31, 149.52, 137.55, 136.96, 134.79, 134.37, 131.23, 130.15, 127.78, 127.15, 126.18, 124.61, 124.06, 61.31, 35.89, 30.59, 28.92, 25.10.; HRMS (ESI $^+$): $[\text{M}+2\text{H}]^{2+}$: calculated for $\text{C}_{20}\text{H}_{23}\text{N}_3\text{O}_2^{2+}$ (m/z): 168.5890; detected: 168.58893. LC-MS > 95 %



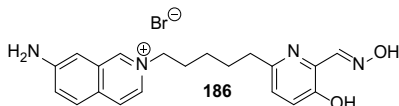
2-(5-(5-hydroxy-6-((1E)-(hydroxyimino)methyl)pyridine-2-yl)pentyl)-1-phenylisoquinolin-2-ium bromide (184): The resulting residue was purified by column chromatography using mobile phase DCM/MeOH (9:1) to afford title product **184** as yellowish oil. Yield 38 %.

^1H NMR (500 MHz, Methanol- d_4) δ 8.99 – 8.80 (m, 1H), 8.67 – 8.52 (m, 1H), 8.42 – 8.32 (m, 1H), 8.26 – 8.17 (m, 2H), 7.96 – 7.85 (m, 1H), 7.84 – 7.72 (m, 3H), 7.72 – 7.64 (m, 3H), 7.24 (d, $J = 8.5$ Hz, 1H), 7.09 (d, $J = 8.5$ Hz, 1H), 4.60 – 4.41 (m, 2H), 2.63 (t, $J = 7.5$ Hz, 2H), 2.05 – 1.85 (m, 2H), 1.68 – 1.49 (m, 2H), 1.45 – 1.18 (m, 5H); ^{13}C NMR (126 MHz, cd_3od) δ 160.72, 154.05, 153.66, 152.73, 139.34, 137.65, 136.36, 136.16, 132.78, 132.50, 131.30, 130.65, 130.59, 130.40, 129.94, 128.83, 127.29, 125.93, 125.36, 60.17, 37.12, 31.75, 30.03, 26.62; HRMS (ESI $^+$): $[\text{M}+2\text{H}]^{2+}$: calculated $\text{C}_{26}\text{H}_{27}\text{N}_3\text{O}_2^{2+}$ (m/z): 206.6046; detected: 206.60463. LC-MS > 96 %



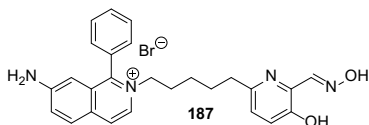
7-amino-1-(5-(5-hydroxy-6-((1E)-(hydroxyimino)methyl)pyridin-2-yl)pentyl)quinolin-1-ium bromide (185): The resulting residue was purified by column chromatography using mobile phase DCM/MeOH (9:1) to afford title product **185** as yellowish oil. Yield 32 %.

¹H NMR (500 MHz, Methanol-*d*₄) δ 8.79 – 8.72 (m, 1H), 8.63 – 8.57 (m, 1H), 8.23 (s, 1H), 7.98 – 7.93 (m, 1H), 7.41 – 7.37 (m, 1H), 7.33 – 7.29 (m, 1H), 7.24 (d, J = 8.5 Hz, 1H), 7.14 (d, J = 8.5 Hz, 1H), 7.12 – 7.09 (m, 1H), 4.67 (t, J = 7.5 Hz, 3H), 2.74 (t, J = 7.6 Hz, 2H), 2.09 – 1.96 (m, 3H), 1.86 – 1.72 (m, 3H), 1.56 – 1.42 (m, 3H); ¹³C NMR (126 MHz, cd₃od) δ 158.01, 154.18, 153.74, 152.73, 146.76, 145.58, 142.99, 136.20, 133.61, 128.77, 126.01, 125.41, 125.35, 122.61, 115.95, 115.02, 57.59, 37.35, 30.39, 29.37, 26.79; HRMS (ESI⁺): [M+2H]²⁺: calculated for C₂₀H₂₄N₄O₂²⁺ (m/z): 176.0944; detected: 176.09436. LC-MS > 95 %



7-amino-1-(5-(5-hydroxy-6-((1E)-(hydroxyimino)methyl)pyridin-2-yl)pentyl)isoquinolin-2-ium bromide (186): The resulting residue was purified by column chromatography using mobile phase DCM/MeOH (9:1) to afford title product **186** as yellowish oil. Yield 84 %.

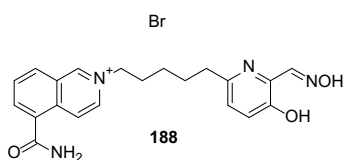
¹H NMR (500 MHz, Methanol-*d*₄) δ 9.41 – 9.34 (m, 1H), 8.22 – 8.19 (m, 1H), 8.19 – 8.18 (m, 1H), 8.09 – 8.05 (m, 1H), 7.89 – 7.84 (m, 1H), 7.61 – 7.53 (m, 1H), 7.21 – 7.19 (m, 1H), 7.18 (d, J = 8.5 Hz, 1H), 7.11 (d, J = 8.5 Hz, 1H), 4.64 (t, J = 7.5 Hz, 3H), 2.68 (t, J = 7.6 Hz, 3H), 2.16 – 2.02 (m, 2H), 1.78 – 1.66 (m, 3H), 1.44 – 1.36 (m, 1H); ¹³C NMR (126 MHz, cd₃od) δ 152.80, 152.27, 151.35, 151.32, 144.86, 134.72, 130.42, 130.14, 129.39, 128.27, 127.90, 125.45, 124.64, 124.09, 105.06, 60.91, 35.96, 30.70, 28.96, 25.18; HRMS (ESI⁺): [M+2H]²⁺: calculated for C₂₀H₂₄N₄O₂²⁺ (m/z): 176.0944; detected: 176.0943. LC-MS > 95 %



7-amino-1-(5-(5-hydroxy-6-((1E)-(hydroxyimino)methyl)pyridin-2-yl)pentyl)-1-phenylisoquinolin-2-ium bromide (187): The resulting residue was purified by

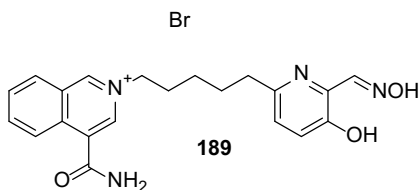
column chromatography using mobile phase DCM/MeOH (9:1) to afford title product **187** as yellowish oil. Yield 25 %.

^1H NMR (500 MHz, Methanol- d_4) δ 8.39 – 8.35 (m, 1H), 8.23 (s, 1H), 8.21 – 8.18 (m, 1H), 8.03 – 7.97 (m, 1H), 7.75 – 7.70 (m, 3H), 7.60 – 7.53 (m, 3H), 7.24 (d, J = 8.5 Hz, 1H), 7.08 (d, J = 8.5 Hz, 1H), 6.53 – 6.50 (m, 1H), 4.38 – 4.31 (m, 2H), 2.61 (t, J = 7.6 Hz, 2H), 1.95 – 1.85 (m, 1H), 1.60 – 1.48 (m, 2H), 1.27 – 1.18 (m, 1H); ^{13}C NMR (126 MHz, cd_3od) δ 154.56, 152.71, 152.35, 151.51, 151.39, 134.84, 131.30, 130.90, 130.79, 130.21, 130.00, 129.32, 128.98, 128.34, 127.61, 125.15, 124.58, 123.98, 105.56, 58.38, 35.77, 30.41, 28.69, 25.26; HRMS (ESI $^+$): $[\text{M}+2\text{H}]^{2+}$: calculated for $\text{C}_{26}\text{H}_{28}\text{N}_4\text{O}_2^{2+}$ (m/z): 214.1101; detected: 214.11003. LC-MS > 98 %.



5-carbamoyl-2-(5-{5-hydroxy-6-[(1E)-(hydroxyimino)methyl]pyridin-2-yl}pentyl)isoquinolin-2-ium bromide (188): The resulting residue was filtered through silica gel pad with acetone to get rid of starting compounds and side products and then washed by MeOH to afford title product **188** as white solid. Yield 45 %.

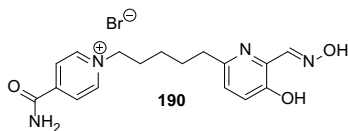
^1H NMR (500 MHz, Methanol- d_4) δ 10.00 (d, J = 1.4 Hz, 1H), 8.95 (d, J = 7.1 Hz, 1H), 8.73 (dd, J = 7.1, 1.5 Hz, 1H), 8.58 (dd, J = 8.4, 1.1 Hz, 1H), 8.47 (dd, J = 7.3, 1.1 Hz, 1H), 8.25 (s, 1H), 8.11 (dd, J = 8.3, 7.3 Hz, 1H), 7.26 (d, J = 8.5 Hz, 1H), 7.16 (d, J = 8.5 Hz, 1H), 4.78 (t, J = 7.5 Hz, 2H), 2.76 (t, J = 7.6 Hz, 2H), 2.25 – 2.13 (m, 2H), 1.81 (p, J = 7.6 Hz, 2H), 1.51 – 1.43 (m, 2H). ^{13}C NMR (126 MHz, cd_3od) δ 169.45, 152.74, 152.39, 151.21, 149.90, 135.89, 135.05, 134.86, 132.90, 132.62, 130.48, 128.36, 124.69, 124.37, 124.02, 61.36, 35.84, 30.48, 28.94, 25.14. HRMS (ESI $^+$): $[\text{M}+2\text{H}]^{2+}$: calculated for $\text{C}_{21}\text{H}_{23}\text{N}_4\text{O}_3^{2+}$ (m/z): 190.0919; detected: 190.09212. LC-MS > 98 %



4-carbamoyl-2-(5-{5-hydroxy-6-[(1E)-(hydroxyimino)methyl]pyridin-2-yl}pentyl)isoquinolin-2-ium bromide (189): The resulting residue was filtered through

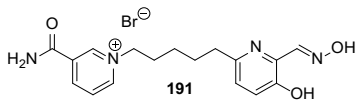
silica gel pad with acetone to get rid of starting compounds and site products and then washed by MeOH to afford title product **189** as white solid. Yield 29 %.

^1H NMR (500 MHz, Methanol- d_4) δ 10.03 (s, 1H), 8.99 (d, $J = 1.3$ Hz, 1H), 8.59 (d, $J = 8.6$ Hz, 1H), 8.57 – 8.51 (m, 1H), 8.32 – 8.24 (m, 1H), 8.23 (s, 1H), 8.12 – 8.05 (m, 1H), 7.23 (d, $J = 8.5$ Hz, 1H), 7.13 (d, $J = 8.5$ Hz, 1H), 4.82 (t, $J = 7.6$ Hz, 2H), 2.73 (t, $J = 7.6$ Hz, 2H), 2.22 – 2.13 (m, 2H), 1.83 – 1.74 (m, 2H), 1.52 – 1.43 (m, 2H). ^{13}C NMR (126 MHz, cd_3od) δ 167.58, 154.16, 153.77, 152.54, 139.02, 136.27, 135.96, 134.95, 134.21, 132.68, 132.37, 129.61, 126.59, 126.06, 125.40, 62.95, 37.34, 31.88, 30.40, 26.58. HRMS (ESI $^+$): $[\text{M}+2\text{H}]^{2+}$: calculated for $\text{C}_{21}\text{H}_{23}\text{N}_4\text{O}_3^{2+}$ (m/z): 190.0919; detected: 190.09209. LC-MS > 99 %.



4-carbamoyl-1-(5-(5-hydroxy-6-((1E)-(hydroxyimino)methyl)pyridin-2-yl)pentyl)pyridin-1-ium bromide (190): The resulting residue was purified by column chromatography using mobile phase MeOH (alone) to afford title product **190** as yellowish foam. Yield 70 %.

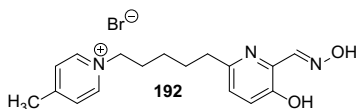
^1H NMR (500 MHz, Methanol- d_4) δ 9.21 – 9.12 (m, 2H), 8.50 – 8.40 (m, 2H), 8.28 (s, 1H), 7.28 (d, $J = 8.5$ Hz, 1H), 7.17 (d, $J = 8.5$ Hz, 1H), 4.78 – 4.63 (m, 2H), 2.85 – 2.66 (m, 2H), 2.19 – 2.05 (m, 2H), 1.84 – 1.71 (m, 2H), 1.52 – 1.39 (m, 2H).; ^{13}C NMR (126 MHz, cd_3od) δ 171.56, 164.39, 152.78, 152.40, 151.33, 148.98, 145.54, 134.91, 126.07, 124.66, 124.03, 61.67, 35.91, 28.96, 25.14, 19.47; HRMS (ESI $^+$): $[\text{M}+2\text{H}]^{2+}$: calculated for $\text{C}_{17}\text{H}_{22}\text{N}_4\text{O}_3^{2+}$ (m/z): 165.0840; detected: 164.08406. LC-MS > 96 %



3-carbamoyl-1-(5-(5-hydroxy-6-((1E)-(hydroxyimino)methyl)pyridin-2-yl)pentyl)pyridin-1-ium bromide (191): The resulting residue was precipitated from MeCN to afford title product **191** as white solid. Yield 55 %.

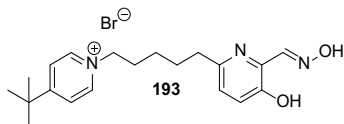
^1H NMR (500 MHz, Methanol- d_4) δ 9.51 – 9.44 (m, 1H), 9.19 – 9.12 (m, 1H), 9.00 – 8.94 (m, 1H), 8.28 (s, 1H), 8.25 – 8.18 (m, 1H), 7.35 – 7.26 (m, 1H), 7.19 (d, $J = 8.5$ Hz, 1H), 4.72 (t, $J = 7.7$ Hz, 2H), 2.76 (t, $J = 7.7$ Hz, 2H), 2.18 – 2.07 (m, 2H), 1.86 – 1.73 (m, 2H), 1.52 – 1.41 (m, 2H); ^{13}C NMR (126 MHz, cd_3od) δ 163.72, 152.72,

152.42, 151.09, 146.22, 144.59, 143.58, 134.83, 134.55, 127.95, 124.84, 124.09, 61.98, 35.81, 30.68, 28.96, 25.13; HRMS (ESI⁺): [M+2H]²⁺: calculated for C₁₇H₂₂N₄O₃²⁺ (m/z): 165.0840; detected: 164.08406. LC-MS > 96 %



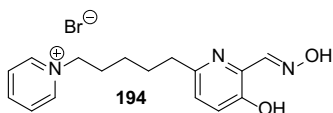
1-(5-(5-hydroxy-6-((1E)-(hydroxyimino)methyl)pyridin-2-yl)pentyl)-4-methylpyridin-1-ium bromide (192): The resulting residue was purified by column chromatography using mobile phase DCM/MeOH (9:1) to afford title product **192** as yellowish oil. Yield 40 %.

¹H NMR (500 MHz, Methanol-*d*₄) δ 8.91 – 8.77 (m, 2H), 8.25 (s, 1H), 8.00 – 7.86 (m, 2H), 7.26 (d, J = 8.5 Hz, 1H), 7.18 (d, J = 8.5 Hz, 1H), 4.61 (t, J = 7.5 Hz, 2H), 2.77 – 2.70 (m, 2H), 2.68 (s, 3H), 2.11 – 1.98 (m, 2H), 1.82 – 1.69 (m, 2H), 1.48 – 1.33 (m, 2H); ¹³C NMR (126 MHz, cd₃od) δ 159.73, 152.87, 152.33, 151.40, 143.51, 134.80, 128.51, 124.69, 124.17, 60.60, 35.91, 30.63, 28.91, 25.01, 20.74; HRMS (ESI⁺): [M+2H]²⁺: calculated for C₁₇H₂₃N₃O₂²⁺ (m/z): 150.5890; detected: 150.58897. LC-MS > 95 %



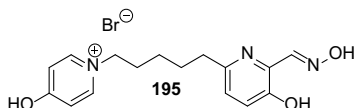
4-tert-butyl-1-(5-(5-hydroxy-6-((1E)-(hydroxyimino)methyl)pyridin-2-yl)pentyl)pyridin-1-ium bromide (193): The resulting residue was purified by column chromatography using mobile phase DCM/MeOH (9:1) to afford title product **193** as yellowish oil. Yield 46 %.

¹H NMR (500 MHz, Methanol-*d*₄) δ 8.94 – 8.86 (m, 2H), 8.27 (s, 1H), 8.15 – 8.07 (m, 2H), 7.26 (d, J = 8.5 Hz, 1H), 7.17 (d, J = 8.5 Hz, 1H), 4.62 (t, J = 7.5 Hz, 2H), 2.74 (t, J = 7.5 Hz, 2H), 2.12 – 2.01 (m, 2H), 1.82 – 1.73 (m, 2H), 1.44 (s, 9H), 1.42 – 1.34 (m, 2H); ¹³C NMR (126 MHz, cd₃od) δ 171.20, 152.84, 152.34, 151.43, 143.84, 134.84, 125.15, 124.65, 124.13, 60.49, 36.16, 35.90, 30.56, 28.88, 25.00; HRMS (ESI⁺): [M+2H]²⁺: calculated for C₂₀H₂₉N₃O₂²⁺ (m/z): 171.6124; detected: 171.6124. LC-MS > 96 %



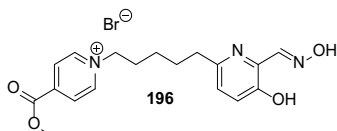
1-(5-(5-hydroxy-6-((1E)-(hydroxyimino)methyl)pyridin-2-yl)pentyl)pyridin-1-ium bromide (194): The resulting residue was purified by column chromatography using mobile phase DCM/MeOH (9:1) to afford title product **194** as yellowish oil. Yield 55 %.

^1H NMR (500 MHz, Methanol- d_4) δ 9.11 – 9.05 (m, 2H), 8.67 – 8.57 (m, 1H), 8.26 (s, 1H), 8.18 – 8.10 (m, 2H), 7.27 (d, $J = 8.5$ Hz, 1H), 7.18 (d, $J = 8.5$ Hz, 1H), 4.70 (t, $J = 7.6$ Hz, 2H), 2.74 (t, $J = 7.6$ Hz, 2H), 2.13 – 2.04 (m, 2H), 1.83 – 1.72 (m, 2H), 1.48 – 1.39 (m, 2H); ^{13}C NMR (126 MHz, cd_3od) δ 152.86, 152.35, 151.39, 145.47, 144.60, 134.83, 128.13, 124.70, 124.15, 61.53, 35.96, 30.82, 28.96, 25.12; HRMS (ESI $^+$): $[\text{M}+2\text{H}]^{2+}$: calculated for $\text{C}_{16}\text{H}_{21}\text{N}_3\text{O}_2^{2+}$ (m/z): 143.5811; detected: 143.58113. LC-MS > 95 %



4-hydroxy-1-(5-(5-hydroxy-6-((1E)-(hydroxyimino)methyl)pyridin-2-yl)pentyl)pyridin-1-ium bromide (195): The resulting residue was purified by column chromatography using mobile phase DCM/MeOH (9:1) to afford title product **195** as yellowish oil. Yield 46 %.

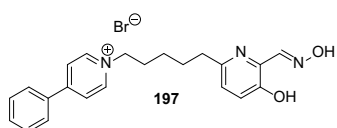
^1H NMR (500 MHz, Methanol- d_4) δ 8.29 (s, 1H), 7.82 – 7.77 (m, 2H), 7.26 (d, $J = 8.5$ Hz, 1H), 7.14 (d, $J = 8.5$ Hz, 1H), 6.46 – 6.42 (m, 2H), 3.98 (t, $J = 7.2$ Hz, 2H), 2.78 – 2.68 (m, 2H), 1.89 – 1.80 (m, 2H), 1.78 – 1.69 (m, 2H), 1.41 – 1.31 (m, 2H); ^{13}C NMR (126 MHz, cd_3od) δ 180.67, 154.30, 153.80, 152.78, 143.14, 136.32, 126.00, 125.36, 118.35, 58.05, 37.46, 31.61, 30.46, 26.57; HRMS (ESI $^+$): $[\text{M}+2\text{H}]^{2+}$: calculated for $\text{C}_{16}\text{H}_{21}\text{N}_3\text{O}_3^{2+}$ (m/z): 151.5786; detected: 151.57855. LC-MS > 97 %



1-(5-(5-hydroxy-6-((1E)-(hydroxyimino)methyl)pyridin-2-yl)pentyl)-4-(methoxycarbonyl)pyridin-1-ium bromide (196): The resulting residue was purified

by column chromatography using mobile phase DCM/MeOH (9:1) to afford title product **196** as yellowish oil. Yield 41 %.

^1H NMR (500 MHz, Methanol- d_4) δ 9.30 – 9.21 (m, 2H), 8.63 – 8.47 (m, 2H), 8.25 (s, 1H), 7.26 (d, J = 8.5 Hz, 1H), 7.18 (d, J = 8.5 Hz, 1H), 4.83 (s, 5H), 4.77 (t, J = 7.6 Hz, 2H), 2.75 (t, J = 7.6 Hz, 2H), 2.16 – 2.06 (m, 2H), 1.78 (m, 2H), 1.50 – 1.41 (m, 2H); ^{13}C NMR (126 MHz, cd_3od) δ 162.25, 152.82, 152.37, 151.35, 145.99, 144.73, 134.84, 128.39, 127.35, 127.29, 124.69, 124.13, 61.98, 35.89, 33.34, 30.79, 28.91, 25.07; HRMS (ESI $^+$): $[\text{M}+2\text{H}]^{2+}$: calculated for $\text{C}_{18}\text{H}_{23}\text{N}_3\text{O}_4^{2+}$ (m/z): 172.5839; detected: 172.58376. LC-MS > 95 %



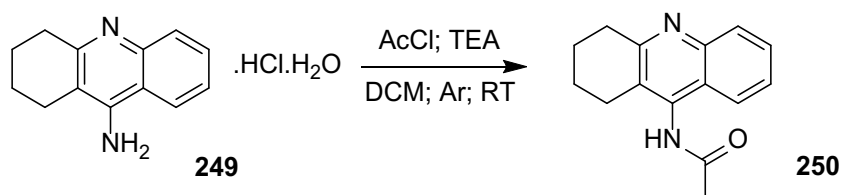
1-(5-(5-hydroxy-6-((1E)-(hydroxyimino)methyl)pyridin-2-yl)pentyl)-4-phenylpyridin-1-ium bromide (197): The resulting residue was purified by column chromatography using mobile phase DCM/MeOH (9:1) to afford title product **197** as yellowish oil. Yield 80 %.

^1H NMR (500 MHz, Methanol- d_4) δ 9.07 – 8.99 (m, 2H), 8.42 – 8.34 (m, 2H), 8.24 (s, 1H), 8.01 – 7.94 (m, 2H), 7.66 – 7.57 (m, 3H), 7.23 (d, J = 8.5 Hz, 1H), 7.16 (d, J = 8.5 Hz, 1H), 4.67 (t, J = 7.5 Hz, 3H), 2.75 – 2.69 (m, 2H), 2.17 – 2.06 (m, 2H), 1.84 – 1.72 (m, 2H), 1.50 – 1.41 (m, 2H); ^{13}C NMR (126 MHz, cd_3od) δ 156.25, 152.85, 152.31, 151.42, 144.47, 134.81, 133.71, 132.03, 129.57, 127.81, 124.69, 124.15, 60.59, 35.99, 30.70, 28.97, 25.15; HRMS (ESI $^+$): $[\text{M}+2\text{H}]^{2+}$: calculated for $\text{C}_{22}\text{H}_{25}\text{N}_3\text{O}_2^{2+}$ (m/z): 181.5968; detected: 181.5968. LC-MS > 96 %

6.1.6 Tacroximes

Preparation of *N*-Acetyl tacrine

N-(1,2,3,4-tetrahydroacridin-9-yl)acetamide (250):

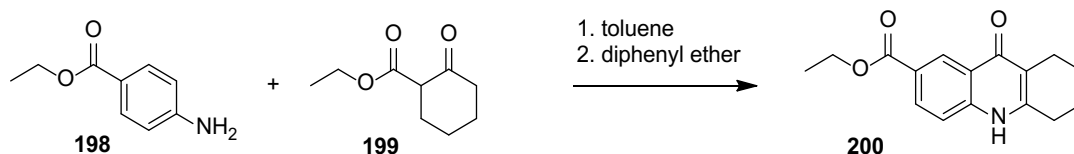


1,2,3,4-tetrahydroacridin-9-amine hydrochloride hydrate (**249**; 1.97 mmol; 1.0 eq) was suspended in anhydrous dichloromethane (DCM; 10 mL) under Ar and acetyl chloride (2.17 mmol; 1.1 eq) was added. After 10 min of stirring triethylamine (TEA; 5.91 mmol; 3.0 eq) was drop wise introduced and the reaction mixture was stirred at room temperature (RT) overnight. The result was diluted with saturated sodium bicarbonate and washed three times with DCM (3x 30 mL). The organic phases were collected, dried with anhydrous sodium sulfate (Na₂SO₄), filtered and concentrated under reduced pressure. The residue was purified by column chromatography using mobile phase DCM and methanol (DCM/MeOH = 40:1) to give crude product **250** (38 mg; 8 %) as sharp yellow solid.

¹H NMR (500 MHz, DMSO-*d*₆) δ 11.04 (s, 1H), 7.94 (dd, *J* = 8.5, 1.3 Hz, 1H), 7.88 (dd, *J* = 8.5, 1.3 Hz, 1H), 7.63 (ddd, *J* = 8.2, 6.7, 1.3 Hz, 1H), 7.49 (ddd, *J* = 8.2, 6.7, 1.3 Hz, 1H), 3.02 (t, *J* = 6.1 Hz, 2H), 2.83 (t, *J* = 6.1 Hz, 2H), 2.20 (s, 3H), 1.89 – 1.79 (m, 4H). ¹³C NMR (126 MHz, dms) δ 171.56, 158.47, 145.77, 138.37, 129.96, 128.74, 128.31, 126.74, 125.81, 123.85, 35.38, 33.95, 25.11, 22.69, 22.38. HRMS (ESI⁺): [M]⁺: calculated for C₁₅H₁₇N₂O⁺ (m/z): 241.1335; found: 241.13329. LC-MS purity > 95 %.

General Procedure and Spectral Data for Tacroxime 1 (**204**)

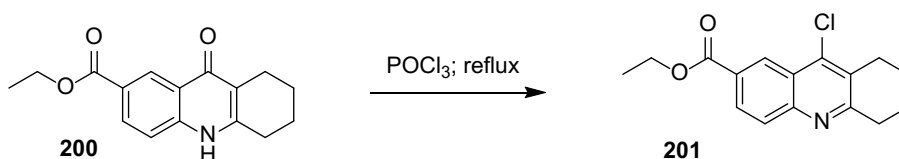
Ethyl 9-oxo-5,6,7,8,9,10-hexahydroacridine-2-carboxylate (**200**):



Benzocaine (**198**; 87.8 mmol; 1.0 eq) and ethyl 2-oxocyclohexanecarboxylate (**199**; 96.6 mmol; 1.1 eq) were dissolved in toluene (150 mL) under Ar atmosphere. The mixture was heated to 150 °C and stirred for 16 hours under Dean-Stark apparatus. Toluene was removed by evaporation under reduced pressure and the residue was mixed with diphenylether (75 mL). The resulting mixture was heated to 230 °C for 2 hours under modified Dean-Stark apparatus. After cooling, the mixture was diluted with heptane (75 mL). The resulting precipitate was filtrated and washed with additional heptane (3x 100 mL) to give the crude product **200** (19.381 g; 81 % yield) as yellowish solid.

^1H NMR (500 MHz, $\text{DMSO-}d_6$) δ 11.61 (s, 1H), 8.68 (d, $J = 2.1$ Hz, 1H), 8.07 (dd, $J = 8.7, 2.1$ Hz, 1H), 7.53 (d, $J = 8.7$ Hz, 1H), 4.33 (q, $J = 7.1$ Hz, 2H), 2.70 (t, $J = 6.2$ Hz, 2H), 2.43 (t, $J = 6.2$ Hz, 2H), 1.81 – 1.73 (m, 2H), 1.73 – 1.66 (m, 2H), 1.34 (t, $J = 7.1$ Hz, 3H). ^{13}C NMR (126 MHz, DMSO) δ 176.07, 165.60, 147.83, 142.19, 130.97, 127.63, 123.38, 122.49, 118.12, 117.08, 60.84, 27.29, 21.82, 21.75, 21.52, 14.41.

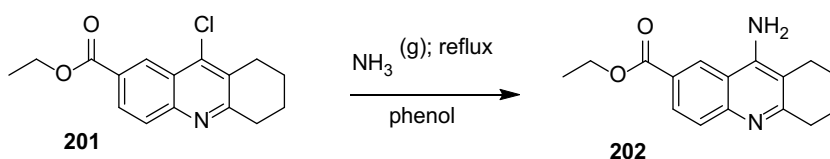
Ethyl 9-chloro-5,6,7,8-tetrahydroacridine-2-carboxylate (**201**):



The compound **200** (18.8 mmol; 1.0 eq) was dissolved with phosphoryl chloride (POCl_3 ; 188.0 mmol; 10.0 eq) in oven-dried round-bottom flask under Ar atmosphere. The mixture was heated to 140 °C for 1 hour. POCl_3 was then distilled under reduced pressure and the residue was diluted with dichloromethane (DCM; 100 mL). The resulting solution was slowly poured in glacial H_2O (100 mL) and then neutralized with ammonium hydroxide 25 % solution to basic pH (pH > 12). The mixture was 3x extracted with DCM (3x 100 mL) and organics were collected, dried with anhydrous sodium sulfate (Na_2SO_4), filtrated and concentrated under reduced pressure. The residue was purified by column chromatography using mobile phase petrol ether (PE) / ethyl acetate (EA) (PE/EA = 2:1) to give crude product **201** (4.397 g; 81 % yield) as yellow solid.

^1H NMR (500 MHz, $\text{DMSO-}d_6$) δ 8.60 (d, $J = 1.9$ Hz, 1H), 8.11 (dd, $J = 8.8, 1.9$ Hz, 1H), 7.93 (d, $J = 8.8$ Hz, 1H), 4.38 (q, $J = 7.1$ Hz, 2H), 3.09 – 2.94 (m, 2H), 2.93 – 2.80 (m, 2H), 1.90 – 1.80 (m, 4H), 1.37 (t, $J = 7.1$ Hz, 3H). ^{13}C NMR (126 MHz, DMSO) δ 165.27, 162.36, 147.89, 141.09, 129.94, 129.34, 128.50, 127.88, 125.65, 123.87, 61.39, 33.92, 27.14, 21.94, 14.34.

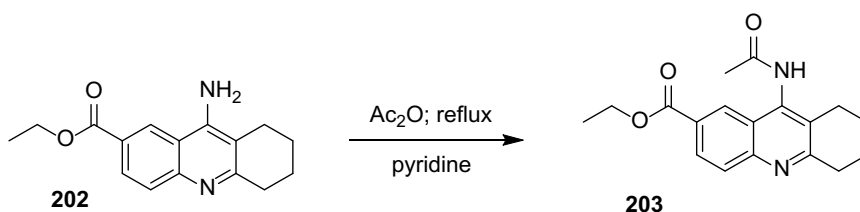
Ethyl 9-amino-5,6,7,8-tetrahydroacridine-2-carboxylate (**202**):



The compound **201** (3.7 mmol; 1.0 eq) was mixed with phenol (70 mL) in double-necked round-bottom flask under Ar atmosphere and heated to 100 °C until homogenated mixture was formed. The mixture was then heated to 180 °C and challenged with ammonia gas (NH₃ (g)) that was *in situ* prepared from sodium hydroxide (s) (NaOH) and saturated solution of ammonium chloride (NH₄Cl) for 30 min. After cooling, the residue was diluted with DCM (100 mL) and slowly neutralized with 10 % NaOH (100 mL). The resulting solution was extracted with DCM (3x 100 mL) and organics were collected, dried with anhydrous Na₂SO₄, filtrated and concentrated under reduced pressure. The residue was purified by column chromatography using mobile phase DCM / methanol (MeOH) and ammonium hydroxide solution (NH₃; 25 % in H₂O) (DCM/MeOH/NH₃ = 9:1:0.1) to give crude product **202** (772 mg; 77 % yield) as yellow solid.

¹H NMR (500 MHz, DMSO-*d*₆) δ 8.89 (d, *J* = 1.9 Hz, 1H), 7.95 (dd, *J* = 8.8, 1.9 Hz, 1H), 7.65 (d, *J* = 8.8 Hz, 1H), 6.76 (bs, 2H), 4.35 (q, *J* = 7.1 Hz, 2H), 2.83 (t, *J* = 6.0 Hz, 2H), 2.54 (t, *J* = 6.0 Hz, 2H), 1.86 – 1.75 (m, 4H), 1.36 (t, *J* = 7.1 Hz, 3H). ¹³C NMR (126 MHz, DMSO) δ 166.17, 159.90, 149.85, 148.54, 128.25, 127.33, 125.76, 123.91, 116.30, 110.00, 60.76, 33.78, 23.78, 22.60, 22.52, 14.49.

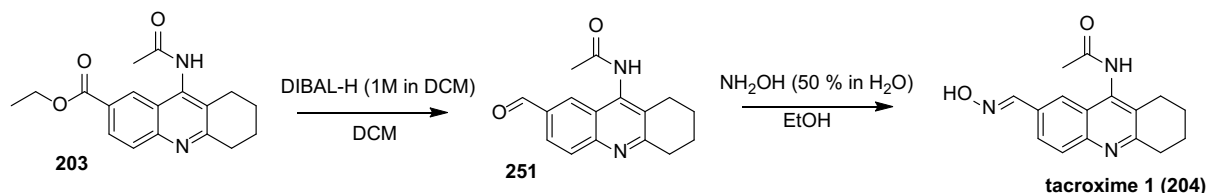
Ethyl 9-acetamido-5,6,7,8-tetrahydroacridine-2-carboxylate (**203**):



The compound **202** (2.12 mmol; 1.0 eq) was dissolved in pyridine under Ar atmosphere. Acetic anhydride (Ac₂O; 2.5 mmol; 1.2 eq) was added and the mixture was heated to 150 °C and stirred for 40 hours. The resulting mixture was concentrated under reduced pressure and directly purified by column chromatography using mobile phase chloroform/methanol (CHCl₃/MeOH = 40:1) to give crude product **203** (198 mg; 30 % yield) as bold yellow solid.

¹H NMR (500 MHz, DMSO-*d*₆) δ 10.17 (s, 1H), 8.53 (d, *J* = 1.9 Hz, 1H), 8.11 (dd, *J* = 8.8, 1.9 Hz, 1H), 7.97 (d, *J* = 8.8 Hz, 1H), 4.38 (q, *J* = 7.1 Hz, 2H), 3.06 (t, *J* = 6.5 Hz,

2H), 2.75 (t, $J = 6.4$ Hz, 2H), 2.23 (s, 3H), 1.92 – 1.84 (m, 2H), 1.84 – 1.75 (m, 2H), 1.36 (t, $J = 7.1$ Hz, 3H). ^{13}C NMR (126 MHz, DMSO) δ 168.64, 165.74, 162.56, 148.18, 140.97, 128.97, 128.48, 127.71, 126.73, 126.29, 123.43, 61.20, 33.79, 25.17, 22.98, 22.37, 21.96, 14.38.



***N*-{7-[(1*E*)-(hydroxyimino)methyl]-1,2,3,4-tetrahydroacridin-9-yl}acetamide (tacroxime 1; 204):**

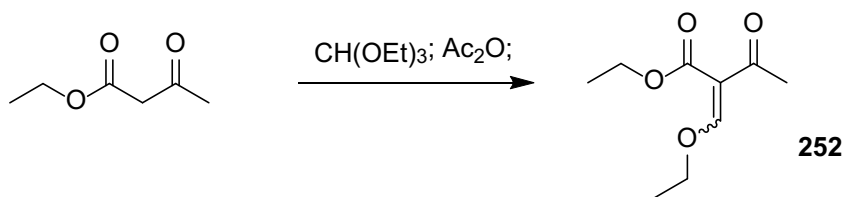
The compound **203** (0.269 mmol; 1.0 eq) was dissolved in anhydrous DCM (15 mL) and cooled to -80 °C under Ar atmosphere. Diisobutylaluminium hydride solution (DIBAL-H (1M in DCM)) (1.13 mmol; 4.2 eq) was drop wise added and the reaction was stirred for 15 min. MeOH (1.5 mL) and Rochelle salt (20 mL) was subsequently added and the mixture was vigorously stirred at RT for 1 hour. The mixture was extracted with DCM (3x 30 mL) and organics were collected, dried with anhydrous sodium sulfate (Na_2SO_4), filtrated and concentrated under reduced pressure. The resulting residue was directly used in the next step without any additional purification.

The mixture of compound **251** (0.269 mmol; 1.0 eq) was dissolved with absolute EtOH (15 mL) and challenged with NH_2OH (50 % in H_2O ; 0.538 mmol; 2.0 eq) for 30 min at RT. The resulting residue was concentrated and directly purified by column chromatography using mobile phase DCM/MeOH (20:1) to give crude product **204** (15 mg; 20 % yield) as light yellow solid.

^1H NMR (500 MHz, $\text{DMSO-}d_6$) δ 11.39 (s, 1H), 9.99 (s, 1H), 8.32 (s, 1H), 7.98 (d, $J = 1.7$ Hz, 1H), 7.92 (d, $J = 1.7$ Hz, 1H), 7.87 (s, 1H), 3.02 (t, $J = 6.5$ Hz, 2H), 2.74 (t, $J = 6.4$ Hz, 2H), 2.20 (s, 3H), 1.91 – 1.83 (m, 2H), 1.82 – 1.74 (m, 2H). ^{13}C NMR (126 MHz, DMSO) δ 168.59, 160.11, 148.18, 146.89, 140.18, 130.33, 128.94, 128.04, 125.61, 124.22, 122.91, 33.59, 25.07, 23.02, 22.52, 22.10. HRMS (ESI $^+$): $[\text{M}]^+$: calculated for $\text{C}_{16}\text{H}_{17}\text{N}_3\text{O}_3^+$ (m/z): 300.1343; found: 300.13367. LC-MS purity > 95 %.

General procedure and Spectral data for Tacroxime 2 (208)

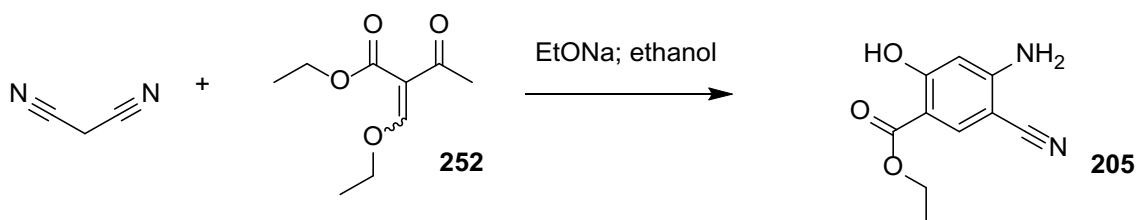
Ethyl 2-(ethoxymethylidene)-3-oxobutanoate (**252**):



Acetylacetonate (47.0 mmol; 1.0 eq), triethyl orthoformate (47.0 mmol; 1.0 eq) and acetic anhydride were stirred and heated at 130 °C for 2 hours. The resulting mixture was neutralized with saturated NaHCO_3 (100 mL) and extracted with DCM (3x 80 mL). The organics were collected, dried with anhydrous Na_2SO_4 , filtrated and concentrated under reduced pressure. The residue was purified by column chromatography using mobile phase PE/EA (4:1) to give both isomers of **252** (1.824 g; 21 % yield) as red liquid.

^1H NMR (500 MHz, Chloroform-*d*) δ 7.72 – 7.56 (m, 2H), 4.43 – 4.13 (m, 8H), 2.46 – 2.27 (m, 6H), 1.46 – 1.22 (m, 12H). ^{13}C NMR (126 MHz, cdCl_3) δ 196.77, 195.27, 165.36, 164.09, 114.26, 113.48, 72.79, 72.71, 60.65, 60.53, 31.62, 28.69, 15.22, 15.17, 14.18, 14.10.

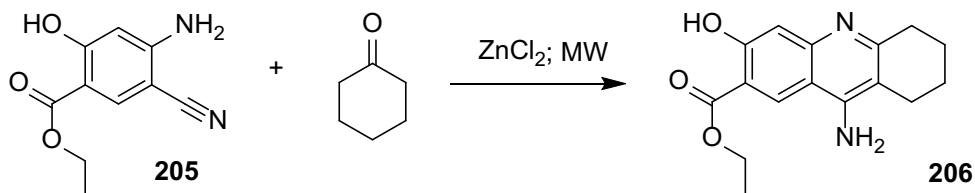
Ethyl 4-amino-5-cyano-2-hydroxybenzoate (**205**):



Malononitrile (80.554 mmol; 1.0 eq) was dissolved in absolute EtOH (15 mL) and was drop wise added to 21 % solution of sodium ethoxide in EtOH (161.11 mmol; 2.0 eq) over half hour under Ar atmosphere. The compound **252** (80.55 mmol; 1.0 eq) was dissolved in absolute EtOH (30 mL) and was drop wise added to the mixture of malononitrile and sodium ethoxide over 1 hour. The resulting mixture was heated to 100 °C and stirred for 40 min. The precipitate was filtrated and dissolved in H_2O . Concentrated HCl (32 % solution; 40 mL) was added and the resulting precipitate was again filtrated. The solid was dissolved in acetic acid at 90 °C and after cooling it was again filtrated to give crude product **205** (3.624 g; 22 % yield) as light brown solid.

^1H NMR (500 MHz, $\text{DMSO-}d_6$) δ 10.98 (s, 1H), 7.87 (s, 1H), 6.78 (bs, 2H), 6.19 (s, 1H), 4.33 – 4.20 (m, 2H), 1.37 – 1.24 (m, 3H). ^{13}C NMR (126 MHz, dms) δ 167.99, 164.32, 156.40, 137.29, 117.22, 102.95, 99.76, 87.55, 61.18, 14.17.

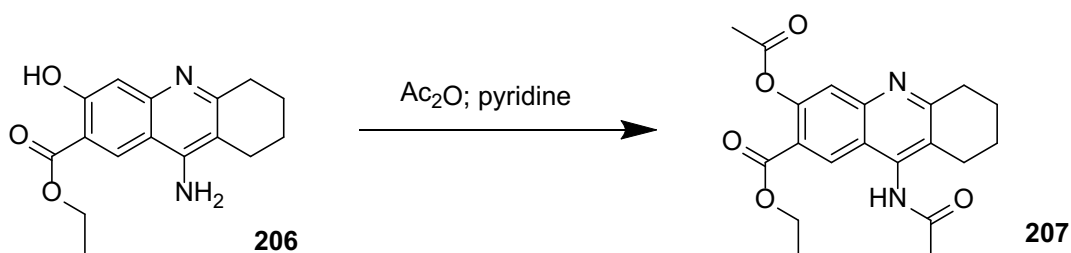
Ethyl 9-amino-3-hydroxy-5,6,7,8-tetrahydroacridine-2-carboxylate (206):



The compound **205** (5.33 mmol; 1.0 eq), ZnCl_2 (10.66 mmol; 2.0 eq) and cyclohexanone (8 mL) were added into microwave-sealed tube and were challenged by microwave irradiation with following settings: dynamic curve, power max cap 150 W, pressure max cap 300 PSI, 150 $^\circ\text{C}$, for 10 min. The resulting mixture was dissolved in ammonium solution (25 %; 20 mL) and DCM (50 mL) and diluted with addition of H_2O (30 mL). The mixture was extracted with DCM (4x 50 mL) and the organics layers were collected, dried with anhydrous Na_2SO_4 , filtrated and concentrated under reduced pressure. The residue was purified by column chromatography using mobile phase DCM/MeOH/ NH_3 (9:1:0.1) to give crude product **206** (672 mg; 44 % yield) as yellow solid.

^1H NMR (500 MHz, $\text{DMSO-}d_6$) δ 8.78 (s, 1H), 7.40 (bs, 2H), 7.01 (s, 1H), 4.37 (q, $J = 7.1$ Hz, 2H), 3.90 (s, 1H), 2.79 (t, $J = 6.0$ Hz, 2H), 2.50 – 2.43 (m, 2H), 1.84 – 1.72 (m, 4H), 1.37 (t, $J = 7.1$ Hz, 3H). ^{13}C NMR (126 MHz, DMSO) δ 168.23, 159.50, 157.16, 152.34, 146.65, 127.60, 114.98, 109.46, 107.71, 107.53, 61.43, 31.40, 23.09, 22.05, 21.82, 14.33.

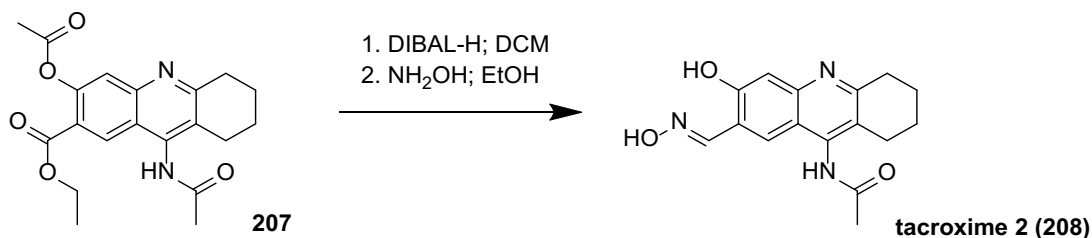
Ethyl 3-(acetyloxy)-9-acetamido-5,6,7,8-tetrahydroacridine-2-carboxylate (207):



The compound **206** (1.52 mmol; 1.0 eq) and acetic anhydride (3.8 mmol; 2.5 eq) were dissolved in distilled pyridine (15 mL) under Ar atmosphere and heated to 140 °C for 40 hours. The resulting mixture was concentrated and directly purified by column chromatography using mobile phase DCM/MeOH (20:1) to give product **207** (183 mg; 33 % yield) as bold yellow solid.

¹H NMR (500 MHz, DMSO-*d*₆) δ 10.17 (s, 1H), 8.47 (s, 1H), 7.69 – 7.61 (m, 1H), 4.33 (q, *J* = 7.1 Hz, 2H), 3.05 (t, *J* = 6.5 Hz, 2H), 2.75 (t, *J* = 6.4 Hz, 2H), 2.33 (s, 3H), 2.22 (s, 3H), 1.92 – 1.83 (m, 2H), 1.85 – 1.73 (m, 2H), 1.32 (t, *J* = 7.1 Hz, 3H).

***N*-{6-hydroxy-7-[(1*E*)-(hydroxyimino)methyl]-1,2,3,4-tetrahydroacridin-9-yl}acetamide (tacroxime 2; **208**):**



The compound **207** (0.42 mmol; 1.0 eq) was dissolved in anhydrous DCM (15 mL) and cooled to -80 °C under Ar atmosphere. DIBAL-H (1M in DCM) (2.1 mmol; 5.0 eq) was drop wise added and the reaction was stirred for 10 min. MeOH (2.5 mL) and Rochelle salt (30 mL) was subsequently added and the mixture was vigorously stirred at RT for 1 hour. The mixture was extracted with DCM (3x 40 mL) and organics were collected, dried with anhydrous Na₂SO₄, filtrated and concentrated under reduced pressure. The resulting residue was directly used in the next step without any additional purification.

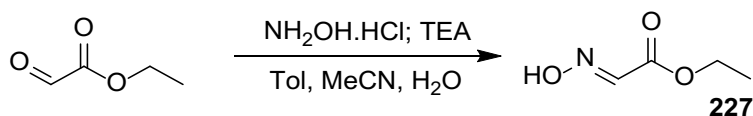
The mixture from the first step (0.42 mmol; 1.0 eq) was dissolved with absolute EtOH (10 mL) and challenged with NH₂OH (50 % in H₂O; 1.68 mmol; 4.0 eq) for 45 min at RT. The resulting residue was concentrated and directly purified by column chromatography using gradient mobile phase DCM/MeOH (from 20:1 to 9:1) to give crude product **208** (9 mg; 7 % yield) as white solid.

¹H NMR (500 MHz, Methanol-*d*₄) δ 8.47 (s, 1H), 7.93 (s, 1H), 7.26 (s, 1H), 3.07 (t, *J* = 6.5 Hz, 2H), 2.79 (t, *J* = 6.4 Hz, 2H), 2.32 (s, 3H), 2.00 – 1.93 (m, 2H), 1.92 – 1.84 (m, 2H). ¹³C NMR (126 MHz, CD₃OD) δ 172.30, 162.73, 158.72, 150.99, 148.88, 141.67, 127.13, 126.08, 121.97, 119.96, 110.76, 110.75, 34.44, 30.75, 26.06, 23.63, 23.47.

HRMS (ESI⁺): [M]⁺: calculated for C₁₆H₁₈N₃O₂⁺ (m/z): 284.1394; found: 284.1387.
LC-MS purity > 95 %.

6.1.7 Uncharged bis-oxime reactivators

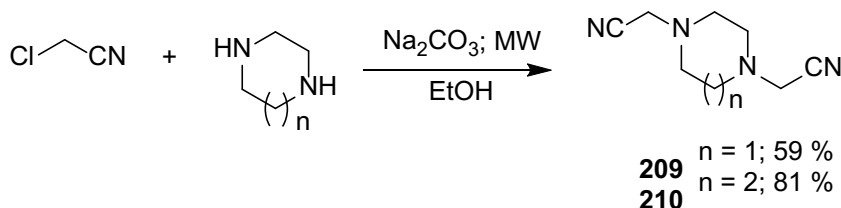
Preparation of oxime fragment (227)



Ethyl (2E)-2-(hydroxyimino)acetate (227): Hydroxylamine hydrochloride (NH₂OH.HCl) (1.0 eq; 50.44 mmol) was dissolved in acetonitrile/water (9:1 ratio = 36:4 mL) and ethyl glyoxalate (50 % solution in toluene) (1.0 eq; 50.44 mmol) was slowly added. After 10 min of stirring triethylamine (TEA) (1.0 eq; 50.44 mmol) was drop wise introduced over 30 min. The reaction mixture was stirred at room temperature (RT) for 24 hours. Then it was concentrated and diluted with H₂O. The aqueous solution was three times washed with dichloromethane (DCM) 3x 100 mL and the organic phases were collected, dried over anhydrous sodium sulfate (Na₂SO₄), filtrated and concentrated to give crude product **227** as colorless oil. Yield 61 %.

¹H NMR (600 MHz, DMSO-*d*₆) δ 12.56 (s, 1H), 7.54 (s, 1H), 4.19 (q, *J* = 7.1 Hz, 2H), 1.23 (t, *J* = 7.1 Hz, 3H).

General procedure A for *N*-alkylation with 2-chloroacetonitrile



Piperazine or homopiperazine (1.0 eq); 2-chloroacetonitrile (2.4 eq) and Na₂CO₃ (4.0 eq) were dissolved in absolute EtOH. The reaction mixture was challenged by microwave (MW) irradiation for 5 hours at 100 °C. The solid was filtered and the filtrate was purified by column chromatography using mobile phase DCM and methanol (MeOH).

2-[4-(cyanomethyl)piperazin-1-yl]acetonitrile (209): Prepared according to the general method A. Piperazine (538 mg; 6.246 mmol); 2-chloroacetonitrile (950 μL;

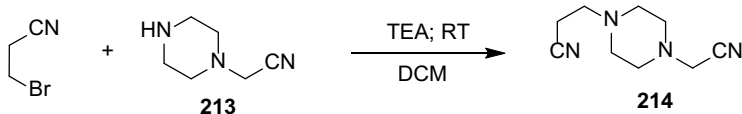
14.99 mmol); Na₂CO₃ (2.648 g; 24.98 mmol) and EtOH (4 mL). Purification was performed using mobile phase DCM:MeOH (98:2) to give crude product **209** as yellow oil. Yield 59 %.

¹H NMR (600 MHz, Chloroform-*d*) δ 3.55 (s, 4H), 2.67 (s, 8H). ¹³C NMR (151 MHz, CDCl₃) δ 114.62, 51.36, 46.03.

2-[4-(cyanomethyl)-1,4-diazepan-1-yl]acetonitrile (210): Prepared according to the general method A. Homopiperazine (638 mg; 6.37 mmol); 2-chloroacetonitrile (970 μL; 15.29 mmol); Na₂CO₃ (2.701 g; 25.48 mmol) and EtOH (4 mL). Purification was performed using mobile phase DCM:MeOH (98:2) to give crude product **210** as yellow oil. Yield 81 %.

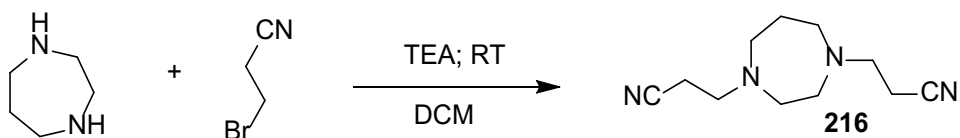
¹H NMR (600 MHz, Chloroform-*d*) δ 3.58 (s, 4H), 2.88 – 2.74 (m, 8H), 1.96 – 1.86 (m, 2H). ¹³C NMR (151 MHz, CDCl₃) δ 115.78, 54.39, 53.47, 47.34, 27.86.

The *N*-alkylation with 3-bromopropionitrile using TEA in DCM



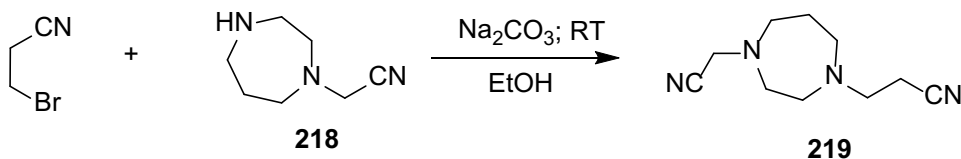
3-[4-(cyanomethyl)piperazin-1-yl]propanenitrile (214): The compound **213** (974 mg; 7.78 mmol) was dissolved in anhydrous DCM (15 mL) and 3-bromopropionitrile (645 μL; 7.78 mmol) was added. After 10 min of stirring, TEA (2.17 mL; 15.56 mmol) was drop wise introduced. The reaction mixture was stirred at RT for 24 hours. The solution was diluted with H₂O, the organic phase was removed and water phase was washed three times with additional DCM (3x 50 mL). The organic phases were collected, dried over Na₂SO₄, filtered, concentrated and purified by column chromatography using mobile phase DCM/MeOH (14:1) to give crude product **214** as dark yellow oil. Yield 66 %.

¹H NMR (600 MHz, Chloroform-*d*) δ 3.52 (s, 2H), 2.72 (t, *J* = 7.0 Hz, 2H), 2.69 – 2.55 (m, 8H), 2.52 (t, *J* = 7.0 Hz, 2H). ¹³C NMR (151 MHz, CDCl₃) δ 118.62, 114.62, 53.08, 52.12, 51.56, 45.82, 15.99.



3-[4-(2-cyanoethyl)-1,4-diazepan-1-yl]propanenitrile (216): Homopiperazine (1.803 mg; 18.0 mmol) was dissolved in anhydrous DCM (20 mL) and 3-bromopropionitrile (2.986 mL; 36.0 mmol) was added. After 10 min of stirring, TEA (10.0 mL; 72.0 mmol) was drop wise introduced. The reaction mixture was stirred at RT for 24 hours. The solution was diluted with H₂O, the organic phase was removed and water phase was washed three times with additional DCM (3x 50 mL). The organic phases were collected, dried over Na₂SO₄, filtered, concentrated and purified by column chromatography using mobile phase DCM/MeOH (9:1) to give crude product **216** as dark yellow oil. Yield 84 %.

¹H NMR (600 MHz, Chloroform-*d*) δ 2.87 (t, *J* = 6.9 Hz, 4H), 2.80 – 2.71 (m, 8H), 2.47 (t, *J* = 6.9 Hz, 4H), 1.80 (p, *J* = 6.9, 5.3 Hz, 2H). ¹³C NMR (151 MHz, CDCl₃) δ 119.01, 54.74, 53.38, 53.31, 27.98, 16.47.

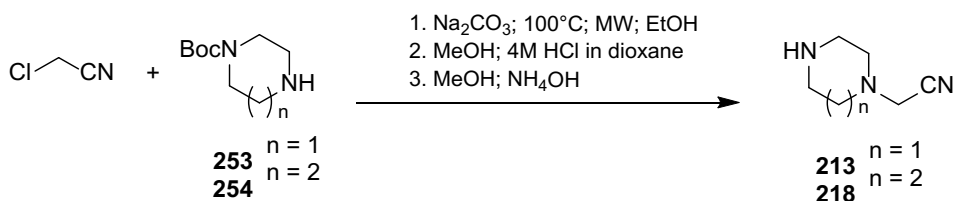


3-[4-(cyanomethyl)-1,4-diazepan-1-yl]propanenitrile (219): The compound **218** (1.229 g; 8.83 mmol) was dissolved in absolute EtOH (20 mL) and subsequently 3-bromopropionitrile (1.5 mL; 17.66 mmol) and Na₂CO₃ (2.808 g; 26.5 mmol) were added. The reaction mixture was stirred at RT for 24 hours, concentrated and directly purified using DCM alone as mobile phase to give crude product **219** as yellow oil. Yield 53 %.

¹H NMR (600 MHz, Chloroform-*d*) δ 3.55 (s, 2H), 2.87 (t, *J* = 7.0 Hz, 2H), 2.81 – 2.73 (m, 8H), 2.46 (t, *J* = 7.0 Hz, 2H), 1.83 (p, *J* = 7.0, 5.9 Hz, 2H). ¹³C NMR (151 MHz, CDCl₃) δ 118.91, 115.69, 54.75, 54.06, 53.56, 53.32, 47.09, 27.77, 16.42.

Multistep reactions

General procedure B



N-Boc-piperazine **253** or *N*-Boc-homopiperazine **254** (1.0 eq) was dissolved in absolute EtOH and subsequently 2-chloroacetonitrile (1.2 eq) and Na_2CO_3 (2.0 eq) were added. The reaction mixture was challenged by MW irradiation for 5 hours at 100 °C. The solution was concentrated, diluted with H_2O and three times washed with DCM (3x 50 mL). The organic phases were collected, dried over Na_2SO_4 , filtered, concentrated and used into next step without any further purification.

The residue was dissolved in MeOH (30 mL) and 1 M solution of HCl in dioxane (15 mL) was added. The mixture was stirred at RT for 20 hours. The result was concentrated and dried under reduced pressure. The residue was again dissolved in MeOH (30 mL) and 25 % solution of ammonium hydroxide (NH_4OH) in water (15 mL) was added. After another 1 hour of stirring the reaction mixture was concentrated and directly purified by column chromatography using mobile phase DCM/MeOH/ NH_4OH (6:1:0.1) to give crude products.

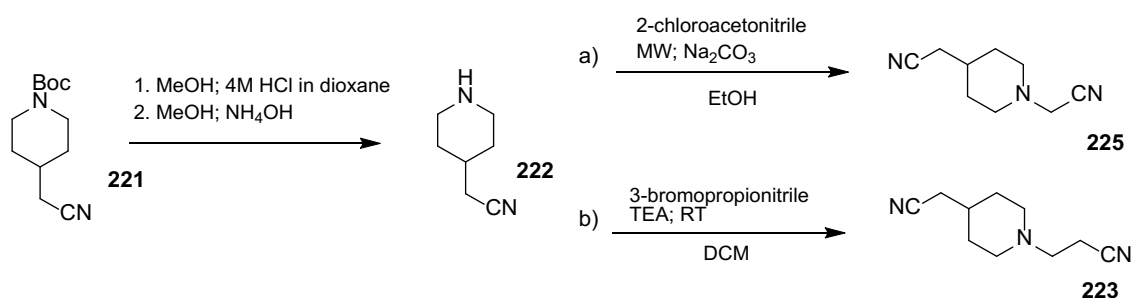
2-(piperazin-1-yl)acetonitrile (213): Prepared according to the general method B. *N*-Boc-piperazine (2.012 g; 10.8 mmol); 2-chloroacetonitrile (820 μL ; 13.0 mmol); Na_2CO_3 (2.289 g; 21.6 mmol) and EtOH (10 mL). Yield 72 %.

^1H NMR (600 MHz, Chloroform-*d*) δ 3.50 (s, 2H), 2.93 (t, $J = 4.9$ Hz, 4H), 2.55 (t, $J = 4.9$ Hz, 4H), 1.74 (bs, 1H). ^{13}C NMR (151 MHz, CDCl_3) δ 114.66, 52.93, 46.56, 45.54.

2-(1,4-diazepan-1-yl)acetonitrile (218): Prepared according to the general method B. *N*-Boc-homopiperazine (2.354 g; 11.75 mmol); 2-chloroacetonitrile (1.8 mL; 14.1 mmol); Na_2CO_3 (2.475 g; 23.5 mmol) and EtOH (10 mL). Yield 86 %.

^1H NMR (600 MHz, Chloroform-*d*) δ 3.60 (s, 2H), 3.19 (bs, 1H), 3.07 – 2.97 (m, 4H), 2.84 – 2.76 (m, 4H), 1.88 (p, $J = 5.9$ Hz, 2H). ^{13}C NMR (151 MHz, CDCl_3) δ 115.59, 56.26, 53.89, 47.88, 47.45, 46.86, 29.20.

General procedure C:



N-Boc-4-cyanomethylpiperidine **221** (4.118 g; 18.36 mmol) was dissolved in MeOH (20 mL) and 1 M solution of HCl in dioxane (10 mL) was added. The mixture was stirred at RT for 20 hours. The result was concentrated and dried under reduced pressure. The residue was again dissolved in MeOH (20 mL) and 25 % solution of ammonium hydroxide (NH₄OH) in water (10 mL) was added. After another 1 hour of stirring the reaction mixture was concentrated and directly purified using very fast column chromatography with mobile phase DCM/MeOH/NH₄OH (6:1:0.1) to give crude product 4-cyanomethylpiperidine **222** as white solid. Yield > 99 %. The amount of 4-cyanomethylpiperidine was halved and used in to next step without characterization.

a) **2-[1-(cyanomethyl)piperidin-4-yl]acetonitrile (225)**: 4-cyanomethylpiperidine **222** (1.14 g; 9.18 mmol) was dissolved in absolute EtOH (10 mL) and subsequently 2-chloroacetonitrile (700 μ L; 11.0 mmol) and Na₂CO₃ (1.946 g; 18.36 mmol) were added. The reaction mixture was challenged by MW irradiation for 10 hours at 100 °C. The result was concentrated and directly purified using column chromatography with mobile phase DCM/MeOH (95:5) to give crude product **225** as yellowish solid. Yield 62 % after 2 steps.

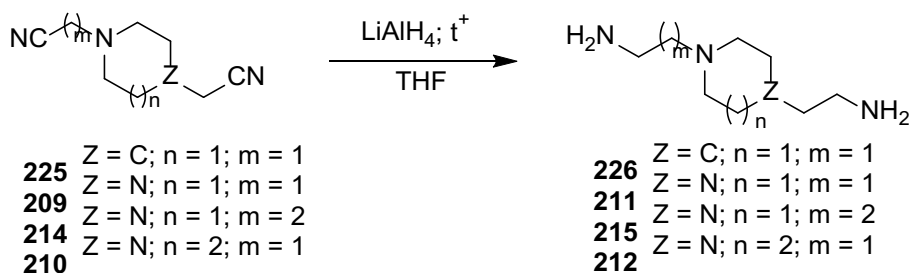
¹H NMR (599 MHz, Chloroform-*d*) δ 3.68 (s, 2H), 3.03 – 2.94 (m, 2H), 2.54 – 2.49 (m, 2H), 2.47 (d, *J* = 6.8 Hz, 2H), 2.06 – 1.97 (m, 2H), 1.91 – 1.81 (m, 1H), 1.65 – 1.54 (m, 2H). ¹³C NMR (151 MHz, CDCl₃) δ 118.16, 114.60, 51.64, 46.22, 32.04, 31.09, 23.83.

b) **3-[4-(cyanomethyl)piperidin-1-yl]propanenitrile (223)**: 4-cyanomethylpiperidine **222** (1.14 g; 9.18 mmol) was dissolved in anhydrous DCM (25 mL) and 3-bromopropionitrile (913 μ L; 11.0 mmol) was added. After 10 min of stirring, TEA (2.6 mL; 18.36 mmol) was drop wise introduced. The reaction mixture was stirred at RT for 24 hours. The solution was diluted with H₂O, the organic phase was removed and water phase was washed three times with additional DCM (3x 30 mL). The organic phases were collected, dried over Na₂SO₄, filtered, concentrated

and purified by column chromatography using mobile phase DCM/MeOH (95:5) to give crude product **223** as yellow oil. Yield 79 % after two steps.

^1H NMR (599 MHz, Chloroform-*d*) δ 3.08 – 2.99 (m, 2H), 2.80 (t, $J = 7.1$ Hz, 2H), 2.62 (t, $J = 7.0$ Hz, 2H), 2.42 (d, $J = 7.0$ Hz, 2H), 2.27 – 2.16 (m, 2H), 1.99 – 1.89 (m, 2H), 1.86 – 1.73 (m, 1H), 1.61 – 1.45 (m, 2H). ^{13}C NMR (151 MHz, CDCl_3) δ 118.89, 118.44, 53.34, 52.59, 32.87, 31.37, 23.88, 15.96.

General procedure D for reduction of carbonitrile groups using LiAlH_4



The 4 M solution of LiAlH_4 in Et_2O (4.6 eq) was added into anhydrous THF under N_2 atmosphere. The compound **209**, **210**, **214** and **225** (1.0 eq) was dissolved in anhydrous THF (20 mL) and the solution was drop wise introduced in the solution of LiAlH_4 . The reaction mixture was heated to 90°C for 4 hours. The result was cooled to 0°C and slowly neutralized by H_2O and then by 10 % solution of NaOH . The solid was filtered and the filtrate was directly purified by column chromatography using mobile phase DCM/MeOH/ NH_4OH (6:3:1) to give crude product **211**, **212**, **215** and **226**.

2-[4-(2-aminoethyl)piperazin-1-yl]ethan-1-amine (211): Prepared according to the general method D. The compound **209** (585 mg; 3.56 mmol); LiAlH_4 (4 M in Et_2O) (4.1 mL; 16.4 mmol). Neutralization 1 mL H_2O and 3 mL of 10 % NaOH . Yield > 99 % as dark yellow oil.

^1H NMR (600 MHz, Chloroform-*d*) δ 2.78 (t, $J = 6.2$ Hz, 8H), 2.48 (bs, 4H), 2.41 (t, $J = 6.2$ Hz, 8H). ^{13}C NMR (151 MHz, CDCl_3) δ 61.34, 53.49, 38.97.

3-[4-(2-aminoethyl)piperazin-1-yl]propan-1-amine (215): Prepared according to the general method D. The compound **214** (921 mg; 5.17 mmol); LiAlH_4 (4 M in Et_2O) (6.5 mL; 25.85 mmol). Neutralization 2 mL H_2O and 4.5 mL of 10 % NaOH . Yield 61 % as dark yellow oil.

^1H NMR (600 MHz, Chloroform-*d*) δ 2.88 (t, $J = 4.9$ Hz, 2H), 2.81 – 2.71 (m, 4H), 2.52 – 2.34 (m, 10H), 1.66 – 1.61 (m, 2H). ^{13}C NMR (151 MHz, CDCl_3) δ 61.77, 61.15, 56.52, 46.10, 40.84, 38.79, 30.43.

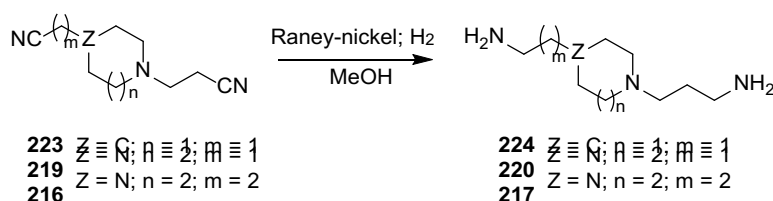
2-[4-(2-aminoethyl)-1,4-diazepan-1-yl]ethan-1-amine (212): Prepared according to the general method D. The compound **210** (785 mg; 4.4 mmol); LiAlH_4 (4 M in Et_2O) (5.0 mL; 20.26 mmol). Neutralization 1 mL H_2O and 4 mL of 10 % NaOH. Yield 84 % as dark yellow oil.

^1H NMR (600 MHz, Chloroform-*d*) δ 2.75 – 2.71 (m, 4H), 2.70 – 2.64 (m, 8H), 2.55 – 2.51 (m, 4H), 1.80 – 1.74 (m, 2H). ^{13}C NMR (151 MHz, CDCl_3) δ 60.83, 55.42, 54.38, 39.58, 27.81.

2-[1-(2-aminoethyl)piperidin-4-yl]ethan-1-amine (226): Prepared according to the general method D. The compound **225** (684 mg; 4.19 mmol); LiAlH_4 (4 M in Et_2O) (4.8 mL; 19.3 mmol). Neutralization 1 mL H_2O and 4 mL of 10 % NaOH. Yield > 99 % as dark yellow oil.

^1H NMR (599 MHz, $\text{DMSO-}d_6$) δ 2.91 (dt, $J = 11.7, 3.4$ Hz, 2H), 2.71 (t, $J = 6.6$ Hz, 2H), 2.69 – 2.63 (m, 2H), 2.38 (t, $J = 6.6$ Hz, 2H), 1.97 (td, $J = 11.7, 2.5$ Hz, 2H), 1.75 – 1.67 (m, 2H), 1.45 – 1.35 (m, 3H), 1.28 – 1.17 (m, 2H).

General procedure E for reduction of carbonitrile groups using Raney-nickel



The compound **216**, **219** and **223** (1.0 eq) was dissolved in anhydrous MeOH under N_2 atmosphere and Raney-nickel (10.0 eq) was added. The N_2 atmosphere was 5 times evacuated and replaced then N_2 was switched to H_2 again 5 times was evacuated and replaced. The reaction mixture was stirred under H_2 atmosphere and controlled by TLC. After finishing the solid was carefully filtered and the filtrate was directly purified by column chromatography using mobile phase DCM/MeOH/ NH_4OH (6:3:1) to give crude product **217**, **220** and **224**.

3-[4-(2-aminoethyl)-1,4-diazepan-1-yl]propan-1-amine (220): Prepared according to the general method E. The compound **219** (831 mg; 4.32 mmol); Raney-nickel (2800,

slurry, in H₂O) (2.536 g; 43.2 mmol); MeOH 25 mL. Yield 44 % of impure product as dark yellow oil. Used in the next reaction without characterization.

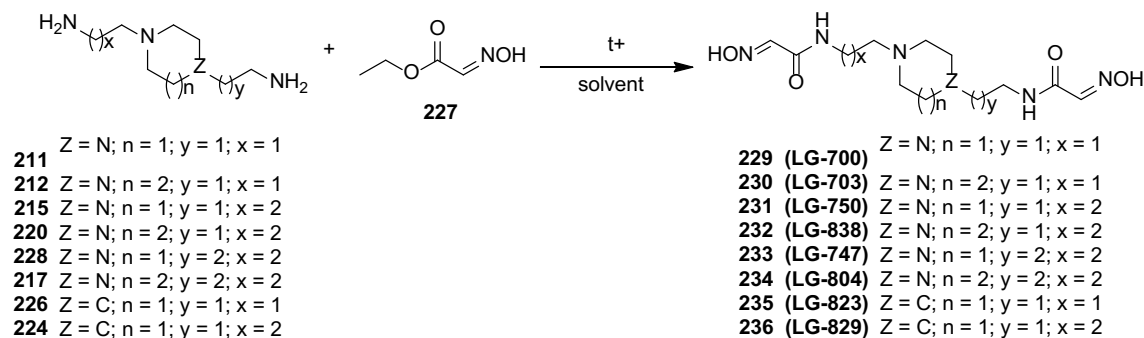
3-[4-(3-aminopropyl)-1,4-diazepan-1-yl]propan-1-amine (217): Prepared according to the general method E. The compound **216** (1.417 g; 6.87 mmol); Raney-nickel (2800, slurry, in H₂O) (4.03 g; 68.7 mmol); MeOH 50 mL. Yield 92 % as dark yellow oil.

¹H NMR (599 MHz, Chloroform-*d*) δ 2.85 (t, *J* = 6.8 Hz, 4H), 2.82 – 2.77 (m, 8H), 2.67 – 2.59 (m, 4H), 1.95 – 1.86 (m, 2H), 1.74 (p, *J* = 7.0 Hz, 4H). ¹³C NMR (151 MHz, CDCl₃) δ 56.19, 54.97, 54.35, 40.62, 30.98, 27.19.

3-[4-(2-aminoethyl)piperidin-1-yl]propan-1-amine (224): Prepared according to the general method E. The compound **223** (1.094 g; 6.17 mmol); Raney-nickel (2800, slurry, in H₂O) (3.621 g; 61.7 mmol); MeOH 30 mL. Yield 73 % as dark yellow oil.

¹H NMR (599 MHz, Chloroform-*d*) δ 3.10 – 2.97 (m, 2H), 2.90 – 2.68 (m, 4H), 2.53 – 2.42 (m, 2H), 2.04 – 1.95 (m, 2H), 1.84 – 1.58 (m, 8H), 1.57 – 1.48 (m, 2H), 1.48 – 1.42 (m, 1H), 1.42 – 1.32 (m, 2H). ¹³C NMR (151 MHz, CDCl₃) δ 56.83, 54.04, 40.88, 39.56, 32.36, 30.79, 26.53.

General procedure F for the final step: bis-amide formation



The compound **211**, **212**, **215**, **217**, **220**, **224**, **226** or **228** (1.0 eq) and oxime-fragment **227** (2.5 eq) was dissolved in solvent (3 mL) and heated for up to several days.

(2E)-2-(N-hydroxyimino)-N-[2-(4-{2-[(2E)-2-(N-hydroxyimino)acetamido]ethyl}piperazin-1-yl)ethyl]acetamide (229): Prepared according general procedure E. **211** (590 mg; 3.425 mmol); oxime fragment **227** (1.003 g ; 8.56 mmol); EtOH (3 mL) heated to 90 °C for 2 days. The solution was

concentrated and directly purified by column chromatography using mobile phase DCM/MeOH (4:1). The result was precipitated in cold MeOH and filtered to give crude product **229** as white solid. Yield 10 %.

^1H NMR (600 MHz, DMSO- d_6) δ 11.94 (s, 2H), 7.95 (t, $J = 5.8$ Hz, 2H), 7.42 (s, 2H), 3.23 (q, $J = 6.5$ Hz, 4H), 2.36 (t, $J = 6.8$ Hz, 12H). ^{13}C NMR (151 MHz, DMSO) δ 162.08, 144.10, 57.09, 53.11, 36.29. HRMS (ESI $^+$): $[\text{M}]^+$: calculated for $\text{C}_{12}\text{H}_{23}\text{N}_6\text{O}_4^+$ (m/z): 315.1775; detected: 315.1772. LC-MS purity > 95 %.

(2E)-2-(N-hydroxyimino)-N-[2-(4-{2-[(2E)-2-(N-hydroxyimino)acetamido]ethyl}-1,4-diazepan-1-yl)ethyl]acetamide (230): Prepared according general procedure E. **212** (305 mg; 1.64 mmol); oxime fragment **227** (480 mg ; 4.1 mmol); EtOH (3 mL) heated to 90 °C for 3 days. The solution was concentrated and directly purified by column chromatography using mobile phase DCM/MeOH (2:1). The result was precipitated in cold MeOH and filtered to give crude product **230** as white solid. Yield 19 %.

^1H NMR (600 MHz, DMSO- d_6) δ 11.95 (s, 2H), 7.93 (t, $J = 5.7$ Hz, 2H), 7.41 (s, 2H), 3.20 (q, $J = 6.5$ Hz, 4H), 2.67 – 2.56 (m, 8H), 2.52 (t, $J = 6.8$ Hz, 4H), 1.65 (p, $J = 5.8$ Hz, 2H). ^{13}C NMR (151 MHz, DMSO) δ 162.09, 144.12, 56.50, 55.04, 54.01, 37.01, 27.69. HRMS (ESI $^+$): $[\text{M}]^+$: calculated for $\text{C}_{13}\text{H}_{25}\text{N}_6\text{O}_4^+$ (m/z): 329.1932; detected: 329.1931. LC-MS purity > 98 %.

(2E)-2-(N-hydroxyimino)-N-[3-(4-{2-[(2E)-2-(N-hydroxyimino)acetamido]ethyl}piperazin-1-yl)propyl]acetamide (231): Prepared according general procedure E. **215** (570 mg; 3.06 mmol); oxime fragment **227** (896 mg ; 7.65 mmol); EtOH (3 mL) heated to 90 °C for 2 days. The solution was concentrated and directly purified by column chromatography using mobile phase DCM/MeOH (2:1). The result was precipitated in cold MeOH and filtered to give crude product **231** as white solid. Yield 14 %.

^1H NMR (600 MHz, DMSO- d_6) δ 11.96 (s, 1H), 11.91 (s, 1H), 8.22 (t, $J = 5.8$ Hz, 1H), 7.98 (t, $J = 5.8$ Hz, 1H), 7.42 (s, 1H), 7.41 (s, 1H), 3.24 (q, $J = 6.5$ Hz, 2H), 3.14 (q, $J = 6.5$ Hz, 2H), 2.46 – 2.25 (m, 12H), 1.58 (p, $J = 7.0$ Hz, 2H). ^{13}C NMR (151 MHz, DMSO) δ 162.13, 144.20, 144.08, 56.98, 55.97, 37.53, 36.26, 26.34. HRMS (ESI $^+$):

[M]⁺: calculated for C₁₃H₂₅N₆O₄⁺ (m/z): 329.1932; detected: 329.1933. LC-MS purity > 98 %.

(2E)-2-(N-hydroxyimino)-N-[3-(4-{2-[(2E)-2-(N-hydroxyimino)acetamido]ethyl}-1,4-diazepan-1-yl)propyl]acetamide (232): Prepared according general procedure E. **220** (369 mg; 1.84 mmol); oxime fragment **227** (539 mg ; 4.6 mmol); EtOH (3 mL) heated to 90 °C for 5 days. The solution was concentrated and directly purified by column chromatography using mobile phase DCM/MeOH (2:1) to MeOH alone to give impure product **232** as orange oil. Yield 5 %.

¹H NMR (599 MHz, DMSO-*d*₆) δ 8.12 – 7.95 (m, 2H), 7.58 – 7.38 (m, 2H), 3.34 – 3.17 (m, 4H), 2.69 – 2.59 (m, 6H), 2.50 (t, *J* = 7.1 Hz, 2H), 1.75 (p, *J* = 5.7 Hz, 2H), 1.64 (p, *J* = 7.2 Hz, 2H), 1.26 – 1.15 (m, 2H), 1.13 (t, *J* = 7.1 Hz, 2H). ¹³C NMR (151 MHz, DMSO) δ 162.16, 162.13, 144.17, 144.06, 56.51, 55.74, 55.13, 54.68, 54.16, 53.96, 37.57, 36.98, 27.39, 27.18. HRMS (ESI⁺): [M]⁺: calculated for C₁₄H₂₇N₆O₄⁺ (m/z): 343.2088; detected: 343.2084. LC-MS purity > 87 %.

(2E)-2-(N-hydroxyimino)-N-[3-(4-{3-[(2E)-2-(N-hydroxyimino)acetamido]propyl}piperazin-1-yl)propyl]acetamide (233): Prepared according general procedure E. **228** (504 mg; 2.516 mmol); oxime fragment **227** (737 mg ; 6.29 mmol); EtOH (3 mL) heated to 90 °C for 3 days. The solution was concentrated and directly purified by column chromatography using mobile phase DCM/MeOH (2:1). The result was precipitated in cold MeOH and filtered to give crude product **233** as white solid. Yield 13 %.

¹H NMR (600 MHz, DMSO-*d*₆) δ 11.89 (s, 2H), 8.19 (s, 2H), 7.40 (s, 2H), 3.14 (q, *J* = 7.0 Hz, 4H), 2.50 – 2.49 (m, 4H), 2.25 (t, *J* = 7.0 Hz, 8H), 1.57 (p, *J* = 7.0 Hz, 4H). ¹³C NMR (151 MHz, DMSO) δ 162.10, 144.22, 56.07, 37.61, 26.52. HRMS (ESI⁺): [M]⁺: calculated for C₁₄H₂₇N₆O₄⁺ (m/z): 343.2088; detected: 343.2086. LC-MS purity > 97 %.

(2E)-2-(N-hydroxyimino)-N-[3-(4-{3-[(2E)-2-(N-hydroxyimino)acetamido]propyl}-1,4-diazepan-1-yl)propyl]acetamide (234): Prepared according general procedure E. **217** (445 mg; 2.076 mmol); oxime fragment **227** (608 mg ; 5.19 mmol); MeCN (3 mL) heated to 50 °C for 2 days. The solution filtered and carefully washed with cold EtOH to give crude product **234** as white solid. Yield 9 %.

^1H NMR (599 MHz, DMSO- d_6) δ 8.21 (t, J = 6.0 Hz, 2H), 7.41 (s, 2H), 3.15 (q, J = 6.7 Hz, 4H), 2.60 – 2.53 (m, 8H), 2.41 (t, J = 7.2 Hz, 4H), 1.72 – 1.62 (m, 2H), 1.60 – 1.49 (m, 4H). ^{13}C NMR (151 MHz, DMSO) δ 162.10, 144.19, 144.18, 55.80, 55.02, 54.17, 37.60, 27.38, 27.26. HRMS (ESI $^+$): $[\text{M}]^+$: calculated for $\text{C}_{15}\text{H}_{29}\text{N}_6\text{O}_4^+$ (m/z): 357.2245; detected: 357.2242. LC-MS purity > 98 %.

(2E)-2-(N-hydroxyimino)-N-[2-(1-{2-[(2E)-2-(N-hydroxyimino)acetamido]ethyl}piperidin-4-yl)ethyl]acetamide (235): Prepared according general procedure E. **226** (694 mg; 4.05 mmol); oxime fragment **227** (1.186 g ; 10.125 mmol); EtOH (3 mL) heated to 90 °C for 1 day. The solution was concentrated and directly purified by column chromatography using mobile phase DCM/MeOH (5:1) to give crude product **235** as yellowish solid. Yield 13 %.

^1H NMR (599 MHz, DMSO- d_6) δ 12.26 (s, 1H), 12.13 (s, 1H), 8.62 (t, J = 5.9 Hz, 1H), 8.43 (t, J = 6.0 Hz, 1H), 7.65 – 7.54 (m, 2H), 3.63 (q, J = 6.3 Hz, 2H), 3.51 – 3.40 (m, 2H), 3.35 – 3.25 (m, 2H), 3.16 – 3.06 (m, 2H), 2.91 – 2.76 (m, 2H), 1.99 – 1.87 (m, 2H), 1.62 – 1.48 (m, 5H). ^{13}C NMR (151 MHz, DMSO) δ 162.66, 162.19, 144.14, 143.83, 68.99, 56.20, 52.42, 45.74, 36.21, 34.38, 30.00. HRMS (ESI $^+$): $[\text{M}]^+$: calculated for $\text{C}_{13}\text{H}_{24}\text{N}_5\text{O}_4^+$ (m/z): 314.1823; detected: 314.1823. LC-MS purity > 95 %.

(2E)-2-(N-hydroxyimino)-N-[3-(4-{2-[(2E)-2-(N-hydroxyimino)acetamido]ethyl}piperidin-1-yl)propyl]acetamide (236): Prepared according general procedure E. **224** (406 mg; 2.19 mmol); oxime fragment **227** (513 mg ; 5.475 mmol); EtOH (3 mL) heated to 90 °C for 3 days. The solution was concentrated and directly purified by column chromatography using mobile phase DCM/MeOH (4:1) to give crude product **236** as yellowish solid. Yield 17 %.

^1H NMR (599 MHz, DMSO- d_6) δ 12.13 – 11.81 (m, 2H), 8.23 (t, J = 5.8 Hz, 1H), 8.13 (t, J = 5.9 Hz, 1H), 7.42 (s, 1H), 7.41 (s, 1H), 3.16 – 3.12 (m, 4H), 2.89 – 2.75 (m, 2H), 2.27 (t, J = 7.1 Hz, 2H), 1.82 (t, J = 11.4 Hz, 2H), 1.67 – 1.51 (m, 4H), 1.36 (q, J = 7.1 Hz, 2H), 1.27 – 1.17 (m, 1H), 1.14 – 1.10 (m, 2H). ^{13}C NMR (151 MHz, DMSO) δ 162.13, 162.07, 144.19, 144.18, 68.97, 56.40, 56.22, 53.75, 37.68, 36.49, 36.08, 32.01, 30.01, 26.46. HRMS (ESI $^+$): $[\text{M}]^+$: calculated for $\text{C}_{14}\text{H}_{26}\text{N}_5\text{O}_4^+$ (m/z): 328.1979; detected: 328.1975. LC-MS purity > 95 %.

6.2 Biological evaluation

6.2.1 Inhibitory assays

Cholinesterase enzymatic activity assay

The enzymatic activities of recombinant *hAChE*, *hBChE* and *AgAChE1* were determined using modified Ellman's assay [143]. Briefly, the recombinant enzymes were mixed with DTNB in 0.1 M phosphate buffer, pH 7.4 and the reactions were initiated by addition of the appropriate substrate (acetylthiocholine or butyrylthiocholine). The final concentrations were 2.0 mM for DTNB and 1.0 mM for substrate. The measurement was performed at 37 °C and the activity was determined as the change in absorbance per one minute ($\Delta A \text{ min}^{-1}$) measured at 412 nm using a Multi-mode microplate reader Synergy 2 (Vermont, USA) in 100 μL reactions. All reactions were measured in at least triplicate and the means were used for statistical analysis.

The recombinant *AgAChE1* enzyme was assayed for enzyme kinetics parameters – the maximum velocity (V_{max}) and Michaelis constant (K_{M}). The enzyme was mixed with various concentrations of substrate (ranging from 3 μM to 10 mM) and the reaction was measured using modified Ellman's assay [143]. The activity data of the enzyme was plotted versus the substrate concentration data and non-linear regression analysis was used to determine the K_{M} and V_{max} values in GraphPad Prism 5 Software.

Inhibition potency and selectivity index determination

The inhibitory potential of novel compounds and standard insecticides was determined spectrophotometrically at inhibitor's maximum inhibition time. All inhibitors were prepared in dimethyl sulfoxide (DMSO) at 10 mM concentration as stock solutions and then diluted in 0.1 M phosphate buffer, pH 7.4 to the final concentrations of 1 μM to – 0.01 nM and below 1% of DMSO concentration. For the half inhibitory concentration values (IC_{50}) determination, the enzymes were incubated with DTNB at five different inhibitors concentrations at their maximum inhibition time prior to addition of the substrates. The IC_{50} values from three independent experiments for each inhibitor concentration in triplicate were calculated using non-linear regression curve analysis in GraphPad Prism 5 Software (San Diego, USA). The selectivity index was determined as ratio of IC_{50} (*hAChE*) / IC_{50} (*AgAChE1*) values.

Potentiometric method

The enzyme activity of *hAChE* was determined using end-point acid-base titration, where the acetic acid derived from the acetylcholine was titrated by 0.01 M NaOH giving the pH of 7.4. The inhibitors in different concentrations were premixed with *hAChE* and the enzyme/inhibitor mixtures were incubated for their maximum inhibition time at 25°C and subsequently added to the potentiometric assay buffer (0.3 M NaCl, pH 7.4). The reaction was started by addition of acetylcholine iodide to the final concentration of 1.6 mM. The enzyme activity was determined by end-point acid-base titration to pH 7.4 by 0.01 M NaOH using a Titrand 842 apparatus (Metrohm-Switzerland). Each inhibitor concentration was assayed at least in triplicate. The activity of non-inhibited enzyme was measured by the same reaction without any present inhibitor. The enzymatic activities of the non-inhibited (A_0) and inhibited enzyme (A_i) were calculated from the amount of NaOH titrant solution used to reach the pH 7.4. The percentage of enzyme remaining activity after inhibition (% A) was calculated according to the formula (Table S1):

$$\%A = \left(1 - \frac{A_0 - A_i}{A_0}\right) \cdot 100$$

Mechanism of the inhibition

The binding mode of the inhibitors was determined using the rapid dilution assay. The enzymes were pre-incubated with appropriate inhibitors in 0.1 M potassium phosphate buffer pH 7.4 for their maximum inhibition time at 25°C. After the inhibition was completed, an aliquot of enzyme/inhibitor mixture was diluted ten times in 0.1 M potassium phosphate buffer pH 7.4 for 10 minutes and the residual activity of the enzyme-inhibitor complex was measured using modified Ellman's assay [143]. The undiluted inhibited enzyme residual activity was used for control reaction.

6.2.2 Reactivation assays

Czech republic – Department of toxicology and military pharmacy

Reactivation potency of standard and tacroximes was evaluated on human recombinant AChE and human plasma BChE. Enzyme was inhibited by the solution of

appropriate cholinesterase inhibitor – tabun, sarin, paraoxon, dichlorvos and VX in propan-2-ol at concentration 10^{-5} M for 60 min. Excess of inhibitor was subsequently removed using octadecylsilane-bonded silica gel SPE cartridge. Inhibited enzyme was incubated for 10 min with solution of reactivator in concentrations 10^{-4} and 10^{-5} M at 37 °C. The reaction was started by addition of substrate acetylthiocholine/butyrylthiocholine. Activity of AChE/BChE was then measured spectrophotometrically at 412 nm by the modified method according to Ellman [143]. Each concentration of reactivator was assayed in triplicate. The obtained data were used to compute reactivation potency (R; Equation 1). Results were corrected for oximolysis and inhibition of AChE/BChE by reactivator.

$$R = \left(1 - \frac{\Delta A_0 - \Delta A_r}{\Delta A_0 - \Delta A_i} \right) \times 100 \quad [\%] \quad (\text{Eq. 1})$$

ΔA_0 indicates absorbance change caused by intact AChE/BChE (phosphate buffer was used instead of AChE/BChE inhibitor solution); ΔA_i indicates absorbance change provided by cholinesterase exposed inhibitors and ΔA_r indicates absorbance change caused by AChE/BChE incubated with solution of reactivator.

USA – SSPPS UCSD

Enzymes – Monomeric hAChE was expressed in stably transfected HEK-293 cells (American Type Culture Collection, Manassas, VA) obtained upon calcium phosphate transfection with pCMV-N-FLAG (Sigma-Aldrich) construct of hAChE encoding cDNA with a stop codon truncating the sequence at amino acid 547. Selection of neomycin-resistant cell colonies using G418 (Invitrogen) enhanced expression. The expressed secreted protein containing the N-terminal FLAG tag was purified in several milligram quantities by an anti-FLAG affinity column (Sigma-Aldrich).

Organophosphates – Nonvolatile, low toxicity fluorescent methylphosphonates (Flu-MPs) (13) were used as analogues of nerve agents sarin, cyclosarin, and VX. The Flu-MPs differ from actual nerve agent OPs only by structure of their respective leaving groups. Inhibition of ChEs by Flu-MPs results in OPChE covalent conjugates identical to the ones formed upon inhibition with nerve agents. Paraoxon was purchased from Sigma-Aldrich.

Oxime Reactivation Assays – *hAChE* activities were measured using a spectrophotometric assay (21) at 37 °C (or 25 °C for tabun conjugates) in 0.1 M sodium phosphate buffer, pH 7.4, containing 0.01% BSA and substrate acetylthiocholine (ATCh) at 1.0 mM *hAChE* concentration. OP-*hAChE* conjugates were prepared by incubating micromolar enzyme stocks with 4-fold molar excess of OP for 2–3 min until inhibition exceeded 95%. Inhibited enzymes and appropriate controls were passed through two consecutive size exclusion Sephadex G-50 spin columns (Roche Diagnostics) to remove excess inhibitor. The reactivation reaction was initiated by adding an oxime reactivator at 0.1, 0.5 and 1.0 mM final concentrations into a nanomolar solution of OP-conjugated enzymes. Control ChE activity was measured in the presence of oxime at concentrations used for reactivation. The time course of *hAChE* reactivation was monitored in 96-well format by parallel consecutive assays of *hAChE* activity in 10 µL of reactivation mixture aliquots diluted 625 times into assay mixture containing ATCh and thiol detection reagent 5,5'-dithiobis-(2-nitrobenzoic acid). The first order reactivation rate constant (k_{obs}) for each oxime + OP conjugate combination was calculated by nonlinear regression. The dependence of reactivation rates on oxime concentrations and determination of maximal reactivation rate constant k_2 , Michaelis-Menten type constant K_{ox} , and the overall second order reactivation rate constant k_r were conducted as previously as described [158].

6.2.3 BBB penetration estimation assays

Pampa assay

The filter membrane of the donor plate was coated with PBL (Polar Brain Lipid, Avanti, AL, USA) in dodecane (4 µL of 20 mg/mL PBL in dodecane) and the acceptor well was filled with 300 µL of PBS pH 7.4 buffer (V_A). Tested compounds were dissolved first in DMSO and that diluted with PBS pH 7.4 to reach the final concentration 100 µM in the donor well. Concentration of DMSO did not exceed 0.5% (v/v) in the donor solution. 300 µL of the donor solution was added to the donor wells (V_D) and the donor filter plate was carefully put on the acceptor plate so that coated membrane was “in touch” with both donor solution and acceptor buffer. Test compound diffused from the donor well through the lipid membrane (Area = 0.28 cm²) to the acceptor well. The concentration of the drug in both donor and the acceptor wells were assessed after 3, 4, 5 and 6 h of incubation in quadruplicate using

the UV plate reader Synergy HT (Biotek, Winooski, VT, USA) at the maximum absorption wavelength of each compound. Concentration of the compounds was calculated from the standard curve and expressed as the permeability (Pe) according the equation:

$$\log P_e = \left\{ C \times \ln \left(1 - \frac{[drug]_{acceptor}}{[drug]_{equilibrium}} \right) \right\} \text{ where } C = \frac{(V_D \times V_A)}{(V_D \times V_A) \text{ Area} \times \text{Time}}$$

MDCK assay

The MDCK assay evaluates the ability of compounds to diffuse from the donor compartment through the MDCK's cell membrane into the acceptor compartment. The MDCK cells were seeded on polycarbonate membrane (area 1.12 cm²) with 3 µm pores of the 12-well plates with 12 mm inserts. The tested compounds were dissolved in DMSO and then diluted with OptiMEM to reach final concentrations (in range XX-XX µM), the concentration of DMSO didn't exceed 0,5 % (V/V). 750 µl of the donor solution was added to the donor compartment (insert) and the same volume of OptiMEM was added into the acceptor. The concentration of the drug in both compartments was measured by UV-VIS spectrophotometry, HPLC-UV or HPLC-MS in 1, 2, 4 and 6 h of incubation in triplicates. The apparent permeability coefficient (P_{app}) was calculated from concentrations ratio. Tightness of MDCK monolayer is assessed by permeability of FITC (fluorescein isothiocyanate) in 0,4 mg/ml. Novel compounds were assessed only once as they show negligible values confirming very low penetrating ability.

$$P_{app} = \left(\frac{dC}{dt} \right) \times \frac{V_r}{(A \times C_0)}$$

A area of the well/cell monolayer

dC/dt amount in the receiver compartment in given time

V_r volume of the receiver compartment

C₀ the initial concentration of tested compounds

6.2.4 Additional measurements

Colorimetric cell viability assay (MTT)

The MTT (3-(4,5-dimethylthiazol-2-yl)-2,5-diphenyl-tetrazolium bromide (Sigma–Aldrich, St. Louis, MO, USA) reduction assay was used for measurement of compounds cytotoxicity according to Mosmann et al. (1983) [159]. MTT is a water soluble tetrazolium salt and it is converted to purple formazan by succinate dehydrogenase in mitochondria of viable cells [159, 160]. Cell viability was detected after 24-hour incubation with the tested substances. For the assay, HepG2 cells were seeded into 96-well plates in 100 μ l volume and density of 15×10^3 per well. Cells were allowed to attach overnight before the treatment. The stock solution of tested compounds were prepared in dimethylsulfoxide (DMSO, Sigma-Aldrich), which were further serially diluted in DMEM and added to the cells in 96-well culture plate. The final concentration of DMSO was less than 0.25% per well.

After 24 hour incubation, the medium containing serially diluted substances was aspirated from each well and replaced by 100 μ L of fresh medium containing MTT (0.5 mg/ml). Plates were subsequently incubated at 37 °C in a CO₂ incubator for 45 min. Medium containing MTT was then aspirated and formazan dissolved in 100 μ L of DMSO. The optical density of each well was measured using Synergy 2 Multi-Mode Microplate Reader (BioTek Instruments, Inc., Winooski, VT, USA) at 570 nm. The cell viability was expressed as the percentage of untreated control. Each experiment was performed in triplicate and repeated four independent times [161].

The IC₅₀ values were calculated using four parametric nonlinear regressions by statistic GraphPad Prism software (version 5.04, GraphPad Software Inc., San Diego, CA) from the logarithmic dose–response curve. The IC₅₀ values were expressed as a mean \pm standard error of the mean (SEM).

7. References

- [1] TOUGU, V. Acetylcholinesterase: Mechanism of Catalysis and Inhibition. *Current Medicinal Chemistry-Central Nervous System Agents* [online]. 2001, **1**(2), 155–170. ISSN 15680150. Dostupné z: doi:10.2174/1568015013358536
- [2] QUINN, Daniel M. Acetylcholinesterase: enzyme structure, reaction dynamics, and virtual transition states. *Chemical Reviews* [online]. 1987, **87**(5), 955–979. ISSN 0009-2665, 1520-6890. Dostupné z: doi:10.1021/cr00081a005
- [3] LOCKRIDGE, Oksana. Review of human butyrylcholinesterase structure, function, genetic variants, history of use in the clinic, and potential therapeutic uses. *Pharmacology & Therapeutics* [online]. 2015, **148**, 34–46. ISSN 1879-016X. Dostupné z: doi:10.1016/j.pharmthera.2014.11.011
- [4] COSTANZI, Stefano, John-Hanson MACHADO a Moriah MITCHELL. Nerve Agents: What They Are, How They Work, How to Counter Them. *ACS Chemical Neuroscience* [online]. 2018, **9**(5), 873–885. Dostupné z: doi:10.1021/acscemneuro.8b00148
- [5] SUSSMAN, J. L., M. HAREL, F. FROLOW, C. OEFNER, A. GOLDMAN, L. TOKER a I. SILMAN. Atomic structure of acetylcholinesterase from *Torpedo californica*: a prototypic acetylcholine-binding protein. *Science (New York, N.Y.)*. 1991, **253**(5022), 872–879. ISSN 0036-8075.
- [6] BERG, Lotta, C. David ANDERSSON, Elisabet ARTURSSON, Andreas HÖRNBERG, Anna-Karin TUNEMALM, Anna LINUSSON a Fredrik EKSTRÖM. Targeting Acetylcholinesterase: Identification of Chemical Leads by High Throughput Screening, Structure Determination and Molecular Modeling. *PLoS ONE* [online]. 2011, **6**(11), e26039. ISSN 1932-6203. Dostupné z: doi:10.1371/journal.pone.0026039
- [7] SINGH, Manjinder, Maninder KAUR, Hitesh KUKREJA, Rajan CHUGH, Om SILAKARI a Dhandeep SINGH. Acetylcholinesterase inhibitors as Alzheimer therapy: from nerve toxins to neuroprotection. *European Journal of Medicinal Chemistry* [online]. 2013, **70**, 165–188. ISSN 1768-3254. Dostupné z: doi:10.1016/j.ejmech.2013.09.050
- [8] BAJDA, Marek, Anna WIĘCKOWSKA, Michalina HEBDA, Natalia GUZIOR, Christoph SOTRIFFER a Barbara MALAWSKA. Structure-Based Search for New Inhibitors of Cholinesterases. *International Journal of Molecular Sciences* [online]. 2013, **14**(3), 5608–5632. ISSN 1422-0067. Dostupné z: doi:10.3390/ijms14035608
- [9] HAREL, M., I. SCHALK, L. EHRET-SABATIER, F. BOUET, M. GOELDNER, C. HIRTH, P. H. AXELSEN, I. SILMAN a J. L. SUSSMAN. Quaternary ligand binding to aromatic residues in the active-site gorge of acetylcholinesterase. *Proceedings of the National Academy of Sciences of the United States of America*. 1993, **90**(19), 9031–9035. ISSN 0027-8424.

- [10] TERRONE L. ROSENBERRY. Acetylcholinesterase. In: *Advances in Enzymology and Related Areas of Molecular Biology*. 22 NOV 2006: John Wiley & Sons, nedatováno, 43, s. 104–112. ISBN 978-0-470-12288-4.
- [11] MASSOULIÉ, J. a S. BON. The molecular forms of cholinesterase and acetylcholinesterase in vertebrates. *Annual Review of Neuroscience* [online]. 1982, **5**, 57–106. ISSN 0147-006X. Dostupné z: doi:10.1146/annurev.ne.05.030182.000421
- [12] BOURNE, Yves, Hartmuth C. KOLB, Zoran RADIĆ, K. Barry SHARPLESS, Palmer TAYLOR a Pascale MARCHOT. Freeze-frame inhibitor captures acetylcholinesterase in a unique conformation. *Proceedings of the National Academy of Sciences of the United States of America* [online]. 2004, **101**(6), 1449–1454. ISSN 0027-8424. Dostupné z: doi:10.1073/pnas.0308206100
- [13] JOHNSON, G. a S. W. MOORE. The peripheral anionic site of acetylcholinesterase: structure, functions and potential role in rational drug design. *Current Pharmaceutical Design*. 2006, **12**(2), 217–225. ISSN 1381-6128.
- [14] SZEGLETES, T., W. D. MALLENDER, P. J. THOMAS a T. L. ROSENBERRY. Substrate binding to the peripheral site of acetylcholinesterase initiates enzymatic catalysis. Substrate inhibition arises as a secondary effect. *Biochemistry* [online]. 1999, **38**(1), 122–133. ISSN 0006-2960. Dostupné z: doi:10.1021/bi9813577
- [15] GORECKI, Lukas, Jan KORABECNY, Kamil MUSILEK, David MALINAK, Eugenie NEPOVIMOVA, Rafael DOLEZAL, Daniel JUN, Ondrej SOUKUP a Kamil KUCA. SAR study to find optimal cholinesterase reactivator against organophosphorous nerve agents and pesticides. *Archives of Toxicology* [online]. 2016, **90**(12), 2831–2859. ISSN 1432-0738. Dostupné z: doi:10.1007/s00204-016-1827-3
- [16] MERCEY, Guillaume, Tristan VERDELET, Julien RENOU, Maria KLIACHYNA, Rachid BAATI, Florian NACHON, Ludovic JEAN a Pierre-Yves RENARD. Reactivators of Acetylcholinesterase Inhibited by Organophosphorus Nerve Agents. *Accounts of Chemical Research* [online]. 2012, **45**(5), 756–766. ISSN 0001-4842, 1520-4898. Dostupné z: doi:10.1021/ar2002864
- [17] WESTERBERG, M. R., K. R. MAGEE a F. E. SHIDEMAN. Effect of 3-hydroxy phenyl-dimethylethylammonium chloride (tensilon) in myasthenia gravis. *Medical Bulletin (Ann Arbor, Mich.)*. 1951, **17**(9), 311–316. ISSN 0196-5336.
- [18] O'CONNOR, A. A new relaxing agent. *Journal of the Royal Naval Medical Service*. 1949, **35**(3), 220. ISSN 0035-9033.
- [19] KOMLOOVA, M., K. MUSILEK, M. DOLEZAL, F. GUNN-MOORE a K. KUCA. Structure-activity relationship of quaternary acetylcholinesterase

inhibitors - outlook for early myasthenia gravis treatment. *Current Medicinal Chemistry*. 2010, **17**(17), 1810–1824. ISSN 1875-533X.

- [20] KORABECNY, Jan, Rafael DOLEZAL, Pavla CABELOVA, Anna HOROVA, Eva HRUBA, Jan RICNY, Lukas SEDLACEK, Eugenie NEPOVIMOVA, Katarina SPILOVSKA, Martin ANDRS, Kamil MUSILEK, Veronika OPLETALOVA, Vendula SEP SOVA, Daniela RIPOVA a Kamil KUCA. 7-MEOTA-donepezil like compounds as cholinesterase inhibitors: Synthesis, pharmacological evaluation, molecular modeling and QSAR studies. *European Journal of Medicinal Chemistry* [online]. 2014, **82**, 426–438. ISSN 1768-3254. Dostupné z: doi:10.1016/j.ejmech.2014.05.066
- [21] NEPOVIMOVA, Eugenie, Jan KORABECNY, Rafael DOLEZAL, Katerina BABKOVA, Ales ONDREJICEK, Daniel JUN, Vendula SEP SOVA, Anna HOROVA, Martina HRABINOVA, Ondrej SOUKUP, Neslihan BUKUM, Petr JOST, Lubica MUCKOVA, Jiri KASSA, David MALINAK, Martin ANDRS a Kamil KUCA. Tacrine-Troxolone Hybrids: A Novel Class of Centrally Active, Nonhepatotoxic Multi-Target-Directed Ligands Exerting Anticholinesterase and Antioxidant Activities with Low In Vivo Toxicity. *Journal of Medicinal Chemistry* [online]. 2015, **58**(22), 8985–9003. ISSN 1520-4804. Dostupné z: doi:10.1021/acs.jmedchem.5b01325
- [22] NEPOVIMOVA, Eugenie, Elisa ULIASSI, Jan KORABECNY, Luis Emiliano PEÑA-ALTAMIRA, Sarah SAMEZ, Alessandro PESARESI, Gregory E. GARCIA, Manuela BARTOLINI, Vincenza ANDRISANO, Christian BERGAMINI, Romana FATO, Dorian LAMBA, Marinella ROBERTI, Kamil KUCA, Barbara MONTI a Maria Laura BOLOGNESI. Multitarget drug design strategy: quinone-tacrine hybrids designed to block amyloid- β aggregation and to exert anticholinesterase and antioxidant effects. *Journal of Medicinal Chemistry* [online]. 2014, **57**(20), 8576–8589. ISSN 1520-4804. Dostupné z: doi:10.1021/jm5010804
- [23] HAMULAKOVA, Slavka, Ladislav JANOVEC, Martina HRABINOVA, Katarina SPILOVSKA, Jan KORABECNY, Pavol KRISTIAN, Kamil KUCA a Jan IMRICH. Synthesis and biological evaluation of novel tacrine derivatives and tacrine-coumarin hybrids as cholinesterase inhibitors. *Journal of Medicinal Chemistry* [online]. 2014, **57**(16), 7073–7084. ISSN 1520-4804. Dostupné z: doi:10.1021/jm5008648
- [24] MINARINI, Anna, Andrea MILELLI, Elena SIMONI, Michela ROSINI, Maria Laura BOLOGNESI, Chiara MARCHETTI a Vincenzo TUMIATTI. Multifunctional tacrine derivatives in Alzheimer's disease. *Current Topics in Medicinal Chemistry*. 2013, **13**(15), 1771–1786. ISSN 1873-4294.
- [25] AXELSEN, Paul H., Michal HAREL, Israel SILMAN a Joel L. SUSSMAN. Structure and dynamics of the active site gorge of acetylcholinesterase: Synergistic use of molecular dynamics simulation and X-ray crystallography. *Protein Science* [online]. 2008, **3**(2), 188–197. ISSN 09618368, 1469896X. Dostupné z: doi:10.1002/pro.5560030204

- [26] POHANKA, Miroslav. Cholinesterases, a target of pharmacology and toxicology. *Biomedical Papers of the Medical Faculty of the University Palacký, Olomouc, Czechoslovakia*. 2011, **155**(3), 219–229. ISSN 1213-8118.
- [27] LEE, Hyun Jung a Dojin RYU. Advances in Mycotoxin Research: Public Health Perspectives. *Journal of Food Science* [online]. 2015. ISSN 1750-3841. Dostupné z: doi:10.1111/1750-3841.13156
- [28] SHAIKH, Sibghatulla, Anupriya VERMA, Saimeen SIDDIQUI, Syed S. AHMAD, Syed M. D. RIZVI, Shazi SHAKIL, Deboshree BISWAS, Divya SINGH, Mohmmad H. SIDDIQUI, Shahnawaz SHAKIL, Shams TABREZ a Mohammad A. KAMAL. Current acetylcholinesterase-inhibitors: a neuroinformatics perspective. *CNS & neurological disorders drug targets*. 2014, **13**(3), 391–401. ISSN 1996-3181.
- [29] KAMIL KUČA AND MIROSLAV POHANKA. Chemical warfare agents. In: *Molecular, Clinical and Environmental Toxicology*. Switzerland: Birkhäuser Verlag, nedatováno, Clinical Toxicology, 2, s. 543–558.
- [30] MAREŠOVÁ, Petra, Hana MOHELSKÁ, Josef DOLEJŠ a Kamil KUČA. Socio-economic Aspects of Alzheimer's Disease. *Current Alzheimer Research*. 2015, **12**(9), 903–911. ISSN 1875-5828.
- [31] SANABRIA-CASTRO, Alfredo, Ileana ALVARADO-ECHEVERRÍA a Cecilia MONGE-BONILLA. Molecular Pathogenesis of Alzheimer's Disease: An Update. *Annals of Neurosciences* [online]. 2017, **24**(1), 46–54. ISSN 0972-7531. Dostupné z: doi:10.1159/000464422
- [32] BLENNOW, Kaj, Mony J. DE LEON a Henrik ZETTERBERG. Alzheimer's disease. *Lancet (London, England)* [online]. 2006, **368**(9533), 387–403. ISSN 1474-547X. Dostupné z: doi:10.1016/S0140-6736(06)9113-7
- [33] PRINCE, Martin J. *World Alzheimer Report 2015: The Global Impact of Dementia* [online]. 25. srpen 2015 [vid. 2019-01-02]. Dostupné z: <https://www.alz.co.uk/research/world-report-2015>
- [34] CONTESTABILE, Antonio. The history of the cholinergic hypothesis. *Behavioural Brain Research* [online]. 2011, **221**(2), 334–340. ISSN 1872-7549. Dostupné z: doi:10.1016/j.bbr.2009.12.044
- [35] ZEMEK, Filip, Lucie DRTINOVA, Eugenie NEPOVIMOVA, Vendula SEPŠOVA, Jan KORABECNY, Jiri KLIMES a Kamil KUČA. Outcomes of Alzheimer's disease therapy with acetylcholinesterase inhibitors and memantine. *Expert Opinion on Drug Safety* [online]. 2014, **13**(6), 759–774. ISSN 1744-764X. Dostupné z: doi:10.1517/14740338.2014.914168
- [36] GIACOBINI, E. Invited review: Cholinesterase inhibitors for Alzheimer's disease therapy: from tacrine to future applications. *Neurochemistry International*. 1998, **32**(5–6), 413–419. ISSN 0197-0186.

- [37] NORDBERG, Agneta, Clive BALLARD, Roger BULLOCK, Taher DARREH-SHORI a Monique SOMOGYI. A review of butyrylcholinesterase as a therapeutic target in the treatment of Alzheimer's disease. *The primary care companion for CNS disorders* [online]. 2013, **15**(2). ISSN 2155-7772. Dostupné z: doi:10.4088/PCC.12r01412
- [38] WANG, Rui a P. Hemachandra REDDY. Role of Glutamate and NMDA Receptors in Alzheimer's Disease. *Journal of Alzheimer's disease: JAD* [online]. 2017, **57**(4), 1041–1048. ISSN 1875-8908. Dostupné z: doi:10.3233/JAD-160763
- [39] SPILOVSKA, Katarina, Filip ZEMEK, Jan KORABECNY, Eugenie NEPOVIMOVA, Ondrej Soukup Manfred WINDISCH a Kamil KUČA. Adamantane - a lead structure for drugs in clinical practice. *Current Medicinal Chemistry*. 2016. ISSN 1875-533X.
- [40] PRATICÒ, Domenico. Evidence of oxidative stress in Alzheimer's disease brain and antioxidant therapy: lights and shadows. *Annals of the New York Academy of Sciences* [online]. 2008, **1147**, 70–78. ISSN 1749-6632. Dostupné z: doi:10.1196/annals.1427.010
- [41] SULTANA, Rukhsana, Patrizia MECOCCI, Francesca MANGIALASCHE, Roberta CECCHETTI, Mauro BAGLIONI a D. Allan BUTTERFIELD. Increased protein and lipid oxidative damage in mitochondria isolated from lymphocytes from patients with Alzheimer's disease: insights into the role of oxidative stress in Alzheimer's disease and initial investigations into a potential biomarker for this dementing disorder. *Journal of Alzheimer's disease: JAD* [online]. 2011, **24**(1), 77–84. ISSN 1875-8908. Dostupné z: doi:10.3233/JAD-2011-101425
- [42] HARDY, J. A. a G. A. HIGGINS. Alzheimer's disease: the amyloid cascade hypothesis. *Science (New York, N.Y.)*. 1992, **256**(5054), 184–185. ISSN 0036-8075.
- [43] SELKOE, Dennis J. a John HARDY. The amyloid hypothesis of Alzheimer's disease at 25 years. *EMBO molecular medicine* [online]. 2016, **8**(6), 595–608. ISSN 1757-4684. Dostupné z: doi:10.15252/emmm.201606210
- [44] MASTERS, C L, G SIMMS, N A WEINMAN, G MULTHAUP, B L MCDONALD a K BEYREUTHER. Amyloid plaque core protein in Alzheimer disease and Down syndrome. *Proceedings of the National Academy of Sciences of the United States of America*. 1985, **82**(12), 4245–4249. ISSN 0027-8424.
- [45] KANG, J., H. G. LEMAIRE, A. UNTERBECK, J. M. SALBAUM, C. L. MASTERS, K. H. GRZESCHIK, G. MULTHAUP, K. BEYREUTHER a B. MÜLLER-HILL. The precursor of Alzheimer's disease amyloid A4 protein resembles a cell-surface receptor. *Nature* [online]. 1987, **325**(6106), 733–736. ISSN 0028-0836. Dostupné z: doi:10.1038/325733a0
- [46] TURNER, Paul R., Kate O'CONNOR, Warren P. TATE a Wickliffe C. ABRAHAM. Roles of amyloid precursor protein and its fragments in regulating

- neural activity, plasticity and memory. *Progress in Neurobiology*. 2003, **70**(1), 1–32. ISSN 0301-0082.
- [47] NALIVAEVA, Natalia N. a Anthony J. TURNER. The amyloid precursor protein: a biochemical enigma in brain development, function and disease. *FEBS letters* [online]. 2013, **587**(13), 2046–2054. ISSN 1873-3468. Dostupné z: doi:10.1016/j.febslet.2013.05.010
- [48] LAFERLA, Frank M., Kim N. GREEN a Salvatore ODDO. Intracellular amyloid-beta in Alzheimer's disease. *Nature Reviews. Neuroscience* [online]. 2007, **8**(7), 499–509. ISSN 1471-003X. Dostupné z: doi:10.1038/nrn2168
- [49] BURDICK, D., B. SOREGHAN, M. KWON, J. KOSMOSKI, M. KNAUER, A. HENSCHEN, J. YATES, C. COTMAN a C. GLABE. Assembly and aggregation properties of synthetic Alzheimer's A4/beta amyloid peptide analogs. *The Journal of Biological Chemistry*. 1992, **267**(1), 546–554. ISSN 0021-9258.
- [50] ROHER, A E, J D LOWENSON, S CLARKE, A S WOODS, R J COTTER, E GOWING a M J BALL. beta-Amyloid-(1-42) is a major component of cerebrovascular amyloid deposits: implications for the pathology of Alzheimer disease. *Proceedings of the National Academy of Sciences of the United States of America*. 1993, **90**(22), 10836–10840. ISSN 0027-8424.
- [51] EGAN, Michael F., James KOST, Pierre N. TARIOT, Paul S. AISEN, Jeffrey L. CUMMINGS, Bruno VELLAS, Cyrille SUR, Yuki MUKAI, Tiffini VOSS, Christine FURTEK, Erin MAHONEY, Lyn HARPER MOZLEY, Rik VANDENBERGHE, Yi MO a David MICHELSON. Randomized Trial of Verubecestat for Mild-to-Moderate Alzheimer's Disease. *The New England Journal of Medicine* [online]. 2018, **378**(18), 1691–1703. ISSN 1533-4406. Dostupné z: doi:10.1056/NEJMoal706441
- [52] AVILA, Jesus, Jose J. LUCAS, Mar PEREZ a Felix HERNANDEZ. Role of tau protein in both physiological and pathological conditions. *Physiological Reviews* [online]. 2004, **84**(2), 361–384. ISSN 0031-9333. Dostupné z: doi:10.1152/physrev.00024.2003
- [53] MEDINA, Miguel a Jesús AVILA. New perspectives on the role of tau in Alzheimer's disease. Implications for therapy. *Biochemical Pharmacology* [online]. 2014, **88**(4), Alzheimer's Disease – Amyloid, Tau and Beyond, 540–547. ISSN 0006-2952. Dostupné z: doi:10.1016/j.bcp.2014.01.013
- [54] BALLATORE, Carlo, Virginia M.-Y. LEE a John Q. TROJANOWSKI. Tau-mediated neurodegeneration in Alzheimer's disease and related disorders. *Nature Reviews Neuroscience* [online]. 2007, **8**(9), 663–672. ISSN 1471-0048. Dostupné z: doi:10.1038/nrn2194
- [55] HUANG, Xudong, Robert D. MOIR, Rudolph E. TANZI, Ashley I. BUSH a Jack T. ROGERS. Redox-active metals, oxidative stress, and Alzheimer's disease pathology. *Annals of the New York Academy of Sciences*. 2004, **1012**, 153–163. ISSN 0077-8923.

- [56] HALLIWELL, B. a J. M. GUTTERIDGE. Oxygen toxicity, oxygen radicals, transition metals and disease. *The Biochemical Journal*. 1984, **219**(1), 1–14. ISSN 0264-6021.
- [57] LEE, Hyun Pil, Xiongwei ZHU, Gemma CASADESUS, Rudy J. CASTELLANI, Akihiko NUNOMURA, Mark A. SMITH, Hyoung-gon LEE a George PERRY. Antioxidant approaches for the treatment of Alzheimer's disease. *Expert Review of Neurotherapeutics* [online]. 2010, **10**(7), 1201–1208. ISSN 1744-8360. Dostupné z: doi:10.1586/ern.10.74
- [58] SHARMA, Abha, Vidhu PACHAURI a S. J. S. FLORA. Advances in Multi-Functional Ligands and the Need for Metal-Related Pharmacology for the Management of Alzheimer Disease. *Frontiers in Pharmacology* [online]. 2018, **9**, 1247. ISSN 1663-9812. Dostupné z: doi:10.3389/fphar.2018.01247
- [59] MEZEIOVA, Eva, Katarina SPILOVSKA, Eugenie NEPOVIMOVA, Lukas GORECKI, Ondrej SOUKUP, Rafael DOLEZAL, David MALINAK, Jana JANOCKOVA, Daniel JUN, Kamil KUCA a Jan KORABECNY. Profiling donepezil template into multipotent hybrids with antioxidant properties. *Journal of Enzyme Inhibition and Medicinal Chemistry* [online]. 2018, **33**(1), 583–606. ISSN 1475-6374. Dostupné z: doi:10.1080/14756366.2018.1443326
- [60] FARLOW, Martin R., Stephen M. GRAHAM a Gustavo ALVA. Memantine for the treatment of Alzheimer's disease: tolerability and safety data from clinical trials. *Drug Safety* [online]. 2008, **31**(7), 577–585. ISSN 0114-5916. Dostupné z: doi:10.2165/00002018-200831070-00003
- [61] HYND, Matthew R., Heather L. SCOTT a Peter R. DODD. Glutamate-mediated excitotoxicity and neurodegeneration in Alzheimer's disease. *Neurochemistry International* [online]. 2004, **45**(5), 583–595. ISSN 0197-0186. Dostupné z: doi:10.1016/j.neuint.2004.03.007
- [62] BLACKARD, W. G., G. K. SOOD, D. R. CROWE a M. B. FALLON. Tacrine. A cause of fatal hepatotoxicity? *Journal of Clinical Gastroenterology*. 1998, **26**(1), 57–59. ISSN 0192-0790.
- [63] SOUKUP, Ondrej, Daniel JUN, Jana ZDAROVA-KARASOVA, Jiri PATOCKA, Kamil MUSILEK, Jan KORABECNY, Jan KRUSEK, Martina KANIAKOVA, Vendula SEPSOVA, Jana MANDIKOVA, Frantisek TREJTAR, Miroslav POHANKA, Lucie DRTINOVA, Michal PAVLIK, Gunnar TOBIN a Kamil KUCA. A resurrection of 7-MEOTA: a comparison with tacrine. *Current Alzheimer Research*. 2013, **10**(8), 893–906. ISSN 1875-5828.
- [64] RECANATINI, M., A. CAVALLI, F. BELLUTI, L. PIAZZI, A. RAMPA, A. BISI, S. GOBBI, P. VALENTI, V. ANDRISANO, M. BARTOLINI a V. CAVRINI. SAR of 9-amino-1,2,3,4-tetrahydroacridine-based acetylcholinesterase inhibitors: synthesis, enzyme inhibitory activity, QSAR, and structure-based CoMFA of tacrine analogues. *Journal of Medicinal Chemistry*. 2000, **43**(10), 2007–2018. ISSN 0022-2623.

- [65] SPILOVSKA, Katarina, Jan KORABECNY, Eugenie NEPOVIMOVA, Rafael DOLEZAL, Eva MEZEIOVA, Ondrej SOUKUP a Kamil KUČA. Multitarget Tacrine Hybrids with Neuroprotective Properties to Confront Alzheimer's Disease. *Current Topics in Medicinal Chemistry* [online]. 2017, **17**(9), 1006–1026. ISSN 1873-4294. Dostupné z: doi:10.2174/1568026605666160927152728
- [66] PRATI, Federica, Andrea CAVALLI a Maria Laura BOLOGNESI. Navigating the Chemical Space of Multitarget-Directed Ligands: From Hybrids to Fragments in Alzheimer's Disease. *Molecules (Basel, Switzerland)* [online]. 2016, **21**(4), 466. ISSN 1420-3049. Dostupné z: doi:10.3390/molecules21040466
- [67] WAGER, Travis T., Xinjun HOU, Patrick R. VERHOEST a Anabella VILLALOBOS. Moving beyond Rules: The Development of a Central Nervous System Multiparameter Optimization (CNS MPO) Approach To Enable Alignment of Druglike Properties. *ACS Chemical Neuroscience* [online]. 2010, **1**(6), 435–449. Dostupné z: doi:10.1021/cn100008c
- [68] KORÁBEČNÝ, Jan, Eugenie NEPOVIMOVÁ, Tereza CIKÁNKOVÁ, Katarína ŠPILOVSKÁ, Lucie VAŠKOVÁ, Eva MEZEIOVÁ, Kamil KUČA a Jana HROUDOVÁ. Newly Developed Drugs for Alzheimer's Disease in Relation to Energy Metabolism, Cholinergic and Monoaminergic Neurotransmission. *Neuroscience* [online]. 2018, **370**, 191–206. ISSN 1873-7544. Dostupné z: doi:10.1016/j.neuroscience.2017.06.034
- [69] WHO | World malaria report 2018. *WHO* [online]. [vid. 2019-01-02]. Dostupné z: <http://www.who.int/malaria/publications/world-malaria-report-2018/report/en/>
- [70] *Vector-borne diseases* [online]. [vid. 2019-01-02]. Dostupné z: <https://www.who.int/news-room/fact-sheets/detail/vector-borne-diseases>
- [71] RAGHAVENDRA, Kamaraju, Tapan K. BARIK, B. P. Niranjan REDDY, Poonam SHARMA a Aditya P. DASH. Malaria vector control: from past to future. *Parasitology Research* [online]. 2011, **108**(4), 757–779. ISSN 1432-1955. Dostupné z: doi:10.1007/s00436-010-2232-0
- [72] CARLIER, Paul R., Jeffrey R. BLOOMQUIST, Max TOTROV a Jianyong LI. Discovery of Species-selective and Resistance-breaking Anticholinesterase Insecticides for the Malaria Mosquito. *Current Medicinal Chemistry* [online]. 2017, **24**(27), 2946–2958. ISSN 1875-533X. Dostupné z: doi:10.2174/0929867324666170206130024
- [73] PANG, Yuan Ping. Insect acetylcholinesterase as a target for effective and environmentally safe insecticides. *Advances in Insect Physiology* [online]. 2014, **46**, 435–494. ISSN 0065-2806. Dostupné z: doi:10.1016/B978-0-12-417010-0.00006-9
- [74] WHO | WHO Pesticides Evaluation Scheme. *WHO* [online]. [vid. 2019-01-02]. Dostupné z: http://www.who.int/neglected_diseases/resources/WHOPES/en/

- [75] MNZAVA, Abraham P., Michael B. MACDONALD, Tessa B. KNOX, Emmanuel A. TEMU a Clive J. SHIFF. Malaria vector control at a crossroads: public health entomology and the drive to elimination. *Transactions of the Royal Society of Tropical Medicine and Hygiene* [online]. 2014, **108**(9), 550–554. ISSN 1878-3503. Dostupné z: doi:10.1093/trstmh/tru101
- [76] CASIDA, J. E. a G. B. QUISTAD. Golden age of insecticide research: past, present, or future? *Annual Review of Entomology* [online]. 1998, **43**, 1–16. ISSN 0066-4170. Dostupné z: doi:10.1146/annurev.ento.43.1.1
- [77] RIVERO, Ana, Julien VÉZILIER, Mylène WEILL, Andrew F. READ a Sylvain GANDON. Insecticide Control of Vector-Borne Diseases: When Is Insecticide Resistance a Problem? *PLoS Pathogens* [online]. 2010, **6**(8). ISSN 1553-7366. Dostupné z: doi:10.1371/journal.ppat.1001000
- [78] HEMINGWAY, J. a H. RANSON. Insecticide resistance in insect vectors of human disease. *Annual Review of Entomology* [online]. 2000, **45**, 371–391. ISSN 0066-4170. Dostupné z: doi:10.1146/annurev.ento.45.1.371
- [79] WEILL, Mylène, Georges LUTFALLA, Knud MOGENSEN, Fabrice CHANDRE, Arnaud BERTHOMIEU, Claire BERTICAT, Nicole PASTEUR, Alexandre PHILIPS, Philippe FORT a Michel RAYMOND. Comparative genomics: Insecticide resistance in mosquito vectors. *Nature* [online]. 2003, **423**(6936), 136–137. ISSN 1476-4687. Dostupné z: doi:10.1038/423136b
- [80] HEMINGWAY, J, N HAWKES, L PRAPANTHADARA, K G JAYAWARDENAL a H RANSON. The role of gene splicing, gene amplification and regulation in mosquito insecticide resistance. *Philosophical Transactions of the Royal Society B: Biological Sciences*. 1998, **353**(1376), 1695–1699. ISSN 0962-8436.
- [81] EDDLESTON, Michael, Nick A. BUCKLEY, Peter EYER a Andrew H. DAWSON. Management of acute organophosphorus pesticide poisoning. *Lancet (London, England)* [online]. 2008, **371**(9612), 597–607. ISSN 1474-547X. Dostupné z: doi:10.1016/S0140-6736(07)61202-1
- [82] MÜNZE, Ronald, Christin HANNEMANN, Polina ORLINSKIY, Roman GUNOLD, Albrecht PASCHKE, Kaarina FOIT, Jeremias BECKER, Oliver KASKE, Elin PAULSSON, Märit PETERSON, Henrik JERNSTEDT, Jenny KREUGER, Gerrit SCHÜÜRMAN a Matthias LIESS. Pesticides from wastewater treatment plant effluents affect invertebrate communities. *Science of The Total Environment* [online]. 2017, **599–600**, 387–399. ISSN 0048-9697. Dostupné z: doi:10.1016/j.scitotenv.2017.03.008
- [83] HAREL, M., G. KRYGER, T. L. ROSENBERRY, W. D. MALLENDER, T. LEWIS, R. J. FLETCHER, J. M. GUSS, I. SILMAN a J. L. SUSSMAN. Three-dimensional structures of *Drosophila melanogaster* acetylcholinesterase and of its complexes with two potent inhibitors. *Protein Science: A Publication of the Protein Society* [online]. 2000, **9**(6), 1063–1072. ISSN 0961-8368. Dostupné z: doi:10.1110/ps.9.6.1063

- [84] GUNNELL, David, Michael EDDLESTON, Michael R. PHILLIPS a Flemming KONRADSEN. The global distribution of fatal pesticide self-poisoning: systematic review. *BMC public health* [online]. 2007, **7**, 357. ISSN 1471-2458. Dostupné z: doi:10.1186/1471-2458-7-357
- [85] BERTOLOTE, José M., Alexandra FLEISCHMANN, Alexander BUTCHART a Nida BESBELLI. Suicide, suicide attempts and pesticides: a major hidden public health problem. *Bulletin of the World Health Organization* [online]. 2006, **84**(4), 260. ISSN 0042-9686. Dostupné z: doi:S0042-96862006000400004
- [86] WATSON, Annetta, Dennis OPRESKO, Robert A. YOUNG, Veronique HAUSCHILD, Joseph KING a Kulbir BAKSHI. Organophosphate Nerve Agents. In: *Handbook of Toxicology of Chemical Warfare Agents* [online]. B.m.: Elsevier, 2015 [vid. 2016-02-15], s. 87–109. ISBN 978-0-12-800159-2. Dostupné z: <http://linkinghub.elsevier.com/retrieve/pii/B9780128001592000099>
- [87] BLACK, R. M. a J. M. HARRISON. The Chemistry of Organophosphorus Chemical Warfare Agents. In: *PATAI'S Chemistry of Functional Groups* [online]. B.m.: John Wiley & Sons, Ltd, 2009 [vid. 2016-12-14]. ISBN 978-0-470-68253-1. Dostupné z: <http://onlinelibrary.wiley.com/doi/10.1002/9780470682531.pat0070/abstract>
- [88] KUČA, Kamil a Miroslav POHANKA. Chemical warfare agents. *EXS*. 2010, **100**, 543–558. ISSN 1023-294X.
- [89] AGARWAL, Reshma, S. K. SHUKLA, S. DHARMANI a A. GANDHI. Biological warfare--an emerging threat. *The Journal of the Association of Physicians of India*. 2004, **52**, 733–738. ISSN 0004-5772.
- [90] PITA, René a Juan DOMINGO. The Use of Chemical Weapons in the Syrian Conflict. *Toxics* [online]. 2014, **2**(3), 391–402. ISSN 2305-6304. Dostupné z: doi:10.3390/toxics2030391
- [91] NG, Eileen. Post-mortem: VX poison killed brother of North Korean leader. *AP NEWS* [online]. 3. říjen 2017 [vid. 2019-01-03]. Dostupné z: <https://apnews.com/90e425dbaf1e44d1ba77e2eea890fc67>
- [92] CHENG, Maria. UK says ex-spy poisoned with Soviet-developed nerve agent. *AP NEWS* [online]. 13. března 2018 [vid. 2019-01-03]. Dostupné z: <https://apnews.com/1a4c95b0e6af4d70b054c8030e177b47>
- [93] WOREK, Franz, Timo WILLE, Marianne KOLLER a Horst THIERMANN. Toxicology of organophosphorus compounds in view of an increasing terrorist threat. *Archives of Toxicology* [online]. 2016, **90**(9), 2131–2145. ISSN 1432-0738. Dostupné z: doi:10.1007/s00204-016-1772-1
- [94] MARRS, T. C. Organophosphate poisoning. *Pharmacology & Therapeutics*. 1993, **58**(1), 51–66. ISSN 0163-7258.

- [95] KING, Andrew M. a Cynthia K. AARON. Organophosphate and carbamate poisoning. *Emergency Medicine Clinics of North America* [online]. 2015, **33**(1), 133–151. ISSN 1558-0539. Dostupné z: doi:10.1016/j.emc.2014.09.010
- [96] MASSON, Patrick, Florian NACHON a Oksana LOCKRIDGE. Structural approach to the aging of phosphylated cholinesterases. *Chemico-Biological Interactions* [online]. 2010, **187**(1–3), 157–162. ISSN 1872-7786. Dostupné z: doi:10.1016/j.cbi.2010.03.027
- [97] TOPCZEWSKI, Joseph J. a Daniel M. QUINN. Kinetic assessment of N-methyl-2-methoxypyridinium species as phosphonate anion methylating agents. *Organic Letters* [online]. 2013, **15**(5), 1084–1087. ISSN 1523-7052. Dostupné z: doi:10.1021/ol400054m
- [98] GORECKI, Lukas, Ondrej SOUKUP, Tomas KUCERA, David MALINAK, Daniel JUN, Kamil KUČA, Kamil MUSILEK a Jan KORABECNY. Oxime K203: a drug candidate for the treatment of tabun intoxication. *Archives of Toxicology* [online]. 2018. ISSN 1432-0738. Dostupné z: doi:10.1007/s00204-018-2377-7
- [99] WILSON, I. B. a B. GINSBURG. A powerful reactivator of alkylphosphate-inhibited acetylcholinesterase. *Biochimica Et Biophysica Acta*. 1955, **18**(1), 168–170. ISSN 0006-3002.
- [100] WONG, L., Z. RADIC, R. J. BRÜGGEMANN, N. HOSEA, H. A. BERMAN a P. TAYLOR. Mechanism of oxime reactivation of acetylcholinesterase analyzed by chirality and mutagenesis. *Biochemistry*. 2000, **39**(19), 5750–5757. ISSN 0006-2960.
- [101] LUO, C., A. SAXENA, M. SMITH, G. GARCIA, Z. RADIC, P. TAYLOR a B. P. DOCTOR. Phosphoryl oxime inhibition of acetylcholinesterase during oxime reactivation is prevented by edrophonium. *Biochemistry* [online]. 1999, **38**(31), 9937–9947. ISSN 0006-2960. Dostupné z: doi:10.1021/bi9905720
- [102] POZIOMEK, EDWARD J., BRENNIE E. HACKLEY a GEORGE M. STEINBERG. Pyridinium Aldoximes1. *The Journal of Organic Chemistry* [online]. 1958, **23**(5), 714–717. ISSN 0022-3263. Dostupné z: doi:10.1021/jo01099a019
- [103] HOBBIER, F., D. G. O’SULLIVAN a P. W. SADLER. New potent reactivators of acetylcholinesterase inhibited by tetraethyl pyrophosphate. *Nature*. 1958, **182**(4648), 1498–1499. ISSN 0028-0836.
- [104] LUETTRINGHAUS, A. a I. HAGEDORN. [QUATERNARY HYDROXYIMINOMETHYLPYRIDINIUM SALTS. THE DISCHLORIDE OF BIS-(4-HYDROXYIMINOMETHYL-1-PYRIDINIUM-METHYL)-ETHER (LUEH6), A NEW REACTIVATOR OF ACETYLCHOLINESTERASE INHIBITED BY ORGANIC PHOSPHORIC ACID ESTERS]. *Arzneimittel-Forschung*. 1964, **14**, 1–5. ISSN 0004-4172.

- [105] HAGEDORN, I., W. H. GÜNDEL a K. SCHOENE. [Reactivation of phosphorylated acetylcholine esterase with oximes: contribution to the study of the reaction course]. *Arzneimittel-Forschung*. 1969, **19**(4), 603–606. ISSN 0004-4172.
- [106] JOKANOVIĆ, Milan. Structure-activity relationship and efficacy of pyridinium oximes in the treatment of poisoning with organophosphorus compounds: a review of recent data. *Current Topics in Medicinal Chemistry*. 2012, **12**(16), 1775–1789. ISSN 1873-4294.
- [107] JOKANOVIĆ, Milan. Medical treatment of acute poisoning with organophosphorus and carbamate pesticides. *Toxicology Letters* [online]. 2009, **190**(2), 107–115. ISSN 1879-3169. Dostupné z: doi:10.1016/j.toxlet.2009.07.025
- [108] KORABECNY, Jan, Ondrej SOUKUP, Rafael DOLEZAL, Katarina SPILOVSKA, Eugenie NEPOVIMOVA, Martin ANDRS, Thuy Duong NGUYEN, Daniel JUN, Kamil MUSILEK, Marta KUCEROVA-CHLUPACOVA a Kamil KUČA. From pyridinium-based to centrally active acetylcholinesterase reactivators. *Mini Reviews in Medicinal Chemistry*. 2014, **14**(3), 215–221. ISSN 1875-5607.
- [109] SAKURADA, Koichi, Kazuo MATSUBARA, Keiko SHIMIZU, Hiroshi SHIONO, Yasuo SETO, Koichiro TSUGE, Mineo YOSHINO, Ikuko SAKAI, Harutaka MUKOYAMA a Takehiko TAKATORI. Pralidoxime iodide (2-pAM) penetrates across the blood-brain barrier. *Neurochemical Research*. 2003, **28**(9), 1401–1407. ISSN 0364-3190.
- [110] BAJGAR, Jiri, Josef FUSEK, Kamil KUČA, Lucie BARTOSOVA a Daniel JUN. Treatment of organophosphate intoxication using cholinesterase reactivators: facts and fiction. *Mini Reviews in Medicinal Chemistry*. 2007, **7**(5), 461–466. ISSN 1389-5575.
- [111] GORECKI, Lukas, Jan KORABECNY, Kamil MUSILEK, Eugenie NEPOVIMOVA, David MALINAK, Tomas KUCERA, Rafael DOLEZAL, Daniel JUN, Ondrej SOUKUP a Kamil KUČA. Progress in acetylcholinesterase reactivators and in the treatment of organophosphorus intoxication: a patent review (2006-2016). *Expert Opinion on Therapeutic Patents* [online]. 2017, **27**(9), 971–985. ISSN 1744-7674. Dostupné z: doi:10.1080/13543776.2017.1338275
- [112] PANG, Y. P., P. QUIRAM, T. JELACIC, F. HONG a S. BRIMIJOIN. Highly potent, selective, and low cost bis-tetrahydroaminacrine inhibitors of acetylcholinesterase. Steps toward novel drugs for treating Alzheimer's disease. *The Journal of Biological Chemistry*. 1996, **271**(39), 23646–23649. ISSN 0021-9258.
- [113] CALAS, André-Guilhem, José DIAS, Catherine ROUSSEAU, Mélanie ARBOLÉAS, Mélanie TOUVREY-LOIODICE, Guillaume MERCEY, Ludovic JEAN, Pierre-Yves RENARD a Florian NACHON. An easy method for the determination of active concentrations of cholinesterase reactivators in blood

- samples: Application to the efficacy assessment of non quaternary reactivators compared to HI-6 and pralidoxime in VX-poisoned mice. *Chemico-Biological Interactions* [online]. 2017, **267**, 11–16. ISSN 1872-7786. Dostupné z: doi:10.1016/j.cbi.2016.03.009
- [114] MUSILEK, Kamil, Daniel JUN, Jiri CABAL, Jiri KASSA, Frank GUNN-MOORE a Kamil KUČA. Design of a potent reactivator of tabun-inhibited acetylcholinesterase--synthesis and evaluation of (E)-1-(4-carbamoylpyridinium)-4-(4-hydroxyiminomethylpyridinium)-but-2-ene dibromide (K203). *Journal of Medicinal Chemistry* [online]. 2007, **50**(22), 5514–5518. ISSN 0022-2623. Dostupné z: doi:10.1021/jm070653r
- [115] CHAMBERS, Janice E., Howard W. CHAMBERS, Edward C. MEEK a Ronald B. PRINGLE. Testing of novel brain-penetrating oxime reactivators of acetylcholinesterase inhibited by nerve agent surrogates. *Chemico-Biological Interactions* [online]. 2013, **203**(1), 135–138. ISSN 1872-7786. Dostupné z: doi:10.1016/j.cbi.2012.10.017
- [116] MERCEY, Guillaume, Tristan VERDELET, Géraldine SAINT-ANDRÉ, Emilie GILLON, Alain WAGNER, Rachid BAATI, Ludovic JEAN, Florian NACHON a Pierre-Yves RENARD. First efficient uncharged reactivators for the dephosphorylation of poisoned human acetylcholinesterase. *Chemical Communications (Cambridge, England)* [online]. 2011, **47**(18), 5295–5297. ISSN 1364-548X. Dostupné z: doi:10.1039/c1cc10787a
- [117] RADIĆ, Zoran, Rakesh K. SIT, Zrinka KOVARIK, Suzana BEREND, Edzna GARCIA, Limin ZHANG, Gabriel AMITAI, Carol GREEN, Bozica RADIĆ, Valery V. FOKIN, K. Barry SHARPLESS a Palmer TAYLOR. Refinement of structural leads for centrally acting oxime reactivators of phosphorylated cholinesterases. *The Journal of Biological Chemistry* [online]. 2012, **287**(15), 11798–11809. ISSN 1083-351X. Dostupné z: doi:10.1074/jbc.M111.333732
- [118] KATZ, Francine S., Stevan PECIC, Timothy H. TRAN, Ilya TRAKHT, Laura SCHNEIDER, Zhengxiang ZHU, Long TON-THAT, Michal LUZAC, Viktor ZLATANIC, Shivani DAMERA, Joanne MACDONALD, Donald W. LANDRY, Liang TONG a Milan N. STOJANOVIC. Discovery of New Classes of Compounds that Reactivate Acetylcholinesterase Inhibited by Organophosphates. *Chembiochem: A European Journal of Chemical Biology* [online]. 2015, **16**(15), 2205–2215. ISSN 1439-7633. Dostupné z: doi:10.1002/cbic.201500348
- [119] OHLOW, Maike J. a Bernd MOOSMANN. Phenothiazine: the seven lives of pharmacology's first lead structure. *Drug Discovery Today* [online]. 2011, **16**(3–4), 119–131. ISSN 1878-5832. Dostupné z: doi:10.1016/j.drudis.2011.01.001
- [120] MITCHELL, S. C. Phenothiazine: the parent molecule. *Current Drug Targets*. 2006, **7**(9), 1181–1189. ISSN 1873-5592.
- [121] SHEN, W. W. A history of antipsychotic drug development. *Comprehensive Psychiatry*. 1999, **40**(6), 407–414. ISSN 0010-440X.

- [122] WHO | The Selection and Use of Essential Medicines. *WHO* [online]. [vid. 2019-01-08]. Dostupné z: <http://www.who.int/medicines/publications/essentialmedicines/trs-1006-2017/en/>
- [123] MURPHY, C. M., Harold RAVNER a Nathan L. SMITH. Mode of Action of Phenothiazine-Type Antioxidants. *Industrial & Engineering Chemistry* [online]. 1950, **42**(12), 2479–2489. ISSN 0019-7866. Dostupné z: doi:10.1021/ie50492a027
- [124] STACK, Cliona, Shari JAINUDDIN, Ceyhan ELIPENAHILI, Meri GERGES, Natalia STARKOVA, Anatoly A. STARKOV, Mariona JOVÉ, Manuel PORTERO-OTIN, Nathalie LAUNAY, Aurora PUJOL, Navneet Ammal KAIDERY, Bobby THOMAS, Davide TAMPELLINI, M. Flint BEAL a Magali DUMONT. Methylene blue upregulates Nrf2/ARE genes and prevents tau-related neurotoxicity. *Human Molecular Genetics* [online]. 2014, **23**(14), 3716–3732. ISSN 1460-2083. Dostupné z: doi:10.1093/hmg/ddu080
- [125] *Cognitive and Functional Connectivity Effects of Methylene Blue in Healthy Aging, Mild Cognitive Impairment and Alzheimer's Disease - Full Text View - ClinicalTrials.gov* [online]. [vid. 2019-01-08]. Dostupné z: <https://clinicaltrials.gov/ct2/show/NCT02380573>
- [126] MERCEY, Guillaume, Julien RENOU, Tristan VERDELET, Maria KLIACHYNA, Rachid BAATI, Emilie GILLON, Mélanie ARBOLÉAS, Mélanie LOIODICE, Florian NACHON, Ludovic JEAN a Pierre-Yves RENARD. Phenyltetrahydroisoquinoline–Pyridinaldoxime Conjugates as Efficient Uncharged Reactivators for the Dephosphorylation of Inhibited Human Acetylcholinesterase. *Journal of Medicinal Chemistry* [online]. 2012, **55**(23), 10791–10795. ISSN 0022-2623, 1520-4804. Dostupné z: doi:10.1021/jm3015519
- [127] BUCHANAN, Katherine A., Milos M. PETROVIC, Sophie E. L. CHAMBERLAIN, Neil V. MARRION a Jack R. MELLOR. Facilitation of long-term potentiation by muscarinic M(1) receptors is mediated by inhibition of SK channels. *Neuron* [online]. 2010, **68**(5), 948–963. ISSN 1097-4199. Dostupné z: doi:10.1016/j.neuron.2010.11.018
- [128] GIESSEL, Andrew J. a Bernardo L. SABATINI. M1 Muscarinic Receptors Boost Synaptic Potentials and Calcium Influx in Dendritic Spines by Inhibiting Postsynaptic SK Channels. *Neuron* [online]. 2010, **68**(5), 936–947. ISSN 0896-6273. Dostupné z: doi:10.1016/j.neuron.2010.09.004
- [129] HORAK, Martin, Kristina HOLUBOVA, Eugenie NEPOVIMOVA, Jan KRUSEK, Martina KANIAKOVA, Jan KORABECNY, Ladislav VYKLICKY, Kamil KUCA, Ales STUHLIK, Jan RICNY, Karel VALES a Ondrej SOUKUP. The pharmacology of tacrine at N-methyl-d-aspartate receptors. *Progress in Neuro-Psychopharmacology & Biological Psychiatry* [online]. 2017, **75**, 54–62. ISSN 1878-4216. Dostupné z: doi:10.1016/j.pnpbp.2017.01.003

- [130] PANG, Yuan-Ping, Stephen BRIMIJOIN, David W. RAGSDALE, Kun Yan ZHU a Robert SURANYI. Novel and viable acetylcholinesterase target site for developing effective and environmentally safe insecticides. *Current Drug Targets*. 2012, **13**(4), 471–482. ISSN 1873-5592.
- [131] SCHMIDT, Monika, Veronika HRABCOVA, Daniel JUN, Kamil KUCA a Kamil MUSILEK. Vector Control and Insecticidal Resistance in the African Malaria Mosquito *Anopheles gambiae*. *Chemical Research in Toxicology* [online]. 2018. ISSN 0893-228X. Dostupné z: doi:10.1021/acs.chemrestox.7b00285
- [132] DOU, Dengfeng, Jewn Giew PARK, Sandeep RANA, Benjamin J. MADDEN, Haobo JIANG a Yuan-Ping PANG. Novel selective and irreversible mosquito acetylcholinesterase inhibitors for controlling malaria and other mosquito-borne diseases. *Scientific Reports* [online]. 2013, **3**, 1068. ISSN 2045-2322. Dostupné z: doi:10.1038/srep01068
- [133] SAINT-ANDRÉ, Géraldine, Maria KLIACHYNA, Sanjeevarao KODEPELLY, Ludivine LOUISE-LERICHE, Emilie GILLON, Pierre-Yves RENARD, Florian NACHON, Rachid BAATI a Alain WAGNER. Design, synthesis and evaluation of new α -nucleophiles for the hydrolysis of organophosphorus nerve agents: application to the reactivation of phosphorylated acetylcholinesterase. *Tetrahedron* [online]. 2011, **67**(34), 6352–6361. ISSN 00404020. Dostupné z: doi:10.1016/j.tet.2011.05.130
- [134] PETROIANU, G. A., K. ARAFAT, S. M. NURULAIN, K. KUCA a J. KASSA. In vitro oxime reactivation of red blood cell acetylcholinesterase inhibited by methyl-paraoxon. *Journal of applied toxicology: JAT* [online]. 2007, **27**(2), 168–175. ISSN 0260-437X. Dostupné z: doi:10.1002/jat.1189
- [135] MUSIL, Karel, Veronika FLORIANOVA, Pavel BUCEK, Vlastimil DOHNAL, Kamil KUCA a Kamil MUSILEK. Development and validation of a FIA/UV–vis method for pKa determination of oxime based acetylcholinesterase reactivators. *Journal of Pharmaceutical and Biomedical Analysis* [online]. 2016, **117**, 240–246. ISSN 07317085. Dostupné z: doi:10.1016/j.jpba.2015.09.010
- [136] ROSENBERG, Yvonne J., Lingjun MAO, Xiaoming JIANG, Jonathan LEES, Limin ZHANG, Zoran RADIC a Palmer TAYLOR. Post-exposure treatment with the oxime RS194B rapidly reverses early and advanced symptoms in macaques exposed to sarin vapor. *Chemico-Biological Interactions* [online]. 2017, **274**, 50–57. ISSN 1872-7786. Dostupné z: doi:10.1016/j.cbi.2017.07.003
- [137] ROSENBERG, Yvonne J., Jerry WANG, Tara OOMS, Narayanan RAJENDRAN, Lingjun MAO, Xiaoming JIANG, Jonathan LEES, Lori URBAN, Jeremiah D. MOMPER, Yadira SEPULVEDA, Yan-Jye SHYONG a Palmer TAYLOR. Post-exposure treatment with the oxime RS194B rapidly reactivates and reverses advanced symptoms of lethal inhaled paraoxon in macaques. *Toxicology Letters* [online]. 2018, **293**, 229–234. ISSN 1879-3169. Dostupné z: doi:10.1016/j.toxlet.2017.10.025

- [138] TRZASKOWSKI, Justyna, Dorothee QUINZLER, Christian BÄHRLE a Stefan MECKING. Aliphatic long-chain C20 polyesters from olefin metathesis. *Macromolecular Rapid Communications* [online]. 2011, **32**(17), 1352–1356. ISSN 1521-3927. Dostupné z: doi:10.1002/marc.201100319
- [139] CHANG, Jun, Si-Ji ZHANG, Yong-Wei JIANG, Liang XU, Jian-Ming YU, Wen-Jiang ZHOU a Xun SUN. Design, synthesis, and antibacterial activity of demethylvancomycin analogues against drug-resistant bacteria. *ChemMedChem* [online]. 2013, **8**(6), 976–984. ISSN 1860-7187. Dostupné z: doi:10.1002/cmdc.201300011
- [140] FUJITA, Daishi, Kosuke SUZUKI, Sota SATO, Maho YAGI-UTSUMI, Eiji KURIMOTO, Yoshiki YAMAGUCHI, Koichi KATO a Makoto FUJITA. Synthesis of a Bridging Ligand with a Non-denatured Protein Pendant: Toward Protein Encapsulation in a Coordination Cage. *Chemistry Letters* [online]. 2012, **41**(3), 313–315. ISSN 0366-7022. Dostupné z: doi:10.1246/cl.2012.313
- [141] SOUKUP, Ondrej, Daniel JUN, Jana ZDAROVA-KARASOVA, Jiri PATOCKA, Kamil MUSILEK, Jan KORABECNY, Jan KRUSEK, Martina KANIAKOVA, Vendula SEPSOVA, Jana MANDIKOVA, Frantisek TREJTNAR, Miroslav POHANKA, Lucie DRTINOVA, Michal PAVLIK, Gunnar TOBIN a Kamil KUCA. A resurrection of 7-MEOTA: a comparison with tacrine. *Current Alzheimer Research*. 2013, **10**(8), 893–906. ISSN 1875-5828.
- [142] KIVRAKIDOU, Olga, Stefan BRÄSE, Frank HÜLSHORST a Nils GRIEBENOW. Solid-phase synthesis of 5-biphenyl-2-yl-1H-tetrazoles. *Organic Letters* [online]. 2004, **6**(7), 1143–1146. ISSN 1523-7060. Dostupné z: doi:10.1021/ol0498848
- [143] ELLMAN, G. L., K. D. COURTNEY, V. ANDRES a R. M. FEATHERSTONE. A new and rapid colorimetric determination of acetylcholinesterase activity. *Biochemical Pharmacology*. 1961, **7**, 88–95. ISSN 0006-2952.
- [144] RIGHI, Marika, Annalida BEDINI, Giovanni PIERSANTI, Federica ROMAGNOLI a Gilberto SPADONI. Direct, One-Pot Reductive Alkylation of Anilines with Functionalized Acetals Mediated by Triethylsilane and TFA. Straightforward Route for Unsymmetrically Substituted Ethylenediamine. *The Journal of Organic Chemistry* [online]. 2011, **76**(2), 704–707. ISSN 0022-3263. Dostupné z: doi:10.1021/jo102109f
- [145] BOULEBD, Houssein, Lhassane ISMAILI, Helene MARTIN, Alexandre BONET, Mourad CHIOUA, José MARCO CONTELLES a Ali BELFAITAH. New (benz)imidazolopyridino tacrines as nonhepatotoxic, cholinesterase inhibitors for Alzheimer disease. *Future Medicinal Chemistry* [online]. 2017, **9**(8), 723–729. ISSN 1756-8927. Dostupné z: doi:10.4155/fmc-2017-0019
- [146] YU, Chengzhi, Bin LIU a Longqin HU. A convenient biphasic process for the monosilylation of symmetrical 1,n-primary diols. *Tetrahedron Letters* [online]. 2000, **41**(22), 4281–4285. ISSN 0040-4039. Dostupné z: doi:10.1016/S0040-4039(00)00626-2

- [147] TRUJILLO-FERRARA, J., Iván VÁZQUEZ, Judith ESPINOSA, Rosa SANTILLAN, Norberto FARFÁN a Herbert HÖPFL. Reversible and irreversible inhibitory activity of succinic and maleic acid derivatives on acetylcholinesterase. *European Journal of Pharmaceutical Sciences: Official Journal of the European Federation for Pharmaceutical Sciences*. 2003, **18**(5), 313–322. ISSN 0928-0987.
- [148] SPILOVSKA, Katarina, Jan KORABECNY, Jan KRAL, Anna HOROVA, Kamil MUSILEK, Ondrej SOUKUP, Lucie DRTINOVA, Zuzana GAZOVA, Katarina SIPOSOVA a Kamil KUČA. 7-Methoxytacrine-adamantylamine heterodimers as cholinesterase inhibitors in Alzheimer's disease treatment--synthesis, biological evaluation and molecular modeling studies. *Molecules (Basel, Switzerland)* [online]. 2013, **18**(2), 2397–2418. ISSN 1420-3049. Dostupné z: doi:10.3390/molecules18022397
- [149] FILOSA, Rosanna, Antonella PEDUTO, Simone Di MICCO, Paolo de CAPRARIIS, Michela FESTA, Antonello PETRELLA, Giovanni CAPRANICO a Giuseppe BIFULCO. Molecular modelling studies, synthesis and biological activity of a series of novel bisnaphthalimides and their development as new DNA topoisomerase II inhibitors. *Bioorganic & Medicinal Chemistry* [online]. 2009, **17**(1), 13–24. ISSN 1464-3391. Dostupné z: doi:10.1016/j.bmc.2008.11.024
- [150] HAREL, M., I. SCHALK, L. EHRET-SABATIER, F. BOUET, M. GOELDNER, C. HIRTH, P. H. AXELSEN, I. SILMAN a J. L. SUSSMAN. Quaternary ligand binding to aromatic residues in the active-site gorge of acetylcholinesterase. *Proceedings of the National Academy of Sciences of the United States of America*. 1993, **90**(19), 9031–9035. ISSN 0027-8424.
- [151] JOHNSON, G. a S. W. MOORE. The peripheral anionic site of acetylcholinesterase: structure, functions and potential role in rational drug design. *Current Pharmaceutical Design*. 2006, **12**(2), 217–225. ISSN 1381-6128.
- [152] WOREK, Franz, Horst THIERMANN, Ladislaus SZINICZ a Peter EYER. Kinetic analysis of interactions between human acetylcholinesterase, structurally different organophosphorus compounds and oximes. *Biochemical Pharmacology* [online]. 2004, **68**(11), 2237–2248. ISSN 0006-2952. Dostupné z: doi:10.1016/j.bcp.2004.07.038
- [153] BLACKARD, W. G., G. K. SOOD, D. R. CROWE a M. B. FALLON. Tacrine. A cause of fatal hepatotoxicity? *Journal of Clinical Gastroenterology*. 1998, **26**(1), 57–59. ISSN 0192-0790.
- [154] PATOCKA, Jiri, Daniel JUN a Kamil KUČA. Possible role of hydroxylated metabolites of tacrine in drug toxicity and therapy of Alzheimer's disease. *Current Drug Metabolism*. 2008, **9**(4), 332–335. ISSN 1389-2002.
- [155] WOREK, F., P. EYER, N. AURBEK, L. SZINICZ a H. THIERMANN. Recent advances in evaluation of oxime efficacy in nerve agent poisoning by in vitro

- analysis. *Toxicology and Applied Pharmacology* [online]. 2007, **219**(2–3), 226–234. ISSN 0041-008X. Dostupné z: doi:10.1016/j.taap.2006.10.001
- [156] DVIR, Hay, Israel SILMAN, Michal HAREL, Terrone L. ROSENBERRY a Joel L. SUSSMAN. Acetylcholinesterase: from 3D structure to function. *Chemico-Biological Interactions* [online]. 2010, **187**(1–3), 10–22. ISSN 1872-7786. Dostupné z: doi:10.1016/j.cbi.2010.01.042
- [157] BARRETT, Kayon a Foday M. JAWARD. A review of endosulfan, dichlorvos, diazinon, and diuron--pesticides used in Jamaica. *International Journal of Environmental Health Research* [online]. 2012, **22**(6), 481–499. ISSN 1369-1619. Dostupné z: doi:10.1080/09603123.2012.667794
- [158] KOVARIK, Zrinka, Zoran RADIĆ, Harvey A. BERMAN, Vera SIMEON-RUDOLF, Elsa REINER a Palmer TAYLOR. Mutant cholinesterases possessing enhanced capacity for reactivation of their phosphonylated conjugates. *Biochemistry* [online]. 2004, **43**(11), 3222–3229. ISSN 0006-2960. Dostupné z: doi:10.1021/bi036191a
- [159] MOSMANN, Tim. Rapid colorimetric assay for cellular growth and survival: Application to proliferation and cytotoxicity assays. *Journal of Immunological Methods* [online]. 1983, **65**(1–2), 55–63. ISSN 0022-1759. Dostupné z: doi:10.1016/0022-1759(83)90303-4
- [160] RISS, Terry L., Richard A. MORAVEC, Andrew L. NILES, Sarah DUELLMAN, Hélène A. BENINK, Tracy J. WORZELLA a Lisa MINOR. Cell Viability Assays. In: G. Sitta SITTAMPALAM, Nathan P. COUSSENS, Henrike NELSON, Michelle ARKIN, Douglas AULD, Chris AUSTIN, Bruce BEJCEK, Marcie GLICKSMAN, James INGLESE, Philip W. IVERSEN, Zhuyin LI, James MCGEE, Owen MCMANUS, Lisa MINOR, Andrew NAPPER, John M. PELTIER, Terry RISS, O. Joseph TRASK a Jeff WEIDNER, ed. *Assay Guidance Manual* [online]. Bethesda (MD): Eli Lilly & Company and the National Center for Advancing Translational Sciences, 2004 [vid. 2016-11-03]. Dostupné z: <http://www.ncbi.nlm.nih.gov/books/NBK144065/>
- [161] MUCKOVA, Lubica, Jaroslav PEJCHAL, Petr JOST, Nela VANOVA, David HERMAN a Daniel JUN. Cytotoxicity of acetylcholinesterase reactivators evaluated in vitro and its relation to their structure. *Drug and Chemical Toxicology* [online]. 2018 [vid. 2018-02-19]. ISSN 10.1080/01480545.2018.1432641. Dostupné z: <http://www.tandfonline.com/doi/abs/10.1080/01480545.2018.1432641>

8. Outputs

Publications

- [1] KORABECNY, Jan, Martin ANDRS, Eugenie NEPOVIMOVA, Rafael DOLEZAL, Katerina BABKOVA, Anna HOROVA, David MALINAK, Eva MEZEIOVA, **Lukas GORECKI**, Vendula SEP SOVA, Martina HRABINOVA, Ondrej SOUKUP, Daniel JUN a Kamil KUCA. 7-Methoxytacrine-p-Anisidine Hybrids as Novel Dual Binding Site Acetylcholinesterase Inhibitors for Alzheimer's Disease Treatment. *Molecules (Basel, Switzerland)* [online]. 2015, **20**(12), 22084–22101. ISSN 1420-3049. Dostupné z: doi:10.3390/molecules201219836
- [2] NEPOVIMOVA, E., J. KORABECNY, R. DOLEZAL, T. D. NGUYEN, D. JUN, O. SOUKUP, M. PASDIOROVA, P. JOST, L. MUCKOVA, D. MALINAK, **L. GORECKI**, K. MUSILEK a Kamil KUCA. A 7-methoxytacrine–4-pyridinealdoxime hybrid as a novel prophylactic agent with reactivation properties in organophosphate intoxication. *Toxicology Research* [online]. 2016, **5**(4), 1012–1016. ISSN 2045-4538. Dostupné z: doi:10.1039/C6TX00130K
- [3] **GORECKI, Lukas**, Jan KORABECNY, Kamil MUSILEK, David MALINAK, Eugenie NEPOVIMOVA, Rafael DOLEZAL, Daniel JUN, Ondrej SOUKUP a Kamil KUCA. SAR study to find optimal cholinesterase reactivator against organophosphorous nerve agents and pesticides. *Archives of Toxicology* [online]. 2016, **90**(12), 2831–2859. ISSN 1432-0738. Dostupné z: doi:10.1007/s00204-016-1827-3
- [4] KUCA, K., J. KORABECNY, R. DOLEZAL, E. NEPOVIMOVA, O. SOUKUP, **L. GORECKI** a K. MUSILEK. Tetroxime: reactivation potency – in vitro and in silico study. *RSC Advances* [online]. 2017, **7**(12), 7041–7045. ISSN 2046-2069. Dostupné z: doi:10.1039/C6RA16499D
- [5] HRABCOVA, Veronika, Jan KORABECNY, Brigita MANYOVA, Lenka MATOUSKOVA, Tomas KUCERA, Rafael DOLEZAL, Kamil MUSILEK, **Lukas GORECKI**, Eugenie NEPOVIMOVA, Kamil KUCA a Daniel JUN. Bis-isoquinolinium and bis-pyridinium acetylcholinesterase inhibitors: in vitro screening of probes for novel selective insecticides. *RSC Advances* [online]. 2017, **7**(62), 39279–39291. Dostupné z: doi:10.1039/C7RA05838A
- [6] **GORECKI, Lukas**, Jan KORABECNY, Kamil MUSILEK, Eugenie NEPOVIMOVA, David MALINAK, Tomas KUCERA, Rafael DOLEZAL, Daniel JUN, Ondrej SOUKUP a Kamil KUCA. Progress in acetylcholinesterase reactivators and in the treatment of organophosphorus intoxication: a patent review (2006-2016). *Expert Opinion on Therapeutic Patents* [online]. 2017, **27**(9), 971–985. ISSN 1744-7674. Dostupné z: doi:10.1080/13543776.2017.1338275
- [7] MEZEIOVA, Eva, Katarina SPILOVSKA, Eugenie NEPOVIMOVA, **Lukas GORECKI**, Ondrej SOUKUP, Rafael DOLEZAL, David MALINAK, Jana JANOCKOVA, Daniel JUN, Kamil KUCA a Jan KORABECNY. Profiling donepezil template into multipotent hybrids with antioxidant properties. *Journal of Enzyme Inhibition and Medicinal Chemistry* [online]. 2018, **33**(1), 583–606. ISSN 1475-6374. Dostupné z: doi:10.1080/14756366.2018.1443326
- [8] SOUKUP, Ondrej, Jan KORABECNY, David MALINAK, Eugenie NEPOVIMOVA, Ngoc L. PHAM, Kamil MUSILEK, Martina HRABINOVA, Vendula HEPNAROVA, Rafael DOLEZAL, Petr PAVEK, Petr JOST, Tereza KOBRLOVA, Jana

- JANKOCKOVA, **Lukas GORECKI**, Miroslav PSOTKA, Thuy D. NGUYEN, Karl BOX, Breeze OUTHWAITE, Martina CECKOVA, Ales SORF, Daniel JUN a Kamil KUCA. In vitro and in silico Evaluation of Non-Quaternary Reactivators of AChE as Antidotes of Organophosphorus Poisoning - a New Hope or a Blind Alley? *Medicinal Chemistry* [online]. 2018, **14**(3), 281–292. ISSN 1573-4064. Dostupné z: doi:10.2174/1573406414666180112105657
- [9] MALINAK, David, Jan KORABECNY, Ondrej SOUKUP, **Lukas GORECKI**, Eugenie NEPOVIMOVA, Miroslav PSOTKA, Rafael DOLEZAL, Thuy D. NGUYEN, Eva MEZEIOVA, Kamil MUSILEK a Kamil KUCA. *A Review of the Synthesis of Quaternary Acetylcholinesterase Reactivators* [online]. červenec 2018 [vid. 2019-01-16]. Dostupné z: <https://www.ingentaconnect.com/contentone/ben/coc/2018/00000022/00000016/art00005>
- [10] **GORECKI, Lukas**, Ondrej SOUKUP, Tomas KUCERA, David MALINAK, Daniel JUN, Kamil KUCA, Kamil MUSILEK a Jan KORABECNY. Oxime K203: a drug candidate for the treatment of tabun intoxication. *Archives of Toxicology* [online]. 2018. ISSN 1432-0738. Dostupné z: doi:10.1007/s00204-018-2377-7

Conference proceedings

7-Methoxytacrine-p-Anisidine Hybrids as Novel Dual Binding Site Acetylcholinesterase Inhibitors for Alzheimer's Disease Treatment. TOXCON 2016, Stará Lesná 22. 6. – 24. 6. 2016. Slovakia, poster presentation

Mono-quaternary reactivators, new lead structures for organophosphorus intoxication. Prague Summer School 2017, Praha, 4. 9. – 9. 9. 2017, Czech Republic, poster presentation.

Novel acetylcholinesterase reactivators to counteract organophosphate poisoning. Chemical and Biological defense science and technology conference 2017, Long Beach, USA, poster presentation

The novel lead candidates for the treatment of organophosphorous intoxication, Rusalka, Malá Úpa, 18. - 20. 1. 2018, Czech Republic, oral presentation

Mono-quaternary reactivators for the treatment of organophosphorous intoxication. 8. Postgraduální a 6. Postdovká konference 2018, Farmaceutická fakulta v Hradci Králové, Univerzita Karlova, 24. 1. 2018, Czech Republic, oral presentation

Novel uncharged bisoximes for treatment of OP intoxication. SSPPS Seminar Series. UCSD, La Jolla 30. 11. 2018, USA

The story of tacroximes, novel unique compounds for the recovery of organophosphorus-inhibited acetylcholinesterase. 9. Postgraduální a 7. Postdocking konference 2018, Farmaceutická fakulta v Hradci Králové, Univerzita Karlova, 23. 1. 2019, Czech Republic, oral presentation

The story of tacroximes, novel unique compounds for the recovery of organophosphorus-inhibited acetylcholinesterase. 26th Young research fellows meeting 2019, Université Paris Descartes, Faculté de Pharmacie de Paris, 20. 2. – 22. 2. 2019, France, poster presentation

9. Attachments

Attachment I

GORECKI, Lukas, Jan KORABECNY, Kamil MUSILEK, David MALINAK, Eugenie NEPOVIMOVA, Rafael DOLEZAL, Daniel JUN, Ondrej SOUKUP a Kamil KUCA. SAR study to find optimal cholinesterase reactivator against organophosphorous nerve agents and pesticides. *Archives of Toxicology* [online]. 2016, **90**(12), 2831–2859. ISSN 1432-0738. Dostupné z: doi:10.1007/s00204-016-1827-3

Attachment II

GORECKI, Lukas, Jan KORABECNY, Kamil MUSILEK, Eugenie NEPOVIMOVA, David MALINAK, Tomas KUCERA, Rafael DOLEZAL, Daniel JUN, Ondrej SOUKUP a Kamil KUCA. Progress in acetylcholinesterase reactivators and in the treatment of organophosphorus intoxication: a patent review (2006-2016). *Expert Opinion on Therapeutic Patents* [online]. 2017, **27**(9), 971–985. ISSN 1744-7674. Dostupné z: doi:10.1080/13543776.2017.1338275

Attachment III

GORECKI, Lukas, Ondrej SOUKUP, Tomas KUCERA, David MALINAK, Daniel JUN, Kamil KUCA, Kamil MUSILEK a Jan KORABECNY. Oxime K203: a drug candidate for the treatment of tabun intoxication. *Archives of Toxicology* [online]. 2018. ISSN 1432-0738. Dostupné z: doi:10.1007/s00204-018-2377-7